COO-2250-25
MITNE-199

EVALUATION OF ADVANCED FAST REACTOR BLANKET DESIGNS

by

J.I. Shin and M.J. Driscoll

March 1977

DEPARTMENT OF NUCLEAR ENGINEERING
MASSACHUSETTS INSTITUTE OF TECHNOLOGY
Cambridge, Massachusetts 02139

ERDA Research and Development

Contract E(11-1)-2250
UC-79P LMFBR - Physics

US. Energy Research and Development Administration

Massachusetts Institute of Technology
Department of Nuclear Engineering
Cambridge, Massachusetts

EVALUATION OF ADVANCED FAST REACTOR BLANKET DESIGNS

by

J.I. Shin and M.J. Driscoll

March 1977

COO-2250-25

MITNE-199

ERDA Research and Development

Contract E(11-1)-2250

UC-79P LMFBR - Physics

U.S. Energy Research and Development Administration

ABSTRACT

Various fast reactor blanket design concepts - moderated, fissile seeded, alternatively fueled, etc. - have been evaluated to develop a more comprehensive understanding of the technical basis for improved breeding and economic performance. Simple analytical models and equations have been developed, verified by state-of-the-art computer calculations, and applied to facilitate interpretation and correlation of blanket characteristics.

All design concepts examined in the study could be fit into a self-consistent methodology: for example, the fissile buildup histories of all blanket compositions and regions, from a single pin to an entire blanket, could be fitted to the same dimensionless correlation, and all blankets have the same dimensionless optimum irradiation time.

It was also found that the external breeding ratio at the beginning of blanket life is a constant multiple of the external breeding ratio averaged over life for an optimally irradiated blanket. Hence one can use beginning-of-life studies to correctly rank the breeding performance of various blanket design options.

Although oxide fuel was found to have economically favorable characteristics given equal fabrication costs per unit mass of heavy metal, thin (2-row) UC-fueled blanket concepts appear to be slightly preferable under projected short-term future economic conditions due to their excellent neutronic and thermal-hydraulic characteristics, and their narrow margin of deficiency even under conditions favoring oxide fuel.

It is confirmed that the non-linear fissile buildup history characteristic of FBR blankets must be considered in making sufficiently accurate fuel management decisions for real reactors, and it is shown that a batch fuel management option produces about 15% less plutonium than other commonly considered options such as In-Out shuffling.

All results were consistent with the observation that very little improvement in external blanket breeding performance can be envisioned unless core design changes are allowed. Breeding ratio improvements were often detrimental to blanket economics (and vice versa).

ACKNOWLEDGMENTS

The work described in this report has been performed primarily by the principal author, J. Shin, who has submitted substantially the same report in partial fulfillment of the requirements for the Sc.D. degree at MIT.

The work was performed under ERDA Contract E(11-1)-2250. The computations were performed at the M.I.T. Information Processing Service Center and at the Laboratory for Nuclear Science. The advice and suggestions of Ms. Rachel Morton on computational problems are gratefully acknowledged.

Typing of this manuscript has been very ably handled by Ms. Cynthia Mitaras.

TABLE OF CONTENTS

Page

LIST OF FIGURES

LIST OF TABLES

CHAPTER 1

INTRODUCTION

1.1 FOREWORD

Energy production has become one of the most urgent issues of the last quarter of this century. The direct and indirect symptoms of diminishing fossil energy resources has motivated efforts to develop practical new energy sources. The fast breeder reactor (FBR) is a technically feasible and economically attractive alternative for future energy production, and is now the focal point of the reactor development program in the U.S. and in most other highly industrialized countries.

A principal attraction of the FBR comes from its ability to breed more fissile fuel than it consumes, which leads to a low fuel cycle cost and to the effective utilization of uranium ore resources.

The superior neutronic performance of the FBR comes from its fast neutron spectrum, as compared to LWR's or epithermal reactors; the resulting long mean free path and large diffusion length also leads to a large neutron leakage probability. These unique characteristics of the FBR induce one to adopt a configuration with the enriched fuel confined to a central core region surrounded by a fertile blanket. The blanket serves many functions: reflection of neutrons (thereby reducing the core size), power production and neutron and gamma shielding and, even more important, fertile-to-fissile conversion by absorbing neutrons leaking from the core region.

Current fast reactor designs for practical large-scale power production promise breeding ratios in the range from 1.2 to 1.4. The blanket region contributes about one third of the total breeding ratio, and reduces the fuel cycle cost by about twenty five percent of total expenses. Achieving a high breeding ratio and a low fuel cycle cost, which are the strong points of the FBR, can not be accomplished without the contributions of the blanket regions. Consequently the selection of attractive blanket design concepts and optimization of the blanket region are important subtasks in the overall LMFBR development program, and are the central topics addressed in this report.

The blanket of the FBR is commonly subdivided into two regions - the axial and radial blankets. The axial blanket region is an extension of the core region, and its design parameters are severely constrained by those of the core region. The radial blanket region is not constrained in this manner, except in terms of overall subassembly size, and consequently a great deal of freedom exists in this design. For that reason most of the attention in the present work is focused on the radial blanket.

1.2 PREVIOUS WORK

1.2.1 Various Blanket Design Concepts

Blanket concepts capable of improved breeding performance and economic contributions have been examined previously at MIT and elsewhere. Concepts examined have been as follows.

1.2.1.1 Moderated Blankets and Spectrum Hardened Blankets

Replacing some blanket fuel with moderator material such as graphite or beryllium oxide softens the blanket spectrum and leads to a higher fissile buildup rate ($KgPu/KgM_{HM}$-yr), which, it is claimed, will result in significantly decreased fuel cycle cost without appreciably reducing the breeding ratio. Munno(M6) and Okrent (O3) have advocated moderated blanket design concepts because they can permit a smaller effective blanket thickness and can decrease fuel cycle costs. On the other hand Mayer (M2) found that a moderated blanket in a steam-cooled fast reactor system offered no significant economic advantages.

Recent concern over the adequacy of the breeding performance of present designs in terms of their ability to produce excess fissile material rapidly enough to fuel on expanding economy has motivated research programs to developed advanced fuels, such as Uranium Monocarbide and Uranium Nitride, which can permit the design of reactors having substantially improved breeding performance (C3),(C4). The economics of metallic blankets (spectrum-hardened blankets) have been evaluated by Klickman (K3), but the low burnup achievable with metallic fuel materials severely disadvantages the metallic blanket, and the oxide blanket was found to be economically preferable.

1.2.1.2 Fissile-Seeded Blankets

Brewer (B4) recommended investigation of fissile-seeded blanket design concepts because of their potentially higher breeding gain due to the higher fertile fission and power in the blanket regions. However, fissile-seeded blankets possess a number of disadvantages, including increased fissile inventory costs and decreased volume available for the fertile material in the blankets.

1.2.1.3 Parfait Blankets, Sandwich Blankets and Heterogeneous Core Concepts

There has been considerable interest of late in heterogeneous core concepts which involve internal axial or radial blankets or both. A succession of studies at MIT (D3),(P2),(A1) found that modest but worthwhile improvements in both breeding performance and safety can be achieved by adoption of the parfait blanket design concept, which involves internal blankets limited in both radial and axial extent.

Kobayashi(K4) has suggested use of a sandwich blanket concept, in which the internal blanket extends the full radial width of the core. More recently, radial internal blankets have been studied for the CRBR (C6). More complicated versions of the heterogeneous core concept were described by Mougniot et al.(M5); the benefits claimed have aroused some controversy over the capabilities of this general class of core designs (C5),(B2).

All of these concepts have demonstrated similar benefits and have a common theoretical basis, as discussed in Ref. (D1).

1.2.2 Optimization of Blanket Fuel Management Parameters

Key fast reactor blanket fuel management parameters-breakeven and optimum irradiation times and maximum revenue have been studied and correlated as a function of variables characterizing the economic environment by Ketabi (K2) and Bruyer (B6), who based their analysis on prior studies by Brewer (B4), Wood (W3) and Tagishi (T1). This work was begun under the assumption of constant local fissile buildup rate and later corrected to deal with more realistic non-linear fissile buildup histories by the adoption of moderatly complicated correction factors.

Blanket fuel management schemes - batch, region scatter, in-out shuffle and out-in shuffle - have been analyzed with respect to fissile production and power distribution by several investigators. Barthold (B1), Wood (W3) and others (W2) concluded that each fuel management scheme produced essentially the same amount of plutonium, and that in-out management produced the flattest radial power and out-in the most skewed. On the other hand, Lake et.al. (L1) found that an out-in blanket fuel shuffling scheme produced more plutonium than in-out shuffling by an amount sufficient to increase the breeding ratio by ∿0.005.

The effects of blanket thickness and reflector composition on blanket depletion-economics have also been addressed in previous studies. Investigations by Brewer (B4) and Tzanos (T4) have indicated that economic considerations are the key factor which determine the optimum thickness of the radial blanket; and reducing the blanket thickness by replacing one or two rows of blanket and the conventional stainless steel reflector with a high-albedo and moderating reflector such as graphite or beryllium can improve the blanket economics substantially.

1.3 OBJECTIVES AND OUTLINE

Various blanket modifications to achieve higher breeding ratios and lower fuel cycle costs have been suggested by previous investigators. However, a clearly defined strategy for improving blanket neutronics and economics has not yet been advanced; most prior work has been conducted on a case-by-case basis in which a limited number of selected alternatives are addressed.

Frequently the alternatives selected as being most attractive in this manner are in conflict: softening the spectrum (UO_2 or UC_2 fueled blankets) vs. hardening the spectrum (UC or UN fueled blankets), or the moderated blanket vs. a fissile-seeded blanket, or thick blankets vs. thin blankets with high-albedo reflectors.

Thus one major objective of this report is to provide a clearer explanation of the technical basis for improved breeding performance and enhanced economic contributions by the blanket region.

Another major objective of this report is evaluation of these advanced/new concepts with respect to their neutronic and economic capability on a consistent analytical and technical basis.

Most of the work reported in this study will be devoted to analysis and evaluation of blanket design concepts in a conventional core and blanket configuration, in which the variation of blanket design parameters does not interfere significantly with core performance. However, "heterogeneous core concepts" will be reviewed briefly.

In practice, all blanket concepts should be evaluated on the basis of a compromise among neutronics, economics and engineering considerations. Evaluation of the neutronic and economic characteristics of FBR blanket systems is emphasized in the present work, although engineering design constraints will be considered where appropriate. The emphasis will be on development of simple analytical models and equations, which will be verified by state-of-the-art computer calculations, and which will be applied to facilitate interpretation and correlation of blanket characteristics.

1.4 ORGANIZATION OF THIS REPORT

The main body of this report consists of four chapters. Chapter 2 describes the computational methods, nuclear data input, and the details of the economic and financial basis for this study. First the specification of reference reactor parameters, cross-sections, blanket fuel materials, and compositions will be discussed. Then the blanket burnup economics involving designation of an economic/financial environment and selecting a method for fuel burnup, will be reviewed.

Chapter 3 treats blanket neutronics, to develop means for evaluating the effects of various blanket design parameters on fissile production and to review possible design modifications for enhancing the breeding ratio.

In Chapter 4, simple but quite useful fuel depletion models will be developed and extended to evaluate fuel management decisions and to assess the fuel cycle cost contribution of the blanket to the overall power generation cost. The first part of this chapter will be devoted to development of generalized simple correlations for fissile buildup histories in FBR blankets, and an FBR fuel depletion model suitable for fuel economic analyses and parameter sensitivity studies will be established. Using these results, optimization of blanket fuel management will be carried out. Finally, blanket fuel management schemes will be reviewed.

In Chapter 5, advanced FBR blanket design concepts will be evaluated based on the analytical grounds developed in Chapters 3 and 4. General design features for each concept will be discussed, followed by detailed analyses of the neutronic and economic characteristics of these blanket configurations. Unique characteristics, advantages and disadvantages of each concept will be identified in order to establish blanket design strategies on a clear analytical basis.

Chapter 6 summarizes these investigations and reiterates the main conclusions. Suggested areas for further work will be discussed in this chapter.

CHAPTER 2

METHODS OF EVALUATION

2.1 INTRODUCTION

The overall objective of this study was to analyze the neutronic and economic characteristics of FBR blanket systems and to evaluate their breeding performance and economic contributions on a consistent analytical and technical basis.

To make meaningful comparisons of FBR blanket concepts, computational methods, nuclear data used for the calculations, and the details of the economic and financcical environment for each design concept should be considered carefully.

The purpose of this chapter is to review the computational methods and input data, and to discuss in a general way their effects on the specific results which will be presented in later chapters.

2.2 PREPARATION OF REACTOR PARAMETERS AND CROSS-SECTIONS

2.2.1 Reference Reactor Configuration

Most of this study has been devoted to analysis and evaluation of blanket design concepts in a conventional core and blanket configuration. The core size (power rating) is not an important variable for the purpose of this study, as shown by Tagishi (T1); however, reference design features of an 1000 MWe LMFBR, selected as the standard system for previous MIT blanket studies, were again chosen as a reference reactor configuration. Figure 2.1 shows the pertinent physical dimensions featuring a two-zone oxide-fueled core, three row (45 cm thick) radial blanket, 40 cm-thick axial blanket, and 50 cm of axial and radial stainless steel reflector-shield. Table 2.1 summarizes the physical characteristics

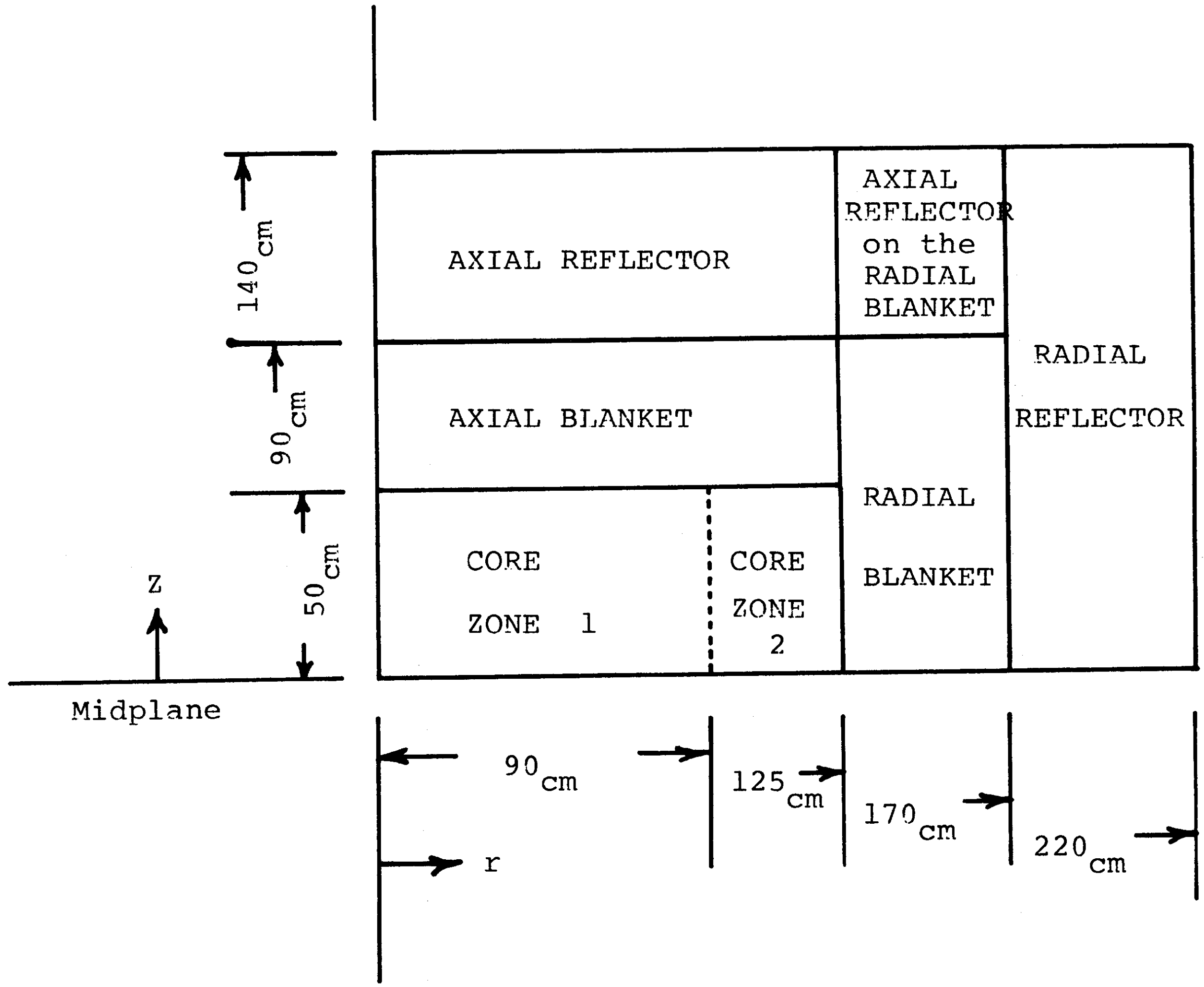

Fig. 2.1 ELEVATION SCHEMATIC VIEW OF THE UPPER RIGHT QUADRANT OF THE STANDARD REACTOR SYSTEM

TABLE 2.1

REFERENCE REACTOR PARAMETERS

1. General		
Plant Rated Power, MWe/MWth	:	1000/2560
Plant Thermal Efficiency, %	:	39.1
Plant Capacity Factor, %	:	82.2
2. Core and Axial Blanket		
Core Height, cm	:	100
Core Diameter, cm	:	250
Core Equivalent Number of Assemblies*	:	245
Material Volume Fractions (Fuel/Na/Structure),%	:	30/50/20
Pellet Smear Density, % T.D.	:	85
Core Average Enrichment (Zone 1/Zone 2) at BOL, %	:	15.2/20.8
Type of Fuel in the Core	:	$(Pu.U)O_2$
Type of Fuel in the Axial Blanket	:	Depleted UO_2
3. Radial Blanket		
Thickness, cm	:	45
Equivalent Number of Assemblies* (3-row)	:	63+70+77
Type of Fuel (reference)	:	Depleted UO_2
Material Volume Fractions (Fuel/Na/Structure), %	:	50/30/20
Pellet Smear Density, % T.D.	:	96.5
4. Reflector		
Thickness (Radial/Axial), cm	:	50/50
Type of Material	:	Stainless Steel
Material Volume Fractions (Steel/Na), %	:	80/20 (axial) 90/100 (radial)

*Assume hexagonal assembly with 15 cm flat-to-flat distance and dimensions of the references reactor system. Table 2.2 summarizes the reference material compositions of the various regions shown in Fig. 2.1. We should note here that the core and axial blanket compositions summarized in Table 2.2 are the beginning-of-life poisoned system compositions.

The equilibrium core and its composition which will be used for most calculations will be discussed in Section 2.5.

2.2.2 Cross-Section Preparation

In the interests of consistency, all studies were performed using the Russian (ABBN) 26-group cross-section set (B3) and 4-group cross-sections prepared by region-collapsing the original ABBN 26-group cross-section set. For simple one-dimensional calculations, the ABBN cross-section set was used, while to reduce the computational cost associated with the burnup analysis, the 26-group self-shielded cross-sections were collapsed into 4-group corss-sections using the ANISN transport code (E1). Separate 4-group sets were prepared for each blanket fuel material. The group structures used for the twenty six and four energy-group sets are specified in Table 2.3, which compares the 4-group structures used by other investigators. As shown, the collapsed group structure is quite similar to those used in other studies. In Appendix D, 4-group cross-sections of Pu-239 (representative fissile material in the core) and U-238 (representative fertile material in the blanket) used for this study are compared with those of the same material used for a benchmark problem examined by the "Large Core Code Evaluation Working Group" (LCCEWG)(K6), and the discrepancies between the two cross-section sets are shown to be quite acceptable for the purpose of this study. All procedures for the preparation of cross-sections followed the same steps already established by previous investigators at MIT (W3),(T1).

TABLE 2.2

MATERIAL COMPOSITIONS OF THE REFERENCE REACTOR SYSTEM AT THE BEGINNING-OF-LIFE

units: 10^3 atoms/barn-cm

Isotope	Core Zone 1 [a]	Core Zone 2 [a]	Axial Blanket [a]	Radial Blanket [b]	Axial Reflector [c]	Radial Reflector [d]
Pu-239	0.8366	1.1206	0.0	0.0	0.0	0.0
Pu-240	0.3453	0.4857	0.0	0.0	0.0	0.0
Pu-241	0.07461	0.10494	0.0	0.0	0.0	0.0
Pu-242	0.04805	0.06756	0.0	0.0	0.0	0.0
U-235	0.00948	0.00831	0.01395	0.02337	0.0	0.0
U-238	4.7288	4.1472	6.963	11.6636	0.0	0.0
Fission Prod.	0.0	0.0	0.0	0.0	0.0	0.0
O - 16	12.0797	11.8686	13.9539	23.3740	0.0	0.0
Fe	12.1300	12.1300	12.1300	12.1300	30.3300	54.5900
Cr	3.1200	3.1200	3.1200	3.1200	7.8000	14.0400
Ni	1.9500	1.9500	1.9500	1.9500	4.8750	8.7750
Na	10.9600	10.9600	10.9600	6.5760	10.9600	2.1920
B - 10	0.1106	0.1106	0.2544	0.0	0.0	0.0

a V_{fuel} = 30 v/o, V_{NA} = 50 v/0, $V_{structure}$ = 20 v/o

b V_{fuel} = 50 v/o, V_{NA} = 30 v/o, $V_{structure}$ = 20 v/o

c V_{steel} = 80 v/o, V_{NA} = 20 v/o

d V_{steel} = 90 v/o, V_{NA} = 10 v/o

TABLE 2.3

THE ENERGY GROUP STRUCTURES USED FOR THE 26-GROUP AND 4-GROUP CROSS-SECTION SETS

Group Number	Upper Energy(eV)	Group Number for 4-group σ-set	Other 4-group structures (Upper Energy in eV)
			• LCCEWG (see Appendix D)
1	10.5×10^6		1. 16.5×10^6
2	6.5×10^6		2. 0.8209×10^6
3	4.0×10^6	Group 1 (groups 1–5)	3. 40.9×10^3
4	2.5×10^6		4. 2.0×10^3
5	1.4×10^6		
6	0.8×10^6		• Fuller*
7	0.4×10^6	Group 2 (groups 6–9)	1. 10.0×10^6
8	0.2×10^6		2. 1.35335×10^6
9	0.1×10^6		3. 40.8677×10^3
10	46.5×10^3		4. 1.2341×10^3
11	21.5×10^3		
12	10.0×10^3	Group 3 (groups 10–14)	• Hoover and Menley**
13	4.65×10^3		1. 10.0×10^6
14	2.15×10^3		2. 0.4979×10^6
15	1.00×10^3		3. 24.79×10^3
16	465		4. 3.355×10^3
17	215		
18	100		
19	46.5		
20	21.5		
21	10.0		
22	4.65	Group 4 (groups 15–26)	
23	2.15		
24	1.0		
25	0.465		
26	Thermal		

*FRA-TM-35, ANL(1972)

**ANL-7710 (1971)

2.3 BLANKET FUEL MATERIAL

2.3.1 Selection of a Representative Fuel Material

Key requirements for blanket fuel materials are that all should be compatible with the maximum operating temperature and possess a good combination of neutronic and thermal characteristics, such as high fertile concentration, phase stability under irradiation, good thermal conductivity, high mechanical strength, high melting point, high corrosion and erosion resistance to the coolant, low porosity and low parasitic neutron capture.

In Table 2.4, the important properties of candidate fuel materials in an LMFBR are summarized. In the early stages of the FBR program, metal and metal-alloy fuels were suggested, however they have serious metallurgical problems such as growth and swelling during temperature fluctuations and irradiation, and phase transformations at low (350 ∿ 600°C) temperatures. The maximum burnup and operating temperature of these fuel materials is accordingly very low.

Oxide fuel materials are well developed and considerable experience has been obtained in LWR's. However, the relatively poor thermal performance and fissile breeding capability of oxide fuel materials has led to the establishment of development programs for advanced fuel materials such as UC, UN and US, on which there is not yet enough information to allow an intelligent choice between these fuels and oxide.

Because fuel performance is a relative factor, and fissile breeding is the most important function of the blankets, considerations for the choice of blanket fuel materials are focused on the allowable linear power rate ($q_{max} \propto k\Delta T_a$ in Table 2.4), the relative softness of the

TABLE 2.4

SELECTED PROPERTIES OF BLANKET FUEL MATERIALS

	Conventional U-Fuel		Advanced U-Fuel		
Fuel	UO_2	UC_2	UC	UN	US
Density (T.D.),g/cc	10.96	11.68	13.6	14.3	10.87
N_{fuel}, 10^{24} $\frac{atoms}{cc}$	0.0244	0.0267	0.0328	0.0342	0.0242
Melting Point*, °C	2750	2375	2290	2850	2460
Thermal Conductivity k, watt/cm °C	0.044(500°C) 0.018(2000°C)	0.343 (50°C) 0.13(1500°C)	0.22-0.25 (500°C-2350°C)	0.16(25°C) 0.21(800°C)	0.11(25°C) 0.17(1000°C)
Coeff. of Thermal Exp. α, 10^6 in/in °C	10∿13	12.5	10.5	9.65	11.6
$k\Delta T_a$**($\propto q'_{max}$)	∿102	∿300	∿385	∿462	∿354
Non-Fuel Component σ_a***, b	0.00126	$3.4x10^{-6}$	$3.4x10^{-6}$	0.022	
Relative Production Cost	Low	Moderate	Moderate	Should be moderate	NA
Max. Burnup Limit†	Excellent (Exp. =10.9%)	Unknown in LMFBR: ∿10%in HTGR	Very good (Exp. =5.2%)	Very Good	Probably (Exp.=2%)
Fuel-Cladding Compatibility	Stainless Steel - no reaction	Unknown	Stainless-Steel - reacts at 1300°F	Minor reaction	Stainless Steel - reacts at 900°C
Remarks (References)	Reference Fuel of LMFBR&GCFR (S1) (T2)	Developed for HTGR (L5) (T3)	Low Parasitic Absorption (S1) (S8)	Hydrogen Buildup by $N^{14}(n,p)C^{14}$ (S1)	(T2)

*Melting Point, decomposition or transformation temperature

**k(at 600°C) · $(T_{melt} - T_{surface}) = k\,(T_{melt} - 1000°F) \propto q'_{max}$.

***for fast-reactor-spectrum neutrons

†Exp. = Empirical irradiation maximum burnup

TABLE 2.4 (continued)

	Early Designs for U Metal-Alloy Fuel		Th-Fuel		
Fuel	U_2Ti	U-M_o (M_o:20 a/o)	ThO_2	ThC_2	ThC
Density(T.D.),g/cc	15.22	17.28	10.0	9.6	10.65
N_{fuel},10^{24}atoms/cc	0.0350	0.0385	0.0228	0.0226	0.0263
Melting Point*,°C	890	565	3220	2655	2625
Thermal Conductivity k, watt/cm °C	0.32(600°C) 0.42(725°C)	0.148 (100°C)	0.048(100°C) 0.032(1200°C)	0.209 (350°C)	0.293(200°C) 0.306(365°C)
Coeff. of Thermal Exp. α ,10^6 in/in °C	~ 20	11 ~ 15	8.0 ~ 9,0	4.0~5.0	3.0~4.0
$k\Delta T_a$**($\propto$ $q_{max.}$)	~113	~ 4.0	~ 94	~ 423	~ 605
Non-Fuel Component σa***, b	0.015	0.131	0.00126	3.4 x 10^{-6}	3.4 x 10^{-6}
Relative Production Cost	NA	NA	NA	NA	NA
Max. Burnup Limit	Good (Exp. = 4.6%)	Very Poor (Exp. = 2%)	Unknown	Unknown	Unknown
Fuel-Cladding Compatibility	Unknown	Reacts with Zr at 1200°C	Similar to UO_2	Unknown	Slight reaction with Ni and Mo at 1100°C
Remarks (References)	High U Concentration (H1) (H5)	High U Concentration (H1) (M3)	(W1) (Y1)	Used in HTGR (L5) (T3)	(L5) (T3)

neutron spectrum, and high fertile density with low parasitic absorption - proper combination of which can lead to a high fissile breeding capability. Based upon these considerations the following were selected as representative fuel materials in this study:

UO_2, UC_2; represent fuels having low fertile density, but having a soft-neutron spectrum,

UC; represents fuels having high fertile density and hard neutron spectrum with low parasitic neutron capture,

U_2Ti; represents fuels having higher fertile density and harder neutron spectrum.

For the most part only Uranium-bearing fuels were considered here. Although Thorium fuel materials were not discussed, the general characteristics of both fuel materials are very similar. Wood, in previous work at MIT, has carried out an extensive comparison of UO_2 vs. ThO_2 fueled LMFBR blankets (W3).

2.3.2 Determination of Material Compositions for Various Blanket Design Concepts

In addition to the reference UO_2-fueled blanket, mono-carbide, di-carbide and Ti-alloy fueled blanket concepts will be considered, and their characteristics compared to derive an understanding of their potential and capabilities. The considerations governing the specification of the material composition of the blanket for different fuel materials were;

a) The same material volume fraction was applied to all fuel materials. Fuel materials having a high thermal conductivity and melting point may allow larger pin diameters. However blanket fuel pins are very tightly packed and the number of fuel pins will therefore have to decrease for a large increase in fuel pin diameter, or in other words the total fuel volume fraction can be expected to remain very nearly constant regardless of fuel pin diameter in the blanket region.

b) The same fuel smear density in % T.D. was applied to all fuel materials. Depending on their metallurgical properties and the effects of irradiation on fuel materials, pellet smear density specifications should be different. However, in the blanket region, burnup and other environmental conditions are less severe than in the core regions, and hence fuel densities close to theoretical can be used - in which case the range of densities under consideration is small and unlikely to have a significant effect on neutronics. Thus we used the same percent of theoretical density in all cases examined.

The ultimate objective of this study is to understand the unique characteristics of various blanket design concepts and to evaluate these concepts with special emphasis on the neutronic and economic viewpoints. Comparison of individually optimized designs for specific fuel materials is not a direct purpose of this study, therefore, the <u>same</u> general blanket design criteria and parameters were applied to all representative fuel materials. Material concentrations in the radial blanket region (blanket region in the spherical geometry) were listed in Appendix A.

Material concentrations for other blanket design concepts such as moderated blankets and fissile-seeded blankets are also summarized in Appendix A. The moderator material chosen for the moderated blanket design concept and the reflector material for the thin blanket concept is BeO, which has a strong moderating effect without any significant neutron absorption. ZrH_2 is a stronger moderator, however, it is also a stronger neutron absorber and it has the least beneficial effect on blanket breeding. Therefore, it was not considered further here.

2.4 BLANKET BURNUP ECONOMICS

2.4.1 Cost Analysis Model

In this work, detailed fuel cycle cost analyses were performed utilizing the cash flow method (CFM) contained in the computer code BRECON, developed by Brewer (B4), and modified by Wood (W3) to permit direct use of 2DB burnup results.

The general CFM expression for the levelized cost of electricity (mills/KwHr) in a region (core, axial blanket, or radial blanket) or subregion under fixed fuel management is

$$e = \frac{1000}{E} M_{HM}(0) \Big[\frac{C_{fiss}\, \varepsilon_o\, F^{MP}(T)}{T} \quad \text{material purchase cost component}$$

$$+ \frac{C_{fab}\, F^{fab}(T)}{T} \quad \text{fabrication cost component}$$

$$+ \frac{C_{rep}\, F^{rep}(T)}{T} \quad \text{reprocessing cost component}$$

$$- \frac{C_{fiss}\, \varepsilon(T) F^{MC}(T)}{T} \Big] \quad \text{material credit cost component} \qquad (2.1)$$

where

e is the local levelized fuel component of the energy cost (mills/KwHr),

E is the electrical energy produced by the reactor in one year (KwHr/yr),

T is the local irradiation time (yr),

C_{fiss} is the fissile price ($/KgPu),

C_{fab} is the unit fabrication cost ($\$/KgM_{HM}$),

C_{rep} is the unit reprocessing cost ($\$/KgM_{HM}$),

ε_o is the initial enrichment,

$\varepsilon(T)$ is the discharge enrichment (Kg fissile discharged per Kg of heavy metal loaded),

$F^q(T)$ is the carrying charge factor for cost component q,

$M_{HM}(0)$ is the mass of heavy metal loaded.

The carrying charge factors, $F^q(T)$, are given by

$$F^q(T) = \frac{1}{1-\tau}\left[\frac{1}{(1+X)^{T_q}} - \tau\right] \quad \text{for capitalized costs or revenue}$$

$$= \frac{1}{(1+X)^{T_q}} \quad \text{for non capitalized costs or revenues (expensed cost or taxed revenue)} \tag{2.2}$$

where

$X = (1-\tau)\, r_b f_b + r_s f_s$ is the discount rate,

τ is the income tax rate,

f_b is the debt (bond) fraction,

f_s is the equity (stock) fraction,

r_b is the debt rate of return,

r_s is the equity rate of return,

T_q is the time between the cash flow transaction q and the irradiation midpoint.

Ketabi (K2) approximated the carrying charge factors expressed by Eq. (2.2) in exponential form to correlate key FBR blanket fuel management parameters as a function of variables characterizing the economic environment under the assumption of constant local fissile buildup rate; namely:

$$F^q(T) \cong e^{\frac{XT_q}{1-\tau}} \qquad \text{for capitalized costs or revenue}$$

$$\cong e^{XT_q} \qquad \text{for noncapitalized cost or revenue}$$

$$= F_q^{\Delta} e^{r_q T} \tag{2.3}$$

where

$F_q^{\Delta} = F_q(\Delta T_q)$, and

ΔT_q is the time between the cash flow transaction q and the beginning of irradiation (for fabrication) or the end of irradiation (for the reprocessing and material credits).

Considering the effects of non-linear fissile buildup histories and using the carrying charge factors expressed Eq. (2.3), Bruyer (B6) established an approximate version of Eq. (2.1), as follows:

$$e = \frac{1000}{E} M_{HM}(0) \left[\frac{\bar{c}_1 e^{r_1 T} + \bar{c}_2 e^{-r_2 T} - \bar{c}_3 \varepsilon(T) e^{-r_3 T}}{T}\right] \tag{2.4}$$

where $\bar{c}_i = c_i \cdot F_i^{\Delta}$ is the modified cost component for operation i (\$/Kg),

Subscript 1 refers to fabrication,

Subscript 2 refers to reprocessing,

Subscript 3 refers to material credit.

Detailed procedures for the derivation of Eq. (2.4) have been summarized in Appendix C.2.

Equation (2.4) will be used for the derivation of all analytic expressions relative to blanket depletion-economics in the present work.

2.4.2 The Reference Economic and Financial Environment

The "Economic environment" is defined here as a set of characteristics: the unit cost for fabrication and reprocessing ($/Kg$M_{HM}$), the fissile Pu market value ($/KgPu) and cash flow timing (ΔT_q).

The financial environment is the set including the debt and equity fractions (f_b, f_s), debt and equity rates of return (r_b, r_s) and the income tax rate, τ. Table 2.5 lists the reference economic and financial parameters used in this study. These conditions are within the range projected for the mature U.S. nuclear fuel cycle economy (Z1): in order to be consistent with prior works at MIT the dollar values are in 1965 dollars, hence are considerably lower then current projections of 1985 costs in 1985 dollars, which are sometimes quoted in the current literature.

It should be noted here that the reference unit fabrication cost was applied to all fuel materials uniformly. The cost of fuel fabrication and processing has many components including fabrication of fuel material and cladding. In the small pin diameter range (0.2 ~ 0.4 in.), tubing costs and total fabrication costs increase rapidly and hence fuel elements with smaller pellet diameter are very expensive (K1), (A2). In the large pin diameter range (>0.4 in.), the unit cost of fabrication is not strongly influenced by the fuel pin diameter. In the (radial) blanket region, typical fuel pin diameters are larger than 0.4 inches (compare to

TABLE 2.5

REFERENCE ECONOMIC AND FINANCIAL ENVIRONMENT

Operation	Unit Fuel Processing Costs*, $/KgM_{HM}$ (Radial Blanket Only)
Fabrication	69
Reprocessing	50
Isotope	**Isotope MARKET Value*, $/KgM_{HM}$**
U-238	0
Pu-239	10,000
Pu-240	0
Pu-241	10,000
Pu-242	0
Financial Parameter	**Value of Parameter (Private Utility)**
Income tax rate, τ	0.5
Capital Structure	
Bond (debt) fraction, f_b	0.5
Stock (equity) fraction, f_s	0.5
Rate of return	
Bonds, r_b	0.07
Stocks, r_s	0.125
Discount rate, $X = (1-\tau)f_b r_b + f_s r_s$	0.08
Cash flow timing	
ΔT_{fab}, yr	0.5
ΔT_{rep}, yr	0.5
ΔT_{MC}, yr	0.5

*1965 dollars, to conform to cases studied by Brewer (B4) core fuel pin diameters (in.) of 0.25 (oxide)/0.354 (carbide)/0.339 (nitride) having unit fabrication costs ($/Kg) of 350 (oxide)/250 (carbide)/275 (nitride) as quoted in Ref. (C3)). Thus the use of the same fabrication costs for all fuel materials may not be far from the actual future circumstances for the blanket region. In any case, this assumption provides a common basis for evaluation of the various blanket design concepts considered in this study.

2.4.3 Cost Accounting Method

Two cost accounting methods, A and B as originally defined by Brewer (B4), were considered for the blanket depletion-economic anlaysis.

In method A, post irradiation transactions are not capitalized-revenue from the sale of plutonium is taxed as ordinary income and reprocessing is treated as a tax deductable expense in the year it occurs. In method B, post irradiation transactions are capitalized.

Unfortunately, there are still many unresolved aspects relating to legal, accounting, tax and financial aspects of the fuel cycle (S7). Therefore, it was considered desirable to carry through a complete analysis on both of the above bases.

2.5 METHOD OF BURNUP

2.5.1 Equilibrium Core Concept

Burnup analysis was performed with the two-dimensional diffusion theory code 2DB (L3). A source of considerable complication in burnup calculations is the requirement that one maintain the system k_{eff} at unity throughout the operating cycle. In practice this is accomplished through the use of movable control rods (i.e., they are progressively withdrawn from the core). For the purpose of this study, it was necessary to simulate this actual operating sequence, since the 2DB code does not have the capability for handling movable control rods. This simulation was made by adding Boron-10 control poison in a "cycle-averaged" concentration and by adopting an "equilibrium" core and axial blanket composition that will remain fixed in time as the irradiation of the radial blanket progresses.

The "equilibrium core" is a "core life-time-averaged" core which occurs at the point where the poisoned k_{eff} is equal to unity. (A "time-averaged" uniform concentration of Boron-10 was added to the core and axial blanket regions of the "unpoisoned equilibrium core"). Since the system k_{eff} varies very nearly linearly with time and fuel burnup, the "equilibium core" concentration can be obtained at the core midcycle (1 yr or 300 full power days for this study). The axial blanket is an integral part of the core, hence an "equilibrium axial blanket" is also determined at the point where the poisoned k_{eff} is equivalent to unity. The poison concentration in the axial blanket was an average of 2.3 times greater than that in the core because of the continuous presence of control and safety rods in that region (Refer to the topical report authored by Wood (W3) for a developement of the factor of 2.3). The detailed procedure to determine equilibrium core concentrations are described in Refs. (A1), (W3), (B5) and (T1).

The effects of the "equilibrium core" approximations on radial blanket neutronics and economics are negligible, because typical radial blanket irradiations are long (on the order of six years) with respect to core refueling intervals (one year). Furthermore, since the same core treatment will be used for all blanket design concepts, any systematic bias, although small, should cancel out so long as relative comparisons are employed.

Table 2.6 lists the "equilibrium" core and axial blanket concentrations corresponding to the BOL system shown in Table 2.2.

2.5.2 Material Included in the Burnup

In the burnup analysis performed by 2DB, materials whose concentration changed as a function of irradiation time were specified, together with the precursor isotope and the reaction which produced the isotope of interest. The fissioning of the following heavy metals contributed to the creation of fission products: Pu-239, Pu-240, Pu-241, Pu-242, U-235, U-238. The buildup of heavy isotopes was assumed to occur by the following neutron capture reactions:

Pu-239 (n,γ) Pu-240

Pu-240 (n,γ) Pu-241

Pu-241 (n,γ) Pu-242

U-238 (n,γ) Pu-239

As shown, neutron capture in U-238 is assumed to lead directly to the production of Pu-239, neglecting the formation of intermediate decay products, which can be shown to lead to a very slight overprediction in the formation rate of Pu-239 (B1). Similarly, Pu-241 decay is neglected, again with justification (B5).

As discussed earlier, the Boron-10 poison concentration in the core and axial blanket was selected to be the time-averaged concentration present in the system. For this reason, the depletion of Boron-10 was neglected in the burnup analysis, leading to a constant Boron-10 concentration throughout core and blanket life.

TABLE 2.6

REFERENCE MATERIAL CONCENTRATIONS OF THE "EQUILIBRIUM" CORE AND AXIAL BLANKET (T1)

unit: 10^3 atoms/barn-cm

Isotope	Core		Axial Blanket
	Zone 1	Zone 2	
Pu-239	0.7543	0.9692	0.1012
Pu-240	0.3595	0.4922	0.00187
Pu-241	0.06438	0.09253	0.00003
Pu-242	0.04677	0.06619	0.0
U-235	0.00560	0.00590	0.01200
U-238	4.4101	3.9607	6.8509
Fission Prod.	0.37101	0.32751	0.01022
O - 16	12.4800	12.4800	13.9500
Fe	12.1300	12.1300	12.1300
Cr	3.1200	3.1200	3.1200
Ni	1.9500	1.9500	1.9500
Na	10.9600	10.9600	10.9600
B-10	0.1106	0.1106	0.2544

*See Table 2.2 for the BOL material concentrations.

2.5.3 Burnup Zones

The 2DB code places a limit of 99 on the sum of the number of burnup zones and cross-section sets. It also treats each burnup zone as a homogeneous mixture during irradiation. Thus, after irradiation each burnup zone has uniform material concentrations, which makes it desirable to have many separate burnup zones in regions of the reactor where the spatial distribution of bred isotopes is important. Figure 2.2 shows the coarse and fine burnup zones for 2DB analysis. The solid lines indicate the coarse burnup zones usually used in this study except for some special blanket designs such as heterogeneously fissile-seeded blankets which used the fine burnup zones indicated by the dotted lines in Fig. 2.2. Table 2.7 shows the correspondence between burnup zones and regions in the reactor as shown in Fig. 2.1.

2.6 METHOD OF COMPUTATION

All of the burnup analyses on which the blanket depletion-economic analysis is based have been performed using the diffusion theory code 2DB (L3).

The one-dimensional transport theory code ANISN(E1) was used for static blanket neutronic analyses, because of the more accurate results which it can in principle provide.

A spherical reactor, whose blanket has the same characteristics as that of the radial blanket was modeled using ANISN. This reactor was analyzed using the S8 angular quadrature approximation, as well as the diffusion theory approximation. Angular quadrature weights and cosines for Gaussian quadrature with constant weight function were derived from Ref. (S5).

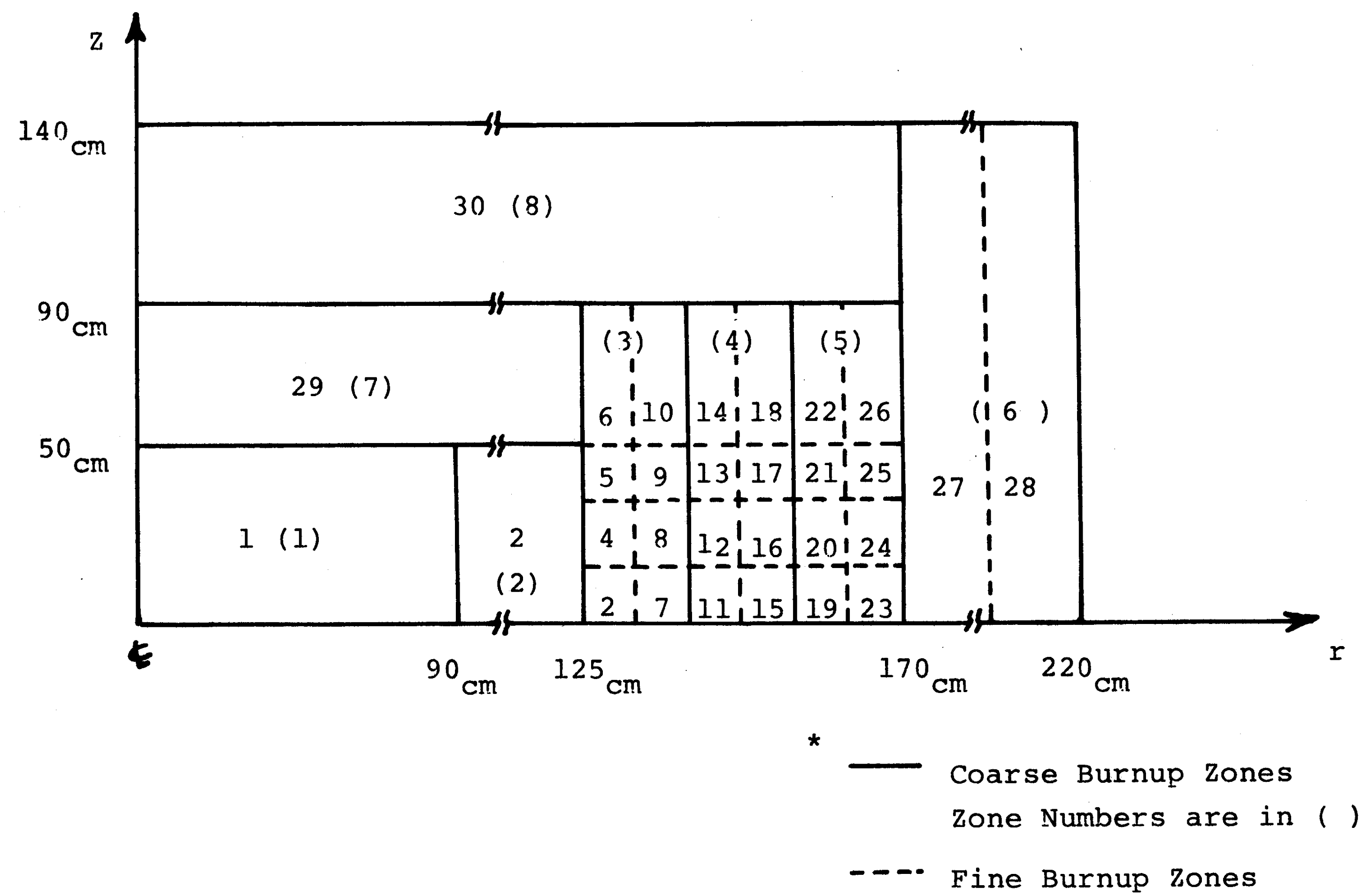

Fig. 2.2 SCHEMATIC ELEVATION VIEW OF THE UPPER RIGHT QUADRANT OF THE REFERENCE 1000 MWe REACTOR SYSTEM WITH BURNUP ZONES INCLUDED

TABLE 2.7

SUMMARY OF BURNUP REGION TYPES

	Fine Burnup Zones	Coarse Burnup Zones
1	Core Zone 1	Core Zone 1
2	Core Zone 2	Core Zone 2
3		Radial Blanket Row 1
4		Radial Blanket Row 2
5		Radial Blanket Row 3
6	Radial Blanket Row 1	Radial Reflector
7		Axial Blanket
8		Axial Reflector
9		
10		
11		
12		
13	Radial Blanket Row 2	
14		
15		
16		
17		
18		
19		
20		
21		
22	Radial Blanket Row 3	
23		
24		
25		
26		
27	Radial Reflector	
28		
29	Axial Blanket	
30	Axial Reflector	

Finally, the BRECON (W3) code was used to provide reference analyses of blanket economics.

2.7 SUMMARY

In this chapter, the computational models and analytical methods used in this work have been discussed.

For the analysis of blanket neutronics, the 26-group ABBN (Russian) cross-section set and a one-dimensional transport theory code were used with a spherical reactor model (to eliminate spurious axial neutron leakage from the system).

All burnup analyses have been performed using the two-dimensional diffusion code 2DB with a 4-group cross-section set prepared by region collapsing the original ABBN cross-section set.

The blanket fuel cycle contribution to the cost of power was computed using the BRECON code, which was developed by Brewer (B4) and later modified by Wood (W3).

Since long burnups (around six years and more) were performed in studying the blanket burnup behavior, an "equilibrium" core and axial blanket were defined which remained fixed in time, containing a cycle-averaged concentration of the poison control material, Boron-10.

The depletion-economic analysis was performed utilizing the same methods and economic/financial environment suggested by previous investigators at MIT.

CHAPTER 3

BREEDING CAPABILITY OF FBR BLANKETS

3.1 INTRODUCTION

The fast breeder reactor (FBR) is expected to be an economically and environmentally favorable energy source in the future due to its breeding capability and low fuel cycle cost. A high fissile gain in the FBR is extremely important if the utility industry is to become relatively independent of the need for expensive mining of low-grade uranium ores by the year 2020, and to thereby assure lower average nuclear power plant fuel cycle costs.

The fast reactor has a relatively small, high-power-density core, and as a result has a very high net neutron leakage from the core region. Therefore, the radial and axial blankets are very important contributors to fissile breeding.

The purpose of this chapter is to evaluate the effects of various design parameters on the fissile production in FBR blankets and to review possible design modifications to enhance the breeding ratio. An evaluation of an analytical method for estimation of the external breeding ratio will be carried out followed by a detailed discussion of the various factors which affect external fissile breeding.

A comparative study of advanced design concepts for FBR blankets will be re-evaluated in Chapter 5 with respect to the blanket economics considerations developed in Chapter 4 and the fissile breeding capabilities reviewed in this chapter.

3.2 BREEDING POTENTIAL OF FBR BLANKETS

3.2.1 Breeding Ratio and Doubling Time

The fissile breeding in an FBR due to neutron capture in fertile materials in the core and blanket regions, is characterized by the breeding ratio, defined by

$$b = \frac{\text{Fissile production rate in core and blanket regions}}{\text{Fissile consumption rate in core and blanket regions}}$$

$$= \frac{\sum_{c,B} (C^{28} + C^{40})}{\sum_{c,B} (A^{49} + A^{41} + A^{25})} \tag{3.1}$$

where

C is the total capture rate in the indicated species,

A is the reactor absorption integral,

c,B are core and blanket regions, respectively.

Considering the neutron balance in each region, i.e.:

$$\underbrace{\nu F_c^{49} + \nu F_c^{28}}_{\text{Production}} - \underbrace{F_c^{49} - F_c^{28} - C_c^{49} - C_c^{28} - A_c^{P,L}}_{\text{Loss and Absorption}} = \underbrace{L_c}_{\text{Leakage}} \tag{3.2}$$

in the core region,

where Pu-239 and U-238 were considered as the representative fissile and fertile species in the core. Similarly,

$$\underbrace{\nu F_B^{28} + \nu F_B^{25}}_{\text{Production}} - \underbrace{C_B^{28} - C_B^{25} - F_B^{28} - F_B^{25} - A_B^{P,L}}_{\text{Loss and Abosrption}} = \underbrace{-L_c}_{\text{Leakage}} \tag{3.3}$$

in the blanket region,

where

F is the total fission rate in the indicated species,

L is the neutron leakage from the core,

P,L refer to parasitic absorption, and neutron loss.

The breeding ratio can then be rewritten as

$$b = \eta_c[1 + \frac{\bar{\nu}-1}{\bar{\nu}} \delta - a(1 + \delta)] - 1 \tag{3.4}$$

where the power production contribution of U-235 and Pu-241 were neglected and,

η_c is the fissile mean neutron yield per neutron absorbed in fissile species in the core region $(\bar{\nu}F_c^{49}/A_c^{49})$,

$\bar{\nu}$ is the mean number of neutrons per fissile and fertile fission,

δ is the ratio of fertile to fissile fissions $([F_c^{28} + F_B^{28}]/\bar{\nu}F_c^{49})$,

a is the parasitic absorptions and neutron loss per fission neutron produced in the core and blanket regions $\left(\frac{A_c^{P,L} + A_B^{P,L}}{\bar{\nu}[F_c^{49} + F_c^{28} + F_B^{28}]}\right)$.

Equation (3.4) indicates that

a) fissile η_c is the dominant term and hence breeding performance can in principle be improved by creating a harder neutron spectrum in the core, which increases η_c of the fissile species. Higher concentrations of heavy isotopes (possible using metal or carbide fuel) in the core leads to a considerably higher breeding ratio, resulting from the harder neutron spectrum and higher η_c. Recent studies involving oxide, carbide, nitride and metal fueled LMFBRs (C3), (O3) have shown that significant fissile production and doubling time advantages exist for metal and carbide fuel over both oxide and nitride fuels. Also, Moorhead and Belcher (M4) found that higher fuel density or higher fuel volume fraction leads to higher breeding ratios.

b) the second term in brackets, $\frac{\bar{\nu}-1}{\bar{\nu}}\,\delta$, indicates a "fast fission bonus" from fertile material, which in practice is usually just about cancelled out by the third term (parasitic absorption and neutron leakage into the reflector region).

c) the third term in brackets, $a(1+\delta)$, indicates that low parasitic absorption is essential for high breeding ratios. The absorption cross-section of fuel materials and the volume fractions of fuel relative to structural materials are important factors here.

Generally, there are two key factors involved in improving the breeding ratio: one is hardening the neutron spectrum and the other is minimizing parasitic absorption.

A second important measure of breeding effectiveness is the doubling time, which we define here as the time necessary to double the initial fissile inventory (note however the present lack of agreement on standard definitions of breeding ratio and doubling time).

Adopting the expression for the linear doubling time from Ref. (D2);

$$DT \equiv \frac{c(1+\delta)}{pgLr(1+\alpha)} = \frac{c\eta(1+\delta)}{pg\bar{\nu}Lr} \qquad (3.5)$$

where

c = constant (numerical conversion factor),

p = specific power (Kw/Kg),

g = breeding gain = b-1,

L = system load factor,

r = fraction of total fuel inventory in reactor, the fractional change caused by the variation of each parameter can be written (A1) as

$$\frac{\Delta DT}{DT} \cong -\frac{\Delta P}{P} - \frac{\alpha}{g}\frac{\Delta\eta}{\eta} - \frac{\Delta f}{f} + \frac{\Delta\delta}{1+\delta} \tag{3.6}$$

where

$$f = Lr \tag{3.7}$$

Equation (3.6) suggests several strategies for decreasing the doubling time, i.e.,

a) increase specific power by power flattening,

b) create a hard spectrum to increase η,

c) decrease δ with higher enrichment.

Actually, δ, the ratio of fertile-to-fissile fissions, is nearly constant, unless one contemplates substituting thorium for uranium as the fertile species - an option not under consideration here. Therefore, hardening the neutron spectrum and achieving a high specific power are in practice the most effective factors which can be altered to shorten the doubling time.

3.2.2 Blanket (External) Breeding Ratio

In this study, our concern was concentrated on blanket breeding capabilities.

The breeding ratio can be split into two parts corresponding to the internal (core) contribution (bi) and the external (blanket) contribution (bx):

$$bi = \frac{\text{Fissile production rate in core}}{\text{Fissile consumption rate in core and blanket regions}}$$

$$= \frac{C_c^{28} + C_c^{40}}{\sum\limits_{c,B} (A^{49} + A^{41} + A^{25})} \tag{3.8}$$

$$bx = \frac{\text{Fissile production rate in blanket}}{\text{Fissile consumption rate in core and blanket regions}}$$

$$= \frac{C_B^{28}}{\sum\limits_{c,B} (A^{49} + A^{41} + A^{25})} \tag{3.9}$$

where it is assumed that no plutonium is present in the blanket at BOL.

Inserting Eq. (3.3) into Eq. (3.9), the external breeding ratio can be rewritten as

$$bx = \frac{1}{\sum\limits_{c,B} (A^{49} + A^{25} + A^{41})} [L_c + (\bar{\nu}-1)F_B - A_B^{P,L,C}] \tag{3.10}$$

where

$$F_B = F_B^{25} + F_B^{28} \text{ and } A_B^{P,L,C} = A_B^{P,L} + C_B^{25}.$$

The fissile consumption rate in the whole reactor, $\sum_{c,B}(A^{49} + A^{41} + A^{25})$, is directly related to the reactor thermal power P, and can be considered as a fixed value. Therefore, Eq. (3.10) indicates that the external breeding ratio depends on

a) the neutron leakage rate from the core (L_c)

b) the neutron production rate in the blanket $[(\bar{\nu}-1)_B F_B]$,

c) the neutron loss rate ($A_B^{P,L,C}$).

Table 3.1 shows typical neutronic characteristics of (spherical) blankets with oxide, carbide and metal alloy fuel driven by the same oxide core. The number of neutrons created in the blanket region is only about 13% of the total available neutrons in this region, and neutron migration from the core is the main source of blanket region neutrons. However, Table 3.1 also shows that if all core parameters were fixed, blanket albedo remains essentially constant regardless of blanket composition.

Neutron loss by parasitic absorption and leakage into the reflectors is nearly equal to the total neutrons generated in the blanket regions. Since the variations of fission cross-sections and $\bar{\nu}$-value resulting from a change of neutron spectrum are insignificant, neutron losses by parasitic absorption and leakage are the key factors which must be reduced to secure high neutron availability and to thereby improve the external breeding ratio.

In Table 3.1, the external breeding ratio of the carbide blanket is the highest because of its low parasitic absorption and leakage loss. Note that the metal alloy fueled blanket, which has the highest atomic density, created the most additional neutrons, but the added neutron absorption of the Ti metal canceled this advantage, and the external breeding ratio is smaller than that of the carbide blanket.

External breeding in an FBR is a composite function of neutron generation, absorption and losses. Since the main neutron source for the blanket region is neutron leakage from the core, which accounts for about 87% of the total available neutrons in the blanket region (for a typical 1000 MWe - sized core), and the total neutron loss caused by parasitic absorption and leakage is around 15% of the total neutrons, we can expect that without changing core parameters, improvement of the external breeding ratio by improving upon the 13% or so of blanket-fission-

TABLE 3.1

COMPARISON OF NEUTRONIC CHARACTERISTICS OF SPHERICAL BLANKETS WITH OXIDE, CARBIDE, OR METAL-ALLOY FUEL†

Fuel Material	UO_2	UC	U_2Ti
$\bar{\nu}_B$	2.68855	2.69986	2.70847
F_B^*	1.44619 + 05	1.60267 + 05	1.62119 + 05
$\bar{\nu}F_B$	3.88816 + 05	4.32698 + 05	4.39094 + 05
$(\bar{\nu}-1)F_B$	2.44197 + 05	2.72431 + 05	2.76975 + 05
Parasitic Absorption (A_B^P)	2.24081 + 05	1.77269 + 05	2.56349 + 05
Leakage Loss (A_B^L)	1.02075 + 05	7.15724 + 04	1.16148 + 05
Neutron Capture by U-235 (C_B^{25})	2.07899 + 04	2.02469 + 04	1.67210 + 04
Leakage from Core (L_c)	2.56408 + 06	2.62047 + 06	2.60308 + 06
A_c^{49}	6.04047 + 06	5.995376 + 06	6.00377 + 06
bx	0.35043	0.37500	0.36053

†Calculated using the ANISN code in Spherical Geometry for 45 cm thick blankets surrounding a large UO_2-Fueled core using representative material compositions.

$*F_B = F_B^{25} + F_B^{28}$

produced neutrons and the 15% or so of neutrons lost in the blanket will be relatively small.

In the following sections, more detailed discussions of the associated factors, and the effects of neutron spectrum and blanket design parameters on external breeding ratio will be presented.

3.3 EVALUATION OF FACTORS WHICH AFFECT EXTERNAL FISSILE BREEDING

3.3.1 Neutron Leakage Rate from the Core Region (L_c)

Most neutrons absorbed in the blanket region come from the core region, and the blanket zone nearest the core has the highest breeding capability and dominates the neutronic characteristics of the entire blanket.

The neutron leakage rate into the blanket is simply related to the blanket diffusion coefficient, D_B, and the geometrical blanket buckling, B_B^2.

The total number of neutrons which escape from the core/blanket interface per second is

$$\int_A \bar{J} \cdot \bar{n} \quad dA = \int_V \text{div } \bar{J} \, dV \tag{3.11}$$

where $\bar{J}$ is the neutron current, $\bar{n}$ is a unit vector normal to the surface element dA and, in accordance with the divergence theorem, the surface integral is changed into one over the reactor volume V.

For a one-group, one-dimensional calculation, Eq. (3.11) can be rewritten in a simpler form;

$$L_c = J_c \cdot S_R \tag{3.12}$$

where J_c is the average neutron current at the core/blanket interface and S_R is the total surface area.

Requiring continuity of neutron current at the core/blanket interface, the neutron leakage from the core can be expressed as

$$L_c = J_c \cdot S_R = J_B \cdot S_R = - D_B \frac{d\phi_B}{dr}\bigg|_{r=a} \cdot \quad S_R \tag{3.13}$$

In Appendix B.1, considerations are discussed which permit the neutron flux distribution in the blanket to be expressed as a simple exponential function, $\phi_B = \phi_o e^{-B_B(r-a)}$, in which case Equation (3.13) can be changed to

$$L_c \propto D_B \; B_B \propto [\frac{\Sigma_{a,B} - \bar{\nu}\Sigma_{f,B}}{\Sigma_{tr,B}}]^{1/2} , \tag{3.14}$$

where we assume that ϕ_o, the neutron flux at the core/blanket interface, remains constant.

Equation (3.14) indicates that the neutron leakage rate from the core is roughly proportional to $[\frac{\Sigma_{a,B}}{\Sigma_{tr,B}}]^{1/2}$, and if we assume that most of the neutrons in the blanket are absorbed by U-238, the neutron leakage rate, L_c, can be written as a simple cross-section ratio for U-238;

$$L_c \propto (\frac{\sigma^{28}_{a,B}}{\sigma^{28}_{tr,B}})^{1/2} \tag{3.15}$$

Table 3.2 summarizes the absorption and transport cross-sections in the blanket, and the neutron leakage rate, for oxide, carbide and Ti-alloy fuels. The carbide fueled blanket has the highest value of $[\frac{\Sigma_{a,B}}{\Sigma_{tr,B}}]^{1/2}$, hence the largest neutron leakage from the core is encountered from this option. However, the variation of the cross-section ratio, $\frac{\Sigma_{a,B}}{\Sigma_{tr,B}}$, is so small that for all practical purposes the change of neutron leakage rate is insignificant as blanket composition is changed.

Table 3.3 shows the variation of neutron leakage rate as blanket design parameters are changed. As can be seen fuel density and reflector composition have a rather unimportant effect on the neutron leakage rate, and blanket thickness and enrichment, while more important, are also negligible (< ± 3%). Hence we can conclude that the neutron leakage rate from the core region into the blanket is only affected by core design parameters (such as power flattening) which will vary ϕ_o, and hence the external breeding ratio is mainly determined by core design parameters.

3.3.2 Increasing $\bar{\nu}$ by Spectrum Hardening

If all core design parameters are fixed, i.e., the neutron leakage rate into the blanket is held essentially constant, the external breeding ratio is directly related to the neutronic economy achieved in the blanket region - namely the detailed balance between neutron production and loss.

Since a higher net neutron production in the blanket region increases the external breeding ratio, achieving a high $\bar{\nu}$ value is one potentially favorable objective for the blanket designer.

TABLE 3.2

COMPARISON OF THE NEUTRON LEAKAGE RATE FROM THE

CORE REGION FOR OXIDE, CARBIDE AND Ti-ALLOY FUELS

Parameter	Units	BLANKET FUEL		
		UO_2	UC	U_2Ti
$\Sigma_{tr,B}$	cm^{-1}	0.3559	0.3716	0.3819
$\Sigma_{a,B}$†	cm^{-1}	5.6127 - 03	6.6964 - 03	6.1849 - 03
$\bar{\nu}\Sigma_{f,B}$	cm^{-1}	7.4601 - 04	9.5900 - 04	8.9404 - 04
$\left[\frac{\Sigma_{a,B} - \nu\Sigma_{f,B}}{\Sigma_{tr,B}}\right]^{1/2}$		0.1169	0.1242	0.1177
$\left[\frac{\Sigma_{a,B}}{\Sigma_{tr,B}}\right]^{1/2}$		0.1256	0.1342	0.1273
$L^*_{c,N}$	neutrons/sec	1.0	1.022	1.015

*relative to UO_2, i.e., $L_{c,N} = L_c/\{L_c\}_{UO_2}$

†$\Sigma_{a,B}$ = Total Absorption by Blanket Material + Right Boundary Leakage (into reflector)

TABLE 3.3

VARIATION OF NEUTRON LEAKAGE RATE

WITH BLANKET DESIGN PARAMETERS†

Design Parameter	Variation in Parameter	Change in Leakage(%)
Fuel Material	$UO_2 \rightarrow UC$	+2.2
Fuel Density	UO_2(96.5% T.D) $\rightarrow UO_2$(65% T.D)	-0.1
Blanket Thickness	UO_2(3 rows) $\rightarrow UO_2$(1 row)	-2.5
Enrichment	UC(0.2% Depleted U) $\rightarrow$UC(0.7% Natural U)	-2.0
Reflector	UO_2 + Steel Reflector $\rightarrow UO_2$ + BeO Reflector	0.0

†For same reference large oxide core and a 3-row blanket.

Note that the leakage referred to is from the core into the blanket and not from the blanket into the reflector.

There is an empirical universal expression for $\bar{\nu}$ values (L2)

$$\bar{\nu}\,(E) = \bar{\nu}_o + aE \qquad (3.16)$$

where $\bar{\nu}_o$ and a are constant, and E is the absorbed neutron energy in MeV. the constants are

for U-235, $\bar{\nu}_o = 2.43$, $a = 0.065$ $(0 \leq E \leq 1)$

$\bar{\nu}_o = 2.35$, $a = 0.150$ $(0 > 1)$

for U-238, $\bar{\nu}_o = 2.30$, $a = 0.160$ (all E)

The average neutron energy in the blanket region is also affected by the core neutron spectrum, because most neutrons come from core, and the magnitude of the neutron flux is sharply attenuated as the distance from the core/blanket interface is increased, as shown in Fig. 3.1. Therefore, the possible range of variation of average neutron energy in the blanket region which can be achieved by varying fuel composition or fuel material is rather small and the $\bar{\nu}$ value remains essentially constant. In Table 3.1 the incremental increase in the $\bar{\nu}$ value due to spectrum hardening (achieved by replacing UO_2 fuel by UC or U_2T_i fuel) is only 0.74%.

Figure 3.2 shows the variation of $\bar{\nu}$ through the blanket region. It decreases slightly with increasing blanket depth, t, because of spectrum softening. Note that $\bar{\nu}$ is a composite quantity involving weighted fissile and fertile fissions, hence the change also reflects the fact that U-238 fissions (a threshold reaction) also fall off much more rapidly than U-235 or Pu-239 fissions.

However, since most fissions occur in the blanket region nearest the

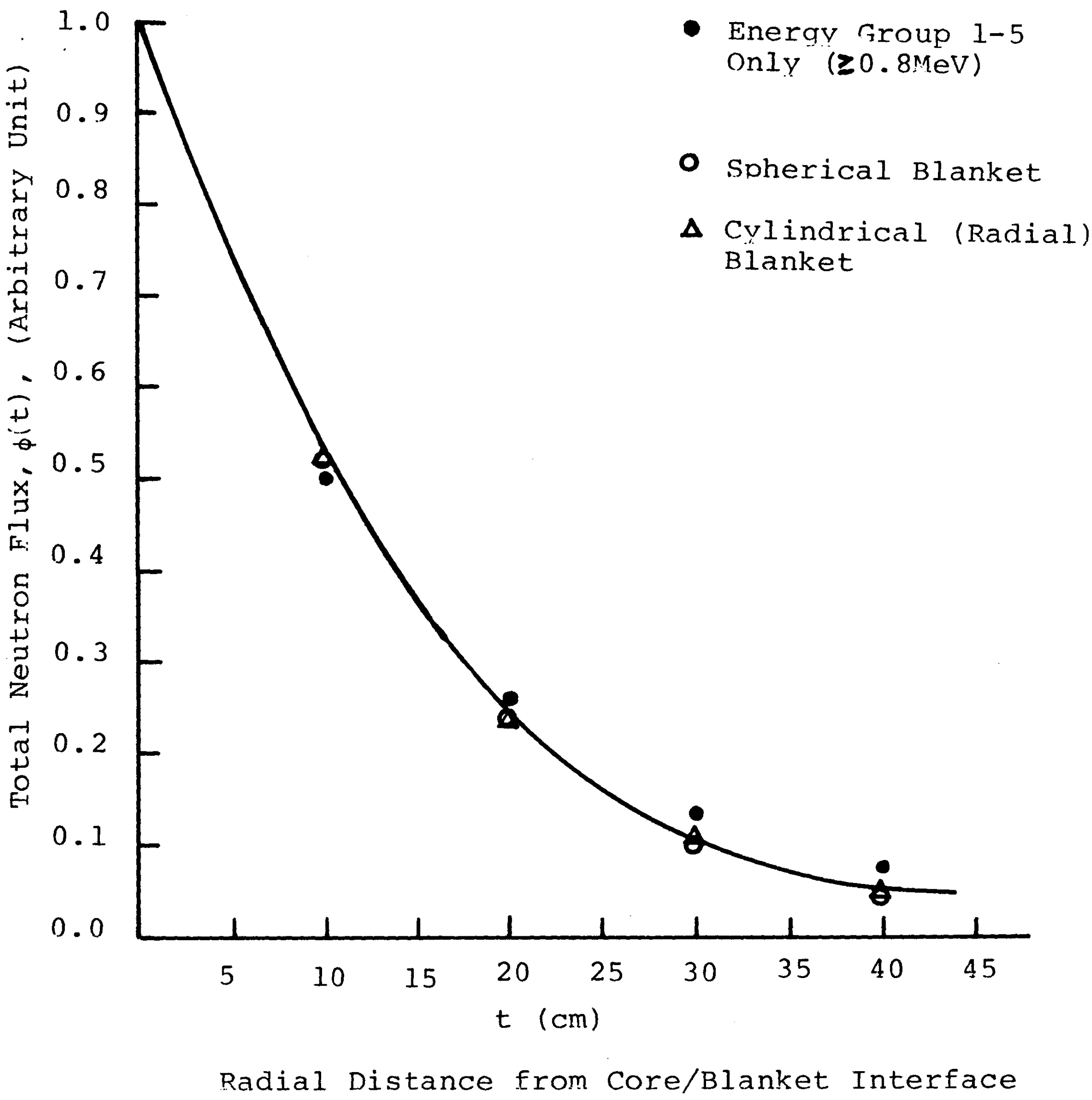

Fig. 3.1 NEUTRON FLUX DISTRIBUTION THROUGH THE BLANKET REGION

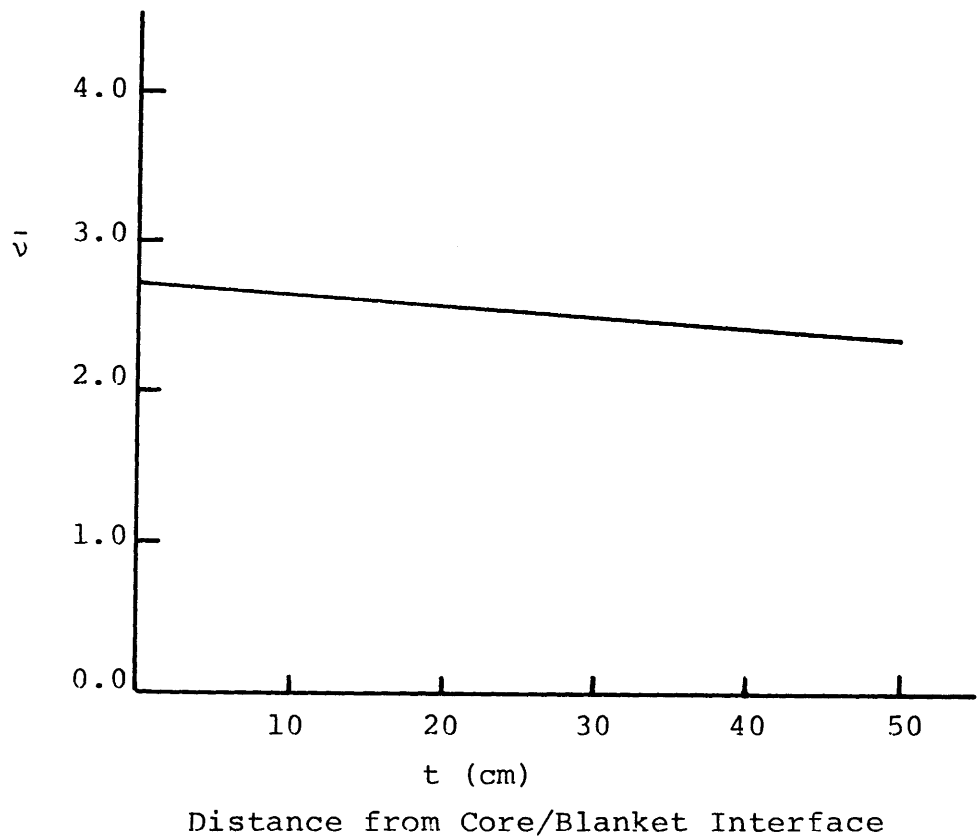

Fig. 3.2 CALCULATED $\bar{\nu}$ -VALUE THROUGH THE BLANKET REGION (BOL)

core (the 1st row of the blanket), the blanket-average $\bar{\nu}$ value is not changed much at all.

For the neutronic analysis of the blanket region, the $\bar{\nu}$ value can be, therefore, simply considered as a constant if core parameters are fixed.

3.3.3 Neutron Fission Rate in the Blanket (F_B)

A high fertile and fissile fission reaction rate in the blanket region are conducive to a larger fast fission bonus. There are two important effects of a high fast fission bonus from U-238 fission - the power contribution and the generation of more available neutrons. The reactor as a whole generates constant total thermal power, hence a high power contribution by the fertile material in the blanket reduces the fissile consumption rate in core, and also offers the potential for a high external breeding ratio.

The number of neutrons consumed in the blanket region by absorption and out-leakage is equal to the sum of the neutron in-leakage from the core and the neutrons produced by fission in blanket, a sum to which the external breeding ratio is linearly proportional. Without for a moment considering options such as addition of moderator or fissile material to the blanket, we can assume that the neutron leakage rate from the core is constant, as described in Section 3.3.1. Hence, increasing the neutron generation in the blanket is an important means to improve the external breeding ratio.

From Equation (3.10), the sensitivity coefficient linking the neutron fission rate in the blanket to the external breeding ratio, $\lambda_{F_B}^{b_x}$, is

$$\lambda_{F_B}^{b_x} \equiv \frac{\frac{\Delta b_x}{bx}}{\frac{\Delta F_B}{F_B}} = [1 + \frac{L_c}{(\bar{\nu}-1)F_B} - \frac{A_B^{P,L,C}}{(\bar{\nu}-1)F_B}]^{-1} \quad (3.17)$$

Employing the typical values of each BOL parameter shown in Table 3.1, the $\lambda_{F_B}^{b_x}$ for oxide, carbide and Ti-alloy are

$$\begin{aligned} \lambda_{F_B}^{b_x} &= 0.0992 \quad \text{(for oxide)} \\ &= 0.1038 \quad \text{(for carbide)} \\ &= 0.1112 \quad \text{(for Ti-alloy)} \end{aligned} \quad (3.18)$$

which are comparable in magnitude to the $\lambda_{A^{P,L,C}}^{b_x}$ sensitivity coefficients for parasitic absorption and neutron leakage developed in the next section. Equation (3.18) indicates that changes in the total fission rate have a small effect on the external breeding ratio, i.e., doubling the fission rate in the blanket only results in a 10% higher external breeding ratio. The dominant term in Eq. (3.17) is the second term, which is the ratio of the number of neutrons leaking from the core to those created in the blanket.

The total fission integral, F_B, in the blanket is the sum of the fission reactions of U-235 and U-238;

$$F_B = (N_B^{28}\, \bar{\sigma}_{f,B}^{28} + N_B^{25}\, \bar{\sigma}_{f,B}^{25})\phi_B \cdot V_B \quad (3.19)$$

Table 3.4 shows the ratio of macroscopic fission cross-sections of fissile and fertile material: U-235 generates about 50% as many neutrons as are produced by U-238 at beginning of life; late in life plutonium fission generates about 400% as many neutrons as those produced by U-238.

3.3.3.1 Variation of the Effective Fission Cross-Section by Changing the Neutron Spectrum

The cross-section for fission by neutrons shows large variations with energy and with the character of the target nucleus. U-238 has a threshold near 1 Mev, while U-235 has a cross-section which increase more-or-less continuously as neutron energy decrease.

Fission reactions in fresh FBR blanketscome from U-238, and an increase in the population of high energy neutrons ($\gtrsim 2.5$ MeV) will increase the "effective" fission cross-section of U-238. Here we should note that a harder neutron spectrum does not improve the "effective" fission cross-section of U-238 without a concurrent increase in the number of high energy ($\gtrsim 2.5$ MeV) neutrons.

Using the ABBN 26-energy group structure (B3), the effective fission cross-section of U-238 in barns can be written as

$$\bar{\sigma}^{28}_{f,B} = \frac{1.0 + 0.58\ \phi_2/\phi_1 + 0.58\ \phi_3/\phi_1 + 0.49\ \phi_4/\phi_1 + 0.02\ \phi_5/\phi_1}{\sum_{i=1}^{26} \phi_i/\phi_1} \tag{3.20}$$

which, also, indicates that only high energy reactions (from first group to fourth group) are important contributions to the effective fission cross-section of U-238.

Table 3.4 shows the neutron spectrum shape at the core/blanket interface and the variation of the structure of the neutron spectrum and fission cross-section for oxide, carbide and Ti-alloy fueled blankets. At the core/blanket interface, the high energy neutron spectrum (the first through the fourth group) is essentially the same for all fuel materials and densities, which means that the high energy neutrons primarily originate in the core

TABLE 3.4

VARIATION OF NEUTRON SPECTRUM AND FISSION CROSS-SECTION

FOR OXIDE, CARBIDE AND Ti-ALLOY FUEL†

Energy Group(i)	ϕ_i/ϕ_i						
	UO_2			UC		U_2Ti	
	A*	B*	C*	A*	B*	A*	B*
1	1.0	1.0	1.0	1.0	1.0	1.0	1.0
2	5.68	5.55	5.62	5.69	5.51	5.63	5.46
3	12.12	11.20	11.74	12.61	11.87	12.52	12.06
4	29.42	28.21	30.39	28.60	26.95	28.29	26.91
5	45.09	44.47	49.34	48.28	53.00	50.67	59.78
ϕ_T/ϕ_1**	9.51+02	1.55+03	1.66+03		1.56+03		1.75+03
$\bar{\sigma}^{28}_{f,B}$	-	1.65-02	1.62-02	-	1.63-02	-	1.46-02
$\Sigma^{25}_{f,B}/\Sigma^{28}_{f,B}$	-	0.44	0.48	-	0.40	-	0.36

*Case A: ϕ_i/ϕ_1 of case B at core/blanket interface

Case B: ϕ_i/ϕ_1 with 96.5% T.D. Fuel Density

Case C: ϕ_i/ϕ_1 with 65% T.D. Fuel Density

** ϕ_T = Total Flux = $\sum_{i=1}^{26} \phi_{i,B}$

† Spherical Blanket, All Driven by Same Large Oxide Core
Calculated by ANISN Code with 26 group σ-set.

region. Spectrum hardening caused by higher fuel density or removing moderator, i.e., replacing oxide by metal, affects mainly the lower energy groups below 2.5 MeV, which lowers the relative ratio of high energy neutrons to the total number of neutrons, and thereby decreases the effective cross-section of U-238.

In view of following facts:

a. Most of neutrons in the blanket come from the core and have an energy spectrum which is a relatively independent of blanket composition.

b. The average energy and the most probably energy of prompt fission neutrons are 1.98 MeV and a 0.85 MeV, respectively.

c. Inelastic scattering makes uranium an effective moderator.

Changing the neutron spectrum at high energy is difficult unless we can change core parameters, hence increasing the effective fission cross-section in the blanket region is for all practical purposes impossible, and moreover, the fission cross-section of the fertile species in the blanket is actually decreased by neutron spectrum hardening.

3.3.3.2 Average Neutron Flux in the Blanket ($\bar{\phi}_B$)

As shown in Appendix B.1, the flux distribution in the blanket is roughly

$$\phi_B(r) = \phi_o \, e^{-B_B(r-a)} \qquad (3.21)$$

and the average neutron flux in a cylindrical blanket should be

$$\bar{\phi}_B = \int_a^{a+t} 2\pi r \cdot \phi_B(r)dr \Big/ \int_a^{a+t} 2\pi r\, dr$$

$$\cong \frac{2\phi_B}{S_B}\left[\frac{a+t}{B_B} + \frac{1}{B_B^2}\right]\left[1 - e^{-B_B t}\right] \qquad (3.22)$$

where

$S_B = (a+t)^2 - a^2$

t = blanket thickness

Equation (3.22) indicates that the average neutron flux in the blanket is a function of blanket thickness, t, and buckling, B_B^2.

A typical value of B_B for a 1000 MWe reactor having a 45 cm thick blanket is 0.1 cm^{-1}, therefore, for thick blanket, $e^{-B_B t}$ approaches zero (i.e. leakage into the reflector is negligible). Thus blanket buckling is the key factor determining the magnitude of the average neutron flux in a blanket; a smaller B_B accompanies a larger $\bar{\phi}_B$.

Blanket buckling, B_B^2, is a product of the macroscopic transport cross-section and the net neutron gain cross-section $(\Sigma_{a,B} - \bar{\nu}\Sigma_{f,B})$ in the blanket, i.e.

$$B_B = \left[\frac{\Sigma_{a,B} - \bar{\nu}\Sigma_{f,B}}{D_B}\right]^{1/2} = 1.732\,\left[\Sigma_{tr,B}\,(\Sigma_{a,B} - \bar{\nu}\Sigma_{f,B})\right]^{1/2} \qquad (3.23)$$

In general, the average neutron flux in the blanket decreases as fuel density increases; all macroscopic cross sections and B_B increase as well.

The macroscopic transport, absorption and neutron fission cross-sections and the average neutron flux for oxide, carbide and Ti-alloy fuel are summarized in Table 3.5.

In this Table we can confirm that $e^{-B_B t}$ is small, and since the outer blanket radius, a+t, is 150 cm, for a large core we can neglect $e^{-B_B t}$ and

TABLE 3.5

COMPARISON OF AVERAGE NEUTRON FLUX

IN BLANKET AND RELATED PARAMETERS†

Parameter ††	UO_2	UC	U_2Ti
$\Sigma_{tr,B}$	0.3559	0.3716	0.3819
$\Sigma_{a,B}$	5.6128-03	6.6964-03	6.1849-03
$\bar{\nu}\Sigma_{f,B}$	7.4604-04	9.6126-04	8.9408-04
$[\Sigma_{tr,B}(\Sigma_{a,B} - \bar{\nu}\Sigma_{f,B})]^{1/2}$	4.1618-02	4.6165-02	4.4951-02
$e^{-B_B t}$**	0.04	0.03	0.03
$B_{B,N}^{-1}$*	1.0	0.90	0.92
$\bar{\phi}^*_{B,N}$	1.0	0.86	0.94

† Calculated by ANISN with 26g σ-set and spherical blankets, all driven by a large oxide-fueled core

†† All units (where required) are cm^{-1}

* Relative values: $B_{B,N}^{-1} = [B_B^{-1}]/[B_B^{-1}]_{UO_2}$, $\bar{\phi}_{B,N} = \bar{\phi}_B/[\bar{\phi}_B]_{UO_2}$

** Blanket thickness, t, is 45 cm

$\frac{1}{B_B^2}$, and the average neutron flux in blanket is approximately proportional to B_B^{-1}, as is also shown in Table 3.5, i.e.

$$\bar{\phi}_B \propto B_B^{-1} \propto [\Sigma_{tr,B}(\Sigma_{a,B} - \nu\Sigma_{f,B})]^{-1/2} \tag{3.24}$$

This observation is also valid for a spherical blanket.

In conclusion, a high fuel density and the relative absence of neutron moderation decreases both the average neutron flux and the average microscopic fission cross-section of U-238, hence the total fission rate in the blanket is not linearly proportional to fuel density.

Combining Eqs. (3.19) and (3.24) and assuming constant microscopic cross-sections, one has, very crudely

$$F_B \propto [N_B^{28}]^{1/2} \tag{3.25}$$

where we also assume that all neutrons are absorbed and removed by U-238.

Table 3.6 verifies Eq. (3.24) and shows that the total fission rate in a fresh blanket is approximately proportional to $[N_B^{28}]^{1/2}$.

3.3.4 Neutron Loss by Parasitic Absorption and Neutron Leakage into the Reflector ($A_B^{P,L,C}$)

In a blanket, neutrons are consumed by absorption in U-238, absorption in blanket materials other than U-238, and neutron leakage into the reflector region. In previous sections, it was shown that a high neutron fission rate in the blanket could not be expected without increasing the U-238 density because the neutron leakage rate from the core and the fission cross-section of U-238 remains constant.

TABLE 3.6

COMPARISON OF NEUTRON FISSION RATE AND

FERTILE DENSITY FOR OXIDE, CARBIDE AND Ti-ALLOY

	UO_2	UC	U_2Ti
F_B†	1.44619 + 05	1.60267 + 05	1.62119 + 05
$F^*_{B,N}$	1.0	1.108	1.121
$[N_B^{28}]^{1/2}$†	0.1080	0.1251	0.1292
$[N_B^{28}]_N^{1/2}$*	1.0	1.158	1.196

†F_B is in Reactions/sec, N_B^{28} is in atoms/barn-cm

*$F_{B,N} = F_B/[F_B]_{UO_2}$, $[N_B^{28}]_N^{1/2} = [N_B^{28}]^{1/2}/[N_B^{28}]_{UO_2}^{1/2}$

In addition to increasing the fuel density, an alternative approach to improvement of the external breeding ratio is to lower parasitic absorption and leakage losses. Typical macroscopic absorption and fission cross-sections for blanket materials are shown in Table 3.7.

Parasitic neutron absorption consumes only 10% of the total available neutrons, and 4% of all neutrons are lost by neutron leakage.

The four main materials which absorb neutrons in a blanket are U-238, U-235, metallic fuel constituents (T_i, M_o etc.) and Iron in structural materials. Neutron absorptions by U-238 and U-235 are directly related to the blanket breeding function, hence to improve external breeding we should

a. reduce the volume fraction of structural material,

b. select structuralmaterials which have low neutron absorption cross-sections,

c. avoid metal-alloy fuel.

As shown in Table 3.7, T_i in U_2T_i fuel absorbs 3% of the total available neutrons, while oxygen and carbon consumes almost no neutrons, hence a metal alloy fueled blanket has a lower external breeding ratio than a carbide fueled blanket even though U_2T_i has the highest fuel density. Design of the fuel clad and the fuel assembly - choice of a material, its dimensions, etc. - is also closely related to reactor safety, reliability and heat transfer problems which should be resolved before focussing on just the breeding capability.

Since low parasitic absorption is paramount, selection of the fuel material is an extremely important task, and oxide, carbide and metal fuels (pure U or Th fuel) are by elimination almost the only favorable

TABLE 3.7

SPECTRUM AND SPACE-WEIGHTED MACROSCOPIC ABSORPTION AND FISSION CROSS-SECTIONS FOR BLANKET MATERIALS

	UO_2	UC	U_2Ti
$\Sigma^{28}_{a,B}$	4.8619 - 03	5.9973 - 03	5.3057 - 03
$\Sigma^{25}_{a,B}$	1.2501 - 04	1.4619 - 04	1.2070 - 04
$\Sigma^{O}_{a,B}$	6.7033 - 06	-	-
$\Sigma^{C}_{a,B}$	-	2.1016 - 08	-
$\Sigma^{Ti}_{a,B}$	-	-	1.7775 - 04
$[\Sigma^{Fuel}_{a,B}]$	4.9935 - 03	6.1435 - 03	5.6042 - 03
$\Sigma^{Fe}_{a,B}$	3.0495 - 04	2.8451 - 04	2.5293 - 04
$\Sigma^{Cr}_{a,B}$	4.7955 - 05	4.3167 - 05	3.6393 - 05
$\Sigma^{Ni}_{a,B}$	4.3843 - 05	4.1630 - 05	3.5764 - 05
$\Sigma^{Na}_{a,B}$	2.6496 - 05	2.4450 - 05	1.9106 - 05
$[\Sigma^{steel}_{a,B}]$	4.2324 - 04	3.9377 - 04	3.4420 - 04
$\nu\Sigma^{28}_{f,B}$	5.3903 - 04	7.1490 - 04	6.8269 - 04
$\nu\Sigma^{28}_{f,B}$	2.0697 - 04	2.4633 - 04	2.1136 - 04
$[\nu\Sigma_{f,B}]$	7.4601 - 04	9.5900 - 04	8.9405 - 04
$\frac{\Sigma^{28}_{a,B}}{\Sigma_{a,B}}$	0.8976	0.9174	0.8919

continued on next page

	UO_2	UC	U_2Ti
$\frac{\Sigma^{28}_{a,B}}{\Sigma^{steel}_{a,B}}$	11.4873	15.2305	15.4146
$\bar{\phi}_B V_B$	5.21175 + 08	4.50135 + 08	4.91115 + 08
bx	0.35043	0.37500	0.36053

*All cross-sections are in cm^{-1}

choices open to blanket designers. In Appendix B.2, one-group LMFBR cross-sections are displayed, in which we can find that Nitrogen, Molybdenum, Silicon, and all possible metallic elements for metal alloy fuel have higher absorption cross-sections than that of Titanium (Ti). Thus all metal-alloy fuels and nitride fuels suffer from high parasitic absorption.

Neutron loss by leakage into the reflector region, which amounts of roughly 4% of total neutrons for a 45 cm thick blanket, is dependent upon blanket thickness, blanket diffusion coefficient and reflector albedo as shown in Equation (3.14).

The determination of an optimum blanket thickness is influenced by fuel cycle cost considerations in addition to blanket neutronic efficiency, a point which is considered in more detail in Section 4.3.

The blanket diffusion coefficient, D_B is a function of the blanket transport cross-section, $\Sigma_{tr,B}$, pertinent values of which are listed in Table 3.2. The variation of the transport cross-section is so small that for fixed blanket thickness we can not expect large reductions of neutron losses.

For thick ($e^{-B_B t} \cong 0$) blankets, the neutron flux near the outside of the blanket is very small, and the practical effects of reflector properties are also negligible.

From Equation (3.10), the sensitivity coefficient of parasitic absorption and neutron leakage to external blanket breeding ratio, $\lambda^{b_x}_{A^{P,L,C}_B}$, is

$$\lambda^{b_x}_{A_B^{P,L,C}} \frac{\frac{\Delta b_x}{bx}}{\frac{\Delta A_B^{P,L,C}}{A_B^{P,L,C}}} = [1 + \frac{L_c}{(\bar{\nu}-1)F_B} - \frac{A_B^{P,L,C}}{(\bar{\nu}-1)F_B}]^{-1} \cdot \frac{A_B^{P,L,C}}{(\bar{\nu}-1)F_B}$$

$$=\lambda^{b_x}_{F_B} \cdot \frac{A_B^{P,L,C}}{(\bar{\nu}-1)F_B} \qquad (3.26)$$

Inserting the reference values shown in Table 3.1, the $\lambda^{b_x}_{A_B^{P,L,C}}$'s are

$$\lambda^{b_x}_{A_B^{P,L,C}} = 0.1410 \text{ (for oxide fuel)}$$

$$= 0.1025 \text{ (for carbide fuel)}$$

$$= 0.1563 \text{ (for Ti-alloy fuel)} \qquad (3.27)$$

Carbide fuel has the lowest parasitic and leakage loss, hence the sensitivity coefficient for carbide fuel is the lowest. Ti-alloy fuel has the highest sensitivity. Here we should note that $\lambda^{b_x}_{A_B^{P,L,C}}$ of oxide and Ti-alloy are higher than $\lambda^{b_x}_{F_B}$ of oxide and Ti-alloy respectively, while for carbide fuel the coefficients are very nearly the same.

The data embodied in Eqs. (3.27) also indicates that only small improvements in breeding ratio are possible through reductions in parasitic absorption.

In summary, a high heavy metal density and a low absorption cross-section for the non-fertile fuel constuents are important if one is to reduce the parasitic absorption in the blanket, and thereby to improve (however slightly the opportunity may be) the external breeding ratio.

3.4 EVALUATION OF BLANKET DESIGN PARAMETERS FOR EXTERNAL FISSILE BREEDING

3.4.1 Fuel Density

High fertile density is perhaps the single most important parameter as far as achieving a high external breeding ratio is concerned. However, as we found in the previous section, a high fuel density reduces the average neutron flux in the blanket, and the overall effect on fertile breeding is seriously reduced. The advantages of high fuel density are:

a. reduction of the relative amount of parasitic absorption because of the high neutron absorption capability of U-238 (assuming that the volume fraction of structural material is fixed).

b. a slight increase in the number of fission reactions, which increases the number of available neutrons slightly.

In Appendix B.1, it is shown that the neutron flux in the blanket is well-represented by a simple exponential function, a result confirmed by both multi-group calculations and experimental data.

The average neutron flux, $\bar{\phi}_B$, is given by Eq. (3.22). Therefore, the integral capture rate of U-238 is

$$C_B^{28} = \Sigma_{C,B}^{28}\, \bar{\phi}_B\, V_B = \Sigma_{C,B}^{28} \cdot \left(\frac{k_1}{B_B}\right) \cdot \left(1 - e^{-B_B t}\right) \qquad (3.28)$$

where k_1 is a constant, t is the blanket thickness and the term containing B_B^{-2} has been neglected.

Assuming U-238 and U-235 (and or Pu-239) dominates the neutron balance and transport-related interactions, the blanket buckling can be rewritten as

$$B_B^2 = [3\Sigma_{tr,B}(\Sigma_{a,B} - \bar{\nu}\Sigma_{f,B})]$$

$$\cong [3N_{28,B}(\sigma_{tr,B}^{28} + \frac{\varepsilon_B}{1-\varepsilon_B}\sigma_{tr,B}^{25}) \cdot N_{28,B}\{(\sigma_{a,B}^{28} + \frac{\varepsilon_B}{1-\varepsilon_B}\sigma_{a,B}^{25})$$

$$- (\nu\sigma_{f,B}^{28} + \frac{\varepsilon_B}{1-\varepsilon_B} \cdot \nu\sigma_{f,B}^{25})\}] \qquad (3.29)$$

where ε_B is the blanket enrichment.

Now the integral capture rate of U-238 is:

$$C_B^{28} = k_1 \cdot k_2 \cdot (1 - e^{-k_3 N_{28,B}}) \qquad (3.30)$$

where

$$k_2 = \frac{\sigma_{C,B}^{28}}{[3(\sigma_{tr,B}^{28} + \frac{\varepsilon_B}{1-\varepsilon_B}\sigma_{tr,B}^{25})\{(\sigma_{a,B}^{28} + \frac{\varepsilon_B}{1-\varepsilon_B}\sigma_{a,B}^{25}) - (\nu\sigma_{f,B}^{28} + \frac{\varepsilon_B}{1-\varepsilon_B} \cdot \nu\sigma_{f,B}^{25})\}]^{1/2}} \qquad (3.31)$$

$$k_3 = \frac{t}{k_2} \cdot \sigma_{c,B}^{28} \qquad (3.32)$$

The sensitivity coefficient for C_B^{28}, $\lambda_{N_{28}}^{C_B^{28}}$, can be derived from Eq. (3.30):

$$\lambda_{N_{28}}^{C_B^{28}} \equiv \frac{\frac{\Delta C_B^{28}}{C_B^{28}}}{\frac{\Delta N_{28}}{N_{28}}} = \frac{\theta}{e^{\theta}-1} \qquad (3.33)$$

where

$$\theta = k_3 N_{28,B}$$

If we neglect fission reactions in the blanket, $\bar{\nu}\Sigma_{f.B}$, and neutron absorption by U-235, θ reduces to

$$\theta = [3 \sigma^{28}_{tr,B} \cdot \sigma^{28}_{a,B}]^{1/2} N_{28,B} \cdot t \tag{3.34}$$

In this limiting case the external breeding ratio is proportional to the neutron capture rate in U-238, and the fractional change in the external breeding ratio, $\frac{\Delta bx}{bx}$, is:

$$\frac{\Delta bx}{bx} = \frac{\theta}{e^{\theta} - 1} \left(\frac{\Delta N_{28,B}}{N_{28,B}}\right) \tag{3.35}$$

For a thick blanket, where t is very large and hence e^{θ} is a dominant term, the variation of the external breeding ratio with fertile density is very small.

Table 3.8 shows the variation of the external breeding ratio and related parameters as fertile density is varied by changing either the density or composition of the fuel ceramic material. If there are no significant absorbing materials present except for U-238, Eq.'s (3.34) and (3.35) provide a useful approximation for evaluating changes on the external breeding ratio, and agreement between Eq. (3.35) and the multigroup results summarized in Table 3.8 is rather good.

TABLE 3.8

VARIATION OF EXTERNAL BREEDING RATIO AS HEAVY METAL DENSITY IS CHANGED

Parameters	Units	UO_2			UC
T.D.	%	96.5	80	65	96.5
$N_{28,B}$	$\frac{\text{atoms}}{\text{barn-cm}}$	1.1664 - 02	9.6696 - 03	7.8566 - 03	1.5665 - 02
θ*	-	1.929315	1.610387	1.319193	2.454809
$\frac{\theta}{e^{\theta}-1} \equiv \lambda$	-	0.3278475	0.402120	0.481387	0.230624
$\lambda \frac{\Delta N_{28,B}}{N_{28,B}}$**	$(\approx \frac{\Delta bx}{bx})$	0.0	-0.03	-0.16	0.08
$\frac{\Delta bx}{bx}$***	-	0.0	-0.04	-0.11	0.07

* $\theta = [3\sigma^{28}_{a,B} \quad \sigma^{28}_{tr,B}]^{1/2} \; N_{28,B} \; t$, t = 45 cm

** $N_{28,B}$ (reference) = $N_{28,B}$ (UO_2 - 96.5% T.D.)

*** bx (reference) = bx (UO_2 - 96.5% T.D.) calculated by ANISN code

3.4.2 Blanket Thickness and Neutronic Blanket Efficiency (E_B)

Blanket neutronic efficiency, E_B, defined here as the ratio of consumed neutrons to total available neutrons in the blanket, is a function of blanket thickness, t.

From Eq. (3.22), the blanket neutronic efficiency, E_B, can be defined as

$$E_B = \frac{\bar{\phi}_B(t)}{\bar{\phi}_B(\infty)} = (1 - e^{-B_B t}) \tag{3.36}$$

Thus, the neutronic blanket thickness, t, in contrast to the economic blanket thickness (expressed by Eq. (4.35), in the next chapter) is given by

$$t = \frac{1}{B_B} \ln [1 - E_B] \tag{3.37}$$

We should note that there is little further improvement of blanket efficiency with increasing thickness, beyond a certain range.

The effect of blanket thickness on external fissile breeding is easily found from Eq. (3.30), namely:

$$\frac{\Delta bx}{bx} = \frac{\theta}{e^{\theta} - 1} (\frac{\Delta t}{t}) \tag{3.38}$$

which has the same sensitivity coefficient for bx,

$$\lambda_t^{bx} \equiv (\Delta bx/bx)/(\Delta t/t) \doteq \frac{\theta}{e\theta - 1}, \text{ as does fuel density.}$$

This should not be a totally unexpected result since we are accustomed to measuring effective thickness of both neutral and charged particle attenuations in terms of the mass per unit surface area intercepting the incident particle current and mass/area $\cong$ density x thickness.

The relationship between blanket thickness, t, and the pertinent economic parameters is simply derived by the combination of Eqs. (3.37) and (4.35).

From Eqs. (4.35) and (3.22),

$$k_4 \quad (1 - e^{-B_B t}) \geq 4 \, \bar{\omega} r_4 \tag{3.39}$$

where

$$k_4 = \frac{2\sigma^{28}_{c,B}\phi_o}{S_B} \left[\frac{a+t}{B_B} + \frac{1}{B_B^2}\right] \cong \frac{2\sigma^{28}_{c,B}\phi_o}{B_B \, t} \tag{3.40}$$

and $\bar{\omega}$ and r_4 are defined in Section 4.3.2, and determined by the economic and financial parameters.

Rearranging Eq. (3.39) for the blanket thickness, one obtains;

$$t \leq \frac{2(1 - 2\bar{\omega} r_4/\sigma^{28}_{c,B}\phi_o)}{B_B} \tag{3.41}$$

which indicates, among other things, that the maximum Pu buildup rate, $\sigma^{28}_{c,B}\phi_o$, should be larger than $2\bar{\omega} r_4$ for the existence of economic blankets of any thickness.

3.4.3 Blanket Enrichment

A main function of the FBR blanket is fissile breeding using neutrons leaking from the core, while power production in blanket is a secondary and concomitant function. Therefore, blanket enrichment is not generally considered a particularly important factor to designers except as it complicates matching blanket power to flow over life. However since blanket breeding capability depends on a high neutron availability, a superficially attractive design option capable of increasing neutron generation in the blanket is fissile seeding, that is, use of enriched fuel in the blanket. This alternative will be evaluated in Chapter 5. However, we can expect that for a fixed core design a high fissile loading in the blanket region reduces core power, and also the neutron leakage rate into the blanket, and hence the external breeding ratio will have suffered a compensatory loss. Without totally prejudging this idea we also note Tzanos' findings (T4) that the maximum breeding ratio is achieved by concentrating all fissile material in the core region, and also the common observation that at end-of-life a blanket has "enriched itself" to ∿4% plutonium content, but without notable benefit to the system breeding ratio relative to BOL.

Thus we will proceed at this point to assume that small variations of enrichment do not change the blanket characteristics significantly. In the review of Eq. (3.29), transport, absorption and fission cross-section of U-235 are related to those of U-238 by the factor of $\frac{\varepsilon_B}{1 - \varepsilon_B}$ ($\approx$ 0.02). The ratio of the transport and absorption cross-sections of U-235 to those of U-238 is ∿1.33 and ∿12.83, respectively, hence the fission ($\frac{\sigma_{f,B}^{25}}{\sigma_{f,B}^{28}}$ = 220) reaction of U-235 is relatively important when the enrichment is increased. However the most important reactions in the blanket with respect to fissile breeding are the neutron transport and absorption reactions, because most available neutrons leak in from the core regions, and fission-produced neutrons in the blankets are of considerably less consequence. Therefore, a small variation in enrichment does not affect the external breeding function appreciably. However, heterogeneous fissile seeding of the blanket region involves many complex effects, and can improve the external breeding ratio very slightly, as will be shown in Chapter 5.

3.4.4 Selection of Optimum Blanket Thickness and Fuel Density

As discussed in previous sections, the sensitivity coefficients for fuel density and blanket thickness of the external breeding ratio are both expressed by $\theta/(e^{\theta} - 1)$, which is sharply decreased as θ increases. This means that further increasing blanket thickness or fuel density beyond an effective optimum value does not change the external breeding ratio significantly. Thus we may determine an optimum value of fuel density or blanket thickness. However, as shown in Eq. (3.41), blanket thickness is also a function of economic/financial parameters, and variation of the blanket thickness in a continuous manner is for all practical purposes precluded by the fixed size of individual fuel assemblies and the number of assembly rows allotted to the blanket. Therefore the only one of this pair of design parameters which will change continuously, is the fuel density. Now if we set an acceptable minimum value for the sensitivity coefficient, λ_{min}, by the considerations of the economic/material/heat transfer aspects, the optimum fuel density will be calculated directly from Eq. (3.38), i.e.;

1. From $\lambda_{min} = (\frac{\theta}{e^{\theta} - 1})_{min}$, calculate the value of θ,

2. Assuming constant microscopic cross-sections, and blanket thickness, $(N_{28,B})_{op}$ can be calculated from Eq. (3.34) and the value of θ.

The selection of λ_{min} is, of course, a designer's choice by the consideration of fuel material and economic parameters. Table 3.9 shows the optimum U-238 concentration (density of U-238) as a function of blanket thickness, t, and λ_{min} for oxide and carbide fuel. If we choose 20% for the sensitivity coefficient (i.e., the variation of fractional external breeding ratio $(\frac{\Delta bx}{bx})$ is 20% of the total change of fertile density) and 45cm for the blanket thickness, the optimum U-238 density is 0.0162 atoms/barn-cm, which corresponds to carbide fuel at 100% T.D. and 50% fuel volume fraction in the blanket. Under these conditions, therefore, the higher U-density achievable with metal fuel is not necessary.

3.5 EFFECT OF NON-LINEAR FISSILE BUILDUP ON EXTERNAL FISSILE BREEDING

In most of the preceding analysis external breeding ratios were estimated using beginning-of-life (BOL) blanket parameters under the assumption of linear fissile buildup as a function of time. As will be discussed in more detail in section 4.2 of the following chapter, the non-linear dependence of the fissile buildup rate should be considered when accuracy is a paramount consideration.

Here we define the "exact" (time-averaged) external breeding ratio, $\overline{bx}$ as

TABLE 3.9

OPTIMUM U-238 CONCENTRATION, $(N_{28,B})_{op}$, AS A FUNCTION OF BLANKET THICKNESS AND THE MINIMUM SENSITIVITY COEFFICIENT†

Thickness / λ^*_{min}	one-row blanket t = 15 cm	two-row blanket t = 30 cm	three-row blanket t = 45 cm
$\lambda_{min} = 0.05$	0.0836	0.0418	0.0279
$\lambda_{min} = 0.0$	0.0670	0.0335	0.0223
$\lambda_{min} = 0.2$	0.0485	0.0243	0.0162
$\lambda_{min} = 0.3$	0.0381	0.0191	0.0127

† $[3\sigma^{28}_{a,B}\ \sigma^{28}_{tr,B}]^{1/2} = 3.6$

$*\lambda_{min} \equiv \left(\frac{\theta}{e^{\theta}-1}\right)_{min}$ where $\theta = [3\sigma^{28}_{a,B}\ \sigma^{28}_{tr,B}]^{1/2} \cdot N_{28,B} \cdot t$

For comparison note that:

$$N_{28} = \begin{cases} 0.0122 \text{ for } UO_2 \text{ at 100\% T.D. and 50\% fuel volume fraction} \\ 0.0164 \text{ for UC at 100\% T.D. and 50\% fuel volume fraction} \\ 0.0173 \text{ for } U_2Ti \text{ at 100\% T.D. and 50\% fuel volume fraction} \end{cases}$$

Values shown in table are volume-averaged, hence are directly comparable.

$$\bar{b}x \equiv \frac{(\text{Fissile Inventory at EOL - Fissile Inventory at BOL})_{\text{Blanket}}}{(\text{Average Fissile Consumption Rate in Core and Blanket})}$$

$$\cdot \frac{1}{(\text{Total Irradiation Time})} \qquad (3.42)$$

Using results which are developed in Chapter 4, i.e.,

a. $\text{Fissile Inventory at EOL}\Big|_{\text{blanket}} = M_{28}(0) S_o T_{op} e^{-\xi \frac{T_{op}}{T_c^\circ}}$

(see Eq. (4.40) for details)

b. $\text{Fissile Inventory at BOL}\Big|_{\text{blanket}} \cong 0,$

c. ξ and $\frac{T_{op}}{T_c^\circ}$ are nearly constant at 2/3 and 0.4 respectively,

(see Table 4.6 for details)

the "exact" external breeding ratio can be rewritten as

$$\bar{b}x = \frac{1}{\bar{M}_a^{\text{fissile}}} [M_{28}(0) \cdot \sigma_{c,B}^{28} \cdot \bar{\phi}_B] \, e^{-\xi \frac{T_{op}}{T_c^\circ}}$$

$$= bx \cdot e^{-\xi \frac{T_{op}}{T_c^\circ}}$$

$$\cong 0.766 \; bx \qquad (3.43)$$

Equation (3.43) indicates that the external breeding ratio calculated using BOL parameters is overestimated by slightly over 20% due to the assumption of a linear fissile buildup time history. However, Eq. (3.43) also indicates that the "exact" time-averaged external breeding ratios of various blankets having different optimum irradiation times are directly proportional to external breeding ratios calculated using BOL blanket parameters. Since the constant of proportionality is the same for all cases, one can use BOL studies to correctly rank the breeding performance of various blanket design options - one should not however use these relative bx values to compute actual reactor fuel cycle material balances, doubling times, etc.

3.6 SUMMARY

The fissile breeding capability of FBR blankets has been reviewed, and the factors and design parameters which affect external fissile breeding have been evaluated in this chapter.

The first point established is that external fissile breeding is primarily determined by neutron leakage from high power density cores, which makes improvement of the external breeding ratio a very difficult task. Since the incident neutron spectrum and total number of available neutrons in blanket region are essentially determined by the core design, low parasitic absorption in the blanket is the most important prerequisite for a higher external breeding ratio. This can be established by the use of high fertile fuel density and the removal of neutron absorbing material wherever possible.

The choice of blanket thickness is related to economic and financial parameters. The relationship between blanket thickness and these parameters has been developed in this chapter. It is shown that one basically must interpose a certain fertile mass loading per unit surface area to achieve a given performance standard.

The effect of blanket fuel density on the external breeding ratio and the determination of an optimum fuel density were also discussed. The analysis showed that high fuel density reduced the parasitic absorption and increased the fission reactions in blanket; and while it reduced the average neutron flux the net result was a slight improvement of the external breeding ratio.

In most parts of this chapter, all analyses were carried out using BOL parameters. The non-linear fissile buildup time history was considered in the final section and it was shown that the BOL external breeding ratio should be corrected by a constant to obtain a valid quantitative estimate of the external breeding ratio averaged over life.

Constant (energy independent) cross-sections were assumed for analysis. The effects of the variation of cross-sections will be estimated in Section 5.2 of Chapter 5.

CHAPTER 4

FUEL DEPLETION AND ECONOMIC ANALYSIS OF FBR BLANKETS

4.1 INTRODUCTION

In the preceding chapters, fissile breeding capabilities in FBR blanket regions were analyzed in detail. However, the primary objective of utility management is not in determining material inventories per se, but in estimating their economic contribution to power generating costs.

In this chapter, simple but accurate fuel depletion models will be developed and employed to evaluate fuel management decisions and to assess the fuel cycle cost contribution of the blanket to the overall power generating cost.

The first section of this chapter is devoted to development of simple, generalized correlations for fissile buildup histories in FBR blankets. This is essential since the analysis of fuel cycle costs requires fuel discharge compositions as a function of irradiation time and fuel position in the blanket. It was found that conventional flux-time correlation methods, which have been recently revived as a useful candidate for FBR applications (S3), could be adapted for this purpose and can establish an FBR fuel depletion model suitable for fuel economic analysis and sensitivity studies.

In the following sections, parametric studies and optimization of parameters governing blanket fuel management decisions will be carried out using simple correlations developed in this initial section. The results are carefully examined using state-of-the-art computer calculations.

Finally, blanket fuel management schemes will be reviewed and the effects of management options on blanket economics will be evaluated.

4.2 GENERALIZED FISSILE MATERIAL BUILDUP HISTORIES FOR FBR BLANKETS

4.2.1 Introduction

The main objective of this section is to develop a simple FBR fuel depletion model for fuel economic analysis and sensitivity studies without expensive computer calculations.

For simple neutronic/economic analyses, a linear fissile buildup approximation has been adopted in some previous work. (K2)(T1) However, Bruyer has shown that the linear buildup approximation can incur appreciable error for fuel depletion and economic calculations in the radial blanket region of a fast reactor. (B1)

Several recent studies have been concerned with the development of accurate methods for fuel depletion calculations which rely upon conventional multi-group time step techniques (L4)(H3) or non-linear perturbation techniques. (S2)(M1) In practice, the fuel discharge composition is a function of both the spectrum and the magnitude of the regional neutron flux, and these neutronic characteristics of the blanket change with the irradiation time due to the relatively large buildup of fissile materials.

Conventional time step depletion calculations are characterized by successive neutron balances and nuclide depletion calculations. The single largest expenditure of computer time is for calculation of a detailed neutron balance, which when normalized to a specified total core power, yields local neutron flux spectra, hence reaction rates, at a given irradiation time. Such calculations are currently performed by the relatively expensive computer programs such as 2DB, (L3) PHENIX, (H2) REBUS, (H4) CITATIØN, (F3) or PDQ.(C1)

Recently, a simpler method based on a non-linear perturbation technique has been developed by Becker (S2) and Masterson (M1) to express the material concentrations analytically and to correlate spectrum-averaged cross-sections with composition for non-linear time-dependent fuel cycle problems. Nodal point concentrations of certain materials are calculated by combining sensitivity parameters. This method apparently avoids the large expenditure of computer time needed to calculate the neutron balance at each time step. However, the complicated correlations involved still require generation of sensitivity parameters, which is an obstacle to widespread use of this approach for fuel cycle analysis.

Brewer (B4) employed a "Semi-Analytic Depletion Method (SAM)" and applied it for the breeding/economic analysis of FBR blankets. This method is based on the assumptions of constant local flux and neutron spectrum, which, while suitable for the core, may be questionable for the blankets due to the large changes in fissile material composition in the blanket.

Bruyer (B6) assumed the experimental time-dependent enrichment in the blankets to be given and proceeded to carry out approximate depletion/ economic calculations, which were demonstrated to be of satisfactory accuracy using illustrative numerical examples.

In review of the partial successes of the prior work referenced above and the fact that practical engineering constraints, such as limitation of refueling to 6, 12 or 18 month intervals, relaxes the degree of accuracy required in estimation of optimum refueling dates, it was considered that a suitable simple model combining both the neutronic and the economic aspects of FBR performance could be synthesized.

As will be seen in the present work, a conventional flux-time correlation method proves to be useful for this purpose.

4.2.2 Derivation of Simple Correlation Equation for Fissile Material Buildup Characteristics

To simplify the derivation, the following assumptions were adopted.

1. In a FBR blanket, consideration can be limited to Pu-239 and U-238 as the representative fissile and fertile species, and Pu-241 buildup or U-235 burnout can be neglected.

2. The local or zone-averaged neutron flux can be considered constant throughout the irradiation life of the fuel in a given location.

3. The local or zone-averaged neutron spectrum does not vary with irradiation time. Hence, spectrum-weighted cross-sections are constant.

The first assumption is valid for all cases of practical interest while the others are valid only for small time intervals. In the next section, the effects of these assumptions are estimated and corrected for.

The differential equation governing nuclide depletion can be rewritten on a mass basis for a given zone of the blanket (ignoring the mass difference per mole of U-238 and Pu-239):

$$\frac{dM_{49}}{dt} = M_{28}\bar{\sigma}_c^{28}\bar{\phi} - M_{49}\bar{\sigma}_a^{49}\bar{\phi} \tag{4.1}$$

and

$$\frac{dM_{28}}{dt} = - M_{28}\bar{\sigma}_a^{28}\bar{\phi} \tag{4.2}$$

Inserting the solution of Eq. (4.2), $M_{28} = M_{28}(0)e^{-\bar{\sigma}_a^{28}\bar{\phi}t}$, into Eq. (4.1) and solving Eq. (4.1), one gets:

$$M_{49}(t) = \hat{M}_{49}\left(e^{-\bar{\sigma}_a^{28}\bar{\phi}t} - e^{-\bar{\sigma}_a^{49}\bar{\phi}t}\right) \tag{4.3}$$

Where $\hat{M}_{49}$ is the maximum fissile inventory achievable, related to the initial U-238 inventory, $M_{28}(0)$, by

$$\hat{M}_{49} = M_{28}(0) \frac{\bar{\sigma}_c^{28}}{\bar{\sigma}_a^{49} - \bar{\sigma}_a^{28}} \tag{4.4}$$

By series expansion of the exponential function, and dropping the negligible terms (> order 2):

$$e^{-at} \cong 1 - at + (at)^2/2 \tag{4.5}$$

$$\text{if } a \ll 1$$

Eq. (4.3) can be changed into a particularly useful form:

$$\frac{M_{49}(t)}{\hat{M}_{49}} = \frac{t}{T_c} e^{-\xi_o \frac{t}{T_c}} \tag{4.6}$$

T_c is a characteristic time constant which can be calculated from reaction rates averaged over the zones in question:

$$T_c = (\bar{\sigma}_a^{49}\bar{\phi} - \bar{\sigma}_a^{28}\bar{\phi})^{-1} \tag{4.7}$$

while

$$\xi_o = 1/2 + [\hat{M}_{49}/M_{28}(0)](\bar{\sigma}_a^{28}/\bar{\sigma}_c^{28}) \tag{4.8}$$

Eq. (4.6) suggests that $M_{49}(t)/\hat{M}_{49}$ can be easily correlated against t/T_c.

4.2.3 Evaluation of Assumptions and Approximations

The simple dimensionless correlation, Eq. (4.6), was derived under three major assumptions, i.e., neglection of Pu-241 buildup, and constant σ's and ϕ's.

The assumptions of constant neutron flux and cross-sections produce opposing errors in calculation of blanket discharge fissile inventory, while the neglection of Pu-241 buildup leads to entirely negligible errors.

The effects of these assumptions were estimated by comparing results with 2DB burnup calculations. In this evaluation the batch fuel management option was employed because it is the most severe case in terms of local changes as a function of time.

In section 4.5, various other fuel management options will be evaluated.

Table 4.1 shows the Pu buildup and Uranium burnup characteristics

TABLE 4.1

PU BUILDUP AND U BURNUP CHARACTERISTICS
OF REPRESENTATIVE RADIAL BLANKETS

Fuel Type	Time / Isotope	0d	300d	600d	1200d	2400d	3600d
UO_2	U-238	17,299	17,208	17,108	16,892	16,411	15,897
	Pu-239	0.0	83.727	167.97	328.18	604.4	817.5
	Pu-240	0.0	1.1317	4.4766	16.7193	56.307	105.58
	Pu-241	0.0	0.0263	0.19913	1.33416	7.2234	16.673
	Pu-242	0.0	0.0	0.00266	0.03730	0.42213	1.48914
UC	U-238	23,233	23,133	23,026	27,790	22,253	21,667
	Pu-239	0.0	92.004	184.85	365.32	694.0	967.4
	Pu-240	0.0	0.9763	3.8711	14.7657	52.293	102.65
	Pu-241	0.0	0.0159	0.12105	0.84219	4.9612	12.298
	Pu-242	0.0	0.0	0.00134	0.01943	0.24061	0.9191
U_2Ti	U-238	24,759	24,661	24,555	24,324	23,804	23,218
	Pu-239	0.0	91.05	182.98	363.77	699.5	989.2
	Pu-240	0.0	0.6946	2.7795	10.8776	40.407	83.271
	Pu-241	0.0	0.0080	0.06209	0.45191	2.8911	7.7788
	Pu-242	0.0	0.0	0.00056	0.00844	0.11309	0.46795

NOTE: (1) 3-row Radial Blankets; all driven by same core.

(2) Δt = 150 days, time step in depletion calculations

(3) All entries are in Kg of heavy metal

calculated by the 2DB burnup code for representative radial blankets on a 1000 MWe LMFBR. Near the optimum irradiation time, 1200 ∿ 2400 days, Pu-241 buildup is so small (∿0.05% of total heavy metal) that we can summarily neglect it in all cases. Uranium oxide fuel, with its softer neutron spectrum, sustained the highest Pu-241 and Pu-242 buildup rates, but the fraction of Pu-241 plus Pu-242 is still less than 1% of total plutonium. Therefore, neutron and power generation from Pu-241 and Pu-242 can be neglected.

Fig. 4.1 shows the variation of the constants used in Eq. (4.6) throughout the fuel life time.

Parameter ξ_o defined by

$$1/2 + \frac{\bar{\sigma}_a^{28}}{\bar{\sigma}_a^{49} - \bar{\sigma}_a^{28}} \quad \text{or} \quad \approx \quad 1/2 + \frac{\hat{M}_{49}}{M_{28}(0)}$$

does not vary significantly. For example, after 3600 full power days, ξ_o of the center row of the blanket increases by ∿5% over the initial (BOL) value. The average value of ξ_o, for a small region or for an entire blanket approaches 0.61, which can, therefore, be considered as a "universal" constant.

The other constants, $\hat{M}_{49}$ and T_c, change more rapidly throughout the irradiation time. T_c of the third row of the radial blanket is decreased by up to 50% of its BOL value at 3600 full power days. which can be attributed to the large increase in neutron flux in this region. Note however that this computation involved irradiation of the inner two blanket rows to beyond their optimum residence times, and also that the third row is at the limit of economic viability.

In all cases, the parameters characterizing the first row, which dominates the behavior of the entire blanket, change only slightly.

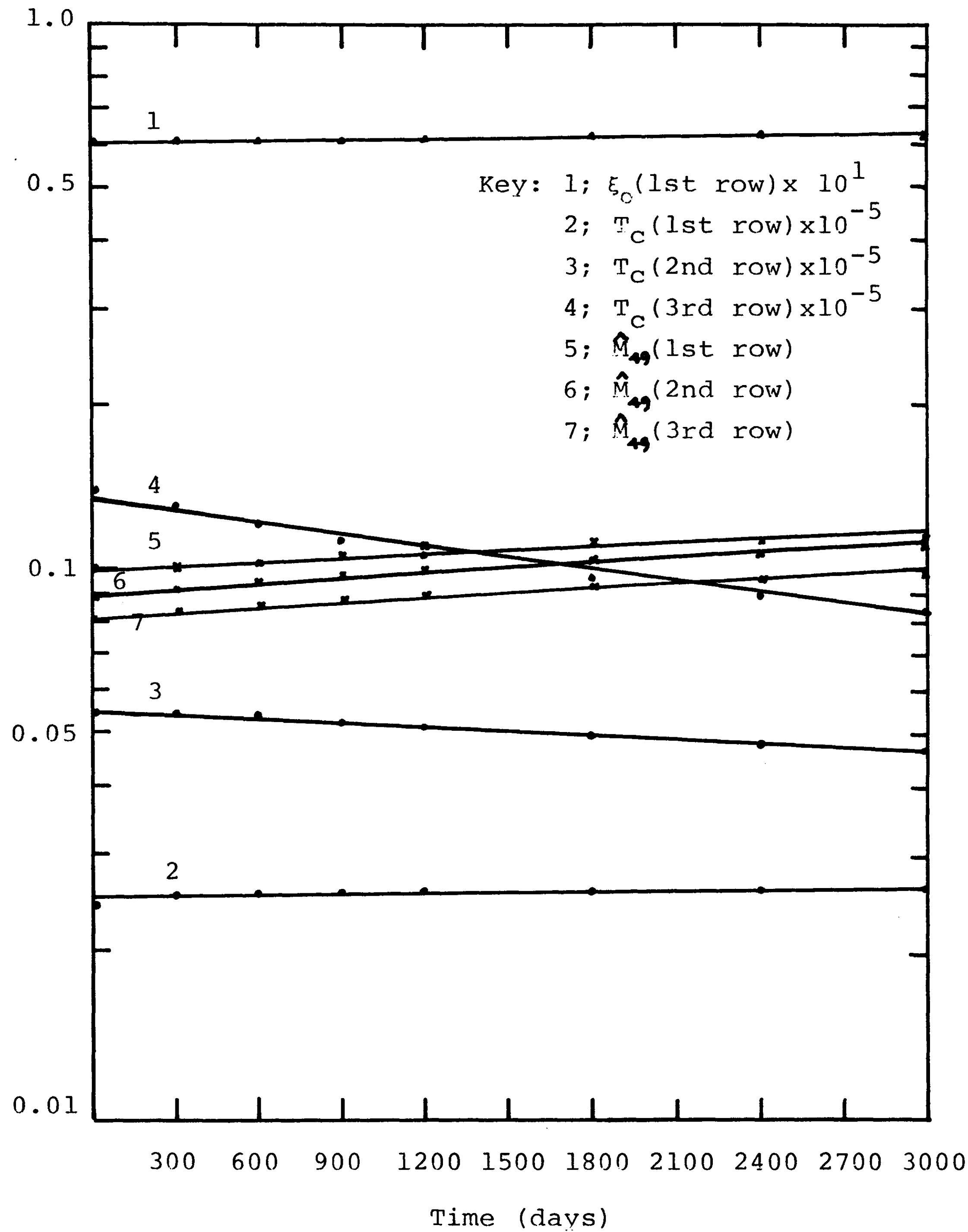

* UO_2 3-row Radial Blanket

Fig. 4.1 VARIATION OF T_c, $\hat{M}_{49}$ AND ξ_o WITH TIME (2DB)

4.2.4 Correction of Constants from BOL Parameters

Equation (4.6) is attractive for fuel cycle and fuel management studies because of its simplicity, its dimensionless form, and the fact that all parameters can be approximated by BOL computations.

The accuracy of Eq. (4.6) using only BOL parameters is obviously limited due to the variation of cross-sections and neutron flux as a function of time. However, empirical observations have shown that use of a corrected constant, ξ, instead of ξ_o can overcome this problem. As shown in Fig. 4.1, the parameters, $\hat{M}_{49}$ and T_c which appear in Equation (4.6) are exponential functions of time (i.e., they plot as straight lines on semi-log paper). From this observation:

$$\hat{M}_{49} = \hat{M}^{\circ}_{49}\ e^{at} \tag{4.9}$$

and

$$T_c = T^{\circ}_c\ e^{bt} \tag{4.10}$$

where a and b are the slopes of the lines shown in Fig. 4.1, and subscript o refers, as usual, to the constant value calculated from BOL parameters.

Combination of Eq. (4.9), (4.10) and (4.6) gives

$$\frac{M_{49}(t)}{\hat{M}^{\circ}_{49}} = \frac{t}{T^{\circ}_c}\ e^{-\xi \frac{t}{T^{\circ}_c}} \tag{4.11}$$

where ξ is the corrected constant which takes non-linear fissile buildup characteristics into account, defined by

$$\xi = \xi_o + (b - a)T_c^\circ \tag{4.12}$$

Equation (4.11) is the modified correlation which will be used henceforth to predict fuel composition over life from BOL static calculations or measurements. For extremely accurate calculations involving small regions, ξ should be individually determined on a case-by-case basis. However, our primary interests involve the analysis of the neutronic and economic behavior of the whole blanket, or the inner (1st and 2nd row) regions of blankets, because most breeding takes place closest to the core. Indeed it is still not clear that a third blanket row is economically competitive. Based on this point of view, we can readily justify selecting a "universal" constant ξ for all fuel materials and regions: our empirical finding is that ξ is $\sim$2/3 for all blankets of interest.

4.2.5 Applications of the Simple Correlation

Equation (4.11) has been derived from a set of general assumptions and corrected for flux-time variations. The applicability of this simple correlation was next demonstrated to hold for a wide variety of blanket compositions and configurations including:

a. Blanket zones of various sizes; from single pins or assemblies to group of assemblies, or to an entire blanket.

b. Axial, radial, and internal blankets.

c. One to several-row-thick radial blankets with steel or moderating reflectors.

d. Oxide, carbide, and metal alloy fueled blankets.

e. Both U-238/Pu-239 and Th-232/U-233 fuel cycles.

Furthermore, based on Ref. (T1) and (K2), we can anticipate that these results will apply to fuel-managed blankets and to blankets driven by cores of all sizes (thermal ratings) of commercial interest. Likewise, the results should apply to GCFR systems.

Fig. 4.2 shows a selection of representative data points from categories (a) through (e) above, calculated using state-of-the-art physics depletion methods (2DB and 4 group σ-sets). The correlation with $\xi = 2/3$ is excellent: all points fall very nearly on the curve defined by Eq. (4.11). Therefore, we have shown that BOL-based comparisons can correctly rank blankets as to fissile production capability over their entire burnup life-time.

Table 4.2 shows a representative comparison of correlated and exact fissile buildup histories for three radial blankets of widely different fuel composition. Again the agreement is good; indeed some of the discrepancy can be attributed to the finite time-step size employed in the burnup code rather than to the correlation.

The preceding results, moreover, are in a form directly usable in the comprehensive economics model developed in the next section, which permits calculation of breakeven and optimum irradiation times in a specified economic environment given the neutronic information embodied in Equation (4.11).

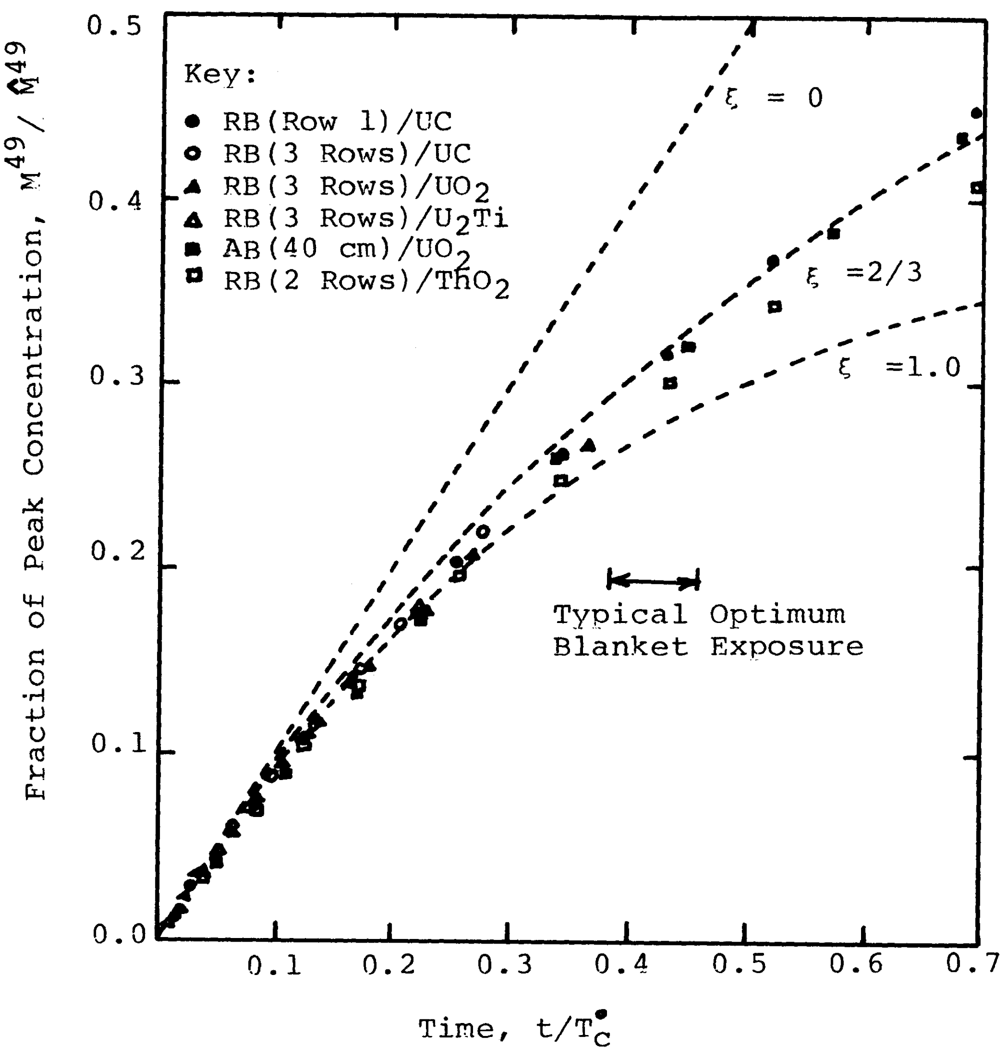

Fig. 4.2 DIMENSIONLESS CORRELATION OF FBR BLANKET BREEDING PERFORMANCE

TABLE 4.2

COMPARISON OF CORRELATED AND EXACT FISSILE BUILDUP HSITORIES*

$M_{49}/\hat{M}_{49}$

FUEL TYPE	UO_2			UC			U_2Ti		
Days	Cal.**	2DB	Δ (%)	Cal.**	2DB	Δ (%)	Cal.**	2DB	Δ (%)
300	0.0597	0.0513	16.4	0.0447	0.0391	14.3	0.0384	0.0342	12.3
900	0.1648	0.1530	7.8	0.1261	0.1175	7.3	0.1092	0.1029	6.1
1800	0.2911	0.2909	0.1	0.2299	0.2283	0.7	0.2019	0.2015	0.2
2400	0.3572	0.3702	-3.5	0.2883	0.2951	-2.3	0.2555	0.2626	-2.7

*3-row radial blankets, all driven by same equilibrium core

**value used for ξ is 2/3; calculated ξ from BOL parameters is ~ 0.6

We should also point out that Equation (4.11) can be reformulated in terms of enrichment:

$$\varepsilon(t) \equiv \frac{M_{49}(t)}{M_{28}(0)} = [\xi_o - \frac{1}{2}] \frac{t}{T_c^o} e^{-\xi \frac{t}{T_c^o}} \quad (4.13)$$

Also, an entirely parallel and equally successful treatment can be applied to correlate higher isotope concentrations. These results are displayed in Appendix C.1. From these simple correlations, useful isotope correlation equations (ICE) are generated and used to predict heavy isotope concentrations in Appendix C.1.

4.3 OPTIMUM ECONOMIC PARAMETERS FOR FBR BLANKETS

4.3.1 Introduction

Work to determine optimum blanket economic parameters has been carried out by Ketabi, Bruyer, and Driscoll (K2), (B6) at MIT and by Y. Furuhashi (F4) in Japan. The present study follows, and improves upon, the methods and procedures for prediction of optimum blanket parameters initiated by Ketabi and Driscoll.

In this study the optimum blanket parameters of concern are the optimum and breakeven irradiation times, optimum enrichment and maximum blanket revenue per assembly. Figure 4.3 illustrates the behavior of the radial blanket fuel cycle cost contribution. Before the breakeven time, T_{BE}, the bred fissile inventory in the blanket is not sufficient to offset the blanket fixed and carrying charges. At T_{op}, the optimum point, net profit produced by the production of valuable plutonium reaches its maximum (e_m). Beyond T_{op}, the carrying charges increase more rapidly than revenue from fissile production. These optimum

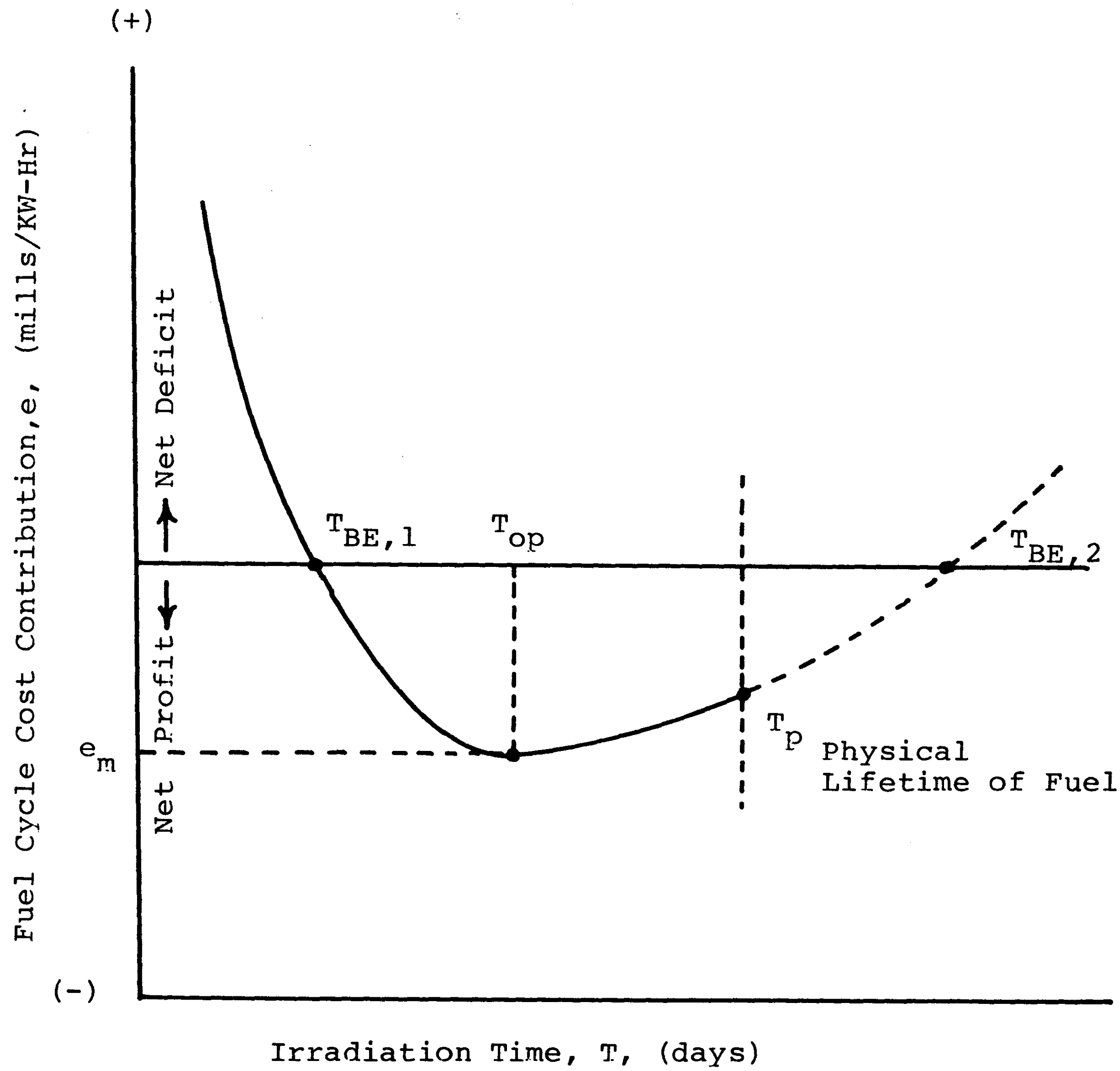

Fig. 4.3 TYPICAL VARIATION OF THE FUEL CYCLE COST CONTRIBUTION FOR A FAST REACTOR BLANKET

blanket parameters are strongly dependent on the economic environment (fabrication, reprocessing and Pu price) as well as the financial environment (income tax rate, discount rate). Simple correlations for each neutronic/economic/financial parameter will be developed and examined for accuracy using the BRECON(W3) code.

Two cost accounting methods, A and B as originally defined by Brewer (B4), were considered. In method A post irradiation transactions are not capitalized (revenue from the sale of plutonium is taxed as ordinary income; reprocessing is treated as a tax deductable expense in the year it occurs; in method B, post irradiation transactions are capitalized. Because many aspects relating to legal accounting, tax and financial aspects of the fuel cycle are still unresolved (S7), it was considered desirable to carry through a complete analysis on both of the above bases. Hopefully in the future a more explicit convention will be established so that only one option need be considered.

4.3.2 Optimum Blanket Parameters

4.3.2.1 Optimum Irradiation Time

From the general expression for the levelized fuel cycle cost, the fuel cycle cost contribution by a given entity of blanket fuel can be expressed as (see Appendix C.2).

$$\frac{e}{M_{HM}} \propto \frac{\bar{c}_1 e^{r_1 T} + \bar{c}_2 e^{-r_2 T} - \bar{c}_3\, \varepsilon(T) e^{-r_3 T}}{T} \qquad (4.14)$$

where

e is the fuel cycle cost contribution in mills/kwhr,

$\bar{c}_i$ are modified cost components for operation i in \$/kg (the actual cost present-worthed to either the beginning or the end of the irradiation , whichever is nearer in time),

r_i are "effective rates of return" used in present worth analysis, as defined by Eq.'s in item 6 of Appendix C.2,

$\varepsilon(T)$ is the time-dependent enrichment,

T is the length of the irradiation period in years,

Subscript 1 refers to fabrication.

Subscript 2 refers to reprocessing

Subscript 3 refers to plutonium credit.

In Equation (4.14), the depleted uranium purchase cost is assumed to be a sub-component of the fabrication cost.

Using the simple correlation which was derived in the previous section, the enrichment, $\varepsilon(T)$, can be expressed in the form;

$$\varepsilon(T) = \frac{M_{49}(T)}{M_{28}(o)} = [\xi_o - 1/2]\,\frac{T}{T_c{}^o}\,e^{-\xi\frac{T}{T_c{}^o}} \tag{4.13}$$

$$= S_o\,T\,e^{-\xi\frac{T}{T_c{}^o}} \tag{4.15}$$

where S_o is the linear enrichment buildup rate determined by BOL conditions, equal to $\bar{\sigma}_c{}^{28}\bar{\phi}$.

Combining Eq's. (4.14) and (4.15), one can get

$$\frac{e}{M_{HM}} \propto \frac{\bar{c}_1 e^{r_1 T} + \bar{c}_2 e^{-r_2 T} - \bar{c}_3 S_o\,T\,e^{-r_4 T}}{T} \tag{4.16}$$

where

$$r_4 = r_3 + \xi/T_c o \tag{4.17}$$

To find the optimum irradiation time, the time derivative of the fuel cycle cost contribution is set equal to zero,

$$\frac{de}{dt} = T\{\bar{c}_1 e^{r_1 T} r_1 - r_2 \bar{c}_2 e^{-r_2 T} - \bar{c}_3 S_o (e^{-r_4 T} - r_4 T e^{-r_4 T},)$$

$$- \{\bar{c}_1 e^{r_1 T} + \bar{c}_2 e^{-r_2 T} - \bar{c}_3 S_o T e^{-r_4 T}\} = 0 \tag{4.18}$$

By series expansion of $e^{r_1 T}$ and $e^{-r_2 T}$, and dropping negligible terms (>2nd order terms), Eq. (4.18) can be rewritten as,

$$\bar{c}_3 S_o r_4 T^2 e^{-r_4 T} - \bar{c}_1 (1 - r_1^2 T^2) - \bar{c}_2 (1 - r_2^2 T^2) = 0 \tag{4.19}$$

The terms $\bar{c}_1 r_1^2 T^2$ and $\bar{c}_2 r_2^2 T^2$ are negligible compared to $\bar{c}_1$ and $\bar{c}_2$, respectively; thus we have

$$T_{op}^2 \; e^{-r_4 T_{op}} = \frac{\bar{c}_1 + \bar{c}_2}{\bar{c}_3 \; S_o r_4} \tag{4.20a}$$

or

$$T_{op} \; e^{-1/2 \; r_4 T_{op}} = \left(\frac{\bar{c}_1 + \bar{c}_2}{\bar{c}_3 \; S_o r_4}\right)^{1/2} \tag{4.20b}$$

Equation (4.20b) is similar to a corresponding expression developed by Bruyer who also considered non-linear enrichment buildup, but who did not develop means for convenient determination of the non-linear correction factor as we have done here.

An approximate but acceptable solution of Eq. (4.20b) can be obtained by inserting the series expansion of $e^{-1/2 r_4 T_{op}}$ and again dropping higher order terms;

$$T_{op}(1 - 1/2 r_4 T_{op}) = \left\{\frac{\bar{c}_1 + \bar{c}_2}{\bar{c}_3\, S_o r_4}\right\}^{1/2} \tag{4.21}$$

If the discriminant of Eq. (4.21) is positive, there are two real solutions,

$$T_{op} = \frac{1}{r_4}\left[1 \pm \sqrt{1 - 2\left\{\frac{(\bar{c}_1 + \bar{c}_2) r_4}{\bar{c}_3\, S_o}\right\}^{1/2}}\right] \tag{4.22}$$

The solution with negative sign is the optimum irradiation time in which we are interested.

Consider the following algebraic relationships;

$$(1 + x)^{1/2} = 1 + 1/2x - 1/8\, x^2 + \ldots. \quad \text{if } |x| < 1 \tag{4.23}$$

and

$$a + (a + d)x + (a + 2d)x^2 + \ldots. = \frac{a}{1-x} + \frac{xd}{(1-x)^2} \quad \text{if } |x| < 1 \tag{4.24}$$

Equation (4.22)can then be simplified as

$$T_{op} = \left[\frac{\bar{\omega}}{S_o\, r_4}\right]^{1/2} F_1 \tag{4.25}$$

where

$$\omega = \frac{\bar{c}_1 + \bar{c}_2}{\bar{c}_3}$$

$$F_1 = (1 + 1/2x_1 + 1/2x_1^2 + 5/8x_1^3 + ...) \cong \text{constant}$$

$$x_1 = \left[\frac{\bar{\omega} r_4}{S_o}\right]^{1/2}$$

The compensation factor F_1 is nearly constant for all fuel materials loaded into the same blanket configuration, if economic parameter $\bar{\omega}$ is fixed. (For radial blankets, F_1 assumes an average value of 1.45.)

Equation (4.25) is similar to an equation developed by Ketabi except that x has now been replaced by r_4 to take into account the non-linear enrichment buildup.

Equation (4.25) shows that the optimum irradiation time is mainly affected by the condensed economic - financial parameters ($\bar{\omega}$ and x), the initial enrichment buildup rate (S_o), and the non-linearity parameters characterizing the fissile material buildup ($\xi/T_c o$). Eq. (4.25) holds for both accounting method A and B: one need only introduce the appropriate discount rates as required - see Appendix C.2 for details.

Comparisons of 2DB/BRECON calculations and the simple correlations are presented in Table 4.3. The optimum irradiation times calculated from the simple correlations are consistent with the 2DB/BRECON results within 2%.

TABLE 4.3

COMPARISON OF OPTIMUM IRRADIATION TIMES
PREDICTED BY 2DB/BRECON AND ANALYTIC EXPRESSIONS***

unit: years

	Accounting Method A†				Accounting Method B††			
Fuel Type**	F_1	2DB/ BRECON	Eq. (4.22)	Eq. (4.25B)*	F_1	2DB/ BRECON	Eq. (4.22)	Eq. (4.25B)*
UO_2	1.4315	7.72	7.40	7.49	1.4240	3.63	3.71	3.77
UC	1.4858	9.21	9.25	9.02	1.4593	4.17	4.34	4.31
U_2T_i	1.5092	10.73	10.18	9.78	1.4838	4.70	4.86	4.75

† 3-row Radial Blanket

†† 1st row of 3-row Radial Blanket

* constant F_1 = 1.45

** All Blankets Driven by the same core

*** Under the Standard Economic/Financial Environment Typical of a U. S. Private Utility as described in Chapter 2.

4.3.2.2 Breakeven Irradiation Time

For the breakeven time, the fuel cycle cost contribution is set equal to zero,

$$e \propto \frac{\bar{c}_1 e^{r_1 T} + \bar{c}_2 e^{-r_2 T} - \bar{c}_3 S_o \, T e^{-r_4 T}}{T} = 0 \qquad (4.26)$$

Expanding the exponential functions in Eq. (4.26) through T^2 and collecting terms, Eq. (4.26) becomes,

$$e\,T \propto -1/2\,\bar{c}_3 S_o r_4^2 T^3 + \left(\frac{\bar{c}_1 r_1^{\,2}}{2} + \frac{\bar{c}_2 r_2^{\,2}}{2} + \bar{c}_3 S_o r_4\right) T^2$$

$$+ (\bar{c}_1 r_1 - \bar{c}_2 r_2 - \bar{c}_3 S_o) T + (\bar{c}_1 + \bar{c}_2) = 0 \qquad (4.27)$$

Since the terms

$$\left|\frac{\bar{c}_1 r_1^2}{2} + \frac{\bar{c}_2 r_2^2}{2}\right| = 0.3 \ll |\bar{c}_3 S_o r_4| \cong 4.6$$

and

$$|\bar{c}_1 r_1 - \bar{c}_2 r_2| \cong 4.1 \ll |\bar{c}_3 S_o| \cong 56.4$$

one has simply

$$f(T_{BE}) = T_{BE}^3 - \frac{2}{r_4} T_{BE}^2 + \frac{2}{r_4^2} T_{BE} - \frac{2(\bar{c}_1 + \bar{c}_2)}{\bar{c}_3 \, S_o \, r_4^2} = 0 \qquad (4.28)$$

By the fact that

$$\frac{2}{r_4}\ ,\ \frac{2}{r_4^2}\ ,\ \frac{2(\bar{c}_1+\bar{c}_2)}{\bar{c}_3\ S_o\ r_4} >> 1$$

the approximate roots of the above cubic equation can be obtained by the neglection of 3rd order terms and solving a quadratic equation,

$$T_{BE}^2 - \frac{1}{r_4}\ T_{BE} + \frac{\bar{\omega}}{S_o r_4} = 0 \qquad (4.29)$$

The solution of Equation (4.29) with positive discriminant is:

$$T_{BE} = \frac{1}{2r_4}\ [1 \pm \sqrt{1 - \frac{4r_4(\bar{c}_1+\bar{c}_2)}{\bar{c}_3 S_o}}\ ] \qquad (4.30)$$

The solution with positive sign is the irradiation time beyond which the profit by breeding is cancelled out by an accumulation of carrying charges.

The solution with negative sign is the real breakeven time of interest beyond which there is a net profit.

Again, we can use Equations (4.23) and (4.24),and (4.30) can be simply approximated as

$$T_{BE} = [\frac{\bar{\omega}}{S_o}]\ F_2 \qquad (4.31)$$

where

$$\bar{\omega} = \frac{\bar{c}_1+\bar{c}_2}{\bar{c}_3} \quad \text{as before}$$

$$F_2 \equiv (1 + x_2 + 2x_2^2 + \ldots.) \cong \text{constant} \tag{4.32}$$

$$x_2 = [\frac{\bar{\omega} r_4}{S_o}] = x_1^2 \tag{4.33}$$

Unlike the optimum irradiation time, the breakeven time is mainly affected only by the composite economic parameter $\bar{\omega}$ and the BOL linear enrichment buildup rate, S_o, and hardly affected at all by the non-linear fissile buildup factor $\xi/T_c°$. This simplicity is due in part to the fact that breakeven times are reached early in fuel life (∿2 years) when the linear fissile buildup model can be used for the prediction of fissile material accumulation in FBR blankets.

In Equation (4.30), the discriminant should be positive for the existence of a breakeven time, which means that blanket fuel cycle cost contributions are negative (i.e., blankets contribute an offsetting profit rather than an expense). This requirement of a non-negative discriminant gives:

$$1 - 4\bar{\omega} r_4 / S_{om} \geq 0 \tag{4.34}$$

or

$$S_{om} \geq 4\bar{\omega} r_4 \tag{4.35}$$

which indicates that the specific enrichment buildup rate (S_{om}) must not be less than a certain value ($4\bar{\omega} r_4$), which is determined by the economic conditions ($\bar{\omega}$,x) and the non-linear factor characterizing fissile buildup ($\xi/T_c°$). Equation (4.35) is very useful for determining the economic blanket thickness - if the local fissile generation rate falls below S_{om}, the region in question will not return a profit.

Table 4.4 presents comparisons of breakeven times from 2DB/BRECON computations and Equations (4.30) and (4.31).

As can be seen agreement is good and the simpler analytic expressions Equations (4.30) and (4.31) are adequate.

4.3.2.3 Maximum Blanket Revenue

The maximum blanket revenue can be calculated by inserting the optimum irradiation time and appropriate economic factors into the general cost equation.

Adopting the same assumptions and approximations of exponential functions which were used to derive the breakeven time in section 4.3.2.2, the maximum blanket revenue (i.e. absolute value of largest negative cost) can be expressed as:

$$e_m = \frac{1000\ M_{HM}}{E} \left[\frac{\bar{c}_1(1+r_1T_{op})}{T_{op}}\right. \qquad \text{Fabrication cost contribution}$$

$$+ \frac{\bar{c}_2(1-r_2T_{op})}{T_{op}} \qquad \text{Reprocessing cost contribution}$$

$$\left. - \bar{c}_3S_o(1-r_4T_{op} + 1/2r_4^2T_{op}^2)\right] \qquad \text{Material credit contribution} \qquad (4.36)$$

In Equation (4.36) the electrical energy produced by the reactor in one year, E(KW-Hr/yr) has been introduced from the general cost equation (e.g. see development of cost equations by Brewer (B4)).

The optimum irradiation time, T_{op}, can be simply expressed as Equation (4.25), $T_{op} = F_1[\frac{\bar{\omega}}{S_or_4}]^{1/2}$, and the maximum blanket revenue can thus be rewritten;

TABLE 4.4

COMPARISON OF BREAKEVEN TIMES CALCULATED USING 2DB/BRECON AND ANALYTIC EXPRESSIONS**

units: years

Fuel Type	Accounting Method A†				Accounting Method B††			
	F_2	2DB/ BRECON	Eq. (4.30)	Eq. (4.31)*	F_2	2DB/ BRECON	Eq. (4.30)	Eq. (4.31)*
UO_2	1.2999	3.09	2.83	2.83	1.2919	1.44	1.40	1.42
UC	1.3573	4.38	3.72	3.56	1.3282	1.55	1.70	1.67
U_2T_i	1.3797	4.58	4.16	3.92	1.3542	1.96	1.95	1.89

† 3-row Radial Blanket

†† 1st row of 3-row Radial Blanket, All Driven by Same Core

* constant F_2 = 1.30

** Under the Standard Economic Environment Typical of a U.S. Private Utility as Described in Chapter 2.

Δt = 50 day time step.

$$e_m = \frac{1000\ M_{HM}}{E} [(\bar{c}_1 + \bar{c}_2)\bar{c}_3\ S_o r_4]^{1/2}\ F_3 \tag{4.37}$$

where

$$F_3 = [\frac{F_1^2 + 1}{F_1} + \frac{(\bar{c}_1 r_1 - \bar{c}_2 r_2)}{\{(\bar{c}_1 + \bar{c}_2)\bar{c}_3\ S_o r_4\}^{1/2}} - \frac{F_1^2}{2}\left(\frac{\bar{\omega} r_4}{S_o}\right)^{1/2} - \left(\frac{S_o}{\bar{\omega} r_4}\right)^{1/2}] \tag{4.38}$$

Equation (4.37) and (4.38) indicate that:

a) F_3 should be negative for positive blanket revenue, i.e.,

$$(\frac{S_o}{\bar{\omega} r_4}) \gtrsim 4.6 \text{ or } S_{om} \gtrsim 4.6\ \bar{\omega} r_4 \tag{4.39}$$

where terms

$$[\frac{F_1^2}{2}\left(\frac{\bar{\omega} r_4}{S_o}\right)^{1/2}] \text{ and } [\frac{(\bar{c}_1 r_1 - \bar{c}_2 r_2)}{\{(\bar{c}_1 + \bar{c}_2)\bar{c}_3\ S_o r_4\}^{1/2}}]$$

are neglected and $F_1 = 1.45$. Equation (4.39) is a more approximate form of Equation (4.35).

b) F_3 and S_o are the dominant parameters determing the |max. fuel cycle cost contribution|, hence UO_2 fuel is more economical even though carbide or metal alloy fuel has large T_{op} and higher M_{HM}, as shown in Table 4.5.

c) For the maximum blanket revenue, $(S_o r_4)$ and $(\frac{S_o}{\bar{\omega} r_4})$ should be as large as possible, which requires a higher neutron capture rate for U-238 (soft spectrum) and low operating (fabrication, reprocessing) costs plus higher Pu-values. Parameter r_4 does not appreciably affect the maximum blanket revenue. In Table 4.3, carbide and metal alloy fuels have

TABLE 4.5

MAXIMUM BLANKET REVENUE AND RELATED PARAMETERS CALCULATED FROM 2DB/BRECON AND SIMPLE CORRELATION

Parameters	Unit	Accounting Method A††			Accounting Method B††		
		UO_2	UC	U_2T_i	UO_2	UC	U_2T_i
$\bar{\omega}$		0.0127797			0.0130972		
$\bar{c}_3$	\$/Kg	9607.8944			9231.1635		
$(\bar{c}_1+\bar{c}_2)$	\$/Kg	122.7863			120.9026		
M_{HM}	Kg	17299	23233	24759	5180	6957	7414
S_o	Kg Pu / Kg_{MHM}Yr	0.005870	0.004663	0.004239	0.012030	0.010204	0.009101
r_4	Yr^{-1}	0.081475	0.0707147	0.066265	0.16065	0.14495	0.13421
F_3**		-0.5064	-0.3881	-0.3443	-0.6420	-0.5744	-0.5366
e_{fab}*	Mills / Kw Hr	0.0767 0.0784	0.0921 0.0959	0.0937 0.0997	0.0371 0.0354	0.0451 0.0475	0.0447 0.0465
e_{rep}*	Mills / Kw Hr	0.0216 0.0231	0.0220 0.0244	0.0206 0.0242	0.0123 0.0117	0.0136 0.0157	0.0124 0.0142
$-e_{max}$*	Mills / Kw Hr	0.1561 0.1548	0.1635 0.1626	0.1574 0.1597	0.0923 0.0824	0.1038 0.0990	0.0979 0.0912
$-e_m$*	Mills / Kw Hr	0.0578 0.0533	0.0494 0.0423	0.0431 0.0358	0.0429 0.0353	0.0451 0.0358	0.0408 0.0305

*Key: Eq.(4.36) / 2DB/BRECON

e_{fab}: fabrication cost contribution
e_{rep}: reprocessing cost contribution
e_{mat}: material credit contribution

**$T_{op} = F_1\left(\frac{\bar{\omega}}{S_o r_4}\right)^{1/2}$ where $F_1 = 1.45$

†3-row Radial Blanket

††1st-row in 3-row Radial Blanket

larger optimum irradiation time, T_{op} and lower r_4 compared to oxide fuel because of their harder spectrum, while oxide fuel has a much larger S_o, which results in larger values of $(S_o r_4)^{1/2}$ and $(\frac{S_o}{\bar{\omega} r_4})^{1/2}$ regardless of the value of r_4. This apparently indicates that a softer neutron spectrum in FBR blankets is preferable for maximum blanket revenue because of the higher resulting enrichment buildup rate, S_o.

d. The modification factor for the optimum irradiation time, F_1, is nearly constant for all fuel materials, and it, therefore, does not appreciably affect the maximum blanket revenue.

e. In Equation (4.38), terms $[\frac{(\bar{c}_1 r_1 - \bar{c}_2 r_2)}{\{(\bar{c}_1 + \bar{c}_2)\bar{c}_3 \; S_o r_4\}^{1/2}}]$ and $\frac{F_1^2}{2}\left(\frac{\bar{\omega} r_4}{S_o}\right)^{1/2}$ are small compared to other terms. Neglecting these two terms can give a rough estimation of e_m (e.g.0.057 mills/KW-Hr vs. 0.020 mills/KW-Hr).

4.3.2.4 Optimum Discharge Enrichment and Dimensionless Optimum Irradition Time

The optimum discharge enrichment can be obtained by inserting the optimum irradiation time, T_{op}, into Equation (4.15):

$$\varepsilon_{op} = \frac{M^{49}(T_{op})}{M_{28}(o)} = S_o T_{op} e^{-\xi \cdot \frac{T_{op}}{T_c^\circ}} \qquad (4.40)$$

where

$$S_o = \bar{\sigma}_c^{28} \bar{\phi}$$

$$T_c^\circ = [(\bar{\sigma}_a^{49} - \bar{\sigma}_a^{28})\bar{\phi}]_{BOL}^{-1}$$

By use of the simple approximate correlation for the optimum irradiation time, $T_{op} = F_1 (\frac{\bar{\omega}}{S_o r_4})^{1/2}$, the dimensionless optimum irradiation time can be defined as:

$$\frac{T_{op}}{T_c^\circ} = F_1 (\frac{\bar{\omega}}{S_o r_4})^{1/2} \quad (\bar{\sigma}_a^{49}\bar{\phi} - \bar{\sigma}_a^{28}\bar{\phi})_{BOL} \tag{4.41}$$

Combining Equations (4.40) and (4.41), one can obtain a simple equation for the optimum discharge enrichment,

$$\varepsilon_{op} = F_1 (\frac{S_o \bar{\omega}}{r_4})^{1/2} e^{-\hat{\xi}(\frac{\bar{\omega}}{S_o r_4})^{1/2}} \tag{4.42}$$

where

$$\hat{\xi} = \xi \cdot F_1 \cdot (\bar{\sigma}_a^{49}\bar{\phi} - \bar{\sigma}_a^{28}\bar{\phi})_{BOL} \tag{4.43}$$

Table 4.6 shows the optimum discharge enrichment for the various fuel materials which were calculated by 2DB/BRECON and the simple correlation, Equation (4.42). The optimum discharge enrichment of oxide, carbide and metal alloy fuels approaches the same value when we fix the economic environment. This result is attributable to the exponential nature of enrichment buildup. Dimensionless optimum irradiation times, $\frac{T_{op}}{T_c^\circ}$, of various fuel materials and different blanket configurations are slightly different, as shown in Table 4.6. However, the actual irradiation time is determined by the plant refueling schedule which will permit fuel discharge only once or twice per year, and we can therefore consider that $\frac{T_{op}}{T_c^\circ}$ of the various fuel materials are the same within the practical error band of $\pm$ 3 to 6 months $\approx \pm$ 10%.

TABLE 4.6

OPTIMUM DISCHARGE ENRICHMENTS PREDICTED BY

2DB/BRECON AND THE ANALYTIC EXPRESSION, EQ. (4.42)†

Parameters	Accounting Method A**			Accounting Method B***		
	UO_2	UC	U_2T_i	UO_2	UC	U_2T_i
$(\frac{S_o\bar{\omega}}{r_4})^{1/2}$	0.03034	0.02903	0.02859	0.03132	0.03036	0.02980
$e^{-\hat{\xi}(\frac{\bar{\omega}}{S_o r_4})^{1/2}}$	0.7328	0.7579	0.7735	0.7375	0.7555	0.7731
$\frac{T_{op}}{T_c^o}$	0.4663	0.4159	0.3853	0.4566	0.4204	0.3861
ε_{op}*	0.0322 0.0343	0.0319 0.0340	0.0321 0.0337	0.0335 0.0344	0.0333 0.0363	0.0334 0.0345

*Key: upper value: Eq.(4.21); lower value: 2DB/BRECON

Constants Used: $F_1 = 1.45$, $\xi = 2/3$

** 3-row Radial Blanket
*** 1st row of 3-row Radial Blanket
† Under the Standard Economic Environment described in Chapter 2

4.4 SENSITIVITY ANALYSIS FOR OPTIMUM BLANKET PARAMETERS

4.4.1 Introduction

To trace the optimum blanket parameters impacted by the variation of the economic and financial environment, sensitivity functions were developed, and the results are examined in this section. Nowadays, variation of economic and financial parameters such as operating costs (c_i) or Pu market value are so rapid and the amplitudes of the changes are so wide that optimum blanket parameters could be subject to considerable uncertainty. The optimum blanket parameters show the sharpest response to Pu market value (c_3), discount rate (X), and enrichment buildup rate (S_o), while they are less sensitive to the other parameters such as reprocessing cost (c_2), and cash flow timing (ΔT).

Sensitivity coefficients have been defined as

$$\lambda_q^P(S) = \lim_{\substack{\Delta q \to 0 \\ q \to S}} \frac{\Delta P/P}{\Delta q/q} = \left[\frac{\partial P}{\partial q} \right]_{q=S} \cdot (q/P) \tag{4.44}$$

where q is the independent parameter such as operating cost (C_i), income tax rate (τ) etc., which has reference value S and small variation Δq,

P is the dependent optimum parameter such as the optimum irradiation time (T_{op}), or breakeven time (T_{BE}) etc., of which the small variation effected by the change of q is ΔP.

By algebraic rules of partial derivatives, we can express the differential or variation of optimum parameter P as follows;

$$\frac{\Delta P(\Delta S)}{P} = \sum_{i=1}^{n} \left[\lambda_q^P(S) \cdot \frac{\Delta q}{q}\right]_i \tag{4.45A}$$

or

$$\Delta P\ (\Delta S) = \sum_{i=1}^{n} [\lambda_q^P(S) \cdot \Delta q \cdot \frac{P}{q}]_i \qquad (4.45B)$$

where n is the total number of independent variables for the optimum parameter P.

If q is also a function of variable u, then

$$\Delta q = \frac{\partial q}{\partial u} \Delta u \qquad (4.46)$$

Combining Equations (4.41), (4.42A) and (4.43), one gets

$$\lambda_u^P(S) = \lambda_q^P(S) \cdot \frac{\partial q}{\partial u} \cdot u/q \qquad (4.47A)$$

and

$$\frac{\Delta P(\Delta S)}{P} = \sum_{i=1}^{n} [\lambda_q^P(S) \cdot \frac{\partial q}{\partial u} \cdot \frac{\Delta u}{q}]_i = \sum_{i=1}^{n} [\lambda_u^P \cdot \frac{\Delta u}{u}]_i \qquad (4.47B)$$

For example, if all parameters are increased by 5% of their reference value, the total percentage change in the optimum parameter of concern is

$$\frac{\Delta P(5\%)}{P} = \sum_{i=1}^{n} [\lambda_q^P(S) \cdot \frac{\partial q}{\partial u} \cdot 5]_i \qquad (4.48)$$

where S is the reference or standard value of independet parameter q.

4.4.2 Sensitivity Coefficients for Optimum Economic Parameters

The optimum economic parameters - optimum irradiation time, breakeven time, optimum enrichment and maximum blanket revenue - are a function of

1. fabrication cost (c_1),
2. reprocessing cost (c_2),
3. Pu market value (c_3),
4. linear enrichment buildup rate (S_o),
5. discount rate (X) which is a function of income tax rate, (τ) bond and stock fractions (f_b, f_s) and the return rates on bond and stock (r_b, r_s),
6. cash flow timing of fabrication (ΔT_1), reprocessing (ΔT_2) and material credit (ΔT_3),
7. non-linear fissile material buildup factor (ξ/T_c°).

Table 4.7 summarizes the sensitivity coefficients for the optimum irradiation time, derived from the simplified correlation, $T_{op} = F_1[\frac{\bar{\omega}}{S_o r_4}]^{1/2}$.

As expected, Pu market value (c_3) and linear enrichment buildup rate (S_o) are the most important factors, and produce 0.5% changes in the optimum irradiation for every 1% of their variation (i.e. $\lambda_q^{T_{op}} = 0.5$).

TABLE 4.7

SENSITIVITY COEFFICIENTS FOR OPTIMUM IRRADIATION TIME†

q / u	$\lambda^{T_{op}}_{q}$* or $\lambda^{T_{op}}_{u}$*	Reference** Value	BRECON Results
$\bar{\omega}$	0.5	0.5	
c_1	$0.5/(1 + \frac{\bar{c}_2}{\bar{c}_1})$	0.304	0.362
c_2	$0.5/(1 + \frac{\bar{c}_1}{\bar{c}_2})$	0.196	0.210
c_3	-0.5	-0.5	-0.45
ΔT_1	$[0.5/(1 + \frac{\bar{c}_2}{\bar{c}_2})] [\frac{X\Delta T_1}{1-\tau}]$	0.024	0.024
ΔT_2	$[-0.5/(1 + \frac{\bar{c}_1}{\bar{c}_2})] [X\Delta T_2]$	-0.008	-0.009
ΔT_3	$0.5\ X\Delta T_3$	0.02	0.021
S_o	-0.5	-0.5	-0.76
r_4	-0.5	-0.5	-0.6
X	$-0.25\ X/r_4$	-0.245	-0.29
τ	0	0.0	
ξ/T_c^o	$-0.5\ \xi/T_c^o/r_4$	-0.255	

†UO_2 Fueled 3-row Radial Blanket for Method A

*$T_{op} = F_1[\frac{\bar{\omega}}{S_o r_4}]^{1/2}$ where F_1 is constant

**With reference economic environment

Note that the sensitivity coefficient for the non-linear factor ξ/T_c° is 0.25, which is a rather high value compared to many of the other sensitivity coefficients. This result illustrates that the non-linear characteristics of Pu buildup in FBR blankets is important to determination of the optimum irradiation time. If the non-linear factor(ξ/T_c°) is increased by the creation of a softer neturon spectrum,then the optimum irradiation time would be decreased substantially. For this reason, the optimum irradiation time of oxide fuel, which has the softest neutron spectrum and the largest value of ξ/T_c° among the possible fuel materials considered here, is much shorter than that of the others.

The variation of cash flow timing (ΔT_i) produces effects which are essentially negligible.

The absolute value of the variation of optimum irradiation time in percent caused by small percentage changes in the independent parameters $\frac{\Delta\bar{\omega}}{\bar{\omega}}$, $\frac{\Delta S_o}{S_o}$ and $\frac{\Delta r_4}{r_4}$ is same. Therefore we can easily predict the optimum irradiation time for small variations of economic/neutronic parameters;

$$T'_{op} = [1 + 0.005 \cdot (\%\text{ change of parameter } \bar{\omega} \text{ or } S_o \text{ or } r_4)]T_{op} \quad (4.49)$$

In Equation (4.31), breakeven time is mainly dependent on economic parameter $\bar{\omega}$ and the linear enrichment buildup rate S_o, while the non-linear fissile buildup factor (ξ/T_c°) and r_3 are included in F_2 which can be considered as a universal constant. Therefore, breakeven time is assumed to be independent of ξ/T_c° and r_3.

Table 4.8 shows the sensitivity coefficients of the variable parameters for the breakeven time, as derived from the simplified correlation, $T_{BE} = F_2[\frac{\bar{\omega}}{S_o}]$.

TABLE 4.8

SENSITIVITY COEFFICIENTS OF THE BREAKEVEN TIME†

u	$\lambda_q^{T_{BE}*}$ or $\lambda_U^{T_{BE}*}$	Reference Value**	BRECON Results
$\bar{\omega}$	1.0	1.0	
c_1	$(1 + \frac{\bar{c}_2}{\bar{c}_1})^{-1}$	0.609	0.7
c_2	$(1 + \frac{\bar{c}_1}{\bar{c}_2})^{-1}$	0.391	0.36
c_3	-1.0	-1.0	-1.1
ΔT_1	$[1 + \frac{\bar{c}_2}{\bar{c}_1}]^{-1} [\frac{X\Delta T_1}{1-\tau}]$	0.048	0.055
ΔT_2	$-[1 + \frac{\bar{c}_1}{\bar{c}_2}]^{-1} [X\Delta T_2]$	-0.016	-0.015
ΔT_3	$X\Delta T_3$	0.040	0.049
S_o	-1.0	-1.0	-0.8

† UO_2 Fueled 3-row Radial Blanket for Method A

* $T_{BE} = F_2[\frac{\bar{\omega}}{S_o}]$ where F_2 is constant

** With reference economic environment

All sensitivity coefficients are increased by a factor of two compared with those of the optimum irradiationtime. Thus the effects on breakeven time arising from variation of economic/neutronic parameters are more serious than in the case of the optimum irradiation time. Figure 4.3 shows that the cost vs. time curve has a very steep slope near the breakeven time, T_{BE}; the location of the intercept with e=0 is most strongly affected by Pu market value (c_3), linear enrichment buildup rate (S_o) and fabrication cost (c_1).

The maximum blanket revenue is given by Eqs. (4.37) and (4.38). Combining these two equations and rewriting, one can obtain;

$$e_m \propto \frac{F_1^2+1}{F_1} [\bar{c}_1 + \bar{c}_2)\bar{c}_3 \; S_o r_4]^{1/2} + \bar{c}_1 r_1 - \bar{c}_2 r_2 - \frac{F_1^2}{2} (\bar{c}_1 + \bar{c}_2) r_4 - \bar{c}_3 S_o$$

$$= [(\bar{c}_1 + \bar{c}_2)\bar{c}_3 \; S_o r_4]^{1/2} F_3 \qquad (4.50)$$

Table 4.9 shows the sensitivity coefficients for maximum blanket revenue determined from Eq. (4.50).

As in the case of the optimum irradiation time, maximum blanket revenue is a function of all of our economic/neutronic variables. The most sensitive variables are Pu-value (c_3), linear enrichment buildup rate (S_o) and fabrication cost (c_1). Discount rate (X) and non-linear buildup factor (ξ/T_c°) are moderately important factors. Fuel reprocessing cost is less important and cash flow times (ΔT_i) are the least significant factors affecting maximum blanket revenue.

This result also illustrates how oxide fuel, which has the highest value of S_o and a relatively larger r_4, can produce the highest maximum

TABLE 4.9

SENSITIVITY COEFFICIENTS FOR MAXIMUM BLANKET REVENUE

g	u	$\lambda_{g}^{e_m^*}$ or $\lambda_{u}^{e_m^*}$	Reference Value	BRECON
$\bar{\omega}$	c_1	$0.5\left(\frac{F_1^2+1}{F_1}\right)\left[\frac{\bar{c}_1}{(\bar{c}_1+\bar{c}_2)F_3}\right] + \frac{\bar{c}_1\left(r_1 - \frac{F_1^2}{2} r_4\right)}{[(\bar{c}_1+\bar{c}_2)\bar{c}_3 S_o r_4]^{1/2} F_3}$	-1.251	-1.4
	c_2	$0.5\left(\frac{F_1^2+1}{F_1}\right)\left[\frac{\bar{c}_1}{(\bar{c}_1+\bar{c}_2)F_3}\right] - \frac{\bar{c}_2\left(r_2 - \frac{F_1^2}{2} r_4\right)}{[(\bar{c}_1+\bar{c}_2)\bar{c}_3 S_o r_4]^{1/2} F_3}$	-0.320	-0.35
	c_3	$0.5\left(\frac{F_1^2+1}{F_1}\right) \cdot \frac{1}{F_3} - \frac{\bar{c}_3 S_o}{[(\bar{c}_1+\bar{c}_2)\bar{c}_3 S_o r_4]^{1/2} F_3}$	2.576	2.84
	ΔT_1	$\lambda_{c_1}^{e_m} \cdot \left[\frac{X\Delta T_1}{1-\tau}\right]$	-0.100	-0.10
	ΔT_2	$-\lambda_{c_2}^{e_m} \cdot [X\Delta T_2]$	0.013	0.018
	ΔT_3	$-\lambda_{c_3}^{e_m} \cdot [X\Delta T_3]$	-0.103	-0.11
S_o		$0.5\left(\frac{F_1^2+1}{F_1}\right) \cdot \frac{1}{F_3} - \frac{\bar{c}_3 S_o}{[(\bar{c}_1+\bar{c}_2)\bar{c}_3 S_o r_4]^{1/2} F_3}$	2.576	2.0
r_4		$0.5\left(\frac{F_1^2+1}{F_1}\right) \frac{1}{F_3} - \frac{F_1^2(\bar{c}_1+\bar{c}_2) r_4}{2[(\bar{c}_1+\bar{c}_2)\bar{c}_3 S_o r_4]^{1/2} F_3}$	-1.238	
	X	$\lambda_{r_4}^{e_m} \cdot 0.5\, X/r_4$	-0.698	
	τ	0	0.0	
	ξ/T_c°	$\lambda_{r_4}^{e_m} \cdot \xi/(T_c^\circ\ r_4)$	-0.630	

†UO_2 Fueled 3-row Radial Blanket for Method A

*F_1 = 1.45

blanket revenue compared to carbide and metal alloy fuels, because S_o is the most influential parameter, along with Pu market value, c_3.

In summary: to achieve the highest blanket revenue, lower fuel fabrication cost, high Pu-value, high Pu production rate per unit heavy metal - this does not necessarily mean high external breeding ratio - a lower discount rate and a lower non-linear buildup factor are preferable.

4.5 THE EFFECTS OF FUEL MANAGEMENT OPTIONS ON BLANKET ECONOMICS

4.5.1 Introduction

In the preceding sections, simple correlations for fissile buildup histories and important blanket parameters have been developed under the batch fuel management option. In this section, the various possible fuel management options for radial blanket assemblies will be reviewed and analyzed with respect to plutonium production (and its economic implications), and power distribution (enrichment swing during burnup).

The most commonly considered options for fuel management of radial blanket assemblies are:

1. No shuffling (batch); all fuel assemblies in the radial blanket are refueled at the same optimum time.
2. Zone or region scatter; each individual assembly is refueled at its own local optimum irradiation time.
3. In-Out shuffling; fresh blanket assemblies are inserted into blanket positions at the core-blanket interface and later moved to outer positions.

4. Out-In shuffling; fresh fuel assemblies are inserted at the blanket periphery and later moved to inner blanket positions.

There are several difficulties involved in comparing fuel management options under truly comparable conditions. Even moving fuel from one row to the next is not simple because the number of fuel assemblies per row differs. Furthermore, both the magnitude of the neutron flux and the spectrum averaged microscopic cross-sections are changed as a function of fuel burnup. Nevertheless some useful insight may be gained by an approximate analytic treatment.

In this section, the following assumptions will be used to permit a simple analysis:

1. Each blanket row has an equal volume and number of fuel assemblies
2. The average neutron flux and group-averaged cross-sections are a function of position only and are not a function of fuel burnup.
3. All fuel assemblies have equal intervals of irradiation time, T_{op}/no. of rows, in each row for the In-Out or Out-In shuffling options.

The fuel management of axial blankets is somewhat different. They are fabricated as an integral part of the core fuel assemblies and are loaded and refueled at core refueling times. Hence we need not consider the axial blanket further.

4.5.2 The Impact of Fuel Management on Pu Production

1. No shuffling (batch) case; the Pu accumulated in the whole blanket ($M^{49}_{NS.0}$) in the optimum irradiation time ($T_{op.0}$), can be expressed as

$$M^{49}_{NS.0}(T_{op,0}) = M^{49}_{NS.1}(T_{op,0}) + M^{49}_{NS.2}(T_{op,0}) + M^{49}_{NS.3}(T_{op,0}) \tag{4.51}$$

where subscripts 0, 1, 2 and 3 refer to the whole blanket, and the first, second and third rows in the blanket, respectively.

Applying Equation (4.3), the plutonium produced in each row can be expressed as

$$M^{49}_{NS.1}(T_{op,0}) = M^{28}_{1}(0) \cdot \Sigma_1 \cdot (e^{-\bar{\sigma}^{28}_{a,1}\bar{\phi}_1 T_{op.0}} - e^{-\bar{\sigma}^{49}_{a,1}\bar{\phi}_1 T_{op,0}}) \tag{4.52}$$

$$M^{49}_{NS.2}(T_{op,0}) = M^{28}_{2}(0) \cdot \Sigma_2 \cdot (e^{-\bar{\sigma}^{28}_{a,2}\bar{\phi}_2 T_{op,0}} - e^{-\bar{\sigma}^{49}_{a,2}\bar{\phi}_2 T_{op,0}}) \tag{4.53}$$

$$M^{49}_{NS.3}(T_{op,0}) = M^{28}_{3}(0) \cdot \Sigma_3 \cdot (e^{-\bar{\sigma}^{28}_{a,3}\bar{\phi}_3\ op,0} - e^{-\bar{\sigma}^{49}_{a,3}\bar{\phi}_3 T_{op,0}}) \tag{4.54}$$

where

$$\Sigma_i = \frac{\bar{\sigma}^{28}_{c,i}}{\bar{\sigma}^{49}_{a,i} - \bar{\sigma}^{28}_{a,i}} \tag{4.55}$$

Since we have assumed the same volume or number of fuel assemblies in each row, the initial heavy metal inventories in each row are the same;

$$M_1^{28}(0) = M_2^{28}(0) = M_3^{28}(0) = 1/3M_{28}(0) \tag{4.56}$$

Expanding the exponential functions, $e^{-at} \cong 1 - at + 1/2(at)^2$, one obtains

$$M^{49}_{NS,1}(T_{op,0}) = 1/3M_{28}(0)\cdot\Sigma_1\cdot(\bar{\sigma}^{49}_{a,1}\bar{\phi}_1 - \bar{\sigma}^{28}_{a,1}\bar{\phi}_1)T_{op,0}\, e^{-1/2(\bar{\sigma}^{28}_{a,1}\bar{\phi}_1 + \bar{\sigma}^{49}_{a,1}\bar{\phi}_1)T_{op,0}}$$

$$= 1/3M_{28}(0)\cdot S_{o,1}\cdot T_{op,0}\, e^{-1/2(\bar{\sigma}^{28}_{a,1}\bar{\phi}_1 + \bar{\sigma}^{49}_{a,1}\bar{\phi}_1)T_{op,0}}$$

$$M^{49}_{NS,2}(T_{op,0}) = 1/3M_{28}(0)\cdot\Sigma_2\cdot(\bar{\sigma}^{49}_{a,2}\bar{\phi}_2 - \bar{\sigma}^{28}_{a,2}\bar{\phi}_2)T_{op,0}\, e^{-1/2(\bar{\sigma}^{28}_{a,2}\bar{\phi}_2 + \bar{\sigma}^{49}_{a,2}\bar{\phi}_2)T_{op,0}}$$

$$= 1/3M_{28}(0)\cdot S_{o,2}\cdot T_{op,0}\, e^{-1/2(\bar{\sigma}^{28}_{a,2}\bar{\phi}_2 + \bar{\sigma}^{49}_{a,2}\bar{\phi}_2)T_{op,0}}$$

$$M^{49}_{NS,3}(T_{op,0}) = 1/3M_{28}(0)\cdot\Sigma_3\cdot(\bar{\sigma}^{49}_{a,3}\bar{\phi}_3 - \bar{\sigma}^{28}_{a,3}\bar{\phi}_3)T_{op,0}\, e^{-1/2(\bar{\sigma}^{28}_{a,3}\bar{\phi}_3 + \bar{\sigma}^{49}_{a,3}\bar{\phi}_3)T_{op,0}}$$

$$= 1/3M_{28}(0)\cdot S_{o,3}\cdot T_{op,0}\, e^{-1/2(\bar{\sigma}^{28}_{a,3}\bar{\phi}_3 + \bar{\sigma}^{49}_{a,3}\bar{\phi}_3)T_{op,0}} \tag{4.58}$$

by

$$S_{o,i} \equiv \bar{\sigma}^{28}_{c,i}\bar{\phi}_i \tag{4.59}$$

Inserting Equations (4.56) through (4.58) into (4.51), the total accumulated Pu in the whole blanket at $T_{op,0}$ can be written;

$$M^{49}_{NS,0}(T_{op,0}) = 1/3M_{28}(0) \cdot T_{op,0} \quad [S_{o,1}\, e^{-1/2(\bar{\sigma}^{28}_{a,1} + \bar{\sigma}^{49}_{a,1}\bar{\phi}_1)T_{op,0}}$$

$$+ S_{o,2}\, e^{-1/2(\bar{\sigma}^{28}_{a,2}\bar{\phi}_2 + \bar{\sigma}^{49}_{a,2}\bar{\phi}_2)T_{op,0}}$$

$$+ S_{o,3}\, e^{1/2(\bar{\sigma}^{28}_{a,3}\bar{\phi}_3 + \bar{\sigma}^{49}_{a,3}\bar{\phi}_3)T_{op,0}}]$$

$$= 1/3M_{28}(0) \cdot T_{op,0} \cdot \sum_{i=1}^{3} S_{o,i}\, e^{-R_{NS,i}T_{op,0}} \qquad (4.60)$$

where

$$R_{NS,1} = 1/2(\bar{\sigma}^{28}_{a,1}\bar{\phi}_1 + \bar{\sigma}^{49}_{a,1}\bar{\phi}_1)$$

$$R_{NS,2} = 1/2(\bar{\sigma}^{28}_{a,2}\bar{\phi}_2 + \bar{\sigma}^{49}_{a,2}\bar{\phi}_2)$$

$$R_{NS,3} = 1/2(\bar{\sigma}^{28}_{a,3}\bar{\phi}_3 + \bar{\sigma}^{49}_{a,3}\bar{\phi}_3) \qquad (4.61)$$

The average fissile production rate per year is

$$\bar{M}^{49}_{NS,0} = \frac{M^{49}_{NS}(T_{op,0})}{T_{op,0}} = 1/3M_{28}(0) \cdot [S_{o,1}\, e^{-1/2(\bar{\sigma}^{28}_{a,1}\bar{\phi}_1 + \bar{\sigma}^{49}_{a,1}\bar{\phi}_1)T_{op,0}}$$

$$+ S_{o,2}\, e^{-1/2(\bar{\sigma}^{28}_{a,2}\bar{\phi}_2 + \bar{\sigma}^{49}_{a,2}\bar{\phi}_2)T_{op,0}} + S_{o,3}\, e^{-1/2(\bar{\sigma}^{28}_{a,3}\bar{\phi}_3 + \bar{\sigma}^{49}_{a,3}\bar{\phi}_3)T_{op,0}}]$$

$$= 1/3M_{28}(0) \cdot \sum_{i=1}^{3} S_{o,i}\, e^{-R_{NS,i}T_{op}} \qquad (4.62)$$

2. In-Out shuffling case; the final plutonium inventory in the assemblies which underwent In-Out shuffling (M_{IO}^{49}) is

$$M_{IO}^{49}(T_{op,0}) = 3 \cdot M_{IO,3}^{49}(T_{op,0}) \tag{4.62}$$

After the first cycle, $1/3T_{op,0}$, the plutonium produced in the first row is

$$M_{IO,1}^{49}(\tfrac{1}{3}T_{op,0}) = 1/3M_{28}(0) \cdot \Sigma_1 \cdot (e^{-\bar{\sigma}_{a,1}^{28}\bar{\phi}_1 \cdot 1/3T_{op,0}} - e^{-\bar{\sigma}_{a,1}^{49}\bar{\phi}_1 \cdot 1/3T_{op,0}})$$

$$= 1/9M_{28}(0) \cdot S_{o,1}T_{op,0} \cdot e^{-1/6(\bar{\sigma}_{a,1}^{28}\bar{\phi}_1 + \bar{\sigma}_{a,1}^{49}\bar{\phi}_1)T_{op,0}} \tag{4.63}$$

Equation (4.63) can be easily obtained from Equation (4.56) by replacing $T_{op,0}$ by $1/3T_{op,0}$.

Considering the solution of the depletion equation, Equation (4.1) with an initial fissile loading (i.e., $M_{49}(0) \neq 0$);

$$M^{49}(T) = M_{28}(0) \cdot \Sigma \cdot (e^{-\bar{\sigma}_a^{28}\bar{\phi}T} - e^{-\bar{\sigma}_a^{49}\bar{\phi}T}) + M_{49}(0)\, e^{-\bar{\sigma}_a^{49}\bar{\phi}T} \tag{4.64}$$

The net plutonium inventory after the second cycle, $2/3T_{op,0}$, is

$$M_{IO,2}^{49}(2/3T_{op,0}) = [1/3M_{28}(0) - M_{IO,1}^{49}] \cdot \Sigma_2 \cdot (e^{-\bar{\sigma}_{a,2}^{28}\bar{\phi}_2 \cdot 1/3T_{op,0}}$$

$$- e^{-\bar{\sigma}_{a,2}^{49}\bar{\phi}_2 \cdot 1/3T_{op,0}}) + M_{IO,1}^{49}\, e^{-\bar{\sigma}_{a,2}^{49}\bar{\phi}_2 \cdot 1/3T_{op,0}}$$

$$= 1/9M_{28}(0) \cdot T_{op,0}[S_{o,1}\, e^{-1/6(\bar{\sigma}^{28}_{a,1}\bar{\phi}_1 + \bar{\sigma}^{49}_{a,1}\bar{\phi}_1 + 2\bar{\sigma}^{49}_{a,2}\bar{\phi}_2)T_{op,0}}$$

$$+ S_{o,2}\, e^{-1/6(\bar{\sigma}^{28}_{a,2}\bar{\phi}_2 + \bar{\sigma}^{49}_{a,2}\bar{\phi}_2)T_{op,0}}] \qquad (4.65)$$

where $(\Sigma_i \cdot \Sigma_j)$ is neglected because of its small value ($\sim$0.01).

After the final cycle, $T_{op,0}$, the plutonium inventory of fuel assemblies in the third row is

$$M^{49}_{IO,3}(T_{op,0}) = [1/3M_{28}(0) - M^{49}_{IO,2}] \cdot \Sigma_3 \cdot (e^{-\bar{\sigma}^{28}_{a,3}\bar{\phi}_3 \cdot 1/3T_{op,0}}$$

$$- e^{-\bar{\sigma}^{49}_{a,3}\bar{\phi}_3 T_{op,0}}) + M^{49}_{IO,2}\, e^{-\bar{\sigma}^{49}_{a,3}\bar{\phi}_3 \cdot 1/3T_{op,0}}$$

$$= 1/9M_{28}(0)T_{op,0}[S_{o,1}e^{-1/6(\bar{\sigma}^{28}_{a,1}\bar{\phi}_1 + \bar{\sigma}^{49}_{a,1}\bar{\phi}_1 + 2\bar{\sigma}^{49}_{a,2}\bar{\phi}_2 + 2\bar{\sigma}^{49}_{a,3}\bar{\phi}_3)T_{op,0}}$$

$$+ S_{o,2}e^{-1/6(\bar{\sigma}^{28}_{a,2}\bar{\phi}_2 + \bar{\sigma}^{49}_{a,2}\bar{\phi}_2 + 2\bar{\sigma}^{49}_{a,3}\bar{\phi}_3)T_{op,0}} + S_{o,3}e^{-1/6(\bar{\sigma}^{28}_{a,3}\bar{\phi}_3 + \bar{\sigma}^{49}_{a,3}\bar{\phi}_3)T_{op,0}}]$$

$$(4.66)$$

Therefore, the total plutonium produced through the third cycle is

$$M^{49}_{IO,0} = 3 \cdot M^{49}_{IO,3} = 1/3M_{28}(0)T_{op,0} \sum_{i=1}^{3} S_{o,i}\, e^{-R_{IO,i}T_{op,0}} \qquad (4.67)$$

where

$$R_{IO,1} = 1/6(\bar{\sigma}^{28}_{a,1}\bar{\phi}_1 + \bar{\sigma}^{49}_{a,1}\bar{\phi}_1 + 2\bar{\sigma}^{49}_{a,2}\bar{\phi}_2 + 2\bar{\sigma}^{49}_{a,3}\bar{\phi}_3)$$

$$R_{IO,2} = 1/6(\bar{\sigma}^{28}_{a,2}\bar{\phi}_2 + \bar{\sigma}^{49}_{a,2}\bar{\phi}_2 + 2\bar{\sigma}^{49}_{a,3}\bar{\phi}_3)$$

$$R_{IO,3} = 1/6(\bar{\sigma}^{28}_{a,3}\bar{\phi}_3 + \bar{\sigma}^{49}_{a,3}\bar{\phi}_3)$$

The steady-stage (average) fissile buildup rate in the whole blanket is

$$\bar{M}_{IO,0} = \frac{M^{49}_{IO,0}}{T_{op,0}} = 1/3M_{28}(0) \cdot \sum_{i=1}^{3} S_{o,i} \; e^{-R_{IO,i} \; T_{op,0}} \qquad (4.68)$$

3) Out-In Shuffling case; all characteristics of the Out-In fuel shuffling option are similar to those of the In-Out Shuffling case. The total plutonium produced and the average plutonium production rate are obtained using Eqs. (4.67) and (4.68), where subscript 3 is replaced by 1 and vice versa.

$$M^{49}_{OI,0} = 3 \cdot M^{49}_{IO,1} = 1/3M_{28}(0)T_{op,0} \sum_{i=1}^{3} S_{o,i} \; e^{-R_{OI,i}T_{op,0}} \qquad (4.69)$$

where

$$R_{OI,1} = 1/6(\bar{\sigma}^{28}_{a,1}\bar{\Phi}_1 + \bar{\sigma}^{28}_{a,1}\bar{\Phi}_1)$$

$$R_{OI,2} = 1/6(\bar{\sigma}^{28}_{a,2}\bar{\Phi}_2 + \bar{\sigma}^{49}_{a,2}\bar{\Phi}_2 + 2\bar{\sigma}^{49}_{a,1}\bar{\Phi}_1)$$

$$R_{OI,3} = 1/6(\bar{\sigma}^{28}_{a,3}\bar{\Phi}_3 + \bar{\sigma}^{49}_{a,3}\bar{\Phi}_3 + 2\bar{\sigma}^{49}_{a,1}\bar{\Phi}_1 + 2\bar{\sigma}^{49}_{a,2}\bar{\Phi}_2)$$

$$\bar{M}^{49}_{OI,0} = M^{49}_{OI,0}/T_{op,0} = 1/3M_{28}(0) \sum_{i=1}^{3} S_{o,i} \; e^{-R_{OI,i} \; T_{op,0}} \qquad (4.70)$$

4) Zone or Region-Scatter Case; In this fuel management option, each individual fuel assembly is refueled at its own local optimim irradiation time.

Let $T_{op,i}$ be the optimum irradiation time of row i, then the plutonium produced up to $T_{op,i}(M^{49}_{RS,i})$ can be written as in Eq. (4.56);

$$M_{RS,1}^{49}(T_{op,1}) = 1/3M_{28}(0) \cdot S_{o,1} \cdot T_{op,1}\, e^{-1/2(\bar{\sigma}_{a,1}^{28}\bar{\phi}_1 + \bar{\sigma}_{a,1}^{49}\bar{\phi}_1)T_{op,1}} \quad (4.71)$$

$$M_{RS,2}^{49}(T_{op,2}) = 1/3M_{28}(0) \cdot S_{o,2} \cdot T_{op,2}\, e^{-1/2(\bar{\sigma}_{a,2}^{28}\bar{\phi}_2 + \bar{\sigma}_{a,2}^{49}\bar{\phi}_2)T_{op,2}} \quad (4.72)$$

$$M_{RS,3}^{49}(T_{op,3}) = 1/3M_{28}(0) \cdot S_{o,3} \cdot T_{op,3}\, e^{-1/2(\bar{\sigma}_{a,3}^{28}\bar{\phi}_3 + \bar{\sigma}_{a,3}^{49}\bar{\phi}_3)T_{op,3}} \quad (4.73)$$

In section 4.3.2.1, a general equation for the optimum irradiation time was derived, culminating in Equation (4.25), which is valid for all blanket regions and various fuel materials.

Recalling Equation (4.25), we can express $T_{op,i}$ as:

$$T_{op,i} = F_1\left[\frac{\bar{\omega}}{S_{o,i} \cdot r_{4,i}}\right]^{1/2} \quad (4.74)$$

where F_1 is a constant. The ratio of local optimum irradiation time to whole blanket optimum irradiation time can be expressed as

$$\frac{T_{op,i}}{T_{op,0}} = \left[\frac{S_{o,0} \cdot r_{4,0}}{S_{o,i} \cdot r_{4,i}}\right]^{1/2} \quad (4.75)$$

Using Equation (4.75), the accumulated plutonium, $M_{RS,i}^{49}$, can be written as a function of $T_{op,0}$;

$$M^{49}_{RS,1}(T_{op,1}) = 1/3M_{28}(0) \cdot S_{o,1} \cdot T_{op,1} \cdot e^{-R_{RS,1}T_{op,0}}$$

$$= 1/3M_{28}(0) \cdot [S_{o,0} \cdot S_{o,1} \cdot r_{4,0}/r_{4,1}]^{1/2} T_{op,0}\ e^{-R_{RS,1}T_{op,0}} \tag{4.76}$$

$$M^{49}_{RS,2}(T_{op,2}) = 1/3M_{28}(0) \cdot S_{o,2} \cdot T_{op,2} \cdot e^{-R_{RS,2}T_{op,0}}$$

$$= 1/3M_{28}(0) \cdot [S_{o,0} \cdot S_{o,1} \cdot r_{4,0}/r_{4,2}]^{1/2} T_{op,0}\ e^{-R_{RS,2}T_{op,0}} \tag{4.77}$$

$$M^{49}_{RS,3}(T_{op,3}) = 1/3M_{28}(0) \cdot S_{o,3} \cdot T_{op,3} \cdot e^{-R_{RS,3}T_{op,0}}$$

$$= 1/3M_{28}(0) \cdot [S_{o,0} \cdot S_{o,1} \cdot r_{4,0}/r_{4,3}]^{1/2} T_{op,0}\ e^{-R_{RS,3}T_{op,0}} \tag{4.78}$$

where

$$R_{RS,1} = 1/2(\bar{\sigma}^{28}_{a,1}\bar{\phi}_1 + \bar{\sigma}^{49}_{a,1}\bar{\phi}_1)\left(\frac{S_{o,0} \cdot r_{4,0}}{S_{o,1} \cdot r_{4,1}}\right)^{1/2}$$

$$R_{RS,2} = 1/2(\bar{\sigma}^{28}_{a,2}\bar{\phi}_2 + \bar{\sigma}^{49}_{a,2}\bar{\phi}_2)\left(\frac{S_{o,0} \cdot r_{4,0}}{S_{o,2} \cdot r_{4,2}}\right)^{1/2}$$

$$R_{RS,3} = 1/2(\bar{\sigma}^{28}_{a,3}\bar{\phi}_3 + \bar{\sigma}^{49}_{a,3}\bar{\phi}_3)\left(\frac{S_{o,0} \cdot r_{4,0}}{S_{o,3} \cdot r_{4,3}}\right)^{1/2}$$

The steady state plutonium production rate of the region scatter fuel management scheme is now

$$\bar{M}^{49}_{RS,0} = \frac{M^{49}_{RS,1}(T_{op,1})}{T_{op,1}} + \frac{M^{49}_{RS,2}(T_{op,2})}{T_{op,2}} + \frac{M^{49}_{RS,3}(T_{op,3})}{T_{op,3}}$$

$$= 1/3M_{28}(0) \sum_{i=1}^{3} (S_{o,i}\, e^{-R_{RS,i}T_{op,0}}) \qquad (4.79)$$

Equations (4.61), (4.68), (4.70) and (4.79) indicate that the steady state plutonium production rate of each fuel management option can be written in the same equation format, i.e.

$$\bar{M}_{FM,0} = 1/3M_{28}(0) \sum_{i=1}^{3} (S_{o,i}\, e^{-R_{FM,i}T_{op,0}}) \qquad (4.80)$$

where subscript FM identifies the fuel management scheme.

The Linear enrichment buildup rates of each row, $S_{o,i}$, were assumed constant for this study. Therefore, the differences caused by the different fuel management schemes are expressed in the exponential function, $e^{-R_{FM,i}T_{op,0}}$. Table 4.10 shows the steady state plutonium production rate, $\bar{M}^{49}_{FM,0}$, and associated parameter $R_{FM,i}$. The batch option produces about 15% less plutonium than the others and the Out-In scheme produces slightly more plutonium than the other options do, which is results from the low $R_{OI,1}$, as shown in Table 4.10.

Barthold (B1) reviewed fuel shuffling schemes in LMFBR blankets, and concluded that the plutonium production in the blanket is in a first order approximation the same for no shuffling, Out-In shuffling and In-Out shuffling. This different conclusion is merely caused by the approximated depletion equations which were developed under the assumption of constant U-238 concentration. On the other hand, Lake et.al. (L1) found that Out-In radial blanket fuel shuffling option offers a 0.005 higher breeding

TABLE 4.10

COMPARISON OF STEADY-STATE PU PRODUCTION RATES OF VARIOUS FUEL MANAGEMENT OPTIONS†

Parameter \ Option	Batch	In-Out	Out-In	Region*** Scatter
$R_{FM,1}(yr^{-1})$	0.07319	0.05191	0.02439	0.04201
$R_{FM,2}(yr^{-1})$	0.03221	0.01844	0.05529	0.03647
$R_{FM,3}(yr^{-1})$	0.01244	0.00415	0.06851	0.02744
$\sum_{i=1}^{3}(S_{o,i}e^{-R_{FM,i}T_{op,0}^{*}})$	0.01238	0.01410	0.01429	0.01392
$\bar{M}_{FM,0}^{49}$**	71.3886	81.3091	82.4291	80.2506
$\bar{M}_{FM,0}^{49}/\bar{M}_{NS,0}^{49}$	1.0	1.139	1.155	1.124

† UO_2 Fueled 3-row Radial Blanket under Reference Economic/Neutronic Environment (Accounting Method A)

* $T_{op,0}$ = 7.49 (yr)

$S_{o,1}$ = 0.01203 (KgPu/Kg M_{HM}yr), $S_{o,2}$ = 0.00489

$S_{o,3}$ = 0.00174 , $S_{o,0}$ = 0.00587

** Unit is KgPu/yr

$M_{28}(0)$ = 17299 Kg

*** $r_{4,1}$ = 0.12065 , $r_{4,2}$ = 0.07629

$r_{4,3}$ = 0.05529 , $r_{4,0}$ = 0.081475 ratio over that of In-Out radial blanket fuel shuffling options; this result coincides with our findings. However, they choose the In-Out fuel shuffling option because of its low power gradient characteristics in radial blankets.

4.5.3 Maximum Enrichment (Power) Swing During Burnup

In the previous section, the plutonium produced in each row and the average plutonium production rate were derived. The discharge enrichment and average enrichment buildup rate can be readily interpreted in terms of these results, i.e., the enrichment of a fuel assembly in row i at total irradiation time T is

$$\varepsilon^{49}_{FM,i} = \frac{M^{49}_{FM,i}(T)}{M^{28}_{i}(0)} \tag{4.82}$$

where FM designates one of the fuel management options.

To compare enrichment changes during burnup with the batch reference option, the maximum enrichment swing (MES) is defined as

$$MES_{FM} \equiv \frac{\text{Max. enrichment change of FM option in 1st row}}{\text{Max. discharge enrichment of Batch option in 1st row}}$$

$$= \varepsilon^{49}_{FM,1}/\varepsilon^{49}_{NS,1} \tag{4.83}$$

Table 4.11 shows the maximum enrichment swing of various fuel management options. The Out-In fuel shuffling scheme is clearly superior to the others with respect to maximum enrichment swing. This means that enrichment changes in the fuel assemblies in the first row (or any other row) from BOL to EOL are minimized by the adoption of Out-In shuffling. This will greatly facilitate orificing of the coolant flow to avoid blanket overcooling and severe sodium striping.

TABLE 4.11

MAXIMUM ENRICHMENT (POWER) SWING IN BLANKET ROW 1
OF VARIOUS FUEL MANAGEMENT OPTIONS†

Option*	MES_{FM}	Duration of Fuel Irradiation
Batch	1.0	$0 \sim T_{op,0}$
In-Out	0.480	$0 \sim 1/3\ T_{op,0}$
Out-In	0.390	$2/3\ T_{op,0} \sim T_{op,0}$
Region Scatter	0.725	$0 \sim T_{op,1}$

† 1000 MWe Reference Core with UO_2 Fuel

* UO_2 Fueled 3-row Radial Blanket Under Reference Economic/Neutronic Environment (Accounting Method A)

4.5.4 Effects of Fuel Management Options on Blanket Optimum Parameters

As shown in Section 4.3, blanket economics are characterized by optimum irradiation time, breakeven time, maximum blanket revenue and optimum discharge enrichment, which are strongly dependent on the economic parameter ($\bar{\omega}$), the linear enrichment buildup rate (S_o), as well as non-linearity parameter (ξ/T_c°) and financial parameter (r_3).

To analyze the characteristics of various fuel management options simply, fixed neutron cross-sections and flux in addition to fixed economic/financial environment were assumed in Section 4.5.1. Therefore, the only parameter which varies in response to a change of fuel management schemes is the non-linearity parameter, ξ/T_c°, i.e., the effects of fuel management options on blanket economics come from the variation of the non-linear characteristics of fissile buildup (ξ/T_c°) or r_4.

For example, if ξ/T_c° is reduced by the switch from the batch to the Out-In shuffling scheme, then r_4, since $r_4 = r_3 + \xi/T_c^\circ$, will be automatically smaller, which will result in a longer optimum irradiation time and higher blanket revenue.

Comparing Eq. (4.80) with the general one-region equation, Eq. (4.11), and rearranging these two equations, the non-linearity parameter, ξ/T_c°, can be correlated with the appropriate parameters of a two or three region (row) blanket, $R_{FM,i}$.

Let

$$S_{o,0} \equiv \frac{S_{o,1} + S_{o,2} + S_{o,3}}{3} \tag{4.84}$$

Equation (4.80) can be equated to Equation (4.11);

$$\bar{M}^{49}_{FM,0} = 1/3M_{28}(0) \sum_{i=1}^{3} (S_{o,i}\, e^{-R_{FM,i}T_{op,0}})$$

$$= M_{28}(0) \cdot S_{o,0} \cdot e^{-\xi\frac{T_{op,0}}{T_c^\circ}}$$

$$= 1/3M_{28}(0) \cdot (S_{o,1} + S_{o,2} + S_{o,3}) \cdot e^{-\xi\frac{T_{op,0}}{T_c^\circ}} \qquad (4.85)$$

where

$$S_{o,0} \equiv \frac{\hat{M}_{49}}{M_{28}(0)} \cdot \frac{1}{T_c^\circ} \text{ in Equation (4.11)}$$

Equation (4.85) can be simplified and rearranged as

$$S_{o,1}\, e^{-R_{FM,1}T_{op,0}} + S_{o,2}\, e^{-R_{FM,2}T_{op,0}} + S_{o,3}\, e^{-R_{FM,3}T_{op,0}}$$

$$= (S_{o,1} + S_{o,2} + S_{o,3})\, e^{-\xi\frac{T_{op,0}}{T_c^\circ}} \qquad (4.86)$$

If we use a first order approximation for the exponential function, Equation (4.86) will become,

$$S_{o,1}(1 - R_{FM,1}T_{op,0}) + S_{o,2}(1 - R_{FM,2}T_{o,0}\ ) + S_{o,3}(1 - R_{FM,3}T_{op,0})$$

$$= (S_{o,1} + S_{o,2} + S_{o,3})(1 - \frac{\sum_{i=1}^{3} S_{o,i}R_{FM,i}T_{op,0}}{\sum_{i=1}^{3} S_{o,i}})$$

$$= (S_{o,1} + S_{o,2} + S_{o,3})(1 - \xi\frac{T_{op,0}}{T_c^\circ}) \qquad (4.87)$$

Solving Equation (4.87) for ξ/T_c°, one obtains

$$\xi/T_c^{\circ} \cong \frac{\sum_{i=1}^{3} S_{o,i} R_{FM,i}}{\sum_{i=1}^{3} S_{o,i}} = \frac{\sum_{i=1}^{3} S_{o,i} R_{FM,i}}{3\, S_{o,0}} \tag{4.88}$$

By the definition of r_4, one can write

$$r_4 \cong r_3 + \xi/T_c^{\circ} = r_3 + \frac{\sum_{i=1}^{3} S_{o,i} R_{FM,i}}{3\, S_{o,0}} \tag{4.89}$$

Table 4.12 summarizes the effects on blanket parameters arising from the variation of r_4. Table 4.12 shows that the No-shuffling scheme is the worst case for blanket economics and In-Out and Out-In shuffling schemes are the best we can choose. The zone scatter schemes are also advantageous compared to the No-shuffling case; however, the plutonium production rate and maximum blanket revenue achieved are less than those of the In-Out or Out-In shuffling schemes.

4.6 SUMMARY

In this chapter, an economic analysis of FBR blankets has been performed. Blanket economics are characterized by certain key parameters - optimum irradiation time, breakeven time, maximum blanket revenue and optimum discharge enrichment, all of which were simply correlated with economic-financial-neutronic factors.

The first part of this chapter was devoted to development of simple, generalized correlations for fissile buildup histories in FBR blankets;

TABLE 4.12

EFFECTS OF FUEL MANAGEMENT OPTIONS ON BLANKET OPTIMUM PARAMETERS

PARAMETER (eq.)	EFFECTS*
Optimum Irradiation Time $T_{op} = F_1 \left(\frac{\bar{\omega}}{S_o r_4}\right)^{1/2}$	Optimum Irradiation Time is slightly increased (by ~10%) because of smaller r_4 (0.097 vs. ~0.078)**
Breakeven Time $T_{BE} = F_2 \left(\frac{\bar{\omega}}{S_o}\right)$	Breakeven Time is not appreciably dependent on r_4. Therefore, it is not affected by the choice of fuel management option.
Maximum Blanket Revenue $e_m \propto [(\bar{C}_1 + \bar{C}_2)\bar{C}_3 S_o \cdot r_4]^{1/2} \cdot F_3$	Lower r_4 and higher Pu production rate offers ~30% higher (0.07 mills/KW-Hr vs. ~0.05 mills/KW-Hr) blanket revenue.

*No Shuffling is Reference Case in Accounting Method A

**Calculated values of r_4 for batch vs. other options are

r_4 (Batch) = 0.0968 (actual 2DB/BRECON value is 0.082)
r_4 (In-Out) = 0.0787
r_4 (Out-In) = 0.0766
r_4 (Region Scatter) = 0.0792

a step which is an essential prerequisite for the analysis of fuel cycle costs and fuel management decisions. These simple correlations can be applied to various blanket compositions and configurations, and can accurately predict isotopic composition during burnup without further recourse to expensive computer calculations.

Economic blanket parameters were optimized using the simple correlations and analyzed with respect to each independent variable.Optimum irradition time is mainly affected by Pu market value (c_3), linear enrichment buildup rate and modified financial factor r_4. In addition to these main factors, the non-linear characterization factor, ξ/T_c°,is also important to determination of the optimum irradition time.

The Breakeven time is simply determined by the economic environment factor, $\bar{\omega}$, and the linear enrichment buildup factor S_o. This simplicity is due in part to the fact that breakeven times are reached early in fuel life when the linear fissile buildup model is valid for the prediction of fissile material accumulation in FBR blankets. An equation for determining the economic blanket thickness was readily derived from the requirement that a breakeven time exist.

Maximum blanket revenue is mainly determined by Pu-market value (c_3), linear enrichment buildup rate (S_o) and fabrication cost (c_1). Analysis shows that oxide fuel, which has the softest spectrum and highest value of S_o, offers the highest maximum blanket revenue compared to carbide and metal alloy fuels. In this study the economic environment, (i.e. costs per kg - c_1, c_2, c_3) was considered the same for all types of fuel materials. Only if fabrication (or less likely, reprocessing) costs of metal or carbide fuels are cheaper than for oxide fuel are these advanced fuels attractive for blanket applications.

A sensitivity study was also performed for the optimum blanket parameters, and possible blanket fuel management options were reviewed and their effects on blanket economics were evaluated.

Accounting method A and B, as originally defined by Brewer, were considered. As shown through comparison of the results summarized in Table 4.13, we have confirmed that the accounting convention employed has a strong effect on blanket management decisions. Accounting method A is to be prefered because blanket revenue is greater.

In summary, a comprehensive and simple model of blanket economics has been developed. The simple analytical expressions derived for optimum blanket parameters indicate that:

1. The most sensitive factors governing blanket economics are fabrication cost, Pu market value and linear enrichment buildup rate.
2. The non-linearity factor, which is related to the neutron spectrum, is important to determination of the optimum irradiation time and maximum blanket revenue.
3. By appropriate attention to fuel management - for example by choice of an Out-In shuffling scheme - plutonium production and maximum blanket revenue can be increased by up to 15% over that in a batch management scheme.

TABLE 4.13

COMPARISON OF ACCOUNTING METHOD A AND B†

Accounting Method	A	B
Modified Cost Component Fab. ($/kg) Rep. ($/kg) Pu-value ($/kg)	 74.7468 48.0395 9607.8944	 74.7468 46.1558 9231.1635
Optimum Irradiation Time (yr)	4.3	3.7
Breakeven Time (yr)	1.3	1.4
Max. Blanket Revenue (mills/KW-Hr)	0.055	0.036
Optimum Discharge Enrichment	0.0391	0.0335

† 1st Row of 3-row Radial Blanket, All Driven by Same Core

CHAPTER 5

EVALUATION OF FBR BLANKET DESIGN CONCEPTS

5.1 INTRODUCTION

In the previous two chapters, the neutronic and economic characteristics of FBR blankets were analyzed using both simple theoretical equations and confirmatory computer calculations.

In practice, the design of FBR blankets involves a compromise between engineering considerations, safety problems, reactor physics and economics. Often, these requirements are in conflict. Low fuel cycle costs can be obtained at the expense of high external breeding ratio, conversely the more complete neutron utilization required to achieve a high breeding ratio leads to thicker blankets and the value of the additional fissile production may not cancel out the increased fabrication and reprocessing costs. Higher fuel density and thicker blankets, on the other hand, are also favorable from a radiation and thermal shielding standpoint, which may, on an overall system basis, provide compensatory savings.

In this chapter, several advanced/new FBR blanket design concepts will be analyzed, not only from the view of fissile production, but also considering economic, engineering and material constraints.

Core variations - heterogeneous cores, parfait and sandwiched internal blankets - will be examined in addition to several simple external blanket modifications involving fissile seeding, improved reflection, or moderator addition, both uniform and heterogeneous.

Advanced blanket design concepts can be classified into the following four categories:

1. Design concepts emphasizing neutron spectrum variations - moderated blankets, spectrum hardened blankets.
2. Design concepts emphasizing high neutron utilization - especially reflected blankets and blankets with high fuel volume fraction.
3. Design concepts emphasizing a high rate of internal neutron generation - fissile seeded blankets.
4. Design concepts emphasizing geometrical rearrangements - parfait blankets, sandwiched blankets, and heterogeneous core concepts.

In this chapter, accounting method A is used for all economic calculations.

5.2 ADVANCED BLANKET DESIGN CONCEPTS INVOLVING NEUTRON SPECTRUM TAILORING

5.2.1 The Moderated Blanket

5.2.1.1 General Design Concepts

Moderated blankets have been examined and analyzed in several past studies. Okrent (O1)(O2)(O3) proposed that the insertion of moderating material such as graphite or beryllium oxide in FBR blankets would allow a smaller effective blanket thickness to be used without appreciably reducing the total amount of fissile produced. Munno (M6) indicated in his calculations that carbon, uniformly distributed in the radial zones resulted in significantly decreased fuel cycle costs. Mayer (M2) on the other hand, considered graphite, ZrH_2, and BeO in a steam cooled fast reactor radial blanket and concluded that moderated blankets offered no significant economic advantages. Perks et al (P1) examined many possible moderator variations (for fixed core parameters) - graphite, graphite-steel, borated graphite and sodium, and found that a conventional design having an 8-in. thick radial blanket adjacent to the core achieved the highest total and external breeding ratio among all the moderated or moderator-seeded blankets considered. Similar results were also described by Butler et al (B7). The purpose of this section is to develop an understanding of the neutronic and economic characteristics of moderated blankets and to evaluate their performance.

In Chapters 3 and 4, the fissile breeding performance and economic contribution of the blankets to the total system were analyzed for the case of a single fuel material and homogeneous fuel distribution in the blankets. As a result of this analysis, we found that a low concentration of fuel material - leading to a soft neutron spectrum in the blanket - has favorable economic aspects because of the high associated fissile breeding rate, while as regards the breeding ratio, achieving high fertile density (hence a hard neutron spectrum) is more important.

These contradictory characteristics complicate blanket design, where both high breeding ratio and good economic performance are desired. If pure fuel materials are used, the fertile density varies considerably more than does the spectrum-averaged microscopic cross section: the ratio of the fertile density of carbide fuel to that of oxide fuel is 1.34 while the ratio of the fertile microscopic capture cross-section of oxide fuel to that of carbide fuel is only 1.09. The purpose of moderator addition to the blankets is to create a softer neutron spectrum, which increases the fertile neutron capture cross-section and the blanket-averaged neutron flux sufficiently to offset the disadvantages of lower fertile density. An important effect of moderator seeding is that the optimum fuel irradiation time, T_{op}, is always shortened due to the spectrum softening. As described in Eq. (4.25), the optimum fuel irradiation time is inversely proportional to $(S_o r_4)^{1/2}$, thus a high fissile buildup rate, S_o, (and r_4) reduces the fuel optimum irradiation time. This feature can be put to good use in its own right if the fuel irradiation would exceed a materials limit if subjected to a longer irradiation; in such cases moderator addition may solve the problem without penalizing the breeding ratio or blanket revenue.

Table 5.1 shows the effects of moderator addition on the optimum irradiation time of UC-fueled radial blankets. The optimum fuel irradiation time is sharply decreased by moderator seeding.

5.2.1.2 Optional Design Features

The Selection of Moderator Material is very important, particularly as regards neutron absorption by the moderator material and compatibility with other fuel constitutents, clad or structural metals, or coolants.

Moderators having a high moderating ratio ($\xi\sigma$ /σ_a) and slowing down power ($\xi\Sigma_s$), such as beryllium oxide, which is used in this study, are preferable.

Heterogeneous and Homogeneous Moderator Seeding have similar effects on fissile breeding and blanket economics, presumable since fast neutron mean free paths are long compared to fuel pin and even subassembly dimensions. Table 5.2 compares results calculated for heterogeneous and homogeneous moderator seeding in the 2nd row of the radial blanket; Figure 5.1 depicts the layout of the heterogeneously-moderated blanket. Reference parameters for the LCCEWG benchmark problem, described in Appendix D, were used for the calculation of the heterogeneously-moderated blankets, while the reference core configuration, design parameters and cross-section set described in

TABLE 5.1

EFFECTS OF MODERATOR SEEDING* ON THE OPTIMUM FUEL IRRADIATION TIME

	UC			
	3-row Blanket		2-row Blanket	
	Reference**	Moderated	Reference**	Moderated
$M_{28}(0)$, Kg	23233	19361	14701	10829
S_o, KgPu/KgM_{HM}Yr	0.00466	0.00553	0.00719	0.00883
r_4	0.07071	0.08211	0.09049	0.11233
T_{op}, yrs	9.25	7.81	6.14	4.99
Internal breeding ratio bi	0.5899	0.5894	0.5898	0.5894
Radial blanket breeding ratio,bxr	0.2824	0.2805	0.2754	0.2688

*25 v/o BeO added homogeneously to 2nd row only.

** Refer to Chapter 2 for reference cases.

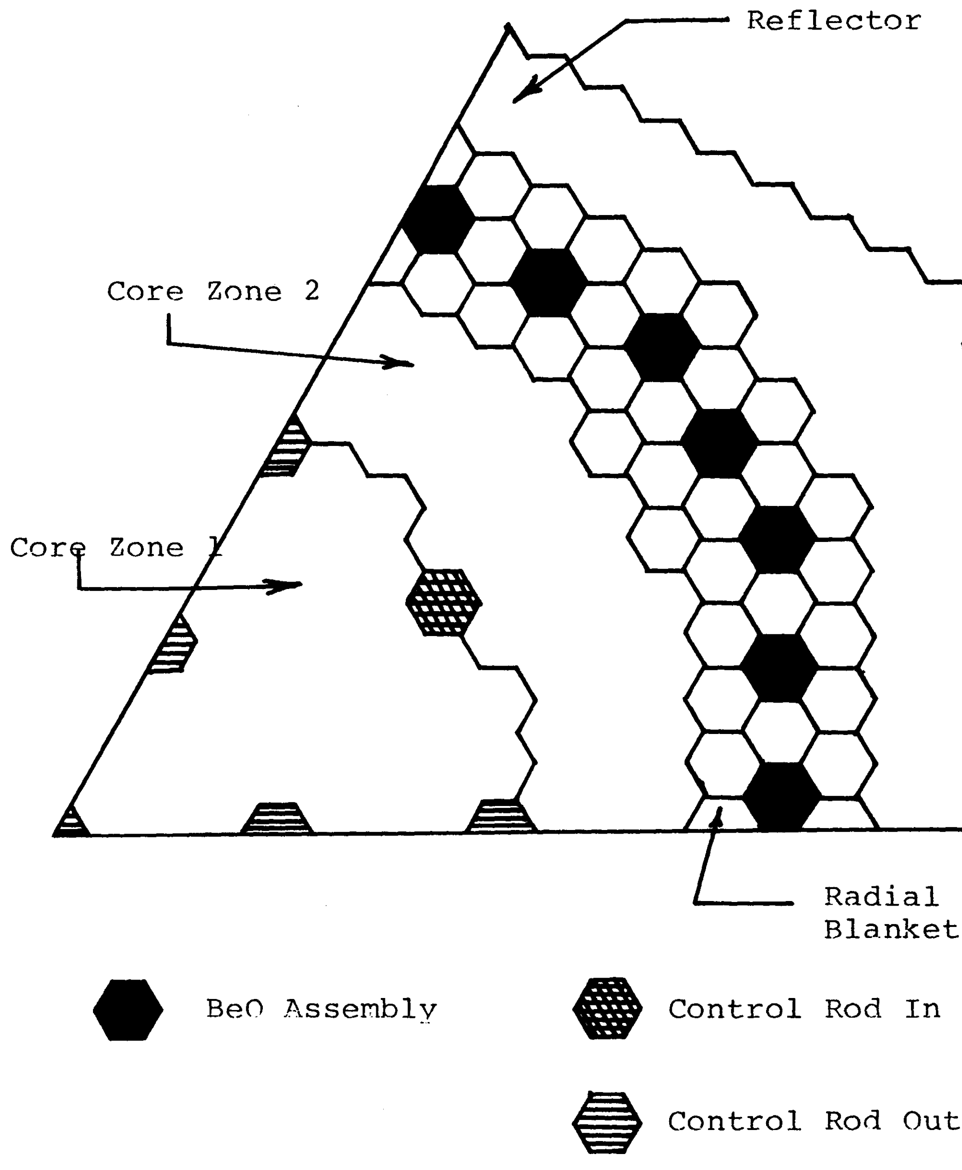

*(1/6 of core shown - calculations used 1/4 core)

Fig. 5.1 CONFIGURATION USED TO STUDY HETEROGENEOUS MODERATOR SEEDING IN THE MIDDLE ROW OF A RADIAL BLANKET

TABLE 5.2

COMPARISON OF RESULTS CALCULATED FOR HETEROGENEOUS AND HOMOGENEOUS MODERATOR SEEDING

	FRACTIONAL CHANGE IN PARAMETER	
Parameter	Heterogeneous Seeding*	Homogeneous Seeding**
M_B^{28}	0.83	0.83
$\sigma_{c,B}^{28}$	1.166	1.162
$\bar{\phi}_B$	1.020	1.042
S_o	1.1902	1.211
bi	1.000	0.998
bxr	0.985	1.004

* Refer to Appendix D for core configurations and material compositions of reference case.
X-Y (triangular) dimension was used for this calculation

** Calculated in cylindrical geometry using the reference case specified for this study

Chapter 2, were used for the calculation of the homogeneously-moderated blankets. Even though the design parameters and cross-sections used to calculate the characteristics of these two moderated blankets were different, all results are consistent within acceptable margins.

Core performance is not affected by moderator seeding in the 2nd row of the blanket and, in particular, the internal breeding ratio is not changed at all. The variation of the fissile buildup rate in the blanket (S_o) depends on the total inventory of moderator material, the neutronic characteristics of the moderator and the neutron spectrum and flux existing in the blankets before moderator seeding.

Since fuel fabrication without the addition of special moderating materials is conventional practice, and thus less expensive, heterogeneous moderator seeding may be the more practical alternative.

Heterogeneous Moderator Seeding in the Middle Row only was chosen for the present study, which was found to be the most favorable alternative with respect to fissile breeding performance (Pl) and blanket economic considerations. This is so because:

a. Most of the important blanket functions are performed in the first row of the blanket. Moderator seeding in the middle row improves the fissile breeding function of the first row due to the increased reflection of low energy neutrons from the second row.

b. Moderator seeding in the middle row helps prevent neutron leakage into the reflector region without significant neutron absorption by the moderator. Moderator seeding in the first row is penalized by neutron absorption by the moderator, which decreases the breeding ratio, and moderator seeding in the third row has an insignificant effect because of the low neutron flux in this region.

5.2.1.3 Neutronic Aspects of Moderated Blankets

The advantages of moderated blankets stem from:

a. high fertile capture cross-sections due to the softened neutron spectrum,

b. higher average neutron flux ($\bar{\phi}_B$) in the blanket region,

c. lower neutron leakage into the reflector region.

The above factors are very favorable as regards achievement of a high external breeding ratio. However, two side effects counter the improvement:

a. fertile inventory is decreased (some fuel must be displaced to make room for the moderator); this decreases the blanket-averaged <u>macroscopic</u> cross-section of the fertile species and also the fertile fast fission bonus.

b. neutron absorption by the moderator increases the parasitic neutron absorption loss.

The net result is that the fraction of total neutrons absorbed by fertile species is actually the same or slightly smaller when the moderator is added, as shown in Table 5.3. As established in Chapter 3, fertile density in the blanket region is the most sensitive parameter as regards breeding performance, and this result is to be expected regardless of the blanket thickness and fuel materials employed.

TABLE 5.3

NEUTRONIC CHARACTERISTICS OF REFERENCE (Ref.) AND MODERATED (Mod.) RADIAL BLANKETS†

Fuel Mat.	UO_2				UC_2				UC			
Thickness	3-row		2-row		3-row		2-row		3-row		2-row	
	Ref.	Mod.	Ref.	Mod.	Ref.	Mod.	Ref.	Mod.	Ref.	Mod.	Ref.	Mod.
$\bar{\sigma}^{28}_{c,B}$ (b)	0.4025	0.4677	0.4173	0.4876	0.4209	0.4709	0.4295	0.4854	0.3692	0.4216	0.3806	0.4386
$\bar{\phi}_B$ ($X10^{-14}$ #/cm^2-sec)	5.6269	5.8655	8.4077	8.9621	5.0691	5.3468	7.6320	8.2292	4.8720	5.0589	7.2872	7.7680
$M_{28}(0)$	17299	14416	10946	8063	18999	15833	12022	8856	23233	19361	14701	10829
A^{49}_c *	3.153	3.154	3.153	3.155	3.153	3.155	3.153	3.157	3.143	3.145	3.143	3.146
bi	0.5888	0.5877	0.5880	0.5879	0.5887	0.5882	0.5887	0.5883	0.5899	0.5894	0.5898	0.5894
bxr	0.2639	0.2650	0.2586	0.2511	0.2729	0.2697	0.2652	0.2568	0.2824	0.2805	0.2754	0.2688

† 25 % BeO was homogeneously added to the 2nd row only

* Neutron Absorption rate in the core region ($X10^{-19}$ #/zone-sec)

The internal core breeding ratio is not affected by moderator seeding in the blanket. The neutron absorption rate of Pu-239 in the core region, A_c^{49}, which is a key factor characterizing core performance, is the same for all blanket fuel materials.

Therefore, the core and blanket characteristics related to the fissile breeding function remain basically unaltered if moderator material is added in the second row of the radial blanket.

5.2.1.4 Economic Aspects of Moderated Blankets

A possible attractive feature of moderated blankets may be their potential for the improvement of blanket revenue due to their high fissile buildup rate (S_o). As shown in Eq. (4.38), the maximum blanket revenue is a function of the total mass of heavy metal loaded in the blankets, fissile buildup rate ($S_o = \bar{\sigma}_{c,B}^{28} \cdot \bar{\phi}_B$), economic parameters, and parameter r_4 which is related to the financial parameter r_3 and to the non-linear nature of the fissile buildup history with time.

If we assume that all economic/financial parameters ($\bar{c}_1$, $\bar{c}_2$, $\bar{c}_3$, r_3) remain constant, the sensitivity coefficients for the maximum blanket revenue, defined in Eq. (4.44) and shown in Table 4.9, are

$$\lambda_{M_{HM}}^{e_m} = 1.0 \tag{5.1}$$

$$\lambda_{S_o}^{e_m} = 0.5\left(\frac{F_1^2+1}{F_1}\right)\frac{1}{F_3} - \frac{\bar{c}_3 S_o}{(\bar{c}_1 + \bar{c}_2)\bar{c}_3 S_o r_4]^{1/2} F_3} = 2.576 \tag{5.2}$$

$$\lambda_{\xi/T_c^\circ}^{e_m} = \frac{\xi}{T_c^\circ \cdot r_4}\left[0.5\left(\frac{F_1^2+1}{F_3}\right)\frac{1}{F_3} - \frac{F_1^2(\bar{c}_1 + \bar{c}_2)r_4}{2\{(\bar{c}_1 + \bar{c}_2)\bar{c}_3 S_o r_4\}^{1/2} F_3}\right] = -0.630 \tag{5.3}$$

where the numerical values are calculated from the reference economic/financial parameters described in Chapter 2 and the neutronic parameters of the 3-row UO_2 reference blanket.

Equations (5.1), (5.2) and (5.3) indicate the following interesting points as shown in Fig. 5.2;

a. The sensitivity coefficient of M_{HM} for the maximum blanket revenue is always 1.0, which means that if the fuel cycle cost contribution of the blanket has a negative sign (F_3 in Eq. (4.37) is negative and the blanket revenue is positive), a high fertile density will increase the maximum blanket revenue, while, if the fuel cycle cost contribution of the blanket has a positive sign (F_3 in Eq.(14.37)) is positive and blanket fuel adds to the net fuel cycle cost), high fertile density will decrease the maximum blanket revenue.

In other words there is an economic optimum fertile content in the blanket. This result must be qualified by noting that it is in part due to the fact that fabrication costs have been assumed to be directly proportional to the heavy metal content.

b. The sensitivity coefficients of S_o and ξ/T_C° for the maximum blanket revenue change their sign depending on whether blanket revenue is positive or negative. Therefore, a high fissile buildup rate (S_o), and a low value of ξ/T_c° always increases the maximum blanket revenue.

c. The sensitivity coefficient for S_o is larger than that of M_{HM} or ξ/T_c°, which indicates that the same fractional variation of S_o would affect the maximum blanket revenue more than a comparable change in M_{HM} or ξ/T_c°, and in a region of high fissile generation (first blanket row), the sensitivity coefficient for S_o is sharply decreased.

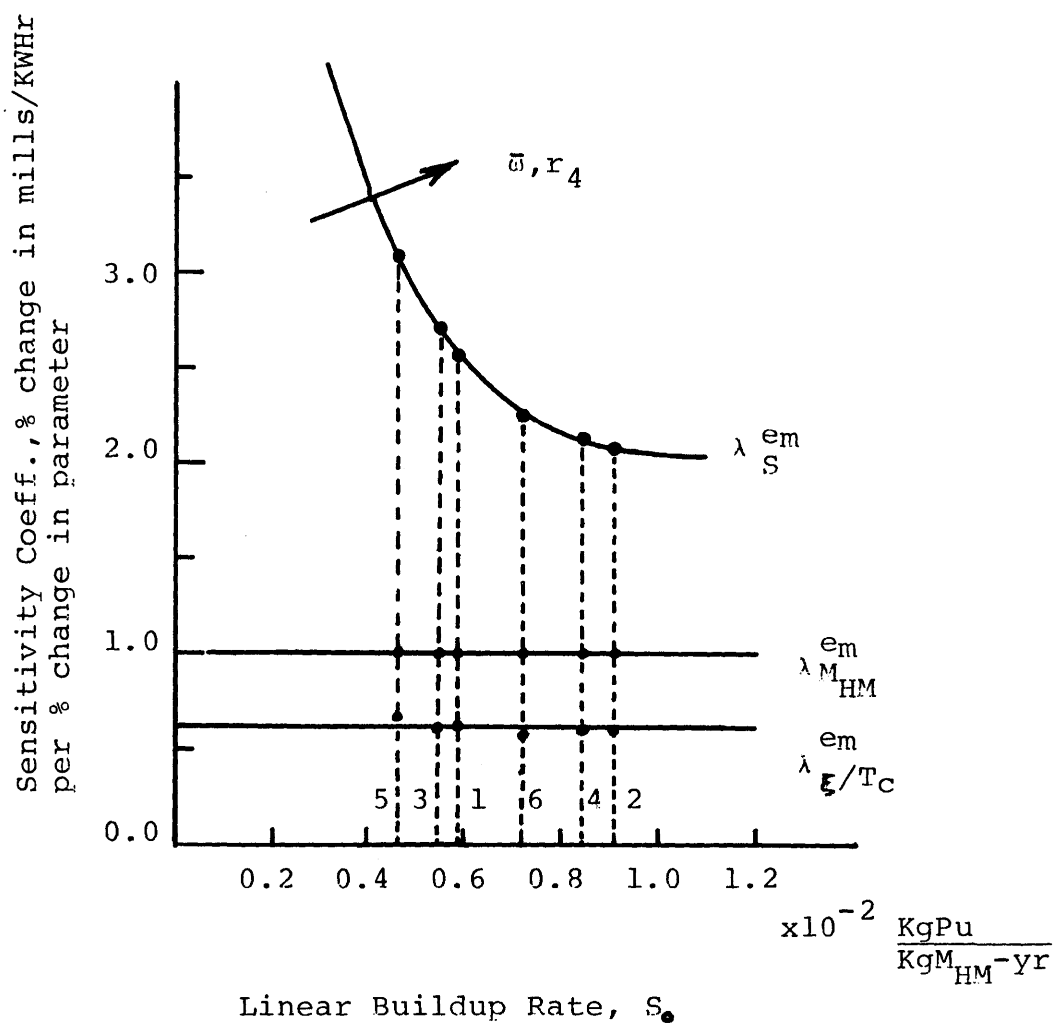

* 1: UO_2/3-row

2: UO_2/2-row

3: UC_2/3-row

4: UC_2/2-row

5: UC/3-row

6: UC/2-row

Fig. 5.2 SENSITIVITY COEFFICIENTS OF THE MAXIMUM BLANKET REVENUE AS A FUNCTION OF $S_\bullet^*$

From the above investigations, we can conclude that;

a. Moderator seeding in the blanket may be effective when the fuel cycle cost contribution of the blanket is positive (the blanket revenue is negative) because of the lower fuel fabrication cost component (due to the smaller heavy metal inventory or the number of fuel rods in the blankets) and the higher neutron capture rate of the remaining fertile material. Since it is a primary goal of the designer and operator to have the blanket defray fuel cycle costs (i.e. have positive revenue/negative costs) one would presumably not face this situation unless economic conditions changed after a plant was already built, and then moderator seeding would have to compete with decreasing the blanket thickness as a fix.

b. The effects of moderator seeding in the blanket on the maximum blanket revenue is less effective when the fuel cycle cost contribution of the blanket is negative (the blanket revenue is positive) because a small heavy metal inventory leads to less fissile production, as explained in the previous section, and hence to a lower fissile material credit.

Table 5.4 compares the improvement in the maximum blanket revenue due to moderator seeding for the above two cases; i.e. positive blanket revenue vs. negative blanket revenue. In both cases shown, moderator seeding is beneficial.

c. Thin blankets having a high fissile buildup rate, So, and a positive blanket revenue exhibit low sensitivity coefficients for So as shown in Eq. (5.2) and moderator seeding loses its advantages. Therefore, moderator seeding is attractive only for a thick blanket containing regions

TABLE 5.4

EFFECTS OF MODERATOR SEEDING ON DESIGNS HAVING POSITIVE AND NEGATIVE BLANKET REVENUES†

	UO_2 Fuel (3-rows)	
	Pos. Blanket Revenue*	Neg. Blanket Revenue**
Economic Parameter $\bar{\omega}$	0.0127797	
$\Delta M_{HM}/M_{HM}$	-0.17	-0.17
$\Delta S_o/S_o$	0.19	0.21
$\Delta r_4/r_4$	0.025	0.22
$\Delta bxr/bxr$	-0.015	0.004
$\Delta e_m/e_m$	-0.976	0.058
(e_m (Ref.) vs. e_m (Mod.))	(0.018853 mills/KwHr vs. 0.0004592 mills/KwHr)	(-0.0578 mills/KwHr vs. -0.06115 mills/KwHr)

† $\frac{\Delta q}{q} = \frac{(q \text{ with moderator seeding}) - (q \text{ without moderator seeding})}{q \text{ without moderator seeding}}$

* Refer to Appendix D (LCCEWG Benchmark Problem) for all parameters used.

** Refer to Chapter 2 for all parameters used.

having a very low fissile buildup rate. Table 5.5 compares important parameters for moderated and reference design blankets, including the sensitivity coefficients for So and ξ/T_c°. The sensitivity coefficients for M_{HM} and ξ/T_c° are not changed significantly, but the sensitivity coefficient for So is decreased significantly as the blanket thickness is decreased or the fissile buildup rate is increased. Actually, $\frac{\Delta So}{S}$ increases slightly as the blanket thickness is decreased; however, the total effect on the blanket revenue,

$$\left.\frac{\Delta e_m}{e_m}\right|_{So} = \lambda_{So}^{e_m} \cdot \frac{\Delta So}{So} ,$$

is decreased.

5.2.1.5 Summary for Moderated Blankets

Moderated blanket concepts have been evaluated by many research organizations from the beginning of the LMFBR program because of their potential for decreasing fuel cycle costs without detracting from the reactor's fissile breeding capability. However, in this study, we found that the moderated blanket concept is only favorable for

a. Thick blankets having a negative blanket revenue,

b. Thick blankets having a very low fissile buildup rate,

c. Thick blankets having a long optimum fuel irradiation time which exceeds allowable fuel or clad/structural exposure times.

Under future economic conditions projected from today's perspective, thin, two-row, blankets will be economically attractive. Thicker blankets will have difficulty in paying their fuel cycle cost because of high fuel fabrication and reprocessing costs.

However thin blankets suffer from several disadvantages, i.e.,

TABLE 5.5

VARIATION IN ECONOMIC CHARACTERISTICS OF BLANKETS DUE TO MODERATOR SEEDING

Fuel Mat.	UO_2				UC_2				UC			
Thickness	3row		2-row		3-row		2-row		3-row		2-row	
	Ref.	Mod.	Ref.	Mod.	Ref.	Mod.	Ref.	Mod.	Ref.	Mod.	Ref.	Mod.
T_{op}*, yr	7.40	6.10	4.90	3.90	7.82	6.63	5.20	4.25	9.25	7.81	6.14	4.99
S_o, $KgPu/Kg_{HM}$ yr	0.00587	0.00711	0.00909	0.01133	0.00553	0.00653	0.00850	0.01035	0.00466	0.00553	0.00719	0.00883
ξ/T_c^o, yr^{-1}	0.04148	0.05935	0.06920	0.10131	0.04052	0.05465	0.06563	0.09141	0.03071	0.04211	0.05049	0.07233
$\lambda^{e_m}_{S_o}$	2.576	-	2.0995	-	2.7432	-	2.1962	-	3.0899	-	2.2641	-
$\frac{\Delta S_0}{S_o}$	0.2112		0.2464		0.1808		0.2176		0.1867		0.2281	
$\lambda^{e_m}_{\xi/T_c^o}$	-0.63	-	-0.5904	-	-0.6062	-	-0.6096	-	-0.6780	-	-0.5753	-
$-e_m$**	0.0578	0.0612	0.073	0.067	0.055	0.058	0.072	0.065	0.049	0.055	0.071	0.066

† 25 v/o BeO
* Calculated from Eq. (4.22)
**Calculated from Eq. (4.36)

high neutron leakage into the reflector region, poor thermal and radiation shielding, a lower external breeding ratio and the potential need for more rapid placement of reflector assemblies.

In plants designed to accommodate 3-row blankets moderator seeding may be considered as an alternative to reducing the blanket thickness, while maintaining a high breeding ratio.

Table 5.6 summarizes the characteristics of moderated blankets, and the effects on blanket parameters due to moderator addition.

5.2.2 <u>Spectrum-Hardened Blankets</u>

5.2.2.1 General Design Concepts

As mentioned in the previous section, projected future economic conditions for fabrication and reporcessing costs and plutonium value (C3)(S4) indicate that thin blankets (e.g. 2 rows) will be economically attractive, hence, high fertile density is desirable to compensate for the disadvantages of thin blankets inherent to their low fertile inventory.

With respect to the neutron spectrum, a soft spectrum is, in general, better both neutronically and economically: a hard neutron spectrum is only a by-product of the use of high-density fuel materials. Therefore, in this study, the terminology "Spectrum-hardened" blankets means only that the blankets in question used high-density fuel materials.

Early experimental fast breeder reactors used metallic fuels both in the core and blanket regions, which created a hard neutron spectrum in both regions. Metallic and metal-alloy fuel having a high fertile density still has an excellent potential for use in the blanket region of fast reactor: (a) high thermal conductivity, (b) high fertile-fissile atom density, (c) good fission gas retention and (d) excellent resistance

TABLE 5.6

SUMMARY OF THE EFFECTS OF MODERATOR SEEDING

Parameters Affected by Moderator Seeding	Effects
1. Fertile Inventory (M_{HM}): • decreased by the lower fuel volume fraction	• Breeding ratio is slightly decreased • If the maximum blanket revenue is negative, fuel cycle costs are improved significantly. • If the maximum blanket revenue is positive, fuel cycle costs will be increased (revenue decreased).
2. Fissile Buildup Rate (S_o): • capture cross-section ($\bar{\sigma}^{28}_{c,B}$) is increased • average neutron flux ($\bar{\phi}_B$) is increased	• Maximum blanket revenue of a thick blanket is affected significantly • Maximum blanket revenue for a thin blanket is less affected • Shorter optimum fuel irradiation time
3. Financial/Non-linear Parameter (r_4): • slightly increased	• Maximum blanket revenue is slightly decreased • Shorter optimum irradiation time
4. Neutron leakage from core (L_c): • if moderator material is inserted near the core, neutron leakage rate from the core is reduced.	• Breeding ratio is worse than without moderator near core • Effect is negligible if moderator is restricted to outer blanket rows
5. Neutron Leakage into Reflector: • reduced	No significant effect; approximately cancelled out by the parasitic absorption of moderator material

Table 5.6 (continued)

Parameters Affected by Moderator Seeding	Effects
6. Power Contribution: • fission reaction of fertile material is decreased • Power generation at EOL is decreased	• Coolant orificing has to accommodate less of a power swing.
7. Fuel Management: • fuel shuffling is possible • fuel irradiation time is shortened • Effective blanket thickness can be controlled by moderator seeding	• Total plutonium production is proportional to bx at BOL (Eq. (3.43)), hence, it is slightly less than without moderator seeding

to sodium corrosion.

These properties are all essential to obtain a high breeding gain in an FBR. However, metallic and metal-alloy fuels are subject to severe metallurgical and neutronic problems - fuel swelling, low maximum burnup limit, high neutron absorption by the alloying additions and low peritectic reaction temperature etc. Hence, metal fuel has been replaced by oxide fuel for all recent FBR plants. Recently, other high density fuel materials, such as carbide and nitride fuels, have received increased attention because of their significant nuclear and economic advantages (C3) (many of which approach those of the metallic fuels), plus the added attribute of good stability (comparable to that of the other ceramic, UO_2), and with the prospect for tolerable fabrication cost.

Spectrum-hardened blankets with carbide and nitride fuels were suggested by Caspersson et al (S3) and Vitti (V1) because of their high breeding gain, the resulting decrease of reactor doubling time, their high allowable maximum peak fuel temperature, and their favorable transient behavior (due to high thermal conductivity).

In the work discussed in this section, attention will be focused on mono-carbide fuel (UC); and nitride and metal-alloy fuel, which have less favorable neutronic characteristics due to their higher parasitic absorption as shown in Tables 3.1 and 3.7 in this report, will not be discussed further. In this study, all fuel design parameters of the blanket fuel assemblies such as fuel pin diameter, heavy metal smear density as a fraction of the maximum theoretical density, clad thickness, clad material, etc. are kept the same as for ceramic oxide fuel.

5.2.2.2 Neutronic Aspects of Spectrum-Hardened Blankets

The average neutron energy in the blanket region is determined by the energy of the incident neutrons from the core and the total energy losses due to inelastic and elastic scattering with blanket fuel atoms. U-238 is a fine moderator for high energy neutrons because it has a large inelastic scattering cross-section between 10 MeV and 50 KeV and the average energy loss per inelastic collision is very high compared to elastic collisions. Light fuel atoms such as oxygen and carbon, on the other hand, have good elastic moderation potential. The ratio of heavy atoms to light atoms is a key factor in determining the average neutron energy in the blankets. A high concentration of heavy atoms leads to a harder neutron spectrum, however the variation of the blanket-averaged neutron energy is not changed significantly by an increase in heavy atom density because of their excellent slowing down power for high energy neutrons. From these facts, we can expect that a given percentage change in fertile atom density is much larger than the accompanying variation of spectrum-averaged cross-sections. Therefore, high fertile density is a more important factor to achieve the highest breeding ratio (in the absence of moderator seeding). As developed in Section 3.4.1, the fractional change of external breeding ratio due to a variation of fertile density can be expressed as

$$\frac{\Delta bx}{bx} \cong \frac{\theta}{e^{\theta}-1}\left(\frac{\Delta N_{28,B}}{N_{28}}\right) \qquad (3.35)$$

$$\text{where } \theta \cong [3\bar{\sigma}^{28}_{a,B} \cdot \bar{\sigma}^{28}_{tr,B}] \cdot N_{28,B} \cdot t \qquad (3.34)$$

Equation (3.35) indicates that the effect of the variation of fertile density on the external breeding ratio depends on the value of θ. If θ is small because the blanket is thin (small t or low $N_{28,B}$), high fertile density will be a very effective way to increase the external breeding ratio. Here we should note that thick blankets, which have large θ values (for example, a 3-row UC blanket), are not affected by the increase of fertile denstiy (for example, using U_2Ti fuel instead of UC). Table 5.7 summarizes the variation of the sensitivity coefficient, $\lambda_{N_{28}}^{bx} = \frac{\theta}{e^{\theta}-1}$, as a function of θ. If θ is larger than about 5.0, the effects of high fertile density on the external breeding ratio will be negligible. This is another explanation for the reason why a U_2Ti fueled blanket has a lower external breeding ratio than that of a UC fueled blanket which has large θ ($\sim$2.5 - a thick blanket) and low sensitivity coefficient $\lambda_{N_{28}}^{bx}$ (0.22). The relatively small improvement contributed by the high fertile atom density of U_2Ti fuel to the external breeding ratio can not offset the parasitic absorption loss by the Ti metal in the fuel material.

Table 5.8 shows the variation of important neutronic parameters achieved by replacing UO_2 fuel by UC fuel. As expected, the improvement of the radial blanket breeding ratio for a 3-row blanket is little less than that of a 2-row blanket, even if the 2-row blanket is used in conjunction with a thick BeO reflector in the 3rd row (while the 3-row blanket is used with a thin steel reflector),which leads to smaller neutron leakage losses.

As discussed in Chapter 3, the variation of neutronic parameters due to spectrum hardening can be characterized as;

TABLE 5.7

VARIATION OF THE SENSITIVITY COEFFICIENT FOR FERTILE DENSITY FOR THE EXTERNAL BREEDING RATIO AS A FUNCTION OF θ†

θ	$\lambda^{28}_{N_{28}} = \frac{\theta}{e^{\theta}-1}$	REMARKS
1.0	0.5820	
1.5	0.4308	UO_2 Fuel with ∿70% T.D.
2.0	0.3130	UO_2 Fuel with ∿97% T.D.
2.5	0.2236	UC Fuel with ∿97% T.D.
3.0	0.1572	Variations of fertile density in this region do not affect bx appreciably because of low sensitivity coefficients and parasitic absorption by fuel materials other than the fertile species.
5.0	0.0339	
10.0	0.0005	

† For 1000 MWe core size and 45cm thick radial blankets.

TABLE 5.8

VARIATION OF NEUTRONIC PARAMETERS FOLLOWING A CHANGE OF UO_2 FUEL TO UC FUEL

	FRACTIONAL CHANGE IN PARAMETER	
Parameter	2-row Blanket*	3-row Blanket**
Initial Heavy Metal Loading (M_{28})	1.343	1.343
$\bar{\sigma}^{28}_{c,B}$	0.9120	0.9175
$\bar{\Phi}_B$	0.8667	0.8658
Blanket Power Fraction (BOL)	1.106	1.118
Internal Breeding Ratio (bi)	1.003	1.002
Radial Blanket Breeding Ratio (bxr)	1.0650	1.0625
Optimum Fuel Irradiation Time	1.25	1.25

*BeO reflector in 3rd row

**Steel reflector outside blanket

a. The low fissile buildup rate, $\bar{\sigma}^{28}_{c,B}\phi_B$, caused by the hard spectrum erodes the advantage of high fertile atom density and the net improvement of the radial blanket breeding ratio is relatively small.

b. The blanket power contribution is increased and the blankets create more fast fission neutrons.

c. The optimum fuel irradiation time is increased; here by 25%.

d. Core performance is not affected by the change in blanket fuel material.

5.2.2.3 Economic Aspects of Spectrum-Hardened Blankets

As described in Section 5.2.1.4, thin blankets having a relatively high fissile buildup rate and a positive blanket revenue are not affected economically by the change of neutron spectrum. The most serious deficiency of the spectrum hardened blanket is its low fissile buildup rate, which leads to low blanket revenue. However, for a thin (2-row) blanket, the effectiveness of the fissile buildup rate on the blanket revenue (positive) is reduced, and the merits of high fertile density overcome this handicap.

Another problem arising from the high fertile density is the longer optimum fuel irradiation time. For a thick (3-row) blanket, the optimum irradiation time of a carbide blanket (batch irradiation of entire blanket) is about 9 years, which is probably beyond the allowable metallurgical irradiation time. Shortening the fuel irradiation time decreases the blanket revenue. Numerical comparisons of the economic parameters and the maximum blanket revenue were summarized in Tables 4.5 and 5.5.

5.2.2.4 Summary for Spectrum-Hardened Blankets

Spectrum-hardened blankets are one of the alternatives which may be applied in optimizing blanket arrangements under future economic environments. While spectrum-hardened blankets can improve the external breeding ratio, they may actually lead to a less favorable economic performance. One would, for example, have to be able to fabricate carbide-fueled blanket assemblies at a lower cost per kilogram heavy metal than oxide-fueled assemblies to offset the economic advantage of the latter attributable to its inherently higher fissile buildup rate and shorter optimum irradiation time.

It may in fact be other advantages of spectrum-hardened blankets which favor their use - for example, their thermal characteristics and transient behavior during scram (C4). The greater thermal conductivity of carbide fuel results in peak fuel temperatures far below its operating capabilities and in shorter time constants during the scram transient.

Table 5.9 summarizes the characteristics of spectrum-hardened blankets.

5.3 FISSILE-SEEDED BLANKETS

5.3.1 General Design Concepts

The fissile breeding performance and fuel cycle cost contribution of the blankets are closely related to three key factors:

a. The fertile atom density or total mass of heavy metals in the blankets,

b. The spectrum-averaged neutron capture cross-section (microscopic) of the fertile species, and

c. The blanket-averaged neutron flux.

TABLE 5.9

SUMMARY OF THE ATTRIBUTES OF SPECTRUM-HARDENED BLANKETS

1. Fissile Breeding Performance:

- High fertile atom density improves the breeding ratio but incurs the handicap of slightly lower fissile buildup rate.

2. Maximum Blanket Revenue:

- For a thick blanket, the maximum blanket revenue is decreased because of the low fissile buildup rate and the long optimum fuel irradiation time.
- For a thin blanket, the benefits of high fertile density offset the reduction of maximum blanket revenue caused by the decrease in fissile buildup rate.

3. Core Performance:

- Power contribution by the blanket fertile fission reaction is increased, hence the internal breeding ratio is increased by 0.2% (which is negligible).
- In general there is no significant effect on core region performance.

4. Fuel Management:

- Due to the good thermal properties of carbide fuel, fuel fabrication costs may be reduced by the use of larger fuel pin diameters.
- Fuel shuffling schemes are not compromised.
- A larger optimum irradiation time is required compared to some highly moderated blankets having softer spectrum

5. Blanket Thermal Performance:

- The high power contribution by the blanket inner row increases radial power peaking factors.
- A larger power gradient exists between the inner row and outer row of the radial blanket.
- Good transient behavior is achieved due to the high thermal conductivity of carbide fuel.

In the previous section, the variation of fertile atom density by changing blanket material, and of microscopic cross-sections by adding moderator material, were examined with respect to neutronic and economic performance. The blanket-averaged neutron flux is determined by the neutron leakage from the core region and the neutronic characteristics of the blanket materials. As reviewed in Chapter 3, neutrons leaking from the core region dominate the total number of neutrons available for fissile breeding in the blankets.

However, for a given core, this term remains nearly constant even if the blanket fuel material is changed. Another method to improve the number of available neutrons (and hence blanket flux) for fertile-to-fissile conversion is the generation of fission neutrons in the blankets by means of fissile seeding.

Brewer (B4) suggested the following potential advantages:

a. Generation of a larger amount of power from the fertile species due to an increased fast fission bonus, which reduces core fissile consumption,

b. Increase of beginning-of-life coolant exit temperature, and reduction of the blanket power-swing over an irradiation cycle.

Fissile seeding has a number of disadvantages, including increased fissile inventory cost, potentially increased pumping power requirements, and a decreased volume fraction available for fertile material in the blankets.

In this section, a more detailed neutronic and economic analysis for fissile-seeded blankets will be presented.

5.3.2 Design Features

In the systems analyzed here, Pu-239 is seeded into the blankets either homogeneously or heterogeneously. The enrichment of fissile material was selected to correspond to a 5% increase of the total Pu-239 inventory in the entire reactor system. This value is not optimized, but was selected to permit evaluation of fissile-seeded blankets under conditions which would not lead to unduly significant effects on core performance. Table 5.10 shows the variation of neutronic characteristics associated with fissile seeding of Types A (ε_{RB_2} = 0.35 w/o Pu in heavy metal, reference case) and B (ε_{RB_2} = 1.1 w/o) Excessive fissile-seeding of the radial blanket (case study B) leads to a small increase in the radial blanket breeding ratio, but a serious decrease in the internal and axial breeding ratios. This result will be analyzed in the next section.

Homogeneous and Heterogeneous Seeding (refer to sketches in Table 5.10) have only slightly different characteristics: fissile seeding in the first row of the radial blanket (under a constant total power constraint) reduces all activities in the core and axial blankets more than activities in the 2nd row of the radial blanket, which results in a slightly lower breeding ratio, as shown in Table 5.11.

One advantage of heterogeneous seeding is a harder internal spectrum in the fissile-seeded regions which leads to a larger fast fission bonus. A more detailed analysis for heterogeneous seeding is described in Appendix E. However in general the difference between homogeneous and heterogeneous seeding is so small as to be considered negligible.

TABLE 5.10

VARIATION OF NEUTRONIC CHARACTERISTICS OF FISSILE-SEEDED BLANKETS†

	FRACTIONAL CHANGE IN PARAMETER	
BOL Parameter	A*	B**
Core Power	0.9970	0.9816
Neutron Flux in Core Zone 1	0.9965	0.9828
Neutron Flux in Core Zone 2	0.9984	0.9812
Axial Blanket Power	0.9959	0.9812
Radial Blanket Power	1.1549	1.9346
Internal Breeding Ratio	0.9965	0.9812
Axial Blanket Breeding Ratio	0.9960	0.9809
Radial Blanket Breeding Ratio	1.0085	1.0493
Total Breeding Ratio	0.9993	0.9983

†Pu-239 is seeded in the 2nd row of the radial blanket homogeneously

*Reference, Case A, ϵ_{RB2} = 0.15%

*Case B Fissile-Seeding, ϵ_{RB2} = 0.92%

TABLE 5.11

FISSILE BREEDING CAPABILITY OF FISSILE-SEEDED BLANKETS

	Fractional Change in Parameter		
Parameter	A*	B*	C*
A_c^{49}	0.9949	0.9975	0.9975
C_B^{28}	1.0150	1.0098	1.0024
Internal Breeding Ratio	0.9933	0.9965	0.9958
Axial Blanket Breeding Ratio	0.9929	0.9960	0.9951
Radial Blanket Breeding Ratio	1.0138	1.0085	1.0014
Total Breeding Ratio	0.9982	0.9993	0.9970

*Arrangements of Fuel Materials (3-row radial blanket)
(ε_{RB} = 0.15%)

(hatched) $U_2Ti + PuO_2$

(open) U_2Ti

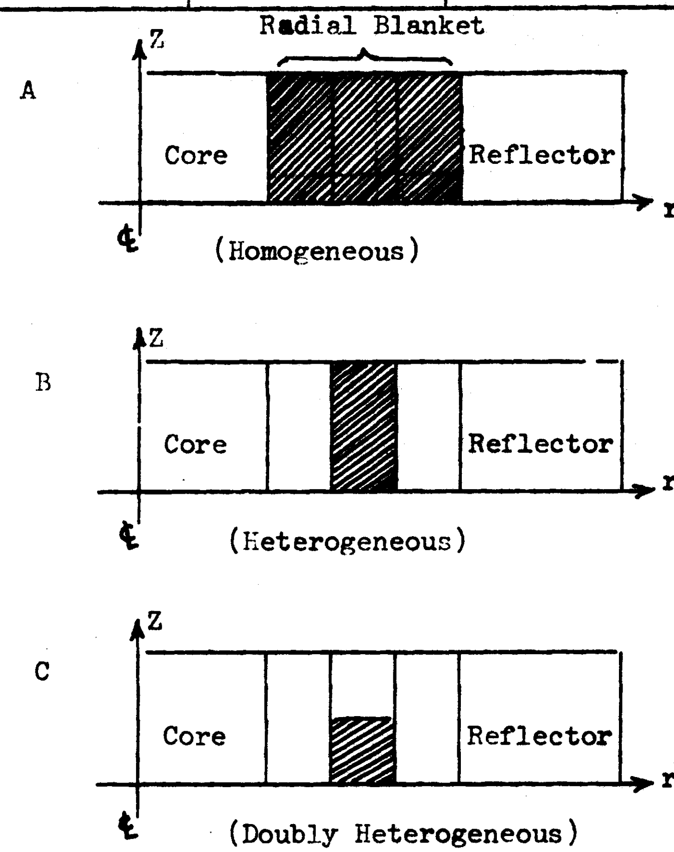

Table 5.11 compares the fissile breeding function of homogeneously and heterogeneously-seeded blankets, which indicates that fissile seeding in the 2nd row which is limited axially, and concentrated at the center region of the row, has a lower breeding ratio than the uniformly fissile-seeded blanket has. Therefore, in this study, uniformly-fissile seeded blankets in the second row will be considered.

5.3.3 Neutronic Aspects of Fissile-Seeded Blankets

We can write the neutron balance as a summation of events over each region of the reactor;

$$\sum_r (\nu F_r^{49} + \nu F_r^{28} - A_r^{49} - C_r^{28} - F_r^{28} - A_r^{P,L}) = 0 \qquad (5.4)$$

where Pu-239 and U-238 were considered as the representative fissile and fertile species in the region and F, A, C and P,L refer to the total fission, absorption, capture and parasitic absorption and neutron leakage rates respectively.

Equation (5.4) can be re-arranged: divide each term by A_r^{49} and then multiply all terms by A_r^{49}/A_T^{49}, where A_T^{49} is the total Pu absorption rate in the entire reactor, $\sum_r A_r^{49}$.

We have

$$\sum_r \left(\frac{\nu F_r^{49} + (\nu-1) F_r^{28} - A_r^{49} - A_r^{P,L}}{A_r^{49}}\right) \cdot \frac{A_r^{49}}{A_T^{49}} - \sum_r \frac{C_r^{28}}{A_T^{49}} = 0 \qquad (5.5)$$

but the second term is the system breeding ratio, $b = \frac{\sum_r C_r^{28}}{A_T^{49}}$, and we also have

$$\eta_r^{49} = \frac{\nu F_r^{49}}{A_r^{49}} \tag{5.6}$$

$$\delta_r^{28} = \frac{F_r^{28}}{F_r^{49}} \tag{5.7}$$

$$a_r = \left(\frac{A_r^{P,L}}{\nu F_r^{49}}\right) \tag{5.8}$$

Thus the neutron balance equation reduces to

$$b = \sum_r \{\eta_r^{49}(1 + \frac{\nu-1}{\nu} \cdot \delta_r^{28} - a_r) - 1\} \left(\frac{A_r^{49}}{A_T^{49}}\right) \tag{5.9}$$

and since $\sum_r \left(\frac{A_r^{49}}{A_T^{49}}\right) = 1$, we can also write

$$b = \sum_r \eta_r^{49}(1 + \frac{\nu-1}{\nu} \delta_r^{28} - a_r)\left(\frac{A_r^{49}}{A_T^{49}}\right) - 1 \tag{5.10}$$

Equation (5.10) shows that we can define core-and blanket-averaged values of the RHS by weighing subregion or zone values by (A_r^{49}/A_T^{49}).

Thus

$$b = \eta_c^{49} \;(1 + \frac{\nu-1}{\nu} \delta^{28} - a_c)\left(\frac{A_c^{49}}{A_T^{49}}\right) + \eta_B^{49}(1 + \frac{\nu-1}{\nu} \delta_B^{28} - a_B)\left(\frac{A_B^{49}}{A_T^{49}}\right) - 1 \tag{5.11}$$

and

$$A_c^{49} + A_B^{49} = A_T^{49}$$

Equation (5.11) is a more detailed expression for the breeding ratio of the core and fissile-seeded blanket systems than is Equation (3.4). If we assume that system power is fixed and that the power is primarily determined by Pu fission (hence absorptions), $A_T^{49} \cong$ constant: $dA_C^{49} = - dA_B^{49}$.

Thus for $\frac{dg}{dA_B^{49}} \geq 0$ we have the criterion:

$$\eta_B^{49} \left(1 + \frac{\nu-1}{\nu} \delta_B^{28} - a_B\right) \geq \eta_c^{49} \left(1 + \frac{\nu-1}{\nu} \delta_c^{28} - a_c\right) \qquad (5.12)$$

where g is the breeding gain, defined by g = b - 1; and hence $\Delta g = \Delta b$.

Equation (5.12) must be satisfied if fissile-seeding in the blankets is to improve breeding gain.

Equation (5.12) shows that it will be difficult to achieve this criterion for the following reasons;

a. $\eta_B^{49} \leq \eta_C^{49}$ because, in general, the blanket spectrum is softer than the core spectrum, even if we surround an oxide core with a metal-fueled blanket.

b. $a_B > a_c$ because of the fact that the concentration of Pu in the blanket is in general smaller than that of the core and because escape into the reflector abets parasitic absorption.

c. Once Pu enrichment in the blanket becomes appreciable, δ_B^{28} becomes relatively small, since fast neutrons are attenuated more rapidly in the blanket than the bulk of the neutron population.

d. Because of the $(\frac{A_B^{49}}{A_T^{49}})$ weighting, the advantage, if any, will be slight, since it is not practical to shift much of the Pu absorptions (fissions) to the blanket.

Because δ_c^{28} and a_c vary with Pu^{49} concentration, Equation (5.12) is really valid only for small perturbations in ΔA_B^{49} about A_B^{49}. Large changes in A_B^{28} affect the core performance, as shown in Table 5.9 (case B); such cases will be analyzed in the succeeding sections.

Table 5.12 summarizes the variations of breeding ratio and η_r^{49} for the fissile-seeded oxide, carbide and Ti-alloy fuels. η_{RB}^{49} is much smaller than η_c^{49} for all fuel materials, and the weighting factor, A_B^{49}/A_T^{49}, is smaller (worse) when fertile atom density is increased and the blanket has a very hard neutron spectrum - all of which works against improving the breeding ratio.

As a result of the above facts, fissile seeding in blankets can not improve the fissile breeding performance significantly. Since the blanket "seeds itself" by accumulating plutonium during its irradiation cycle, and since breeding performance does not improve with irradiation time, hindsight suggests that there was very little reason to expect that artificially enriching a beginning-of-life blanket would be helpful in the first place.

5.3.4 Economic Aspects of Fissile-Seeded-Blankets

Possibly favorable characteristics of fissile-seeded blankets as regards blanket economics are their high fissile buildup rate, due to the increased average neutron flux, and shorter fuel optimum irradiation time. Table 5.13 summarizes the key parameters and the maximum blanket revenue of the fissile-seeded blankets studied here. In this calculation,

TABLE 5.12

VARIATION OF NEUTRONIC CHARACTERISTICS OF FISSILE-SEEDED BLANKETS†

	UO_2	UC	U_2Ti
ϵ_{RB2}, %	0.50	0.42	0.35
η_c^{49}	2.3325	2.3352	2.3383
η_{RB}^{49*}	1.9264	1.9969	2.1560
A_B^{49}/A_T^{49}	0.0076	0.0053	0.0036
	FRACTIONAL CHANGES:		
bi	0.9933	0.9955	0.9965
bxa	0.9929	0.9951	0.9960
bxr	1.0071	1.0104	1.0085
b	0.9963	0.9990	0.9993

†Pu-239 was seeded in the second row of the radial blanket homo-geneously.

*Radial Blanket only

TABLE 5.13

COMPARISON OF ECONOMIC PARAMETERS FOR

REFERENCE AND FISSILE-SEEDED UO_2 BLANKETS

	REFERENCE	FISSILE-SEEDED*
M_{HM}, Kg	17299	17124
$\bar{\sigma}^{28}_{c,B}$, b	0.40252	0.39391
$\bar{\phi}_B$, 10^{-14} #/cm^2-sec	5.6269	5.9032
S_o, KgPu/KgM_{HM} yr	0.00587	0.006027
T^o_c, yr^{-1}	16.0738	15.9960
r_4	0.081475	0.081677
T_{op}, yr	7.40	7.23
T_{BE}, yr	2.83	2.73
e_{fab}, mills/kw-hr	0.0767	0.0776**
e_{rep}, mills/kw-hr	0.0216	0.0225**
$-e_{mat}$ mills/kw-hr	0.1561	0.1608**
$-e_m$, mills/kw-hr	0.0578	0.0607**

*Pu-239 was seeded in the second row of the radial blanket

**Additional costs (fissile purchase, fabrication penalty) for the initial fissile loading were neglected.

additional costs (fissile purchase, fabrication penalty) for the initial fissile loading were not considered. Even so the "improvement" of the maximum blanket revenue due to the slightly higher fissile buildup rate, So, is negligible.

Moderated blankets are similar to fissile-seeded blankets in some respects. However, moderator addition does not affect core performance seriously, and blanket fuel shuffling is easier to implement than when heterogeneous fissile-seeding is used, because of smaller power generation in the blankets.

5.3.5 Summary for Fissile-Seeded Blankets

The neutronic and economic characteristics of fissile-seeded blankets are very similar to those of moderated blankets. As shown in Appendix E, total breeding gain can be improved by fissile seeding only if η_B^{49} is larger than 2 + go ($\sim$2.2), however η_B^{49} is usually less than 2.0. Large scale fissile seeding in the blanket also affects core performance and leads to large neutron leakage into the reflector region, which leads to a low breeding ratio.

The harder spectrum created by fissile seeding reduces the spectrum-averaged microscopic capture cross-section of the fertile species, and this cancels out part of the advantages of the fissile-seeded blankets. The displacement of fertile material is another minor detriment.

We should note that while analysis was done for plutonium seeding the same conclusions must apply for uranium (U-235) seeding. Hence natural uranium fuel will not be superior to depleted uranium fuel in the blanket region.

The fissile-seeded blanket may have an advantage from the thermal-hydraulic view point. Increased fissile power generation in the blanket can increase the BOL coolant exit temperature and reduce blanket power-swing over an irradiation interval.

Table 5.14 summarizes the effects of fissile seeding on blanket neutronic and economic parameters.

5.4 PARFAIT BLANKET CONCEPT FOR FAST BREEDER REACTORS

5.4.1 General Design Concepts

In the preceeding sections, blanket design variations which could be implemented without any perturbation of core performance were evaluated. However, few significant benefits were found under this constraint.

In this section, advanced design concepts which involve rearranging core and blanket configurations will be briefly analyzed: for more detailed discussions refer to references (D1),(D3) and (A1).

To achieve a uniformly high average fuel burnup and smaller temperature gradient in the core, core fuel subassemblies are generally arranged in two or three radial zones of roughly equal volume, each zone's subassemblies differing in fissile material enrichment, i.e., power flattening. The lowest fissile enrichment is in the inner-most core region. In general the fissile enrichment is uniform within each core zone - that is, zone loading is homogeneous. An alternative approach is to heterogeneously load the zone using a combinatin of fissile-loaded and fertile-only assemblies. Many versions of these "heterogeneous" FBR core designs are now under intensive scrutiny by the international fast reactor community.

TABLE 5.14

SUMMARY OF THE EFFECTS OF FISSILE SEEDING

Parameters Affected by Fissile Seeding	Effects
1. Fertile Inventory (M_{HM}):	
• decreased by the lower volume fraction	• Breeding ratio is slightly decreased
2. Fissile Buildup Rate (S_o):	
• capture cross-section is decreased due to the hard spectrum	• Maximum blanket revenue is slightly increased
• average neutron flux is increased	• Larger neutron leakage losses especially for thin blankets
• S_o is slightly increased	• Blanket breeding ratio is increased
3. Maximum Blanket Revenue ($-e_m$):	
• slightly higher than without fissile seeding	• If there are additional costs for the initial fissile loading, this benefit will be lost.
4. Power Contribution:	
• large power contribution at BOL and EOL	• Increase of BOL coolant exit temperature • Reduced blanket power-swing over an irradiation time • High fast fission bonus increases blanket-averaged neutron flux • Increase in pumping power may result
5. Fuel Management:	
• fuel shuffling is possible but may be more difficult if heterogeneous seeding is used	• Total Pu production is not improved (see Eq. (3.43))
• shorter fuel optimum irradiation time due to large S_o and r_4	

TABLE 5.14 (continued)

Parameters Affected by Fissile Seeding	Effects
6. Breeding Ratio • internal breeding ratio is slightly decreased • axial blanket breeding ratio without fissile seeding is decreased • radial blanket breeding ratio is increased	• Total breeding ratio is decreased

Internal blankets limited in both radial and axial extent (designated "parfait" blankets here) were developed and investigated in some detail by Ducat (D3), Pinnock (P2) and Aldrich (A1) at MIT.

Conventional and parfait core configurations are shown in Fig. 5.3. Table 5.15 compares representative parfait and conventional 1000 MWe designs constrained to have the same external core dimensions and volumetric compositions. The total breeding ratio is increased by 2%, and the resulting reduction of doubling time is about 6%. Most additional advantages are related to core thermal-hydraulic performance and, perhaps, reactor safety. One of the drawbacks of the parfait blanket concept is its high fissile inventory which, if not compensated for by design trade-offs, can lead to higher fuel cycle costs.

5.4.2 Design Features (D3)

In the designs studied at MIT, the radial extent of the internal blanket is the same as that of the inner enrichment zone, as shown in Fig. 5.3. This design decision was a result of several criterion - the need to achieve a reasonable local peak power density in the core and internal blanket regions, and the desire to retain a simple fuel management scheme (each core comprised of only two types of fuel assemblies).

The axial extent or thickness of the internal blanket is determined by considerations involving power flattening (which directly affects the magnitude of the increased fissile inventory) and the breeding ratio. Thick parfait blankets exhibit a very small improvement in breeding ratio (<1%) and a low fissile buildup rate in the internal blanket. These factors will be discussed further in the next section.

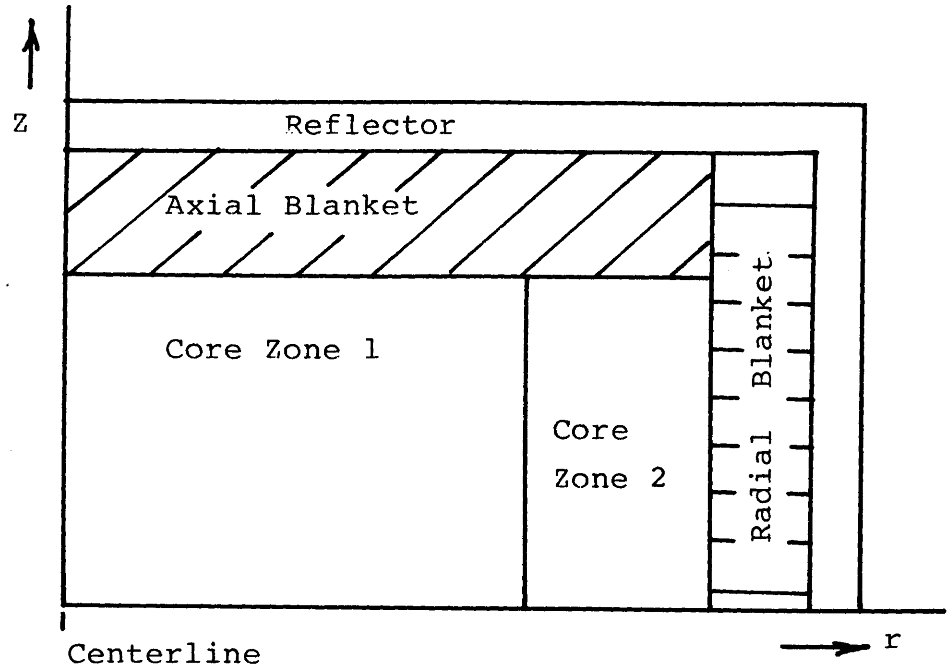

CONVENTIONAL DESIGN

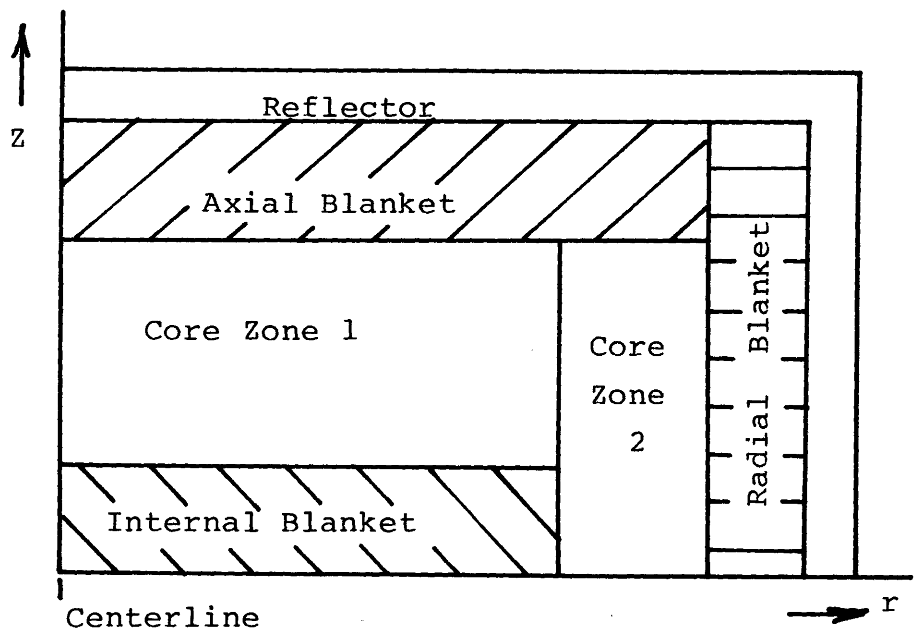

PARFAIT CONFIGURATION

Fig. 5.3 CONVENTIONAL AND PARFAIT CORE CONFIGURATIONS

TABLE 5.15

COMPARISONS BETWEEN A REPRESENTATIVE PAIR OF PARFAIT AND CONVENTIONAL CORE DESIGNS†

Advantageous Changes

Decreased Sodium Void Coefficient (25 - 50%)
Decreased Sodium Temperature Coefficient (40%)
Decreased Peak Power Density (5%)
Increased Overpower Operating Margin* (7%)
Decreased power production by the fissile-fueled zones (9% at mid-cycle) due to increased blanket power production (including the internal blanket)
Decreased Peak Fuel Burnup (8%)
Decreased average fissile-fueled zone burnup (5%)
Decreased Burnup Reactivity Swing (25%)
Decreased Peak Fast Flux (25%)
Decreased average fissile-fueled zone flux (15%)
Decreased Wrapper Tube Elongation in Inner Core Zone (29%)
Decreased Wrapper Tube Dilation in Inner Core Zone (50%)
Decreased Radial Flux Gradient in Inner Core Zone (50%)
Decreased Fluence-Induced Bowing in Inner Core Zone (90%)
Increased Breeding Ratio (2%)
Decreased Doubling Time (6%)

Disadvantageous Aspects

Increased Core Fissile Inventory (4%)
Reduced Doppler Power Coefficient (8%)
Increased Isothermal Doppler Coefficient (7%)
Higher Peak Clad Temperature (17°F)
Increased average fissile-fueled zone power density (15%)
Reduced prompt neutron lifetime (3%)
Reduced delayed neutron fraction (1%)
Magnitude and Gradients of fluence/power/temperature are not improved in the outer core zone or radial blanket
Increased Coherence: above 32% overpower more fuel is molten-at 50% overpower 23% of parfait fuel reaches C_L melting vs. 18% of the conventional core; more of the parfait core goes into boiling at higher power/flow ratios
Increased leakage to reflector (11%) hence blankets (radial and axial) may have to be thicker to realize the full breeding advantages of the parfait design

†Both cores are rated at 1000 MWe and operated for the same number of full power days between refuelings. The parfait design has a 30cm thick internal blanket, otherwise the core and fuel assembly dimensions are identical. Note that all results can be modified by changing the dimensions of the internal blanket.

*Percent steady state power (at 100% flow) at which incipient fuel centerline melting will occur.

The material composition of the internal blanket is the same as that of the axial blanket and the initial core enrichment is chosen to achieve $k_{eff} = 1.0$ at the end of a normal burnup cycle (here 300 days). Detailed data and procedures are described in Refs. (D3),(P2),(A1).

5.4.3 Neutronic Aspects of Parfait Blanket Systems

The breeding ratio was defined in terms of a neutron balance in Section 3.2.1, and expressed by Eq. (3.4):

$$b = \eta_c^{49} \, [1 + \frac{\bar{\nu}-1}{\bar{\nu}} \delta - a(1 + \delta)] - 1 \qquad (3.4)$$

or

$$b = \eta_c^{49} \, [1 + (1 - \frac{1}{\bar{\nu}} - a) \, \delta - a] - 1 \qquad (5.13)$$

If we consider $\bar{\nu}$ as a constant (see section 3.3.2) the change in breeding ratio due to the introduction of an internal blanket will be:

$$\Delta b = \frac{\partial b}{\partial \eta_c^{49}} \cdot \Delta\eta_c^{49} + \frac{\partial b}{\partial \delta} \cdot \Delta\delta + \frac{\partial b}{\partial a} \cdot \Delta a$$

$$= [1 + (1 - \frac{1}{\bar{\nu}} - a)\delta - a] \cdot \Delta\eta_c^{49} + \eta_c^{49}(1 - \frac{1}{\bar{\nu}} - a) \cdot \Delta\delta - (1 + \delta) \cdot \Delta a \qquad (5.14)$$

For a small variation of parameters, we can substitute typical values for FBR parameters into Eq. (5.14), i.e.,

$$\bar{\nu} \cong \bar{\nu}F/F \cong 2.90$$

$$\delta = (F_c^{28} + F_B^{28})/\bar{\nu}F_c^{49} \cong 0.15$$

$$a = (A_c^{P,L} + A_B^{P,L})/\bar{\nu}F \cong 0.20$$

$$\eta_c^{49} = \bar{\nu}F_c^{49}/A_c^{49} \cong 2.45$$

and Eq. (5.14) can be approximated as

$$\Delta b \cong 0.87\ \Delta\eta_c^{49} + 1.1\ \Delta\delta - 1.15\ \Delta a \tag{5.15}$$

which indicates that reducing parasitic absorption ($-\Delta a$) and core fissile consumption (hence $+\Delta\delta$) and increasing η_c^{49} ($+\Delta\eta_c^{49}$) are essentially equally important approaches to increasing the breeding ratio.

It is at least conceptually possible that by adopting the parfait blanket concept, the above three requirements can be satisfied, and a higher breeding ratio achieved, for example:

a. Higher η_c^{49}: The breeding performance of a fast reactor can almost always be improved by subdividing a large core into a number of smaller cores (see, for example, Feinberg's explanation of the rationale underlying a multi-fissile-zone GCFR design (F1), because the increased average fissile concentration in the smaller cores creates a harder neutron spectrum and hence η_c^{49} is increased. Aldrich (A1) found the empirical correlation between $\frac{\Delta\eta}{\eta}$ and $\frac{\Delta\varepsilon}{\varepsilon}$ to be

$$\frac{\Delta\eta_c}{\eta_c} \approx 0.04\ \frac{\Delta\varepsilon_c}{\varepsilon_c} \tag{5.16}$$

Hence, an increase in η_c permits an increase in η_c^{49} and hence the breeding ratio. For example, in an oxide fueled LMFBR, increasing the average fissile enrichment from 12.8% to 15.8%, increases η_c^{49} by approximately 0.023; from Eq. (5.15) a corresponding increase in b of approximately 0.02 would be anticipated.

b. Lower fissile consumption in the core $(+\Delta\delta)$:

An additional benefit is the large fertile fission contribution in the blankets which decreases the core power production ratio and hence fissile consumption in the core.

From the definition of δ, i.e.,

$$\delta \equiv \frac{1}{\bar{\nu}} \left(\frac{1}{F_c^{49}/F_c^{28}} + F_B^{28}/F_c^{49} \right)$$

$$= \frac{1}{\bar{\nu}} \left(\frac{\bar{\sigma}_{f,c}^{28}}{\bar{\sigma}_{f,c}^{49}} \quad \frac{1-\varepsilon_c}{\varepsilon_c} + \frac{F_B^{28}}{F_c^{49}} \right)$$

$$\cong 0.0088 \frac{1-\varepsilon_c}{\varepsilon_c} + 0.34 \frac{F_B^{28}}{F_c^{49}} \tag{5.17}$$

We see that $\Delta\delta$ can be positive or negative following an increase of core enrichment because the first term of Eq. (5.17) decreases as the core enrichment increases, while on the other hand, our experience shows that the second term of Eq. (5.17) generally increases when internal blankets are installed.

As a result of the previous studies already referenced, it was found that the core average power density should be increased as the volume of the internal blanket is increased. Therefore, the optimum axial thickness of the internal blanket should be decided by the following criterion, derived by requiring that $\Delta\delta$ be positive in Eq. (5.17):

$$\Delta\left(\frac{F_B^{28}}{F_c^{49}}\right) >> 0.026\ \Delta\left(\frac{1-\varepsilon}{\varepsilon}\right)_c \qquad (5.18)$$

Pinnock (P2) found that the core power production ratio (BOL) was decreased from 93.4% to 88.5% by the adoption of a 30 cm thick parfait blanket, while core average fissile-loaded-zone enrichment was increased from 15.6% to 19.6%. This increases δ by approximately 0.009 and the corresponding increase of b is around 0.01.

c. <u>Decrease of parasitic absorption by increasing fuel volume fraction ($-\Delta a$)</u>: Other advantages of parfait blanket systems found by previous investigators are the reduced swelling and bowing attributable to the lower neutron flux and better power shaping. This should permit increasing the volume fraction of heavy metal oxide in the core and thereby decreasing the parasitic absorption. For example, reduced control requirements permit increasing the fuel volume fraction in the core by 0.5%, and reduced swelling and bowing permits increasing fuel fraction in the core by ∿2%, which together can increase the breeding ratio by ~0.03.

Additional improvements in total breeding gain can be anticipated by concurrent changes in core thermal-hydraulic design features, i.e., by trading away some of the margin (e.g. on peak power and burnup) shown in Table 5.15.

Table 5.16 summarizes the possible improvements in breeding gain which may be achievable by the adoption of parfait blanket systems. It should be noted that use of a non-optimized internal blanket configuration can easily lead to decreased breeding gain, particularly if sufficient power flattening is not achieved to offset the critical mass penalty. This, in fact, is often observed for internal blankets which extend the full

TABLE 5.16

POSSIBLE IMPROVEMENTS IN BREEDING GAIN OF "PARFAIT BLANKET" SYSTEMS

Change of Design Parameter	Numerical Example	Δb
1. Higher Core Enrichment ($\bar{\varepsilon}_c$) which increases η_c^{49}	ε_c: 12.8% → 15.8% ($\Delta\eta_c^{49}$: 0.023)	∿0.02
2. Lower Power Production Ratio which reduces the fissile consumption in the core	$\frac{P_B}{P_c}$: $\frac{6.6}{93.4} \rightarrow \frac{11.5}{88.5}$	∿0.01
3. Higher Fuel Volume Fraction in the Core which reduces the parasitic absorption	ΔV_f v/o: 0.5 (reduced control requirement) ∿2.0 (reduced swelling and bowing)	∿0.03
	Total*	∿0.06

*Note that this does not reflect the impact of offsetting penalties (e.g. on critical mass) which may lead to an increase in doubling time.

length of the core (hence which do not contribute to axial power shaping).

5.4.4 Economic Aspects of Parfait Blanket Systems

The technical feasibility of the parfait concept, especially as related to fuel fabrication and reprocessing costs, was investigated by Ducat (D3) who concluded that there were not apparent obstacles to the operation of a fast reactor with an internal blanket, and the same appeared to be true for the preirradiation and post-irradiation steps in the fuel cycle.

Based on the above results, and a consistently applied basis of financing charges, and fabrication and reprocessing costs, one can compare the economic performance of the reference and parfait configurations.

Assesment of the economic (fuel cycle cost) effects of parfait blanket systems can be most easily done by considering their influence on the fuel depletion economics of the core and the external blankets.

A parfait blanket system can affect core fuel economics in three ways:

a. by affecting the core fissile inventory required for criticality and substaining a specified burnup reactivity lifetime, and thereby affecting core inventory costs,

b. by perturbing the magnitude and spectrum of the flux in the core, causing changes in depletion, and thus material credits,

c. by reducing the core fertile inventory (hence internal breeding ratio), resulting in a smaller material credit.

These effects generally increase the fuel cycle cost contribution in the core regions.

External blanket economics are indirectly affected by the internal blanket, since it increases their fissile buildup rate by increasing the neutron leakage from the core regions; this leads to a higher material credit from the external blankets.

Table 5.17 compares the fuel cycle cost contribution by each region for the reference and parfait blanket systems. The increased expenses in the core region can be cancelled by the internal blanket revenue and the increased external blanket revenues. The total fuel cycle costs of the reference and parfait systems differ by small (negligible) margins, when the internal blanket thickness is properly optimized. There are, however, several characteristics of the parfait configuration (not accounted for in Table 5.17) which will enhance its economic performance relative to the reference reactor. The results shown in Table 5.16 were obtained under the assumption of equal unit fabrication costs for the core regions and internal blanket (\$314/Kg M_{HM}). If fabrication costs for the internal blanket are equal to those estimated for the axial blanket (\$80/Kg M_{HM}), the fuel cycle cost of the parfait system may be favorable.

In addition, the capability of employing higher core fuel volume fractions in the parfait designs as the result of reduced fuel swelling, reduced metal swelling and reduced control rod requirements would further enhance the economic performance of the parfait concepts.

5.4.5 Brief Review of the "Heterogeneous Core" and "Sandwich - Blanket" Concepts

Recently, there has been considerable interest, both in the U.S. and abroad, relative to the potentially superior safety and breeding characteristics of LMFBR cores having internal blankets. The "Parfait

TABLE 5.17

FUEL CYCLE COST CONTRIBUTIONS OF REFERENCE AND PARFAIT CONFIGURATIONS

	Cost Contribution, mills/kwhr		
	Reference	30-cm IB Parfait	50-cm IB* Parfait
Core			
Direct burnup	0.1964	0.3385	0.4144
Inventory carrying charges	0.6568	0.6687	0.6804
Direct fabrication	0.3093	0.2533	0.2210
Fabrication carrying charges	0.0990	0.0810	0.0706
Net reprocessing charges	0.0456	0.0373	0.0326
Subtotal	1.3071	1.3788	1.4190
Internal Blanket			
Net material credit	-	-0.1092	-0.1556
Net reprocessing charges	-	0.0083	0.0130
Direct fabrication	-	0.0560	0.0883
Fabrication carrying charges	-	0.0180	0.0284
Subtotal		-0.0269	-0.0259
Axial Blanket			
Net material credit	-0.1873	-0.2052	-0.2113
Net reprocessing charges	0.0356	0.0356	0.0356
Direct fabrication	0.0616	0.0616	0.0616
Fabrication carrying charges	0.0196	0.0196	0.0196
Subtotal	-0.0705	-0.0884	-0.0945
Radial Blanket			
Net material credit	-0.2120	-0.2338	-0.2420
Net reprocessing charges	0.0349	0.0349	0.0349
Direct fabrication	0.0520	0.0520	0.0520
Fabrication carrying charges	0.0333	0.0333	0.0333
Subtotal	-0.0918	-0.1136	-0.1218
Total Expenses	1.5441	1.6981	1.7857
Total Material Credits	-0.3993	-0.5482	-0.6089
TOTAL FUEL CYCLE COSTS	1.1448	1.1499	1.1768

*Oversized

Blanket" concept discussed in this section is one of these "heterogeneous cores", in which the internal blanket is limited in both radial and axial extent. Fully heterogeneous concepts, which employ both axial and radial internal blanket zones, are also under study elsewhere, in France in particular (M5).

The "Sandwich - blanket" concept has design options similar to those of the parfait blanket system except that the internal blanket is extended radially through both core regions (see Fig. 5.4 (a)), as described by Kobayashi et. al. (K4).

Mougniot et. al. (M5) have suggested substantial improvements in breeding performance for more complicated versions of the heterogeneous concept (see Fig. 5.4 (c)), which has aroused some controversy over the capabilities of this general class of core designs (see the preliminary review by Chang (C5)), Chang (C6) has also studied and applied a simple heterogeneous core concept constrained to fit within the CRBR configuration. (see Fig. 5.4(b)). All of these new concepts have very nearly the same design benefits and theoretical basis as already discussed for the "parfait blanket" concept. Proponents claim that:

a. higher breeding ratios and shorter doubling times can be achieved.

b. using a single fissile enrichment, better core power flattening can be achieved,

c. better safety-related characteristics can be expected (e.g. reduced fuel swelling and bowing, sodium void coefficient and power peaking factor).

Although these concepts appear to have modest neutronic advantages,

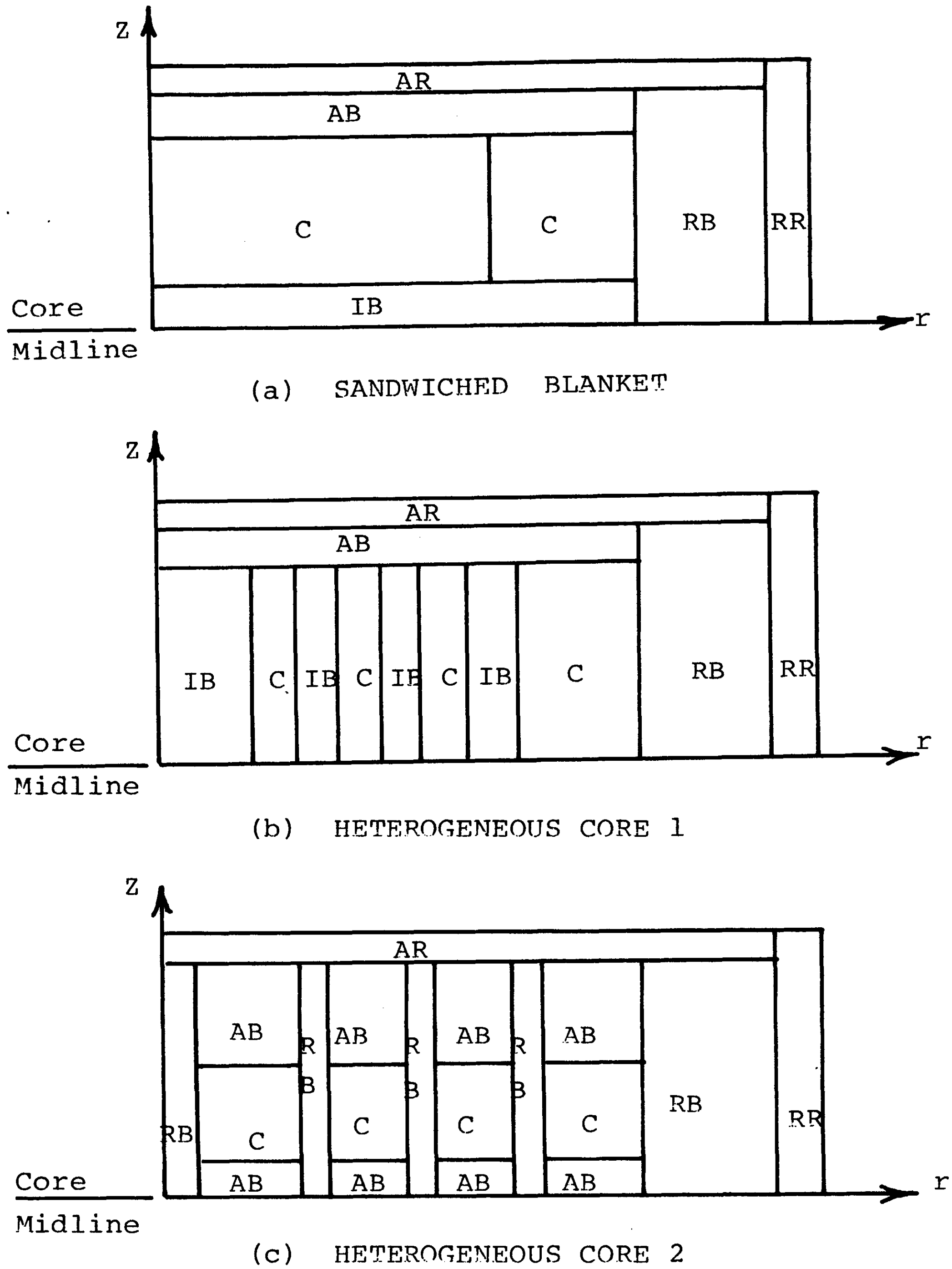

* C: Core, AB: Axial Blanket, RB: Radial Blanket
IB: Internal Blanket, AR: Axial Reflector, RR: Radial Reflector

Fig. 5.4 CONFIGURATION OF "SANDWICHED-BLANKET" AND "HETEROGENEOUS CORE" DESIGNS they may also entail several practical disadvantages such as high fuel linear heat rating in the internal blankets at end of life and sodium striping problems where hot and cold (blanket) sodium effluent from adjacent assemblies mixes.

With respect to fuel utilization and the fuel cycle cost of the entire reactor system, these design concepts will not offer substantial improvements unless they permit increasing the volume fraction of fuel loaded within the core envelope, since this is the only practical way to achieve significantly better breeding ratios and doubling times.

5.5 SUMMARY

Analyses emphasizing the neutronic and economic performance of various blanket concepts have been presented in this chapter.

Most of the chapter was devoted to evaluation of blanket modifications involving variations of blanket neutron spectrum (moderated and spectrum-hardened blankets) and of the blanket average neutron flux (fissile-seeded blanket) which could be achieved without any perturbation of core performance.

Few significant benefits were found under this constraint; in some cases slightly higher breeding ratio could be realized at the expense of reduced blanket revenue (or vice versa). Thin (2-row), spectrum-hardened (UC fueled) blanket concepts appear to be slightly preferable under future economic conditions, while the moderated-blanket is only an alternative way to re-optimize already-built systems committed to thick ($\geq$ 3 row) blankets. Fissile-seeded blankets have some characteristics similar to those of moderated blankets, however the neutronic and economic potential of a moderated blanket is superior to that of fissile-seeded blankets.

In the final two sections, advanced design concepts which involve rearranging core and blanket configurations were evaluated briefly. The "parfait blanket" concept which has been studied at MIT offers the possibility of good neutronic and economic performance providing that a complete design trade off is carried out to fully realize its potential. Increasing the volume fraction fuel in the core has been identified as the key to superior performance (D1). "Heterogeneous core" concepts have been evaluated by several investigators elsewhere, and identified some still controversial problems related to the core thermal-hydraulic performance, severe power mis-match at zone boundaries and possible difficulties in fuel management which must be resolved. Moreover, economic aspects of these advanced design concepts may not be favorable, as fuel cycle cost and average fuel utilization may well be nearly the same as those of equivalent homogeneous cores.

An extensive evaluation program is currently underway in the U.S. in this area, however, and a completely definitive assessment of heterogeneous cores must await their completion.

Throughout the present analysis, the most promising fuel materials have been found to be oxide and mono-carbide fuels because of their good neutronic and economic aspects in the blanket region.

Carbide fuel has a better potential in the thermal-hydraulic and neutronic areas than does oxide fuel. Oxide fuel on the other hand creates the largest blanket revenue (among the mono-carbide, di-carbide and metal alloy fuels) due to its high fissile buildup rate. This conclusion holds when the same economic and financial basis applies to all fuel materials, and in particular when the same fabrication and reprocessing costs are charged per unit mass of heavy metal. In practice the fabrication cost is more sensitive to the number of pins fabricated than the fuel mass in the pin. The total number of fuel pins to be fabricated in the blanket region is about the same for all fuel materials, hence the fabrication cost per unit mass of carbide fuel might well be less than that of oxide fuel. If the unit fabrication cost for the carbide fuel ($\$/KgM_{HM}$) is less than about 90% of that for oxide fuels (based on the reference core configurations and economic environments used in this study), carbide fuel will be better than oxide fuel from a neutronic/economic point of view.

CHAPTER 6

SUMMARY AND CONCLUSIONS

6.1 INTRODUCTION

The fast breeder reactor (FBR) is a technically feasible and economically attractive alternative for future energy production. A principal attraction of the FBR comes from its ability to breed more fissile fuel than it consumes, which leads to a low fuel cycle cost and to the effective utilization of uranium ore resources. Current fast reactor designs for practical large-scale power production promise breeding ratios in the range from 1.2 to 1.4. The blanket region contributes about one third of the total breeding ratio, and reduces the fuel cycle cost by about twenty five percent of total expenses. Achieving a high breeding ratio and a low fuel cycle cost, which are the strong points of the FBR, can not be accomplished without the contributions of the blanket regions.

Various modifications to improve blanket performance have been suggested by many previous investigators. However, a clearly defined strategy for improving blanket neutronics and economics has not yet been advanced. Frequently the alternatives selected as being most attractive in this manner are in conflict: softening the spectrum (UO_2 or UC_2 fueled blankets) vs. hardening the spectrum (UC or UN fueled blankets) or a moderated blanket vs. a fissile-seeded blanket, or thick blankets vs. thin blankets with high-albedo reflectors.

Thus the central objective of this work has been to provide a clearer explanation of the technical basis for improved breeding performance and enhanced economic contributions by the blanket region.

Another major objective has been evaluation of these advanced/new blanket concepts with respect to their neutronic and economic capability on a consistent analytical and technical basis.

In practice, all blanket concepts should be evaluated on the basis of a compromise among neutronics, economics and engineering considerations. Evaluation of the neutronic and economic characteristics of FBR blanket systems is emphasized in the present work, although engineering design constraints have been considered where appropriate. The emphasis is also on development of simple analytical models and equations, which are verified by state-of-the art computer calculations, and which are then applied to facilitate interpretation and correlation of blanket characteristics.

6.2 METHODS OF EVALUATION

To permit meaningful comparisons of FBR blanket concepts, the computational methods, the nuclear data used for the calculations, and the details of the economic and financial environment were all carefully considered.

6.2.1 Reference Reactor Configuration

The core size (power rating) is not an important variable for the purpose of this study as shown by Tagishi (T1); however, reference design features of an 1000 MWe LMFBR, selected as the standard system for previous MIT blanket studies, were again chosen as a reference reactor configuration. Figure 6.1 shows the pertinent physical dimensions and summarizes the important physical characteristics of the reference reactor system. The main features to note in this cylindrically symmetric layout are two approximately-equal-volume

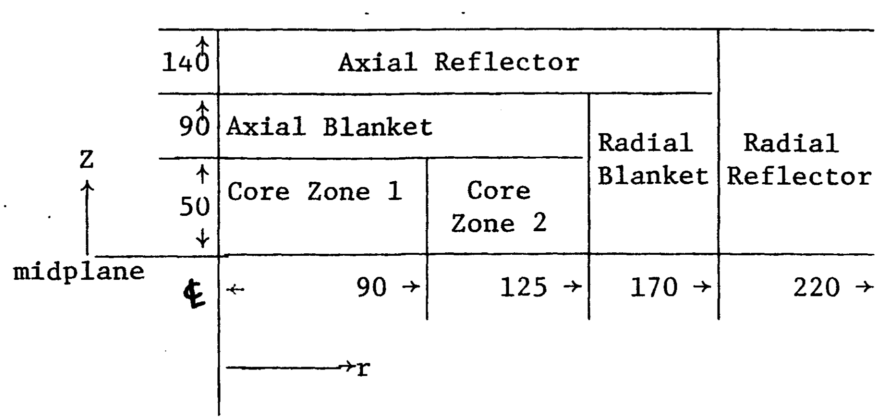

* All dimensions in cm

*Physical Characteristics of Reference Reactor

General:

Rated power, MWe/MWth = 1000/2560
Capacity factor, % = 82.2

Core and Axial Blanket:

Flat-to-Flat distance of a fuel assembly, cm = 15
Material Volume Fractions (Fuel/Na/Structure), % = 30/50/20
Pellet Smear Density, % T.D. = 85
Core Average Enrichment (Zone 1/Zone 2) at BOL, % = 15.2/20.8
Type of Fuel in the Core: $(Pu.U)O_2$

Radial Blanket:

Number of rows = 3
Type of fuel (reference): Depleted UO_2
Material volume fractions (Fuel/Na/Structure), % = 50/30/20
Pellet smear density, % T.D. = 96.5

Reflectors:

Type of material: stainless steel
Material Volume Fractions (Steel/Na), % = 80/20 (axial)
90/10 (radial)

Fig. 6.1 Elevation Schematic View of the Upper Right Quadrant of the Reference Reactor System core enrichment zones (for radial power-flattening), a 40-cm thick axial blanket on the top and bottom of the core, and a three-row, 45 cm-thick radial blanket surrounded by a steel reflector.

6.2.2 Methods of Burnup and Neutronic Computations

Burnup analysis was performed with the two-dimensional diffusion theory code 2DB (L3). To determine the initial material compositions for various blanket design concepts, the same material volume fraction and fuel smear density (in % T.D.) were applied to all blanket fuel materials, because in the blanket region burnup and other environmental conditions are less severe than in the core regions. "Equilibrium" core and axial blanket compositions that remain fixed in time as the irradiation of the radial blanket progresses were adopted for this study.

In the interests of consistency, all computations were performed using the Russian (ABBN) 26-group cross-section set (B3) and a 4-group cross-sections prepared by region-collapsing the original ABBN 26-group cross-section set using the one-dimensional transport theory code ANISN (E1). For simple neutronic calculations, a spherical reactor geometry whose blanket has the same characteristics as that of the radial blanket was also modeled.

6.2.3 Blanket Burnup Economics

6.2.3.1 Cost Analysis Model

Detailed fuel cycle cost analyses were performed utilizing the cash flow method (CFM) contained in the computer code BRECON, developed by Brewer (B4) and modified by Wood (W3).

The general CFM expression for the levelized cost of electricity (mills/KW-Hr) in a region or subregion under fixed fuel management is

$$e = \frac{1000}{E} M_{HM}(0) \Big[\frac{C_{fiss}\, \varepsilon_o\, F^{MP}(T)}{T} \quad \text{material purchase cost component}$$

$$+ \frac{C_{fab}\, F^{fab}(T)}{T} \quad \text{fabrication cost component}$$

$$+ \frac{C_{rep}\, F^{rep}(T)}{T} \quad \text{reprocessing cost component}$$

$$- \frac{C_{fiss}\, \varepsilon(T)\, F^{MC}(T)}{T} \Big] \quad \text{material credit cost component} \qquad (6.1)$$

where

e is the local levelized fuel component of the energy cost (mills/KW-Hr),

E is the electrical energy produced by the reactor in one year (KW-Hr/yr),

T is the local irradiation time (yr),

C_{fiss} is the fissile price (\$/Kg Pu),

C_{fab} is the unit fabrication cost (\$/KgM_{HM}),

C_{rep} is the unit reprocessing cost (\$/KgM_{HM}),

ε_o is the initial enrichment,

$\varepsilon(T)$ is the discharge enrichment (Kg fissile discharged per Kg of heavy metal loaded),

$F^q(T)$ is the carrying charge factor for cost component q,

$M_{HM}(0)$ is the mass of heavy metal loaded.

The carrying charge factors, $F^q(T)$, are given by

$$F^q(T) = \frac{1}{1-\tau}\left[\frac{1}{(1-X)^{T_q}} - \tau\right] \quad \text{for capitalized costs or revenues}$$

$$= \frac{1}{(1+X)^{T_q}} \quad \text{for noncapitalized costs or revenues (expensed costs or taxed revenues)}$$

where (6.2)

$X = (1-\tau)r_b f_b + r_s f_s$ is the discount rate,

τ is the income tax rate,

f_b is the debt (bond) fraction,

f_s is the equity (stock) fraction,

r_b is the debt rate of return,

r_s is the equity rate of return,

T_q is the time between the cash flow transaction q and the irradiation midpoint.

An approximate form of Eq. (6.2), developed by Ketabi (K2), is

$$F^q(T) \cong e^{\frac{XT_q}{1-\tau}} \quad \text{for capitalized costs or revenues}$$

$$\cong e^{XT_q} \quad \text{for noncapitalized costs or revenues}$$

$$= F_q^{\Delta}\, e^{r_q T} \qquad (6.3)$$

where

$F_q^{\Delta} = F_q(\Delta T_q)$, and

ΔT_q is the time between the cash flow transaction q and the beginning of irradiation (for fabrication) or the end of irradiation (for the reprocessing and material credits).

Considering the effects of non-linear fissile buildup histories and using the carrying charge factors expressed in Eq. (6.3), Equation (6.1) can be approximated as follows:

$$e = \frac{1000}{E} M_{HM}(0) \left[\frac{\bar{c}_1 e^{r_1 T} + \bar{c}_2 e^{-r_2 T} - \bar{c}_3 \varepsilon(T) e^{-r_3 T}}{T}\right] \qquad (6.4)$$

where

$\bar{c}_i = c_i \cdot F_i^{\Delta}$ is the modified cost component for operation i (\$/Kg),

Subscript 1 refers to fabrication,

Subscript 2 refers to reprocessing,

Subscript 3 refers to material credit.

6.2.3.2 The Reference Economic and Financial Environment

Table 6.1 lists the reference economic and financial parameters used in this study. These conditions are within the range projected for the mature U.S. nuclear fuel cycle economy (Z1). (Note that 1965 dollars are employed to insure consistency with prior work at MIT by Brewer (B4)).

The reference unit fabrication and reprocessing costs shown in Table 6.1 were applied to all fuel materials uniformly because the unit fuel processing costs are not strongly influenced by the fuel pin diameter in the larger pin diamter range (>0.4 in.; a common fuel pin diameter in the radial blanket region is around 0.52 in.). In any case, this assumption provides a common basis for evaluation of the various blanket design concepts considered in this study.

Two cost accounting methods, A and B as originally defined by Brewer (B4), were considered for the blanket depletion - economic analysis. In method A, post irradiation transactions are not capitalized and in method B, post irradiation transactions are capitalized.

TABLE 6.1

REFERENCE ECONOMIC AND FINANCIAL ENVIRONMENT

Operation	Unit Fuel Processing Cost *, $/Kg M_{HM} (Radial Blanket Only)
Fabrication	69
Reprocessing	50
Isotope	**Isotope Market Value* $/Kg$M_{HM}$**
U-238	0
Pu-239	10,000
Pu-240	0
Pu-241	10,000
Pu-242	0
Financial Parameters	**Value of Parameters (Private Utility)**
Income Tax rate, τ	0.5
Capital Structure	
Bond (debt) fraction, f_b	0.5
Stock (equity) fraction, f_s	0.5
Rate of Return	
Bonds, r_b	0.07
Stocks, r_s	0.125
Discount Rate, $X = (1-\tau)f_b r_b + f_s r_s$	0.08
Cash Flow Timing	
ΔT_{fab}, yr	0.5
ΔT_{rep}, yr	0.5
ΔT_{mc}, yr	0.5

*1965 dollars, to conform to cases studied by Brewer (B4)

6.3 BREEDING CAPABILITY OF FBR BLANKETS

A high fissile gain in the fast breeder reactor (FBR) is extremely important if the utility industry is to become relatively independent of the need for mining of expensive low-grade uranium ores in the next 50 years or so, and to thereby assure lower average nuclear power plant fuel cycle costs.

The fast reactor has a relatively small, high-power-density core, and as a result has a very high net neutron leakage from the core region. Therefore, the radial and axial blankets make very important contributions to fissile breeding.

The purpose of this section is to evaluate the effects of various design parameters on the fissile production in FBR blankets and to review possible design modifications to enhance the breeding ratio. An evaluation of an analytical method for estimation of the external breeding ratio will be carried out followed by a detailed discussion of the various factors which affect external fissile breeding.

6.3.1 Breeding Potential of FBR Blankets

The fissile breeding in an FBR due to neutron capture in fertile materials in the core and blanket regions, is characterized by the breeding ratio, defined by

$$b = \frac{\text{Fissile production rate in core and blanket regions}}{\text{Fissile consumption rate in core and blanket regions}}$$

$$= \frac{\sum_{c,B} (C^{28} + C^{40})}{\sum_{c,B} (A^{49} + A^{41} + A^{25})} \qquad (6.5)$$

where

C is the total capture rate in the indicated species,

A is the reactor absorption integral,

c,B are core and blanket regions, respectively.

The breeding ratio can be split into two parts corresponding to the internal (core) contribution (b_i) and the external (blanket) contribution (bx):

$$b_i = \frac{\text{Fissile production rate in core}}{\text{Fissile consumption rate in core and blanket regions}}$$

$$= \frac{C_c^{28} + C_c^{40}}{\sum_{c,B}(A^{49} + A^{41} + A^{25})} \tag{6.6}$$

$$bx = \frac{\text{Fissile production rate in blanket}}{\text{Fissile consumption rate in core and blanket regions}}$$

$$= \frac{C_B^{28}}{\sum_{c,B}(A^{49} + A^{41} + A^{25})} \tag{6.7}$$

Considering the neutron balance in the region r, i.e.;

$$\nu F_r^{49} + \nu F_r^{28} + \nu F_r^{25} - F_r^{49} - F_r^{28} - F_r^{25} - C_r^{49} - C_r^{28} - C_r^{25} - A_r^{P,L} = L_r \tag{6.8}$$

where

Pu-239, U-238 and U-235 were considered as the representative fissile and fertile species in the core and blanket, and

F is total fission rate in the indicated species

L_r is neutron leakage from the region r, and

P,L refers to parasitic absorption and neutron leakage losses, The breeding ratio can then be rewritten as

$$b = \eta_c \left[1 + \frac{\bar{\nu}-1}{\bar{\nu}} \delta - a(1 + \delta) \right] - 1 \tag{6.9}$$

where the power production contribution of U-235 was neglected and,

η_c is the fissile mean neutron yield per neutron absorbed in the fissile species in the core region ($\bar{\nu}F_c^{49}/A_c^{49}$),

$\bar{\nu}$ is the mean number of neutrons per fissile and fertile fission,

δ is the ratio of fertile to fissile fissions ($[F_c^{28} + F_B^{28}]/\bar{\nu}F_c^{49}$),

a is the parasitic absorptions and neutron leakage losses per fission neutron produced in the core and blanket regions

$$\left(\frac{A_c^{P,L} + A_c^{P.L}}{\bar{\nu}[F_c^{49} + F_c^{28} + F_B^{28}]}\right)$$

Equation (6.9) has the following interpretation:

a. fissile η_c is the dominant term and hence breeding performance can in principle be improved by creating a harder neutron spectrum in the core, which increases η_c of the fissile species: hence higher concentrations of heavy isotopes (metal and carbide fuel) in the core leads to a considerably higher breeding ratio,

b. the second term in brackets, $\frac{\bar{\nu}-1}{\bar{\nu}} \delta$, accounts for the "fast fission bonus" from fertile material,

c. the third term in brackets, $a(1+\delta)$, indicates that low parasitic absorption is essential for a high breeding ratio. The absorption cross-section of the fuel and non-fuel materials and the volume ratio of fuel to structural material are important factors here.

Generally speaking then, there are two basic approaches to improving the breeding ratio: one is to harden the neutron spectrum and the other is to decrease the relative amounts of parasitic absorption.

Inserting Eq. (6.8) into Eq. (6.7), the external breeding ratio can be rewritten as

$$bx = \frac{1}{\sum_{c,B}(A^{49} + A^{25} + A^{41})} \left[L_c + (\bar{\nu}-1)F_B - A_B^{P,L,C}\right] \quad (6.10)$$

where

$$F_B = F_B^{25} + F_B^{28},$$

$$A_B^{P,L,C} = A_B^{P,L} + C_B^{25} \text{ and}$$

it is assumed that no plutonium is present in the blanket at BOL.

The fissile consumption rate in the whole reactor, $\sum_{c,B} (A^{49} + A^{41} + A^{25})$, is directly related to the reactor thermal power P, and can be considered as a fixed value. Therefore, Eq. (6.10) suggests several strategies for increasing the external breeding ratio, i.e.,

a) increase $\bar{\nu}$ by hardening the blanket neutron spectrum,

b) increase the fertile fission rate, F_B^{28}, by hardening the blanket neutron spectrum,

c) minimize parasitic absorptions

A high neutron leakage rate leads to a high external breeding ratio however it also reduces the internal breeding ratio and thus is not an appropriate means to improve the external breeding ratio.

Actually, δ, the ratio of fertile-to-fissile fissions, and $\bar{\nu}$ are nearly constant, unless one contemplates substituting thorium for uranium as the fertile species - an option not under consideration here. Therefore neutron wastage by parasitic absorption and leakage is the key factor.

6.3.2 Evaluation of Factors which Affect External Fissile Breeding

6.3.2.1 Neutron Leakage Rate from the Core Region (L_c)

Most neutrons absorbed in the blanket region come from the core region, and the blanket zone nearest the core has the highest breeding capability and dominates the neutronic characteristics of the entire blanket region.

The neutron leakage rate into the blanket is simply related to the blankets diffusion coefficient, D_B, and buckling, B_B^2, i.e.;

$$L_c \propto D_B B_B \propto \left[\frac{\Sigma_{a,B} - \nu\Sigma_{f,B}}{\Sigma_{tr,B}}\right]^{1/2} \triangleq \left[\frac{\bar{\sigma}^{28}_{a,B}}{\bar{\sigma}^{28}_{tr,B}}\right]^{1/2} \qquad (6.11)$$

The variation of the cross-section ratio, $\left[\frac{\Sigma_{a,B}}{\Sigma_{tr,B}}\right]^{1/2}$, is so small in cases of practical interest that for all practical purposes the change in neutron leakage rate is insignificant as blanket composition is changed. The results of ANISN calculations show that blanket fuel density is not an important factor affecting the neutron leakage rate, and that while blanket thickness (e.g.1 vs 3 rows) and enrichment (Depleted U vs. Nat. U) are more sensitive parameters, their effects are also negligible ($< \pm$ 3%). Hence we can conclude that the neutron leakage rate from the core region into the blanket is affected only by core design parameters. We also reiterate that in all of the work reported here the core design and composition was held fixed.

6.3.2.2 Variation of $\bar{\nu}$-value by Spectrum Hardening

Since a higher net neutron production in the blanket region increases the external breeding ratio, achieving a high $\bar{\nu}$ value is one potentially favorable objective for the blanket designer. There is an empirical universal expression for $\bar{\nu}$-values (L2).

$$\bar{\nu}(E) = \bar{\nu}_o + aE \tag{6.12}$$

where $\bar{\nu}_o$ and a are constant and E is the incident neutron energy in MeV. The constants are

for U-235, $\bar{\nu}_o = 2.43$, $a = 0.065$ $(0 \leq E \leq 1)$

$\bar{\nu}_o = 2.35$, $a = 0.150$ $(E > 1)$

for U-238 $\bar{\nu}_o = 2.30$, $a = 0.160$ (all E)

The average neutron energy in the blanket region is also affected by the core neutron spectrum, because most neutrons come from the core, and the magnitude of the neutron flux is sharply attenuated as the distance from the core/blanket interface is increased. Therefore, the possible range of variation of the average neutron energy in the blanket region, which can be achieved by varying blanket fuel composition or fuel materials is rather small, and the $\bar{\nu}$ value remains essentially constant. The incremental increase in the $\bar{\nu}$ value due to spectrum hardening (achieved by replacing UO_2 fuel by UC or U_2Ti fuel) is only 0.74%.

6.3.2.3 Neutron Fission Rate in the Blanket (F_B)

The number of neutrons consumed in the blanket region by absorption and out-leakage is equal to the sum of the neutron in-leakage from the core and the neutrons produced by fission in the blanket, a sum to which the external breeding ratio is linearly proportional. Without for a moment considering options such as addition of moderator or fissile material to the blanket, we can assume that the neutron leakage rate from the core is constant, hence increasing the neutron generation in the blanket is an important means to improve the external breeding ratio.

The total fission integral, F_B, in the blanket is the sum of the fission reactions of U-235 and U-238;

$$F_B = (N_B^{28}\,\bar{\sigma}_{f,B}^{28} + N_B^{25}\,\bar{\sigma}_{f,B}^{25})\bar{\phi}_B \cdot V_B \tag{6.13}$$

Fission reactions in a fresh FBR blanket are predominently in U-238, and an increase in the population of high energy neutrons ($\geq$ 2.5 MeV) will increase the "effective" fission cross-section of U-238 because U-238 has a threshold near 1 MeV. Here we should note that a harder neutron spectrum does not improve the "effective" fission cross-section of U-238 without a concurrent increase in the number of high energy ($\geq$ 2.5 MeV) neutrons.

Since (a) most neutrons in the blanket come from the core and have an energy spectrum which is relatively independent of blanket composition, (b) the average energy and the most probable energy of prompt fission neutrons are 1.98 MeV and 0.85 MeV respectively and (c) inelastic scattering in Uranium itself dominates fast neutron downscattering, changing the neutron spectrum at high energies is difficult unless we can change <u>core</u> parameters. Hence increasing the effective U-238 fission cross-section in the blanket region is for all practical purposes impossible, and moreover multigroup calculations typically show that the space and spectrum averaged fission cross-section of the fertile species in the blanket is actually decreased by neutron spectrum hardening.

The average neutron flux, $\bar{\phi}_B$, shown in Eq. (6.13) should be, in a cylindrical blanket:

$$\bar{\phi}_B \cong \frac{2\phi_o}{S_B}\left[\frac{a+t}{B_B} + \frac{1}{B_B^2}\right]\left[1 - e^{-B_B t}\right] \tag{6.14}$$

where the flux distribution in the blanket was approximated as

$\phi_B(r) \cong \phi_o \, e^{-B_B(r-a)}$, and

a = the core radius,

ϕ_o = the neutron flux at the core/blanket interface,

$S_B = (a+t)^2 - a^2$

t = blanket thickness,

B_B^2 = the blanket geometrical buckling

A typical value of B_B for a 1000 MWe reactor having a 45 cm thick blanket is $\sim$0.1 cm^{-1}. Therefore, for thick blankets $e^{-B_B t}$ is small, and since the outer blanket radius, a+t, is 150 cm for a large core we can neglect $e^{-B_B t}$ and $\frac{1}{B_B^2}$; and hence the average neutron flux in the blanket is approximately proportional to B_B^{-1} , i.e.:

$$\bar{\phi}_B \propto B_B^{-1} \propto [\Sigma_{tr,B}(\Sigma_{a,B} - \nu\Sigma_{f,B})]^{-1/2} \qquad (6.15)$$

From the above analysis one may conclude that a high fuel density and the relative absence of neutron moderation decreases both the average neutron flux and the average microscopic fission cross-section of U-238, hence the total fission rate in the blanket is not linearly proportional to fuel density. Combining Eqs. (6.13) and (6.15) and assuming constant microscopic cross-sections, one has, very crudely

$$F_B \propto [N_B^{28}]^{1/2} \qquad (6.16)$$

6.3.2.4 Neutron Loss by Parasitic Absorption and Neutron Leakage into the Reflector ($A_B^{P,L,C}$)

In addition to increasing the fuel density, an alternative approach to improvement of the external breeding ratio is to lower parasitic absorption and leakage losses. Parasitic neutron absorption consumes about 10% of the total available neutrons, and 4% of all neutrons are lost by neutron leakage into (and absorption in) the reflector regions external to the blankets.

The four main materials which absorb neutrons in a blanket are U-238, U-235, alloying constituents if metallic fuel is used (Ti, Mo etc.), and Iron in structural materials. Neutron absorptions by U-238 and U-235 are directly related to the blanket breeding function, hence to improve external breeding we should (a) reduce the volume fraction of structural material, (b) select structural materials which have low neutron absorption cross-sections, and (c) avoid metal-alloy fuel.

Ti in U_2T_i fuel absorbs $\sim$3% of the total available neutrons, while the oxygen and carbon in ceramic fuels consume almost no neutrons. Since low parasitic absorption is paramount, selection of the fuel material is an extremely important task, and oxide, carbide and pure metal fuels are by elimination almost the only favorable choices open to blanket designers.

Neutron loss by leakage into the reflector region, which amounts to roughly 4% of the total neutrons for a 45 cm thick blanket, is dependent upon blanket thickness, which is in turn determined by fuel cycle cost considerations.

The blanket diffusion coefficient, D_B, is a function of the blanket transport cross-section, $\Sigma_{tr,B}$, which remains nearly constant for composition changes of practical interest. Accordingly, we can not expect large reductions of neutron leakage losses.

In summary, a high heavy metal density and a low absorption cross-section for the non-fertile fuel constuents are important if one is to reduce the parasitic absorption in the blanket, and thereby to improve (however slightly the opportunity may be) the external breeding ratio.

6.3.3 Evaluation of Blanket Design Parameters for External Fissile Breeding

6.3.3.1 Fuel Density

High fertile density is perhaps the single most important parameter as far as achieving a high external breeding ratio is concerned. Although it reduces the average neutron flux in the blanket, a high fuel density reduces the relative amount of parasitic absorption and increases slightly the number of fission reactions, with the overall result that fertile breeding is improved.

The integral capture rate of U-238 is

$$C_B^{28} = k_1 \cdot k_2 \cdot (1 - e^{-k_3 N_{28,B}}) \tag{6.17}$$

where

k_i = a constant,

$$k_2 = \frac{\sigma_{c,B}^{28}}{[3(\sigma_{tr,B}^{28} + \frac{\varepsilon_B}{1-\varepsilon_B}\sigma_{tr,B}^{25})]^{1/2}} \cdot$$

$$\frac{1}{[(\sigma_{a,B}^{28} + \frac{\varepsilon_B}{1-\varepsilon_B}\sigma_{a,B}^{25}) - (\nu\sigma_{f,B}^{28} + \frac{\varepsilon_B}{1-\varepsilon_B}\nu\sigma_{f,B}^{25})]^{1/2}} \tag{6.18}$$

$$k_3 = t/k_2 \cdot \sigma^{28}_{c,B} \tag{6.19}$$

t = blanket thickness

The external breeding ratio is proportional to the neutron capture rate in U-238, and the fractional change in the external breeding ratio, $\frac{\Delta bx}{bx}$, is :

$$\frac{\Delta bx}{bx} = \frac{\theta}{e^{\theta}-1} \left(\frac{\Delta N_{28,B}}{N_{28}}\right) \tag{6.20}$$

where

$$\theta = k_3 N_{28,B} \triangleq [3\sigma^{28}_{tr,B} \cdot \sigma^{28}_{a,B}]^{1/2} \cdot N_{28,B} \cdot t \tag{6.21}$$

If there are no significant absorbing materials present except for U-238, Eq. (6.20) provides a useful approximation for evaluating changes in the external breeding ratio, and the agreement between Eq. (6.20) and multigroup results is rather good.

6.3.3.2 Blanket Thickness and Blanket Neutronic Efficiency (E_B)

Blanket neutron efficiency, E_B, defined here as the ratio of consumed neutrons to total available neutrons in the blanket, is a function of blanket thickness, t.

$$E_B = \frac{\bar{\phi}_B(t)}{\bar{\phi}_B(\infty)} = (1 - e^{-B_B t}) \tag{6.22}$$

thus, the neutronic blanket thickness, t, in contrast to the economic blanket thickness is given by

$$t = \frac{1}{B_B} \ln [1 - E_B] \tag{6.23}$$

We should note that there is little further improvement of blanket efficiency with increasing thickness, beyond a certain range.

The effect of blanket thickness on external fissile breeding is easily found from Eq. (6.17), namely:

$$\frac{\Delta bx}{bx} = \frac{\theta}{e^{\theta}-1} \left(\frac{\Delta t}{t}\right) \tag{6.24}$$

The relationship between blanket thickness, t, and the pertinent economic parameters is simply derived by the combination of Eqs. (6.14) and (6.46), i.e.:

$$k_4(1 - e^{-B_B t}) \geq 4\, \bar{\omega} r_4 \tag{6.25}$$

where

$$k_4 = \frac{2\bar{\sigma}^{28}_{c,B}\, \phi_o}{S_B} \left[\frac{a+t}{B_B} + \frac{1}{B_B^2}\right] \cong \frac{2\bar{\sigma}^{28}_{c,B}\, \phi_o}{B_B t} \tag{6.26}$$

and $\bar{\omega}$ and r_4 are defined in Section 6.4.

Rearranging Eq. (6.26) for the blanket thickness, one obtains;

$$t \leq \frac{2(1 - 2\bar{\omega} r_4/\bar{\sigma}^{28}_{c,B}\, \phi_o)}{B_B} \tag{6.27}$$

which indicates, among other things, that the maximum Pu buildup rate, $\bar{\sigma}^{28}_{c,B}\, \phi_o$, should be larger than $2\bar{\omega} r_4$ for the existence of economic blankets of any thickness.

6.3.3.3 Blanket Enrichment

A main function of the FBR blanket is fissile breeding using neutrons leaking from the core, while power production in the blanket is a secondary and concomitant function. Therefore, blanket enrichment is not generally considered a particularly important factor to designers except as it complicates matching blanket power to flow over life. However, since blanket breeding capability depends on a high neutron availability, a superficially attractive design option capable of increasing neutron generation in the blanket is fissile seeding, that is, use of enriched fuel in the blanket. However we can expect that for a fixed core design a high fissile loading in the blanket region reduces core power, and also the neutron leakage rate into the blanket, and hence the external breeding ratio will suffer a compensatory loss.

Thus we will proceed at this point to assume that small variations of enrichment do not change the blanket characteristics significantly. In Eq. (6.18), transport, absorption and fission cross-section of U-235 are weighted relative to those of U-238 by the factor $\frac{\varepsilon_B}{1-\varepsilon_B}$ (~ 0.02). The ratio of the transport and absorption cross-sections of U-235 to those of U-238 is ~ 1.33 and ~ 12.83, respectively, hence the fission ($\frac{\bar{\sigma}^{25}_{f,B}}{\bar{\sigma}^{28}_{f,B}} \simeq 220$) reaction of U-235 is relatively important when the enrichment is increased. However the most important reactions in the blanket with respect to fissile breeding are the neutron transport and absorption reactions, because most available neutrons leak in from the core regions, and fission-produced neutrons in the blankets are of considerably less consequence. Therefore, a small variation in enrichment does not affect the external breeding function appreciably.

6.3.4 Effect of Non-linear Fissile Buildup on External Fissile Breeding

In most of the preceding analysis the external breeding ratios were estimated using beginning-of-life (BOL) blanket parameters under the assumption of linear fissile buildup as a function of time. As discussed in more detail in Section 4.2, the non-linear dependence of the fissile buildup rate should be considered when accuracy is a paramount consideration.

Here we define the "exact" (time-averaged) external breeding ratio, $\bar{b}x$ as

$$\bar{b}x \equiv \frac{\text{(Fissile Inventory at EOL - Fissile Inventory at BOL) Blanket}}{\text{(Average Fissile Consumption Rate in Core and Blanket)}} \cdot \frac{1}{\text{(Total Irradiation Time)}} \qquad (6.28)$$

Using results which were developed in the body of this report the "exact" external breeding ratio for an optionally-irradiated balnket can be expressed as

$$\bar{b}x = \frac{1}{\bar{M}_a^{fissile}} [M_{28}(0) \cdot \bar{\sigma}^{28}_{c,B} \cdot \bar{\Phi}_B] \, e^{-\xi \frac{T^o_{op}}{T_c}}$$

$$= bx \cdot e^{-\xi \frac{T^o_{op}}{T_c}}$$

$$\cong 0.766 \text{ bx} \qquad (6.29)$$

Equation (6.29) indicates that the external breeding ratio calculated using BOL parameters is overestimated by slightly over 20% due to the assumption of a linear fissile buildup time history.

However, Eq. (6.29) also indicates that the "exact" time-averaged external breeding ratio of various blankets having different optimum irradiation times are directly proportional to the external breeding ratio calculated using BOL blanket parameters. Since the constant of proportionality is the same for all cases (to a very good approximation), one can use BOL studies to correctly rank the breeding performance of various blanket design options.

6.3.5 Summary

The fissile breeding capability of FBR blankets has been reviewed, and the factors and design parameters which affect external fissile breeding have been evaluated in this section.

The main neutron source for the blanket region is neutron leakage from the core, which typically accounts for almost 90% of the total available neutrons in the blanket region; and non-fertile absorptions account for about 15% of the losses as shown in Table 6.2. Hence we can expect that without changing core parameters, improvement of the external breeding ratio by improving upon the 10% or so of blanket-fission-produced neutrons and the 15% or so of neutrons lost in the blanket will be relatively small.

The non-linear fissile-buildup-time-history was also considered in this section, and it was noted that the BOL external breeding ratio should be modified by a constant to obtain a valid quantitative estimate of the external breeding ratio averaged over life for blankets which are irradiated to their economically optimum exposure.

TABLE 6.2

SPECTRUM AND SPACE-WEIGHTED MACROSCOPIC ABSORPTION AND FISSION CROSS-SECTIONS FOR BLANKET MATERIALS

	UO_2	UC	U_2Ti
$\Sigma^{28}_{a,B}$	4.8619 E-03	5.9973 E-03	5.3057 E-03
$\Sigma^{25}_{a,B}$	1.2501 E-04	1.4619 E-04	1.2070 E-04
$\Sigma^{O}_{a,B}$	6.0733 E-06	-	-
$\Sigma^{C}_{a,B}$	-	2.1016 E-08	-
$\Sigma^{Ti}_{a,B}$	-	-	1.7775 E-04
$[\Sigma^{Fuel}_{a,B}]$	4.9935 E-03	6.1435 E-03	5.6042 E-03
$\Sigma^{Fe}_{a,B}$	3.0495 E-04	2.8451 E-04	2.5293 E-04
$\Sigma^{Cr}_{a,B}$	4.7955 E-05	4.3167 E-05	3.6393 E-05
$\Sigma^{Ni}_{a,B}$	4.3843 E-05	4.1630 E-05	3.5764 E-05
$\Sigma^{Na}_{a,B}$	2.6496 E-05	2.4450 E-05	1.9106 E-05
$[\Sigma^{Steel}_{a,B}]$	4.2324 E-04	3.9377 E-04	3.4420 E-04
$\nu\Sigma^{28}_{f,B}$	5.3903 E-04	7.1490 E-04	6.8269 E-04
$\nu\Sigma^{25}_{f,B}$	2.0697 E-04	2.4633 E-04	2.1136 E-04
$[\nu\Sigma_{f,B}]$	7.4601 E-04	9.5900 E-04	8.9405 E-04
$\frac{\Sigma^{28}_{a,B}}{\Sigma_{a,B}}$	0.8976	0.9174	0.8919
$\frac{\Sigma^{28}_{a,B}}{\Sigma^{steel}_{a,B}}$	11.4873	15.2305	15.4146
$\phi_B V_B$	5.21175 E+08	4.50135 E+08	4.91115 E+08
bx	0.35043	0.37500	0.36053

*All cross-sections are in cm^{-1}.

6.4 FUEL DEPLETION AND ECONOMIC ANALYSIS OF FBR BLANKETS

6.4.1 Generalized Fissile Material Buildup Histories for FBR Blankets

For simple neutronic/economic analyses, a linear fissile buildup approximation has been adopted in some previous work (K2),(T1). However, the linear buildup approximation can incur appreciable error for fuel depletion and economic calculations in the radial blanket region of a fast reactor (B6).

Several recent studies have been concerned with the development of accurate methods for fuel depletion calculations which rely upon conventional multigroup time step techniques (L4),(H3) or non-linear perturbation techniques (S2), (M1), which are currently performed using relatively expensive computer programs, and offer little insight upon which generalizations of the type of interest in this study can be based.

In view of the partial successes of prior work (B4), (B6) and the fact that practical engineering constraints, such as limitation of refueling to 6, 12 or 18 month intervals, relaxes the degree of accuracy required in estimation of optimum refueling dates, it was considered that a suitable simple model combining both the neutronic and the economic aspects of FBR performance could be synthesized.

The differential equation governing nuclide depletion can be rewritten on a mass basis for a given zone of the blanket (ignoring the mass difference per mole of U-238 and Pu-239):

$$\frac{dM_{49}}{dt} = M_{28}\,\bar{\sigma}_c^{28}\,\bar{\phi} - M_{49}\,\bar{\sigma}_a^{49}\,\bar{\phi} \qquad (6.30)$$

and

$$\frac{dM_{28}}{dt} = -M_{28}\,\bar{\sigma}_a^{28}\,\bar{\phi} \qquad (6.31)$$

Here, Pu-241 buildup was neglected and consideration was limited to Pu-239 and U-238 as the representative fissile and fertile species.

The solution for the fissile buildup history can be written in a particularly simple dimensionless form; after some rearrangement the following equation results:

$$M_{49}(t)/\hat{M}_{49} = \frac{t}{T_c} e^{-\xi_o \frac{t}{T_c}} \tag{6.32}$$

where

$T_c = (\bar{\sigma}_a^{49} \bar{\phi} - \bar{\sigma}_a^{28} \bar{\phi})^{-1}$ = the characteristic time constant,

$$\hat{M}_{49} = M_{28}(0) \quad \left(\frac{\bar{\sigma}_c^{28}}{\bar{\sigma}_a^{49} - \bar{\sigma}_a^{28}}\right)$$

$$\xi_o = 1/2 + [\hat{M}_{49}/M_{28}(0)](\bar{\sigma}_a^{28}/\bar{\sigma}_c^{28}).$$

The accuracy of Eq. (6.32) using only BOL parameters is obviously limited due to the variation of cross-sections and neutron flux as a function of time. However, empirical observations have shown that use of a corrected constant, ξ, instead of ξ_o can overcome this problem because the parameters, $\hat{M}_{49}$ and T_c, are exponential functions of time. Thus Eq. (6.32) can be rewritten as

$$M_{49}(t)/\hat{M}_{49} = \frac{t}{T_c^o} e^{-\xi \frac{t}{T_c^o}} \tag{6.33}$$

where subscript o refers, as usual, to the (constant) values calculated from BOL parameters.

Equation (6.33), together with the empirical finding that $\xi \cong 2/3$ for all blankets of interest, suggests that $M_{49}(t)/\hat{M}_{49}$ can be correlated against t/T_c^o. Figure 6.2 shows a selection of representative data points calculated using state-of-the-art physics depletion methods (2DB code and 4-group σ sets). The correlation is excellent and all points fall very nearly on the curve defined by Eq. (6.33).

We should also point out that Eq. (6.33) can be reformulated in terms of enrichment:

$$\varepsilon(t) = \frac{M_{49}(t)}{M_{28}(0)} = [\xi_o - 1/2] \frac{t}{T_c^o} e^{-\xi \frac{t}{T_c^o}} \tag{6.34}$$

Also, an entirely parallel and equally successful treatment can be applied to correlate higher isotope concentrations (see Appendix C.1).

6.4.2 Optimum Economic Parameters for FBR Blankets

In this study the optimum blanket parameters of concern are the optimum and breakeven irradiation times, optimum enrichment and maximum blanket revenue per assembly, which are illustrated in Fig. 6.3.

6.4.2.1 Optimum Irradiation Time (T_{op})

From the general expression for the levelized fuel cycle cost shown in Eq. (6.4), the fuel cycle cost contribution by a given entity of blanket fuel can be expressed as

$$\frac{e}{M_{HM}} \propto \frac{\bar{c}_1 e^{r_1 T} + \bar{c}_2 e^{-r_2 T} - \bar{c}_3 \varepsilon(T)\, e^{-r_3 T}}{T} \tag{6.35}$$

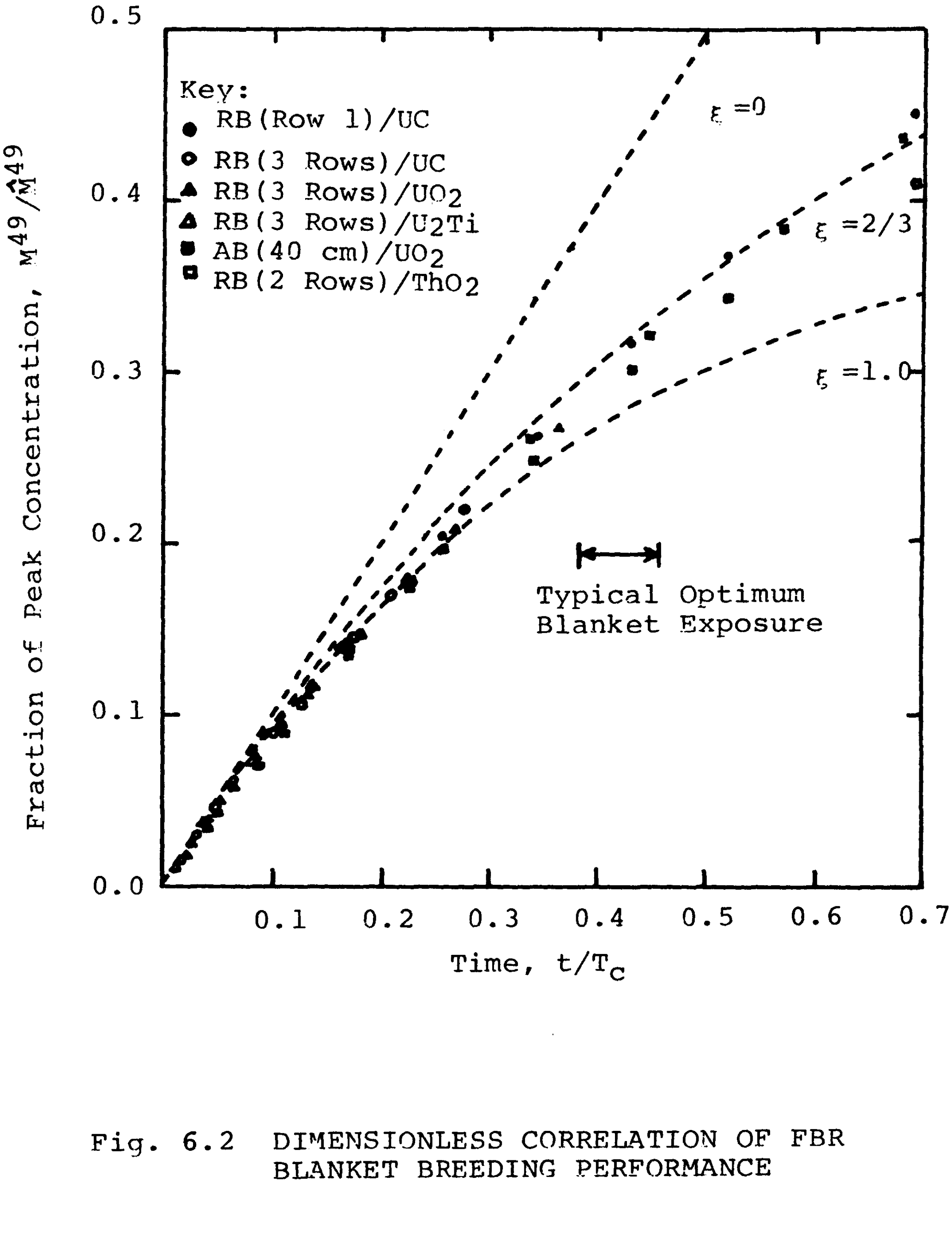

Fig. 6.2 DIMENSIONLESS CORRELATION OF FBR BLANKET BREEDING PERFORMANCE

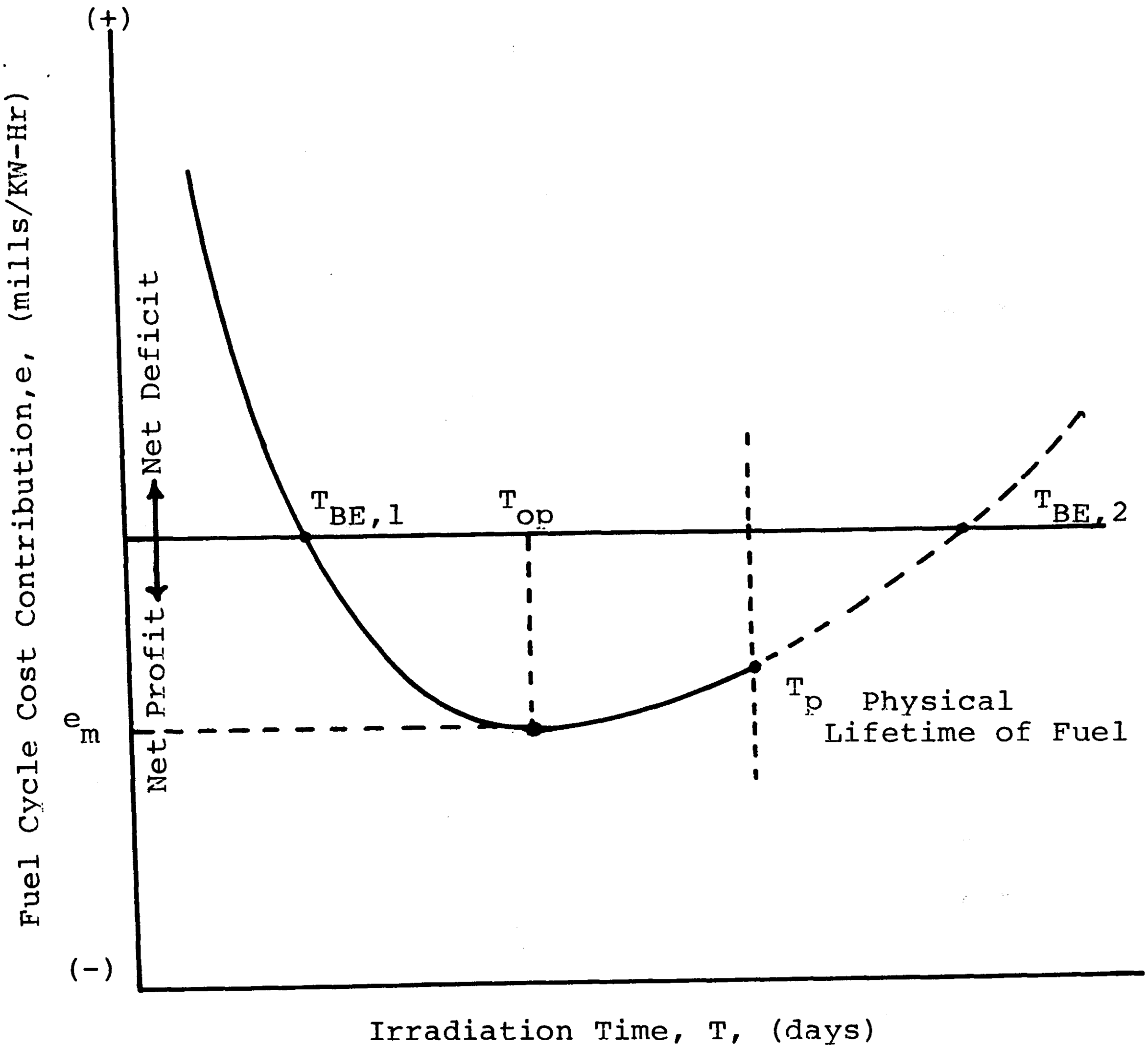

Fig. 6.3 TYPICAL VARIATION OF THE FUEL CYCLE COST CONTRIBUTION FOR A FAST REACTOR BLANKET

Using the simple correlation for the enrichment which was derived in the previous section, i.e.,

$$\varepsilon(T) = [\xi_o - 1/2] \frac{T}{T_c^o} e^{-\xi \frac{T}{T_c^o}} = S_o T e^{-\xi \frac{T}{T_c^o}} \qquad (6.36)$$

(where S_o is the linear enrichment buildup rate determined by BOL conditions, equal to $\bar{\sigma}_c^{28} \bar{\phi}$.)

Eq. (6.35) can be rewritten as

$$\frac{e}{M_{HM}} \propto \frac{\bar{c}_1 e^{r_1 T} + \bar{c}_2 e^{-r_2 T} - \bar{c}_3 S_o T e^{-r_4 T}}{T} \qquad (6.37)$$

where

$$r_4 = r_3 + \xi / T_c^o \qquad (6.38)$$

To find the optimum irradiation time, the time derivative of the fuel cycle cost contribution is set equal to zero and the solution of this equation is approximated by the series expansion of the exponential function, dropping negligible terms. Thus one can obtain:

$$T_{op} = 1/r_4 \; [1 \pm \sqrt{1 - 2 \left\{ \frac{(\bar{c}_1 + \bar{c}_2) r_4}{\bar{c}_3 S_o} \right\}^{1/2}}] \qquad (6.39)$$

Equation (6.39) can be futher simplified by algebraic rearrangements;

$$T_{op} = \left[\frac{\bar{\omega}}{S_o r_4}\right]^{1/2} F_1 \qquad (6.40)$$

where

$$\bar{\omega} = \frac{\bar{c}_1 + \bar{c}_2}{\bar{c}_3} ,$$

$$F = (1 + 1/2\, x_1 + 1/2\, x_1^2 + 5/8\, x_1^3 + \ldots) \cong \text{constant},$$

$$x_1 = [\frac{\bar{\omega} r_4}{S_o}]^{1/2}$$

The compensation factor, F_1, is nearly constant for all fuel materials loaded into the same blanket configuration, as shown in Table 4.3, if the economic parameter $\bar{\omega}$ is fixed (for radial blankets, F_1 assumes an average value of 1.45).

The optimum irradiation times calculated from the simple correlations are consistent with 2DB/BRECON results within $\pm 2\%$, as shown in Table 4.3.

6.4.2.2 Breakeven Irradiation Time

For the breakeven time, the fuel cycle cost contribution is set equal to zero,

$$e \propto \frac{\bar{c}_1 e^{r_1 T} + \bar{c}_2 e^{-r_2 T} - \bar{c}_3 S_o T\, e^{-r_4 T}}{T} = 0 \qquad (6.41)$$

Expanding the exponential functions through T^2 and neglecting the negligible terms, Eq. (6.41) becomes:

$$T_{BE}^2 - \frac{1}{r_4} T_{BE} + \frac{\bar{\omega}}{S_o r_4} = 0, \qquad (6.42)$$

which has the solutions:

$$T_{BE} = \frac{1}{2r_4} [1 \pm \sqrt{1 - \frac{4r_4\bar{\omega}}{S_o}}] \quad (6.43)$$

or

$$T_{BE} = [\frac{\bar{\omega}}{S_o}]F_2 \quad (6.44)$$

where

$$F_2 = (1 + x_2 + 2x_2^2 + \ldots) \cong \text{constant},$$

$$x_2 = [\frac{\bar{\omega}r_r}{S_o}] = x_1^2.$$

In equation (6.42), the discriminant should be positive for the existence of a breakeven time, which means that blanket fuel cycle cost contributions are negative and the blanket is economic. This requirement of a non-negative discriminant gives:

$$1 - 4\bar{\omega}r_4/S_{om} \geq 0 \quad (6.45)$$

or

$$S_{om} \geq 4\bar{\omega}r_4 \quad (6.46)$$

which indicates that the specific enrichment buildup rate (S_{om}) must not be less than a certain value ($4\bar{\omega}r_4$) if a given blanket region is to justify its existence on economic grounds.

6.4.2.3 Maximum Blanket Revenue

The maximum blanket revenue can be calculated by inserting the optimum irradiation time (T_{op}) and appropriate economic factors into the general cost equation.

If we select the approximate expression for the optimum irradiation time, $T_{op} = F_1[\frac{\bar{\omega}}{S_o r_4}]^{1/2}$, the maximum blanket revenue can thus be rewritten as

$$e_m = \frac{1000\ M_{HM}}{E}[(\bar{c}_1 + \bar{c}_2)\bar{c}_3 S_o r_4]^{1/2}\ F_3 \tag{6.47}$$

where

$$F_3 = [\frac{F_1^2 + 1}{F_1} + \frac{(\bar{c}_1 r_2 - \bar{c}_1 r_2)}{\{(\bar{c}_1 + \bar{c}_2)\bar{c}_3 S_o r_r\}^{1/2}} - \frac{F_1^2}{2}(\frac{\bar{\omega} r_4}{S_o})^{1/2} - (\frac{S_o}{\bar{\omega} r_4})^{1/2}] \tag{6.48}$$

Equation (6.47) indicates that

a. F_3 should be negative for positive blanket revenue,

b. F_3 and S_o are the dominant parameters determining the maximum balnket revenue, hence UO_2 fuel is more economical, as shown in Table 6.3.

Table 6.3 summarizes the maximum blanket revenue and the related parameters of oxide, carbide and metal-alloy fueled blankets. A hard neutron spectrum (UC or U_2Ti) leads to longer T_{op}, while a softer neutron spectrum (UO_2) forms a shorter T_{op} and large e_m due to the higher value of S_o.

6.4.2.4 Optimum Discharge Enrichment and Dimensionless Optimum Irradiation Time

The optimum discharge enrichment can be obtained by inserting the optimum irradiation time, T_{op}, into Eq. (6.36):

TABLE 6.3

OPTIMUM BLANKET PARAMETERS AND RELATED FACTORS FOR SIMPLE CORRELATIONS

	Accounting Method A†			Accounting Method B††		
	UO_2	UC	U_2Ti	UO_2	UC	U_2Ti
M_{HM}, Kg	17,299	23,233	24,759	5,180	6,957	7,414
So, KgPu/KgM$_{HM}$,yr	0.005870	0.004663	0.004239	0.012030	0.010204	0.009101
r_4, yr^{-1}	0.081475	0.0707147	0.066265	0.16065	0.14495	0.13421
T_{op}, yr	7.49 7.72	9.02 9.21	9.78 9.73	3.77 3.63	4.31 4.17	4.75 4.70
T_{BE}, yr	2.83 3.09	3.56 4.38	3.92 4.58	1.42 1.44	1.67 1.55	1.87 1.96
F^*_3	-0.5064	-0.3881	-0.3443	-0.6420	-0.5744	-0.5366
e_{fab}, mills/KwHr	0.0767 0.0784	0.0921 0.0959	0.0937 0.0997	0.0371 0.0354	0.0451 0.0475	0.0447 0.0465
e_{rep}, mills/KwHr	0.0216 0.0231	0.0220 0.0244	0.0206 0.0242	0.0123 0.0117	0.0136 0.0157	0.0124 0.0142
$-e_{mat}$, mills/KwHr	0.1561 0.1548	0.1635 0.1626	0.1574 0.1597	0.0923 0.0824	0.1038 0.0990	0.0979 0.0912
$-e_m$, mills/KwHr	0.0578 0.0533	0.0494 0.0423	0.0431 0.0358	0.0429 0.0353	0.0451 0.0358	0.0408 0.0305

Key: (upper value in cell) Eq. (6.39) or (6.43) or (6.47); (lower value in cell) 2DB/BRECON RESULT

† 3-row Radial Blanket

†† 1st-row in 3-row radial blanket

* $T_{op} = 1.45\ (\bar{\omega}/S_o r_4)^{1/2}$

$$\varepsilon_{op} = \frac{M^{49}(T_{op})}{M_{28}(0)} = S_o T_{op} \, e^{-\xi \frac{T_{op}}{T_c^\circ}} \tag{6.49}$$

or

$$\varepsilon_{op} \cong F_1 \left(\frac{S_o \bar{\omega}}{r_4}\right)^{1/2} e^{-\hat{\xi} \left(\frac{\bar{\omega}}{S_o r_4}\right)^{1/2}} \tag{6.50}$$

where

$$\hat{\xi} = \xi \cdot F_1 \cdot (\bar{\sigma}_a^{49} \bar{\phi} - \bar{\sigma}_a^{28} \bar{\phi})_{BOL}$$

The dimensionless optimum irradiation time can be defined as

$$\frac{T_{op}}{T_c^\circ} = F_1 \left(\frac{\bar{\omega}}{S_o r_4}\right)^{1/2} \cdot (\bar{\sigma}_a^{49} \bar{\phi} - \bar{\sigma}_a^{28} \bar{\phi})_{BOL}$$

The values of T_{op}/T_c° computed using Eq. (6.51) for various fuel materials and different blanket configurations are very nearly the same. Considering that the actual irradiation time is determined by the plant refueling schedule, which will permit fuel discharge only once or twice per year, we can therefore consider that T_{op}/T_c° of the various fuel materials are the same within practical limits.

This result is an important input for calculations estimating the time-varying characteristics of the blanket breeding ratio, as described in Section 6.3.4.

6.4.3 Sensitivity Analysis for Optimum Blanket Parameters

To trace the optimum blanket parameters impacted by the variation of the economic and financial environment, sensitivity functions were developed and evaluated.

Sensitivity coefficients have been defined as

$$\lambda_q^P(S) = \lim_{\substack{\Delta q \to 0 \\ q \to S}} \frac{\Delta P/P}{\Delta q/q} = \left[\frac{\partial P}{\partial q}\right]_{q=S} \cdot (q/P) \tag{6.52}$$

where q is the independent parameter such as operating cost (Ci), income tax rate (τ) etc., which has reference value S and a small variation Δq; and P is the dependent optimum parameter such as the optimum irradiation time or breakeven time, etc.

By the algebraic rules of partial derivatives, we can express the differential, or variation, of optimum parameter P as follows:

$$\Delta P(\Delta S) = \sum_{i=1}^{n} \left[\lambda_q^P(S) \cdot \Delta q \cdot \frac{P}{q}\right]_i \tag{6.53}$$

Table 6.4 summarizes the sensitivity coefficients for the optimum economic parameters.

As expected, the Pu market value ($\bar{c}_3$) and linear enrichment buildup rate (S_o) are the most important factors for all optimum economic parameters.

Note that the sensitivity coefficient for the non-linear factor, ξ/T_c°, has a rather high value compared to many of the other sensitivity coefficients, which illustrates that the non-linear characteristic of Pu buildup in FBR blankets is very important to determination of the optimum economic parameters (except for the breakeven time).

These results summarized in Table 6.3 also illustrate how oxide fuel, which has the highest value of S_o and a relatively large r_4, can produce the highest maximum blanket revenue compared to carbide and metal alloy fuels, because S_o is the most influential parameter, along with Pu market valve c_3. Therefore, to achieve the highest blanket revenue, a high fissile production rate - this does not necessarily mean high external

TABLE 6.4 SENSITIVITY COEFFICIENTS FOR OPTIMUM ECONOMIC PARAMETERS†

q	$T_{op} = F_1[\frac{\bar{\omega}}{S_o r_4}]^{1/2}$		$T_{BE} = F_2[\frac{\bar{\omega}}{S_o}]$		e_m	
u	$\lambda_q^{T_{op}}$	Reference Value*	$\lambda_q^{T_{BE}}$	Reference Value*	$\lambda_q^{e_m}$	Reference Value*
$\bar{\omega}$	0.5	0.5	1.0	1.0		-
c_1	$0.5/(1 + \bar{c}_2/\bar{c}_1)$	0.304	$(1 + \bar{c}_2/\bar{c}_1)^{1/2}$	0.609	$0.5(\frac{F_1^2+1}{F_1})[\frac{\bar{c}_1}{(\bar{c}_1+\bar{c}_2)F_3}] + \frac{\bar{c}_1(r_1 - \frac{F_1^2}{2}r_4)}{[(\bar{c}_1+\bar{c}_2)\bar{c}_3 S_o r_4]^{1/2}F_3}$	-1.251
c_2	$0.5/(1 + \bar{c}_1/\bar{c}_2)$	0.196	$(1 + \bar{c}_1/\bar{c}_2)^{1/2}$	0.391	$0.5(\frac{F_1^2+1}{F_1})[\frac{\bar{c}_2}{(\bar{c}_1+\bar{c}_2)F_3}] + \frac{\bar{c}_2(r_2 - \frac{F_1^2}{2}r_4)}{[(\bar{c}_1+\bar{c}_2)\bar{c}_3 S_o r_4]^{1/2}F_3}$	-0.320
c_3	-0.5	-0.5	-1.0	-1.0	$0.5(\frac{F_1^2+1}{F_1})(\frac{1}{F_3}) - \frac{\bar{c}_3 S_o}{[(\bar{c}_1+\bar{c}_2)\bar{c}_3 S_o r_4]^{1/2}F_3}$	2.576
ΔT_1	$\lambda_{c_1}^{T_{op}} \cdot (X\Delta T_1/1-\tau)$	0.024	$\lambda_{c_1}^{T_{BE}} \cdot (X\Delta T_1/1-\tau)$	0.048	$\lambda_{c_1}^{e_m} \cdot (X\Delta T_1/1-\tau)$	-0.1
ΔT_2	$\lambda_{c_2}^{T_{op}} \cdot (-X\Delta T_2)$	-0.008	$\lambda_{c_2}^{T_{BE}} \cdot (-X\Delta T_2)$	-0.016	$\lambda_{c_2}^{e_m} \cdot (-X\Delta T_2)$	0.013

continued on next page

ΔT_3	$0.5\ X\Delta T_3$	0.02	$X\Delta T_3$	0.040	$\lambda_{c_3}^{e_m} \cdot (-X\Delta T_3)$	-0.103
S_o	-0.5	-0.5	-1.0	-1.0	$0.5(\frac{F_1^2+1}{F_1}) \cdot \frac{1}{F_3} - \frac{\bar{c}_3 S_o}{[(\bar{c}_1+\bar{c}_2)\bar{c}_3 S_o r_4]^{1/2} F_3}$	2.576
r_4	-0.5	-0.5	-	-	$0.5(\frac{F_1^2+1}{F_1}) \cdot \frac{1}{F_3} - \frac{F_1^2(\bar{c}_1+\bar{c}_2) r_4}{2[(\bar{c}_1+\bar{c}_2)\bar{c}_3 S_o r_4]^{1/2} F_3}$	-1.238
X	$-0.25\ X/r_4$	-0.245	-	-	$\lambda_{r_4}^{e_m} \cdot (0.5\ X/r_4)$	-0.608
τ	0	0.0	-	-	0	0.0
ξ/T_c°	$-0.5\ \xi/T_c^\circ/r_4$	-0.255	-	-	$\lambda_{r_4}^{e_m}\ \ \xi/(T_c^\circ \cdot r_4)$	-0.63

†UO_2 Fueled 3-row Radial Blanket for Accounting Method A

*For the reference economic environment

breeding ratio - is a very important factor. Also note that this conclusion of oxide superiority is predicated on equal fuel fabrication costs per Kg of heavy metal for all fuels; if carbide fuel assemblies can be fabricated more cheaply then this may offset the economic disadvantages noted here.

6.4.4 The Effect of Fuel Management Options on Blanket Economics

The most commonly considered options for the fuel management of radial blanket assemblies are:

a. No Shuffling or Batch (NS); All fuel assemblies in the radial blanket are refueled at the same optimum time.

b. Zone or Region Scatter (RS): Each individual assembly is refueled at its own local optimum irradiation time.

c. In-Out Shuffling (IO): Fresh blanket assemblies are inserted into blanket positions at the core-blanket interface and later moved to outer positions.

d. Out-In Shuffling (OI); Fresh fuel assemblies are inserted at the blanket periphery and later moved to inner blanket positions.

There are several difficulties involved in comparing fuel management options under truly comparable conditions, and the following assumptions were used to permit a simple analysis in this study:

a. Each blanket "row" has an equal volume and number of fuel assemblies.

b. The average neutron flux and group-averaged cross-section are a function of position only and are not a function of fuel burnup.

c. All fuel assemblies have equal intervals of irradiation time, T_{op}/(no. of rows), in each row for the In-Out or Out-In Shuffling options.

6.4.4.1 The Impact of Fuel Management on Pu Production

The steady state fissile production rate of each fuel management option ($\bar{M}^{49}_{FM,0}$) which is defined as

$$\bar{M}^{49}_{FM,0} = \left(\frac{\text{Total Amount of Plutonium at the End of the Fuel Cycle}}{\text{Total Irradiation Time}}\right)_{\text{blanket}}$$

can be written in the general format:

$$\bar{M}^{49}_{FM,0} = 1/3\ M_{28}(0) \sum_i \left(S_{o,i}\ e^{-R_{FM,i}\ T_{op,0}}\right) \qquad (6.54)$$

where

subscript FM identifies the fuel management scheme

i refers to ith row of the blanket and

0 refers to the whole blanket.

The linear enrichment buildup rates of each row, $S_{o,i}$, were assumed constant for this study. Therefore, the differences caused by the different fuel management schemes are expressed in the exponential function, $e^{-R_{FM,i}T_{op,0}}$. Table 6.5 shows the steady state plutonium production rate, $\bar{M}^{49}_{FM,0}$, and associated parameter $R_{FM,i}$. The batch option produces about 15% less plutonium than the others and the Out-In scheme produces slightly more plutonium than do the other options.

Barthold (B1) reviewed fuel shuffling schemes in LMFBR blankets, and concluded that the plutonium production in the blanket is to a first order approximation the same for all shuffling schemes. Ketabi's

TABLE 6.5

COMPARISON OF STEADY-STATE Pu PRODUCTION RATES OF VARIOUS FUEL MANAGEMENT OPTIONS

Parameter \ Option	Batch (NS)	In-Out (IO)	Out-IN (OI)	Region Scatter (RS)
$R_{FM,1}$, yr^{-1}	0.07319	0.05191	0.02439	0.04201
$R_{FM,2}$, yr^{-1}	0.03221	0.01844	0.05529	0.03647
$R_{FM,3}$, yr^{-1}	0.01244	0.00415	0.06851	0.02774
$\sum_{i=1}^{3} (S_{o,i}\, e^{-R_{FM,i}\, T_{op,0}})$	0.01238	0.01410	0.01429	0.01392
$\bar{M}^{49}_{FM,0}$ KgPu/yr	71.3886	81.3091	82.4291	80.2506
$\bar{M}^{49}_{FM,0}/\bar{M}^{49}_{NS,0}$	1.0	1.139	1.155	1.124

† UO_2 Fueled 3-row Radial Blanket under Reference Economic/Neutronic Environment (for Accounting Method A)

work at MIT reached similar conclusions (K2). This difference in conclusions is caused in part, if not entirely, by the approximation in Bathold depletion equations of constant U-238 concentration. On the other hand, Lake et. al. (L1) found that the Out-In Shuffling option offers ≈0.005 higher breeding ratio over that of In-Out fuel shuffling options, a result which agrees with that of the present work.

6.4.4.2 Effects of Fuel Management Options on Blanket Optimum Parameters

To analyze the characteristics of various fuel management options simply, fixed neutron cross-sections and flux (in addition to a fixed economic/financial environment) were assumed.

Therefore, the only parameter which varies in response to a change of fuel management scheme is the non-linearity parameter, ξ/T_c°. For example, if ξ/T_c° is reduced by the switch from the batch to the Out-In Shuffling scheme, the r_4 (since $r_4 = r_3 + \xi/T_c^\circ$) will be smaller and will result in a longer optimum irradiation time and higher blanket revenue.

Using the definition of r_4 and a series combinations of equations, one can write

$$r_4 = r_3 + \xi/T_c^\circ \cong r_3 + \frac{\sum_{i=1}^{3} S_{o,i} \, R_{FM,i}}{3\, S_{\bullet,0}} \qquad (6.55)$$

Table 6.6 summarizes the effects on blanket parameters arising from the variation of r_4. Table 6.6 shows that the No-Shuffling option is the worst case for blanket economics and In-Out and Out-In Shuffling schemes are the best. The Region-scatter schemes are also advantageous compared to the No-Shuffling case; however the plutonium production rate and maximum blanket revenue achieved are less than those of the In-Out or Out-In shuffling schemes.

TABLE 6.6

EFFECTS OF FUEL MANAGEMENT OPTIONS ON BLANKET OPTIMUM PARAMETERS†

PARAMETER (EQ.)	EFFECTS OF SHUFFLING*
Optimum Irradiation Time $[T_{op} = F_1(\frac{\bar{\omega}}{S_o r_4})^{1/2}]$	• Optimum irradiation time is slightly increased (by ∿10%) because of smaller r_4 (0.097 vs. 0.078)
Breakeven Time $[T_{BE} = F_2(\frac{\bar{\omega}}{S_o})]$	• Breakeven time is not appreciably dependent on r_4. Therefore, it is not affected by the choice of fuel management option.
Maximum Blanket Revenue $[e_m \propto [(\bar{c}_1 + \bar{c}_2)\bar{c}_3 S_o r_4]^{1/2} F_3]$	• Lower r_4 and higher Pu production rate offers ∿30% higher (∿0.07 mills/KwHr vs. 0.05 mills/KwHr) blanket revenue.

*No-shuffling is reference case, using Accounting Method A;

†UO_2 fueled 3-row radial blanket.

6.5 EVALUATION OF FBR BLANKET DESIGN CONCEPTS

In practice, the design of FBR blankets involves a compromise between engineering considerations, safety problems, reactor physics and economics. Often, these requirements are in conflict. Low fuel cycle costs can be obtained at the expense of a low external breeding ratio, conversely the more complete neutron utilization required to achieve a high breeding ratio leads to thicker blankets, and the value of the additional fissile production may not cancel out the increased fabrication and reprocessing costs.

In this section, several advanced/new FBR blanket design concepts will be analyzed, emphasizing their neutronic and economic performance, although engineering desing constraints will be considered where appropriate.

Advanced blanket design concepts can be classified into the following four categories:

1. Design concepts emphasizing neutron spectrum variations -moderated blankets and spectrum-hardened blankets.
2. Design concepts emphasizing high neutron utilization -especially reflected blankets and blankets with high fuel volume fraction.
3. Design concepts emphasizing a high rate of internal neutron generation - fissile seeded blankets.
4. Design concepts emphasizing geometrical rearrangements, -parfait blankets, sandwiched blankets, and heterogeneous core concepts.

6.5.1 The Moderated Blanket

As described in the previous sections, a low relative density of fuel material (i.e. high diluent content), which leads to a soft neutron spectrum in the blanket, is favorable from an economic aspect because of the high fissile breeding rate attainable; while, as regards breeding ratio, achieving a high fertile density (hence hard neutron spectrum) is a more important goal.

The ratio of the fertile density of carbide fuel to that of oxide fuel is 1.34 which is much larger than the ratio of the (space and spectrum-averaged) fertile microscopic cross-sections which is only about 1.09.

The purpose of adding moderator to the blankets is to create a softer neutron spectrum, which increases the fertile neutron capture cross-section and the blanket-averaged neutron flux: hopefully enough to offset the disadvantages of low fertile density.

The impacts of heterogeneous-seeding instead of homogeneous-seeding was also examined and both found to have similar effects on fissile breeding and blanket economics. Hence we need not make this distinction in our summarized discussions.

6.5.1.1 Neutronic Aspects of Moderated Blankets

The advantages of moderated blankets stem from high fertile capture cross-sections, high average neutron flux in the blanket region and lower neutron leakage into the reflector region. These factors are very favorable as regards achievement of a high external breeding ratio. However, two side effects counter the improvement; a) fertile inventory is decreased (some fuel must be displaced to make room for the moderator) and b) neutron absorption by the moderator increases the parasitic neutron absorption loss.

The net result is that the fraction of total neutrons absorbed by fertile species is actually the same or slightly smaller when the moderator is added, as shown in Table 6.7. As described in Section 6.3, fertile density in the blanket region is the most sensitive parameter as regards breeding performance, and this result is to be expected regardless of the blanket thickness and fuel materials.

The internal (core) breeding ratio is not affected by moderator seeding in the blanket.

6.5.1.2 Economic Aspects of Moderated Blankets

A possibly attractive feature of moderated blankets may be their potential for the improvement of blanket revenue due to their high fissile buildup rate (S_o), achieved without significant loss of fissile breeding.

The sensitivity coefficient for S_o, $\lambda_{S_o}^{e_m} \equiv (\Delta e_m/e_m)/(\Delta S_o/S_o)$, is much larger than that of M_{HM} or ξ/T_c°, as shown in Fig. 6.4, which indicates that the same fractional variation of S_o would affect the maximum blanket revenue more than a comparable change in M_{HM} or ξ/T_c°. The sensitivity coefficient of M_{HM} for the maximum blanket revenue is always 1.0; therefore we may anticipate higher blanket revenue by adding moderator to increase S_o. However, it should be noted that it is easier to achieve large percentage changes in M_{HM} than in S_o, and in the high fissile breeding rate regions, the sensitivity coefficient for S_o sharply decreases, as shown in Fig. 6.4; hence, moderator-seeding loses its purported advantages.

Moderator seeding in the blanket is very effective when the fuel cycle cost contribution of the blanket is positive (the blanket revenue is negative) because of the lower fuel fabrication cost (due to the smaller heavy metal inventory or the number of fuel rods in the blankets) and the higher neutron capture rate of the remaining fertile material. Moderator seeding in the blanket is less effective when the

TABLE 6.7

NEUTRONIC CHARACTERISTICS OF REFERENCE (REF.) AND MODERATED (MOD.) RADIAL BLANKETS

Fuel Mat.	Thickness (rows)	Unit	b	10^{-14} #/cm^2-sec	kg	10^{-19} #/zone-sec		
			$\sigma_{c,B}^{-28}$	$\bar{\phi}_B$	$M_{28}(0)$	A_c^{49}	bi	bxr
UO_2	3	Ref.	0.4025	5.6269	17299	3.153	0.5888	0.2639
		Mod.	0.4677	5.8655	14416	3.154	0.5877	0.2650
	2	Ref.	0.4173	8.4077	10946	3.153	0.5880	0.2586
		Mod.	0.4876	8.9621	8063	3.155	0.5879	0.2511
UC_2	3	Ref.	0.4209	5.0691	18999	3.153	0.5889	0.2729
		Mod.	0.4709	5.3468	15833	3.155	0.5882	0.2697
	2	Ref.	0.4295	7.6320	12022	3.153	0.5887	0.2652
		Mod.	0.4854	8.2292	8856	3.157	0.5883	0.2568
UC	3	Ref.	0.3692	4.8720	23233	3.143	0.5899	0.2824
		Mod.	0.4216	5.0589	19361	3.145	0.5894	0.2805
	2	Ref.	0.3806	7.2872	14701	3.143	0.5898	0.2754
		Mod.	0.4386	7.7680	10827	3.146	0.5894	0.2688

All moderator material was seeded homogeneously in the 2nd row.

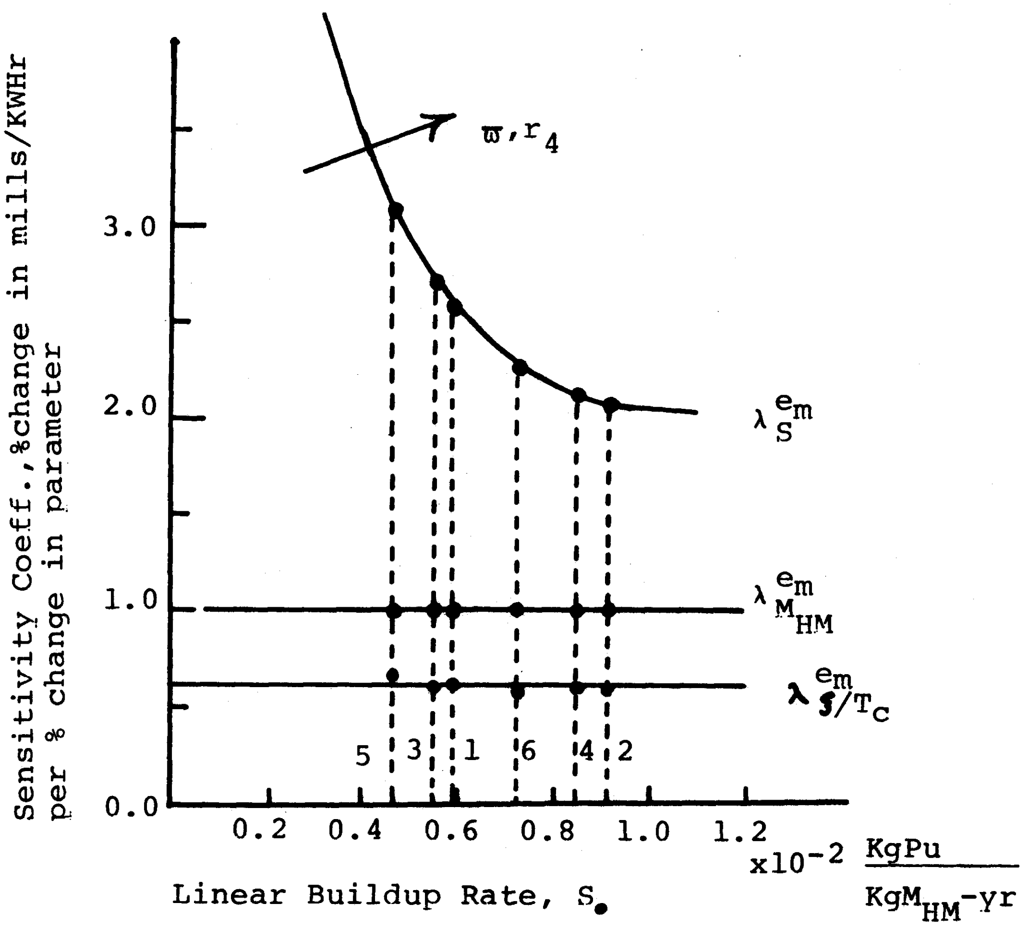

* 1: UO_2/3-row
2: UO_2/2-row
3: UC_2/3-row
4: UC_2/2-row
5: UC/3-row
6: UC/2-row

Fig. 6.4 SENSITIVITY COEFFICIENTS OF THE MAXIMUM BLANKET REVENUE AS A FUNCTION OF $S_\bullet^*$

fuel cycle cost contribution of the blanket is negative (positive blanket revenue) because a small heavy metal inventory leads to less fissile production and hence to a lower fissile material credit. The detrimental effect of moderator seeding in the blanket on the maximum blanket revenue is more pronounced for thin blankets, which have a high fissile buildup rate, because of the low effectiveness of improved S_o in this region. Table 6.8 compares the effects on maximum blanket revenue of moderator seeding.

In conclusion, the moderated blanket concept is only favorable for:

a. Thick blankets having a negative blanket revenue,

b. Thick blankets having a very low fissile buildup rate,

c. Thick blankets having a long optimum fuel irradiation time which is out of range of the metallurgically allowable fuel irradiation time, because the high fissile buildup rate always shortens the optimum irradiation time.

Under future economic conditions projected from todays perspective, only one or two-row (i.e. thin) blankets will be economically attractive. In this respect moderator seeding may be considered as an alternative to re-optimizing already-built systems committed to thick ($\geq$ 3 row) blankets.

6.5.2 Spectrum Hardened Blankets

As mentioned in the previous section, projected future economic conditions for fabrication and reprocessing costs and plutonium value (L3), (S4) indicate that thin blankets may be more economically attractive, hence, high fertile density is desirable to compensate for the disadvantages of thin blankets inherent to their low fertile inventory.

TABLE 6.8

EFFECTS OF MODERATOR SEEDING ON MAXIMUM BLANKET REVENUE

$\frac{\Delta q}{q}$ †	UO_2 Fuel (3-rows)		UC Fuel	
	Positive Blanket Revenue*	Negative Blanket Revenue**	Thick (3-row) Blanket	Thin (2-row) Blanket
$\frac{\Delta M_{HM}}{M_{HM}}$	-0.17	-0.17	-0.17	-0.26
$\frac{\Delta S_o}{S_o}$	0.19	0.21	0.19	0.23
$\frac{\Delta r_4}{r_4}$	0.025	0.22	0.16	0.24
$\frac{\Delta bxr}{bxr}$	-0.015	0.004	-0.007	-0.024
$\frac{\Delta e_m}{e_m}$	-0.976	0.058	0.122	-0.070
e_m*** (Ref.)	0.018853	-0.0578	-0.049	-0.071
e_m*** (Mod.)	0.000459	-0.0612	-0.055	-0.066

† $\frac{\Delta q}{q} = \frac{(q \text{ with moderator seeding}) - (q \text{ without moderator seeding})}{(q \text{ without moderator seeding})}$

* Refer to Appendix D for all parameters used.

** Refer to Chapter 2 for all parameters used.

With respect to the neutron spectrum, a soft spectrum is, in general, better both neutronically and economically: a hard neutron spectrum is only a by-product of the use of high-density fuel materials. Therefore, in this study "spectrum-hardened" blankets means only that the blankets in question used high-density fuel materials.

6.5.2.1 Neutronic Aspects of Spectrum-Hardened Blankets

As developed in section 6.3.3.1, the fractional change of external breeding ratio due to a variation of fertile density can be expressed as

$$\frac{\Delta bx}{bx} = \frac{\theta}{e^{\theta}-1} \left(\frac{\Delta N_{28,B}}{N_{28,B}}\right) \qquad (6.20)$$

where

$$\theta \cong [3\bar{\sigma}^{28}_{a,B}\, \bar{\sigma}^{28}_{tr,B}]^{1/2} \cdot N_{28,B} \cdot t \qquad (6.21)$$

Equation (6.20) indicates that the effect of fertile density on the external breeding ratio depends on the value of θ. If θ is small because the blanket is thin (small t), increasing fertile density will be a very effective way to improve the external breeding ratio. Here we should note that thick blankets, which have large θ values, are not improved by an increase of fertile density. Table 6.9 summarizes the variation of the sensitivity coefficient, $\lambda^{b_x}_{N_{28}} = \frac{\theta}{e^{\theta}-1}$, as a function of θ. If θ is larger than about 2.5 (which corresponds to that of a UC fueled blanket at 97% T.D.), the effect of high fertile density on the external breeding ratio will be negligible (hence metallic fuel does not improve the external breeding ratio significantly.)

TABLE 6.9

VARIATION OF $\lambda^{bx}_{N_{28,B}}$ * AS A FUNCTION OF θ

θ	$\lambda^{bx}_{N_{28,B}}$	Remarks
1.5	0.4308	UO_2 Fuel at ∿70% T.D.
2.0	0.3130	UO_2 Fuel at ∿97% T.D.
2.5	0.2236	UC Fuel at ∿97% T.D.
3.0	0.1572	bx may not improve in this region, because of low $\lambda^{bx}_{N_{28,B}}$ and high parasitic absorption
5.0	0.0339	

$$* \ \lambda^{bx}_{N_{28,B}} \equiv \frac{\Delta bx/bx}{\Delta N_{28}/N_{28}} = \frac{\theta}{e^{\theta}-1}$$

Table 6.10 shows the variation of important neutronic parameters achieved by replacing UO_2 fuel by UC fuel, which can be generalized as:

a. lower fissile buildup rate (which erodes the advantage of high fertile density); and the net improvement of bx is relatively small,

b. increased blanket power contribution,

c. longer optimum fuel irradiation time,

d. no effect on core performance.

6.5.2.2 Economic Aspects of Spectrum Hardened Blankets

The most serious deficiency of the spectrum hardened blanket is its low fissile buildup rate, which leads to lower blanket revenue. However, for a thin(2-row) blanket, the effectiveness of the fissile buildup rate on the (positive) blanket revenue is reduced, as shown in Fig. 6.3, and the mertis of high fertile density overcome this handicap.

Another problem arising from the high fertile density is the longer optimum fuel irradiation time. For a thick blanket (3-row), the optimum (batch) irradiation time of a carbide blanket (3-row) is about 9 years, which is possibly beyond the allowable metallurgical irradiation time. Shortening the fuel irradiation time decreases the blanket revenue.

Numerical comparisons of the economic parameters and the maximum blanket revenue are summarized in Table 6.2.

6.5.3 Fissile-Seeded Blankets

Neutrons leaking from the core region dominate the total number of neutrons available for fissile breeding in the blankets, however this value remains very nearly constant even if the blanket fuel material is changed. An alternative method to improve the number of neutrons

TABLE 6.10

CHANGES IN NEUTRONIC PARAMETERS WHEN UO_2 FUEL IS CHANGED TO UC FUEL

Fractional changes of Parameters	2-row Blanket	3-row Blanket
Initial Heavy Metal Loading ($M_{28}(0)$)	1.343	1.343
$\bar{\sigma}^{28}_{c,B}$	0.9120	0.9175
$\bar{\phi}_B$	0.8667	0.8658
Blanket Power Fraction (BOL)	1.106	1.118
Internal Breeding Ratio	1.003	1.002
Radial Blanket Breeding Ratio	1.0650	1.0625
Optimum Fuel Irradiation Time(T_{op})	1.25	1.25

available for fissile breeding is the generation of more fast fission neutrons in the blankets by means of fissile seeding.

6.5.3.1 Neutronic Aspects of Fissile-Seeded Blankets

From the neutron balance equation shown in Eq. (6.8), the breeding ratio in a fissile-seeded blanket can be expressed as

$$b = \eta_c^{49} \left(1 + \frac{\nu-1}{\nu}\delta_c^{28} - a_c\right)\left(\frac{A_c^{49}}{A_T^{49}}\right) + \eta_B^{49}\left(1 + \frac{\nu-1}{\nu}\delta_B^{28} - a_B\right)\left(\frac{A_B^{49}}{A_T^{49}}\right) - 1 \quad (6.56)$$

where

$$\eta_r^{49} = F_r^{49}/A_r^{49}, \text{ fissile neutron yield} \quad (6.57)$$

$$\delta_r^{28} = F_r^{28}/F_r^{49}, \text{ the fertile-to-fissile fission ratio} \quad (6.58)$$

$$a_r = (A_r^{P,L}/\nu F_r^{49}), \text{ parasitic losses per fissile fission neutron} \quad (6.59)$$

If plutonium exists only in the core region (as in a conventional core-blanket system at BOL), Eq. (6.56) reduces to Eq. (6.9), as shown in Section 6.3.1.

If we assume that system power is fixed and that the power is primarily determined by plutonium fissions (hence absorptions), $A_T^{49} \cong \text{constant} \;:\; dA_c^{49} = -\, dA_b^{49}$.

Thus for $\frac{dg}{dA_b^{49}} \geq 0$, we have the criterion:

$$\eta_B^{49}\left(1 + \frac{\nu-1}{\nu}\delta_B^{28} - a_B\right) \geq \eta_c^{49}\left(1 + \frac{\nu-1}{\nu}\delta_c^{28} - a_c\right) \quad (6.60)$$

where g is the breeding gain defined by g = b - 1; hence $\Delta g = \Delta b$.

Equation (6.60) shows that it will be difficult to achieve this criterion for the following reasons;

a. $\eta_B^{49} \leq \eta_c^{49}$ (because the blanket spectrum is softer than the core spectrum),

b. $a_B > a_c$ (because of the smaller plutonium concentration in the blanket region than in the core),

c. δ_c^{28} decreases if Pu enrichment in the blanket becomes appreciable,

d. because of the $(\frac{A_B^{49}}{A_T^{49}})$ weighting, the advantage, if any, will be slight.

The differences in neutronic characteristics between homogeneous and heterogeneous seeding were also examined and found to be negligible.

Table 6.11 summarizes the parametric changes in fissile-seeded blankets.

6.5.3.2 Economic Aspects of Fissile-Seeded Blankets

Potentially favorable benefits of fissile-seeded blankets on blanket economics could come from a higher fissile buildup rate and a shorter fuel optimum irradiation time. Table 6.12 summarizes the key parameters and the maximum blanket revenue of fissile-seeded blankets. In this calculation, additional costs for the initial fissile loading were not considered. However, even so the economic improvement due to the slightly higher fissile buildup rate, S_o, is negligible because of a) the decreased total amount of fertile material loaded in the blankets, b) the decreased microscopic capture cross-section of U-238.

In conclusion, the total breeding gain can be increased by fissile-seeding only if η_B^{49} is larger than 2-g. ($\geq$ 2.2) - but η_B^{49} is usually less than 2.0 (as discussed in Appendix E). Economic advantages are also

TABLE 6.11

PARAMETRIC CHANGES OF FISSILE-SEEDED BLANKETS

	UO_2	UC	U_2Ti
ε_B (RB2) ω/o	0.050	0.42	0.35
η_c^{49}	2.3325	2.3352	2.3383
η_{RB}^{49}	1.9264	1.9969	2.1560
A_{RB}^{49}/A_T^{49}	0.0076	0.0053	0.0036
Fractional Change of:			
bi	0.9933	0.9955	0.9965
bxa	0.9929	0.9951	0.9960
bxr	1.0071	1.0104	1.0085
b	0.9963	0.9990	0.9993

† Pu-239 was seeded homogeneously in the second row of the radial blanket

TABLE 6.12

COMPARISON OF ECONOMIC PARAMETERS FOR REFERENCE AND FISSILE-SEEDED UO_2 BLANKETS

	Reference Blanket	Fissile-Seeded*
M_{HM}, kg	17, 299	17,124
$\bar{\sigma}^{28}_{c,B}$, b	0.40252	0.39391
$\bar{\phi}_B$, 10^{-14} #/cm^2-sec	5.6269	5.9032
S_o, KgPu/(KgM_{HM}, yr)	0.00587	0.006027
T^o_c, yr^{-1}	16.0738	15.9960
r_4	0.081475	0.081677
T_{op}, yr	7.40	7.23
T_{BE}, yr	2.83	2.73
e_{fab}, mills/KwHr	0.0767	0.0776
e_{rep}, mills/KwHr	0.0216	0.0225
$-e_{mat}$, mills/KwHr	0.1561	0.1608
$-e_m$, mills/KwHr	0.0578	0.0607

*Pu-239 was seeded in the second row of the radial blanket ($\epsilon_B = 0.50\%$).

negligible because of the lower fertile volume fraction and decreased $\bar{\sigma}^{28}_{c,B}$.

These findings are compatible with the observation that breeding performance does not improve with irradiation - which may be regarded as a method for "self-seeding".

6.5.4 Parfait Blanket Concept for Fast Breeder Reactors

To achieve a uniformly high fuel burnup, core fuel subassemblies are generally arranged in two or three radial zones of roughly equal volume, each zone's subassemblies differing in fissile material enrichment, with the lowest fissile enrichment in the innermost core region. In general the fissile enrichment is uniform within each core zone - that is, zone loading is homogeneous. An alternative approach is to heterogeneously load the zone using a combination of fissile-loaded and fertile-only assemblies (or zones within an assembly). Many versions of these "heterogeneous" FBR core designs are now under intensive scrutiny by the international fast reactor community.

Parfait blanket concepts which adopt internal blankets limited in both radial and axial extent were developed and investigated in some detail previously at MIT (D3), (P2), (A1). Conventional and parfait core configurations are shown in Fig. 6.5.

6.5.4.1 Neutronic Aspects of Parfait Blanket Systems

From Eq. (6.9), the change in the breeding ratio due to the internal blanket will be

$$\Delta b = [1 + (1 - \frac{1}{\bar{\nu}} - a)\delta - a] \cdot \Delta\eta_c^{49} + \eta_c^{49}(1 - \frac{1}{\bar{\nu}} - a) \cdot \Delta\delta - (1 + \delta) \cdot \Delta a \qquad (6.61)$$

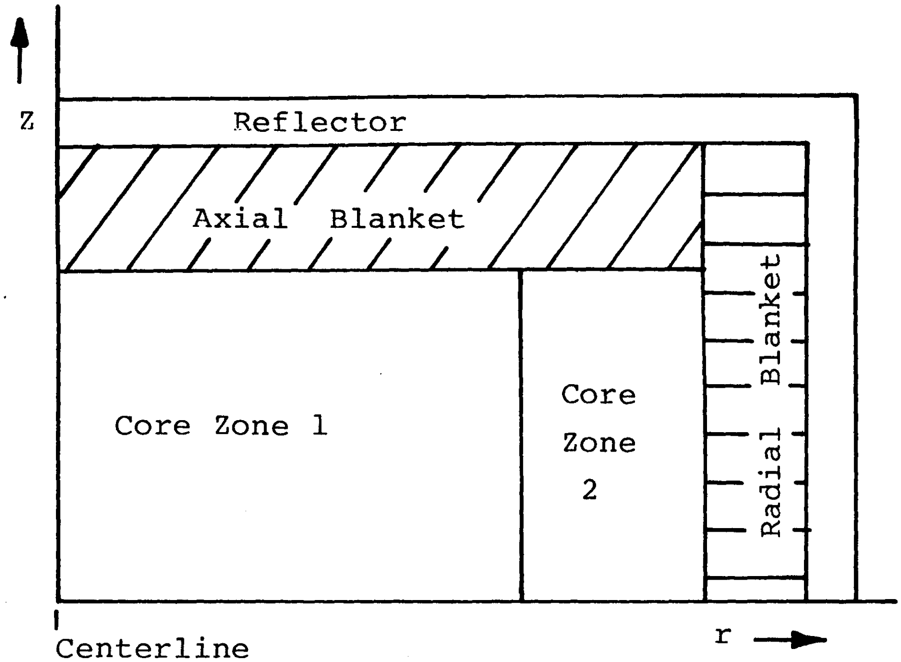

CONVENTIONAL DESIGN

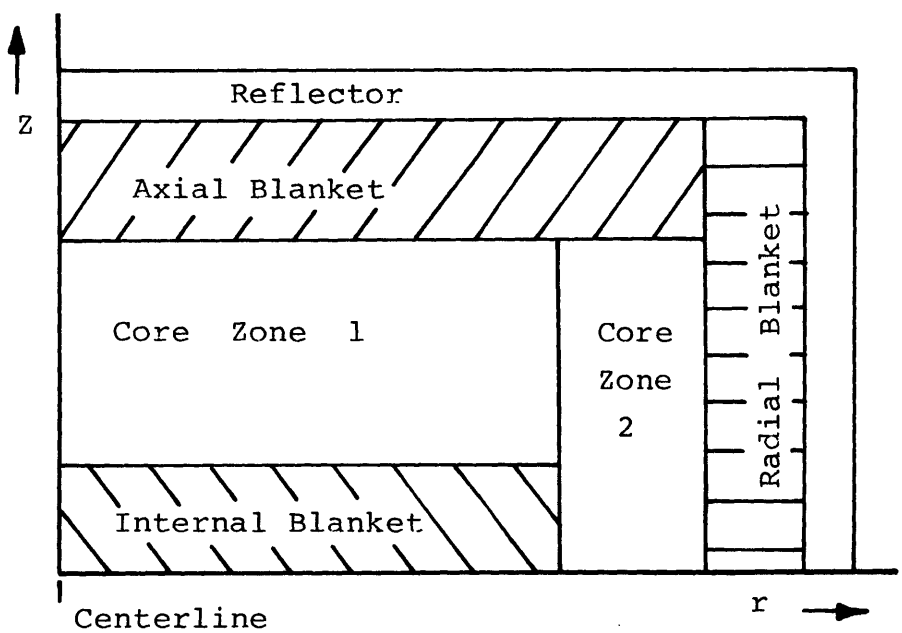

PARFAIT CONFIGURATION

Fig. 6.5 CONVENTIONAL AND PARFAIT CORE CONFIGURATIONS where $\bar{\nu}$ was considered as a constant.

Equation (6.61) indicates that reduction of the parasitic absorption ($-\Delta a$) and core fissile consumption (hence $+\Delta\delta$) and increasing η_c^{49} ($+ \Delta\eta_c^{49}$) are all important to increasing the breeding ratio.

Parfait blanket concepts can satisfy these requirements because

a. η_c^{49} is higher because of the harder core neutron spectrum created by higher core fissile-zone enrichment ($\Delta\eta_c/\eta_c \approx 0.04 \frac{\Delta\varepsilon_c}{\varepsilon_c}$; see Ref. (A1) for details),

b. a positive $\Delta\delta$ may be possible if
$$\Delta\left(\frac{F_B^{28}}{F_c^{49}}\right) >> 0.026\ \Delta\left(\frac{1-\varepsilon_c}{\varepsilon_c}\right),$$

c. a negative Δa can be achieved by increasing the fuel volume fraction (permissible due to reduced control requirements and reduced fuel swelling and bowing).

The possible improvement in total breeding ratio is approximately 0.06, and more improvements can be anticipated by concurrent changes in core thermal-hydraulic design features. However it should be noted that use of a non-optimized internal blanket configuration can easily lead to a decreased breeding gain.

6.5.4.2 Economic Aspects of Parfait Blanket Systems

Assesment of the economic (fuel cycle cost) effects of parfait blanket systems can be most easily done by considering the influence of the internal blankets on the fuel depletion economics of the core and the external blankets.

A parfait blanket system can affect core fuel economics in three ways: a) by affecting the core fissile inventory required for criticality and sustaining a specified burnup-reactivity life-time, and thereby affecting core inventory costs, b) by perturbing the magnitude and spectrum of the flux in the core, causing changes in depletion, and thus material credits, c) by reducing the core fertile inventory (hence internal breeding ratio), resulting in a smaller material credit.

These effects generally cause a net increase in the fuel cycle cost contribution in the core regions, but this can be compensated by the internal blanket revenue and increased external blanket revenues. In general, the differences in fuel cycle costs between the reference and parfait systems are negligible (e.g.1.1448 vs. 1.1499 mills/KwHr) as described in more detail in Ref. (D3).

6.5.5 Brief Review of the "Heterogeneous Core" and "Sandwich-Blanket" Concepts

Recently, fully heterogeneous core concepts which employ both axial and radial internal blanket zones have received considerable interest, both in the U.S. and abroad. The "parfait blanket" and "sandwiched-blanket" concepts are simpler versions of the fully heterogeneous concept. In the "sandwiched-blanket" concept the internal blanket is extended radially through both core regions (see Fig. 6.6.(a)),as described by Kobayashiet. al. (K4). Mougniot et. al. (M5) have suggested more complicated versions of the heterogeneous concept (see Fig. 6.6.(c)), which has aroused some controversy over the capabilities of this general class of core designs (C5). Chang (C6) has also studied a simple heterogeneous core concept constrained to fit within the CRBR configuration (see Fig. 6.6 (b)). All of these new concepts have very nearly the same design benefits and theoretical basis as already discussed for the "parfait

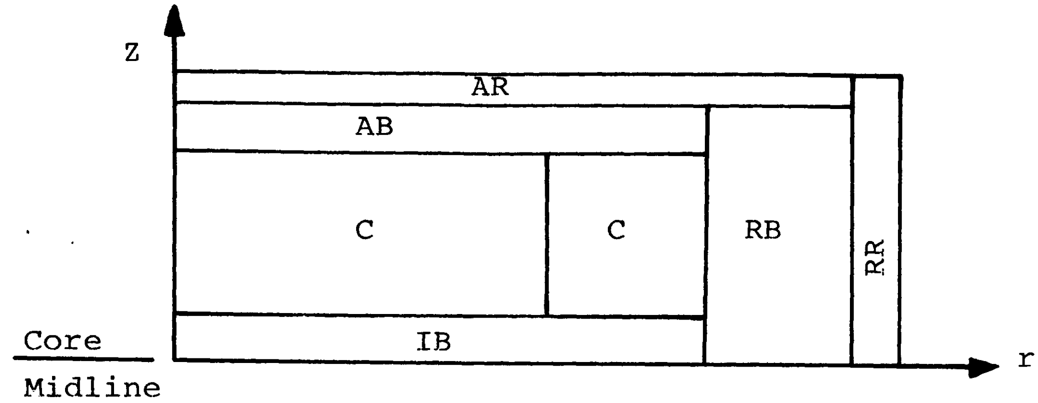

(a) SANDWICHED BLANKET

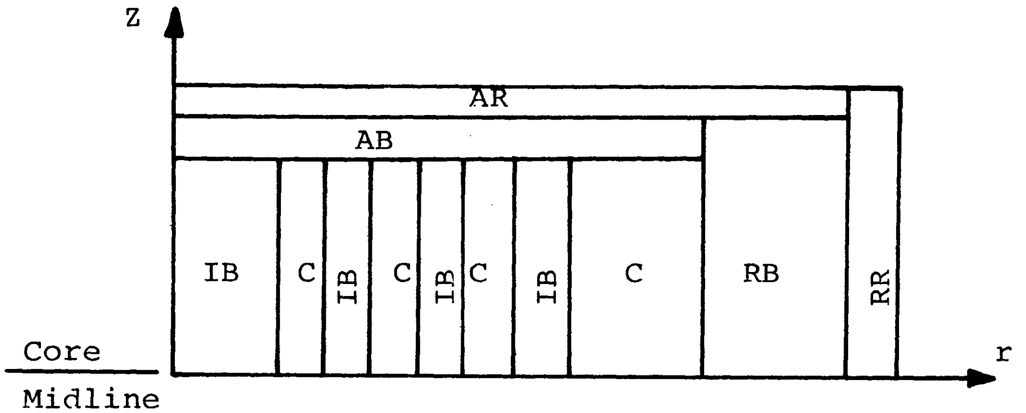

(b) HETEROGENEOUS CORE 1

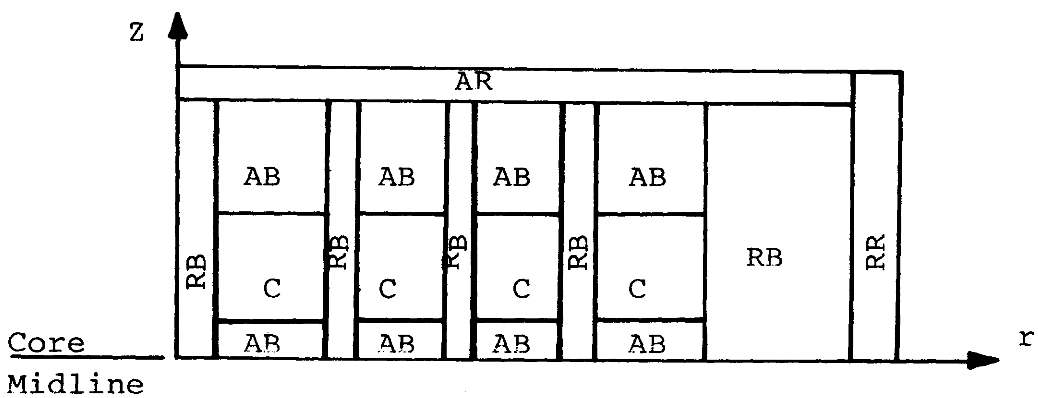

(c) HETEROGENEOUS CORE 2

* C: Core, AB: Axial Blanket, RB: Radial Blanket, IB: Internal Blanket, AR: Axial Reflector, RR: Radial Reflector

Fig. 6.6 CONFIGURATION OF "SANDWICHED-BLANKET" AND "HETEROGENEOUS CORE" DESIGNS blanket" concept. Proponents claim: a) higher breeding ratio and shorter doubling times, b) better core power-flattening using a single fissile enrichment, c) better safety-related characteristics (e.g. reduced fuel swelling and bowing etc.).

However, with respect to fuel utilization and the fuel cycle cost of the entire reactor system, these design concepts will not offer substantial improvements unless they permit increasing the volume fraction of fuel loaded within the core envelope, since this is the only practical way to achieve significantly better breeding ratios and doubling times.

6.5.6 Summary

Analyses emphasizing the neutronic and economic performance of various blanket concepts have been presented.

Most of the evaluations have been devoted to blanket modifications which could be achieved without any perturbation of core performance. Few significant benefits were found under this constraint; in some cases a slightly higher breeding ratio could be realized at the expense of reduced blanket revenue (or vice versa).

Thin (2-row), spectrum-hardened (UC fueled) blanket concepts appear to be slightly preferable under future economic conditions, while moderated-blankets are only (at best) an alternative way to re-optimize already-built systems committed to thick ($\geq$ 3 row) blankets.

Fissile-seeded blankets have some characteristics similar to those of moderated blankets, however their potential is inferior to that of moderated blankets.

Heterogeneous core concepts having internal blanket(s) have been evaluated by several investigators. However the economic aspects of these advanced design concepts may not be particularly favorable, as fuel cycle cost and average fuel utilization may well be nearly the same as those of equivalent homogeneous cores.

Throughout the present analysis, the most promising fuel materials have been found to be oxide and mono-carbide fuels. Carbide fuel has a better potential in the thermal-hydraulic and neutronic areas than does oxide fuel. Oxide fuel on the other hand creates the largest blanket revenue due to its high fissile buildup rate. However, if the unit fabrication cost for the carbide fuel ($\$/Kg\ M_{HM}$) is less than about 90% of that for oxide fuels (based on the reference core configurations and economic environments used in this study), carbide fuel will be better than oxide fuel from an economic point of view as well.

6.6 RECAPITULATION OF MAJOR FINDINGS

In conclusion, the present work has established the following major points:

As regards fissile breeding capability:

1. External fissile breeding is primarily determined by neutron leakage from the core which makes improvement of the external breeding ratio a very difficult task without changes in core parameters; conversely, even extreme changes in external blanket design have very little effect on core performance.
2. Since the incident neutron spectrum and the total number of available neutrons in the blanket region are essentially determined by the core design, low parasitic absorption in the blanket is the single most important prerequisite for a higher external breeding ratio.

3. High blanket fuel density reduces the parasitic absorption and increases the fertile fission reaction in the blanket; although the average neutron flux is concurrently reduced, the net result is a slight improvement of the external breeding ratio.

4. It was shown that the external breeding ratio at the beginning of blanket life can be corrected by a constant to obtain a valid quantitative estimate of the external breeding ratio averaged over life for an optimally irradiated blanket. Hence one does not need to carry out burnup calculations to evaluate the effects of blanket design or composition changes.

As regards fuel depletion and economic analysis:

1. The fissile buildup history in the blanket can be expressed in a particularly simple dimensionless form, i.e.

$$\frac{M_{49}(t)}{\hat{M}_{49}} = \frac{t}{T_c^o} e^{-\xi\frac{t}{T_c^o}}$$

Thus all blankets (metal, oxide, carbide fuel, etc.) or subregions of a blanket (from pin to subassembly to whole blanket) can be correlated on a single functional plot.

2. The non-linear enrichment vs. time characteristics of plutonium buildup in FBR blankets is very important to determination of the optimum economic parameters (except for the breakeven time). Simple linearized models, while pedagogically attractive, are not adequate for fuel management in real reactors.

3. Oxide fuel, which has a higher fissile buildup rate, can produce a higher maximum blanket revenue than carbide or metal alloy fuels (note that this conclusion of oxide superiority is predicated on equal fuel fabrication costs per kg of heavy metal for all fuels). If carbide fuel assemblies can be fabricated on the order of 10% more cheaply then this may offset the foregoing disadvantage.
4. The batch fuel management option produces about 15% less plutonium than other commonly considered strateges, and an Out-In scheme produces slightly more plutonium than do the other shuffled options.

As regards FBR blanket design concepts:

1. Few significant benefits were found among those blanket modifications which could be achieved without any perturbation of core performance. In some cases a slightly higher breeding ratio could be realized at the expense of reduced blanket revenue or vice versa.
2. Thin (2-row), spectrum-hardened (UC fueled) blanket concepts appear to be slightly preferable under future economic conditions due to their excellent thermal and neutronic characteristics (hence higher external breeding ratios) and very minor economic deficiencies, while moderated-blankets are only at best an alternative way to re-optimize already-built systems committed to thick ($\geq$ 3 row) blankets.

Although particular emphasis has been placed on generalizing the results in the present work, there is no assurance that it encompasses all possible design options for external blankets on FBR's. However, all cases examined could be fit into a self-consistent methodology, and all are consistent with the observation that very little improvement in external blanket breeding performance can be envisioned unless core design changes are allowed. On the other hand a wide latitude of design changes in the blanket could be accommodated without affecting core neutronics or breeding performance. The only option not yet resolved is the use of internal blankets to improve system performance, and it is recommended that an investigation of comparable scope to that of the present work be carried out on these "heterogeneous" or "parfait" core concepts.

6.7 RECOMMENDATIONS FOR FUTURE WORK

In fulfilling the goals of the present work several areas have been identified in which further analysis is required.

a. Blanket Design Concepts:

1. More detailed analyses relating to the "heterogeneous core" concept should be carried out. The present work was confined almost exclusively to external blankets, which have virtually no effect on core performance.
2. Further work on blanket shape optimization (S6) would appear worthwhile.

b. Evaluation Methods and Data:

1. Parameters characterizing the economic and financial environments should be updated; reprocessing costs in particular, as they become better known. In order to be consistent with prior work at MIT, values used in this report are quoted 1965 dollars.

2. Throughout the evaluation of the various blanket design concepts, Brewer's accounting method A (in which material purchases and fabrication charges were capitalized and consequently depreciated for tax purposes; whereas reprocessing charges and material credit were treated as an expensed cost and taxable revenue, respectively.) was employed. Further work on Brewer's accounting method B will be necessary if method A can not be agreed on as a definitive convention.

3. Optimization of key blanket parameters (e.g. blanket thickness, enrichment, fertile density, etc.) should be performed in more detail for specific designs; carbide vs. oxide fueled blankets in particular, and using current best estimates of fabrication costs.

c. Evaluation of Blanket Performance:

1. This report has concentrated on the neutronic and economic aspects of the various blanket design concepts. Other aspects of blanket design - thermal - hydraulic aspects in particular (e.g. transient temperature behavior, blanket overcooling, etc.) should be reviewed.

APPENDIX A

MATERIAL CONCENTRATIONS USED FOR THE ANALYSIS OF VARIOUS BLANKET DESIGN CONCEPTS (BOL)

A.1 Blanket Fuel Variations*

units: 10^3 atoms/barn-cm

Element / Fuel	U-235	U-238	Oxygen	Carbon	Titanium
UO_2 (Reference)	0.02337	11.6636	23.374	-	-
UC	0.03139	15.6646	-	15.696	-
UC_2	0.02567	12.8090	-	25.6700	-
U_2Ti	0.03345	16.6935	-	-	8.3635

*$V_{fuel}/V_{structure}/V_{NA}$ = 50% v/o / 20 v/o / 30 v/o

A.2 Moderated Blankets*

units: 10^3 atoms/barn-cm

Element / Fuel	U-235	U-238	Oxygen	Carbon	Titanium	Beryllium
UO_2	0.01169	5.8318	29.353	-	-	17.666
UC	0.0157	7.8323	17.666	7.8480	-	17.666
UC_2	0.01284	6.4045	17.666	12.8350	-	17.666
U_2Ti	0.01673	8.3468	17.666	-	4.1818	17.666

*$V_{fuel}/V_{moderator}/V_{structure}/V_{NA}$ = 25 v/o / 25 v/o / 20 v/o / 30 v/o

A.3 Fissile-Seeded Blankets*

units: 10^3 atoms/barn-cm

Element / Fuel	U-235	U-238	Pu-239	Oxygen	Carbon	Titanium
UO_2	0.02266	11.3100	0.1594	22.9800	-	-
UC	0.03097	15.4554	0.1594	0.3188	15.4866	-
U_2Ti (case A)	0.03807	19.0000	0.1594	0.3188	-	9.5180
U_2Ti (case B)	0.02882	16.9900	0.7970	1.5940	-	8.5110

$$* \frac{M^{49}_{RB}}{M^{49}_{core}} \cong 0.05$$

Pu-239 is homogeneously seeded in the second row of the radial blanket.

A.4 Radial Reflectors

units : atoms/barn-cm

Element / Reflector	Fe	Cr	Ni	Na	Be	O
Steel*	0.05459	0.01404	0.008775	0.002192	-	-
BeO**	0.007380	0.001944	0.000924	0.001100	0.06046	0.06046

$*V_{steel + structure}/V_{NA}$ = 90 v/o /10 v/o

$*V_{BeO}/V_{structure}/V_{NA}$ = 83 v/o / 12 v/o / 5 v/o

APPENDIX B.1

SUMMARY OF FLUX EQUATIONS FOR LARGE FBR CORES AND BLANKETS

B.1.1 Nomenclature

a	:	The core radius, cm
B_i^2	:	The geometrical buckling of region i, cm^{-2}
B_B	:	The geometrical buckling of the blanket, cm^{-2}
B_{c1}	:	The geometrical buckling of core zone 1, cm^{-2}
B_{c2}	:	The geometrical buckling of core zone 2, cm^{-2}
D_i	:	The diffusion coefficient of region i
k_i, j_i	:	constants
r	:	Radius, measured from the center of the core, cm
re	:	The extrapolated radius, cm
r_1	:	The radius of the innermost core zone, cm
r_2	:	The radius of the outermost core zone, cm
$\Sigma_{a,i}$	:	The macroscopic absorption cross-section of region i, cm^{-1}
$\nu\Sigma_{f,i}$	:	The macroscopic neutron production cross-section of region i, cm^{-1}
ϕ_i	:	Neutron Flux of region i, neutrons/cm^2-sec
ϕ_o	:	The neutron flux at the core/blanket interface, neutrons/cm^2-sec

B.1.2 Differential Equation for Region i and General Solutions

A. Diffusion Equation for Region i:

$$D_i \nabla^2 \phi_i - \Sigma_{a,i} \phi_i + \nu \Sigma_{f,i} \phi_i = 0 \qquad \text{(B.1)}$$

or

$$\nabla^2 \phi_i + B_i^2 \phi_i = 0 \qquad \text{(B.2)}$$

B. General Solution for One-dimensional Cylindrical Coordinates:

$$\phi_i = k_i J_o(B_i r) + j_i Y_o(B_i r) \qquad \text{(B.3)}$$

$$(\text{if } B_i^2 > 0)$$

$$= k_i I_o(B_i r) + j_i K_o(B_i r) \qquad \text{(B.4)}$$

$$(\text{if } B_i^2 < 0)$$

$$= \text{constant} \qquad (\text{if } B_i^2 = 0) \qquad \text{(B.5)}$$

C. General Solution for One-dimensional Spherical Coordinates:

$$\phi_i = \frac{k_i}{r} \sin (B_i r) + \frac{j_i}{r} \cos (B_i r) \qquad \text{(B.6)}$$

$$(\text{if } B_i^2 > 0)$$

$$= \frac{k_i}{r} \sinh (B_i r) + \frac{j_i}{r} \cosh (B_i r) \qquad \text{(B.7)}$$

$$(\text{if } B_i^2 < 0)$$

$$= \text{constant} \qquad (\text{if } B_i^2 = 0) \qquad \text{(B.8)}$$

B.1.3 Normalized (Core Central Flux = 1.0) Flux Equation for Radially-Power-Flattened Core

(One-dimensional Cylindrical Coordinates)

A. Power Flattening ($\Sigma_f(r)\phi(r)$ = constant):

$$\phi_c(r) = [1 - \frac{I_o(B_c r)}{I_o(B_c re)}] \quad (B.9)$$

(See Ref. (T1) for detailed derivations)

B. Flux Flattening ($\phi(r)$ = constant):

$$\phi_{c1} = 1 \quad (B.10)$$

$$\phi_{c2}(r) = k_{c2}[J_o(B_{c2}r)Y_o(B_{c2}re) - Y_o(B_{c2}r)J_o(B_{c2}re)] \quad (B.11)$$

where

$$k_{c2} = [J_o(B_{c2}r_1)Y_o(B_{c2}r_1) - J_o(B_{c2}re)Y_o(B_{c2}r_1)]^{-1} \quad (B.12)$$

(see Ref. (G1) for detailed derivations)

B.1.4 Approximate Flux Equation for FBR Blankets

A. Cylindrical Coordinates:

From Eq. (B.4) and with B.C., $r \to \infty$ $\phi_B \to 0$;

$$\phi_B(r) = \phi_o \frac{K_o(B_B r)}{K_o(B_B a)} \quad (B.13)$$

Using the following approximations;

$$K_o(B_B x) \cong \frac{1}{\sqrt{2\pi B_B x}} e^{-B_B x} \quad (B.14)$$

$$t/a = 0 \text{ or } \left.\frac{r}{a}\right|_{\text{blanket}} \cong 1.0 \qquad \text{(B.15)}$$

then

$$\phi_B \rightarrow \phi_o \, e^{-B_B(r-a)} \qquad \text{(B.16)}$$

B. Spherical Coordinates:

From Eq. (B.7) and with B.C., $r \rightarrow \infty$ $\phi_B \rightarrow 0$;

$$\phi_B = \frac{\phi_o a}{r} \, e^{-B_B(r-a)} \qquad \text{(B.17)}$$

Using Eq. (B.15)

$$\phi_B \rightarrow \phi_o \, e^{-B_B(r-a)} \qquad \text{(B.18)}$$

APPENDIX B.2

ONE-GROUP LMFBR CROSS-SECTION SET (D2)

* All Cross-sections are in barns

Nuclide	$\nu\sigma_f$	σ_f	σ_a	σ_{tr}
Pu-239	5.878	2.007	2.481	8.593
Pu-240	1.104	0.367	1.093	8.384
Pu-241	8.663	2.894	3.337	8.713
Pu-242	0.827	0.269	0.695	8.404
U-235	5.297	2.156	2.844	8.246
U-238	0.142	0.051	0.404	8.181
Na			0.00180	3.728
Fe			0.00867	3.594
O			0.0026	3.104
C			3.4×10^{-6}	3.211
Al			0.0040	6.990
B-10			2.592	3.754
Be			0.0056	3.628
N			0.022	3.104
H			51.7×10^{-6}	2.448
Mo			0.1310	6.360
Zr			0.0197	6.357
Cu			0.0686	4.678
Ni			0.0244	4.771
Cr			0.00869	3.287
V			0.02055	4.941
Ti			0.01523	3.621
K			0.02017	2.104
W			0.3270	7.1300

APPENDIX C.1

DERIVATION OF SIMPLE CORRELATIONS FOR HEAVY ISOTOPE BUILDUP IN FBR BLANKETS

C.1.1 INTRODUCTION

In Chapter 4, a simple but quite useful correlation for Pu-239 buildup during irradiation was derived. Equations for the concentrations of other heavy isotopes can also be developed by following the same procedures as previously shown in section 4.2.

Isotopic correlation techniques (ICT) have recently been shown to be a very useful tool in fuel management and analysis of reactor or fuel performance in LWR's (K5), (C2), (C7). This suggests that the application of isotopic correlation techniques to FBR blanket calculations to check analytical results, nuclear material balances, reprocessing and post-irradiation analyses, and optimization of the fuel cycle would also be very useful.

The simplest application of ICT is as a consistency check of post-irradiation data generated by computer calculations or post-reprocessing anlaysis. For example, the concentration of M_{41} can be predicted from the linear correlation between the product $(M_{49} \cdot M_{41})$ and $(M_{40})^2$, since as will be shown in this Appendix, the isotopic ratio, $\frac{(M_{49} \cdot M_{41})}{(M_{40})^2}$, is constant over a wide burnup range - an observation which is also valid in LWR Systems (K5).

In this appendix, the correlation equations for heavy isotopes will be summarized and isotopic correlations to permit their use to predict heavy isotope concentration will be introduced.

C.1.2 Coupled Depletion Equations on Mass Basis

1. General Equation:

$$\frac{dM_j}{dr} = - \lambda_j M_j \quad \text{(decay loss)}$$

$$- M_j \sum_{k=1}^{n} \phi_k \sigma_{k,a}^{j} \quad \text{(absorption loss)}$$

$$+ \lambda_i M_i \quad \text{(decay source)}$$

$$+ \sum_m M_m \sum_{k=1}^{n} \phi_k \sigma_{k,c}^{m} \quad \text{(capture source)}$$

$$+ \sum_q M_q Y_{q,j} \sum_{k=1}^{n} \phi_k \sigma_{k,f}^{q} \quad \text{(fission source)} \qquad \text{(C.1.1)}$$

where

j = nuclide index

k = energy group index

m = capture parent index

i = decay parent index

q = fission parent index

M_j = total mass of nuclide j in the zone (Kg)

ϕ_k = group k neutron flux in the zone ($\#/cm^2$-sec)

$\sigma_{k,c}^{j}$ = microscopic cross-section for event c, group k, nuclide j (cm^2)

λ_j = decay constant of nuclide j (sec^{-1})

t = time (sec)

$Y_{q,j}$ = yield of nuclide j per fission of nuclide q

Note that we have neglected the small mass differences between M_j, M_i etc., in converting from a per nucleus to a per unit mass basis. Applying Eq. C.1.1 to heavy isotopes of interest one obtains:

2. Pu-239:

$$\frac{dM_{49}}{dt} = M_{28}\,\bar{\phi}\,\bar{\sigma}_c^{28} - M_{49}\,\bar{\phi}\,\bar{\sigma}_a^{49} \qquad (C.1.2)$$

3. Pu-240:

$$\frac{dM_{40}}{dt} = M_{49}\,\bar{\phi}\,\bar{\sigma}_c^{49} - M_{40}\,\bar{\phi}\,\bar{\sigma}_a^{40} \qquad (C.1.3)$$

4. Pu-241:

$$\frac{dM_{41}}{dt} = M_{40}\,\bar{\phi}\,\bar{\sigma}_c^{40} - M_{41}\,\bar{\phi}\,\bar{\sigma}_a^{41} \qquad (C.1.4)$$

(the Pu-241 decay reaction has been neglected)

5. Pu-242:

$$\frac{dM_{42}}{dt} = M_{41}\,\bar{\phi}\,\bar{\sigma}_c^{41} - M_{42}\,\bar{\phi}\,\bar{\sigma}_a^{42} \qquad (C.1.5)$$

6. U-238:

$$\frac{dM_{28}}{dt} = -\,M_{28}\,\bar{\phi}\,\bar{\sigma}_a^{28} \qquad (C.1.6)$$

7. U-235:

$$\frac{dM_{25}}{dt} = -\,M_{25}\,\bar{\phi}\,\bar{\sigma}_a^{25} \qquad (C.1.7)$$

C.1.3 Solution of Coupled Depletion Equations

1. Assumptions:

   Constant neutron cross-sections and flux as a function of time.

2. Pu-239:

$$M_{49} = \hat{M}_{49}\,(e^{-\bar{\sigma}_a^{28}\bar{\phi}t} - e^{-\bar{\sigma}_a^{49}\bar{\phi}t}) \qquad \text{(C.1.8)}$$

3. Pu-240:

$$M_{40} = \hat{M}_{49}\,[B_1(e^{-\bar{\sigma}_a^{28}\bar{\phi}t} - e^{-\bar{\sigma}_a^{40}\bar{\phi}t}) - B_2(e^{-\bar{\sigma}_a^{49}\bar{\phi}t} - e^{-\bar{\sigma}_a^{40}\bar{\phi}t})] \qquad \text{(C.1.9)}$$

4. Pu-241:

$$M_{41} = \hat{M}_{49}[B_1C_1\,(e^{-\bar{\sigma}_a^{28}\bar{\phi}t} - e^{-\bar{\sigma}_a^{41}\bar{\phi}t}) - B_2C_2\,(e^{-\bar{\sigma}_a^{49}\bar{\phi}t} - e^{-\bar{\sigma}_a^{41}\bar{\phi}t})$$

$$+ (B_2C_3 - B_1C_3)(e^{-\bar{\sigma}_a^{40}\bar{\phi}t} - e^{-\bar{\sigma}_a^{41}\bar{\phi}t})] \qquad \text{(C.1.10)}$$

5. Pu-242:

$$M_{42} = \hat{M}_{49}\,[B_1C_1D_1\,(e^{-\bar{\sigma}_a^{28}\bar{\phi}t} - e^{-\bar{\sigma}_a^{42}\bar{\phi}t})$$

$$- B_2C_2D_2\,(e^{-\bar{\sigma}_a^{49}\bar{\phi}t} - e^{-\bar{\sigma}_a^{42}\bar{\phi}t})$$

$$- (B_1C_3D_3 - B_2C_3D_3)(e^{-\bar{\sigma}_a^{40}\bar{\phi}t} - e^{-\bar{\sigma}_a^{42}\bar{\phi}t})$$

$$- (B_1C_1D_4 - B_2C_2D_4 + B_2C_3D_4 - B_1C_3D_4)(e^{-\bar{\sigma}_a^{41}\bar{\phi}t} - e^{-\bar{\sigma}_a^{42}\bar{\phi}t})]$$

$$\text{(C.1.11)}$$

6. U-238:

$$M_{28} = M_{28}(0)\;e^{-\bar{\sigma}_a^{28}\bar{\phi}t} \qquad \text{(C.1.12)}$$

7. U-235:

$$M_{25} = M_{25}(0)\;e^{-\bar{\sigma}_a^{25}\bar{\phi}t} \qquad \text{(C.1.13)}$$

where

$$\hat{M}_{49} = M_{28}(0) \left(\frac{\bar{\sigma}_c^{28}}{\bar{\sigma}_a^{49} - \bar{\sigma}_a^{28}}\right)$$

$$B_1 = \frac{\bar{\sigma}_c^{49}}{\bar{\sigma}_a^{40} - \bar{\sigma}_a^{28}} , \qquad B_2 = \frac{\bar{\sigma}_c^{49}}{\bar{\sigma}_a^{40} - \bar{\sigma}_a^{49}}$$

$$C_1 = \frac{\bar{\sigma}_c^{40}}{\bar{\sigma}_a^{41} - \bar{\sigma}_a^{28}} , \qquad C_2 = \frac{\bar{\sigma}_c^{40}}{\bar{\sigma}_a^{41} - \bar{\sigma}_a^{49}}$$

$$C_3 = \frac{\bar{\sigma}_c^{40}}{\bar{\sigma}_a^{41} - \bar{\sigma}_a^{40}} , \qquad D_1 = \frac{\bar{\sigma}_c^{41}}{\bar{\sigma}_a^{42} - \bar{\sigma}_a^{28}}$$

$$D_2 = \frac{\bar{\sigma}_c^{41}}{\bar{\sigma}_a^{42} - \bar{\sigma}_a^{49}} , \qquad D_3 = \frac{\bar{\sigma}_c^{41}}{\bar{\sigma}_a^{42} - \bar{\sigma}_a^{40}}$$

$$D_4 = \frac{\bar{\sigma}_c^{41}}{\bar{\sigma}_a^{42} - \bar{\sigma}_a^{41}}$$

C.1.4 Approximation by Expansion of Exponential Functions and Neglection of Insignificant Terms

1. Expansion of Exponential Functions:

$$e^{-at} = 1 - at + 1/2(at)^2 \tag{C.1.14}$$

2. Pu-239:

$$M_{49} \cong \hat{M}_{49} \left[\frac{t}{T_C^\circ} \; e^{-\xi_o \, t/T_{c0}}\right] \tag{C.1.15}$$

(Refer to Section 4.2 of Chapter 4 for the detailed procedure used to derive this equation)

3. Pu-240:

$$M_{41} \cong \hat{M}_{49} \left[(t/Tc_1)^2 \, e^{-\xi_1 t/Tc_1} \right] \tag{C.1.16}$$

4. Pu-241:

$$M_{41} \cong \hat{M}_{49} \left[(t/T_{c2})^3 \, e^{-\xi_2 t/T_{c2}} \right] \tag{C.1.17}$$

5. Pu-242:

$$M_{42} \cong \hat{M}_{49} \left[(t/T_{c3})^4 \, e^{-\xi_3 t/T_{c3}} \right] \tag{C.1.18}$$

where

$$T_{c0} = (\bar{\sigma}_a^{49}\bar{\phi} - \bar{\sigma}_a^{28}\bar{\phi})^{-1} \quad , \quad \xi_o/T_{c0} = 1/2(\bar{\sigma}_a^{49}\bar{\phi} + \bar{\sigma}_a^{28}\bar{\phi})$$

$$T_{c1} = \frac{(\bar{\sigma}_c^{49}\bar{\phi})^{-1/2}}{2T_{c0}} \quad , \quad \xi_1/T_{c1} = 1/4(\bar{\sigma}_a^{49}\bar{\phi} + \bar{\sigma}_a^{28}\bar{\phi} + 2\bar{\sigma}_a^{40}\bar{\phi})$$

$$T_{c2} = \frac{(\bar{\sigma}_c^{49}\bar{\phi} \cdot \bar{\sigma}_c^{40}\bar{\phi})^{-1/3}}{8T_{c0}} \quad , \quad \xi_2/T_{c2} = 1/8(\bar{\sigma}_a^{49}\bar{\phi} + \bar{\sigma}_a^{28}\bar{\phi} + 2\bar{\sigma}_a^{40}\bar{\phi} + 4\bar{\sigma}_a^{41}\bar{\phi})$$

$$T_{c3} = \frac{(\bar{\sigma}_c^{49}\bar{\phi} \cdot \bar{\sigma}_c^{40}\bar{\phi} \cdot \bar{\sigma}_c^{41}\bar{\phi})^{-1/4}}{64T_{c0}} \quad , \quad \xi_3/T_{c3} = 1/16(\bar{\sigma}_a^{49}\bar{\phi} + \bar{\sigma}_a^{28}\bar{\phi} + 2\bar{\sigma}_a^{40}\bar{\phi} + 4\bar{\sigma}_a^{41}\bar{\phi} + 8\bar{\sigma}_a^{42}\bar{\phi})$$

C.1.5 Isotope Correlations - A Simple Tool for the Prediction of Isotope Ratios and Concentrations

In the previous section simple depletion equations for heavy isotopes were introduced, all of which were expressed in the same general form, involving terms of $(t/T_{ci})^{i+1}$ and $e^{-\xi_i(t/T_{ci})}$. Numerical results indicate that the value of (ξ_i/T_{ci}) is both small and roughly the same for all isotopes, as shown in Table C.1.1. Therefore, we can generate even simpler isotope correlations by neglecting the exponential term, and find linear cross-section-time relationships between adjacent Pu isotopes, (Pu-239, Pu-240, Pu-241, Pu-242). The calculational error resulting from use of these correlations is remarkably small if a best-fit weighting coefficient is employed.

Combining Eqs. (C.1.15) and (C.1.16), one obtains,

$$M_{40}/M_{49} = a_{40}t \tag{C.1.19}$$

where a_{40} is a linear coefficient determined by fitting computed or experimental results.

From the isotope ratios M_{49}/M_{40}, M_{40}/M_{41}, and M_{41}/M_{42}, and neglecting the small differences among exponential terms in Eqs. (C.1.15) through (C.1.18), one can write

$$M_{41} = a_{41}\ [M_{40}]^2/M_{49} \tag{C.1.20}$$

$$M_{42} = a_{42}\ [M_{41}]^2/M_{40} \tag{C.1.21}$$

TABLE C.1.1

VALUES OF $\frac{\xi_i}{T_{c_i}}$ DETERMINED USING MULTIGROUP CALCULATIONS

units: days^{-1}

$\frac{\xi_i}{T_{c_i}}$ Fuel Type*	UO_2 - entire 3-row blanket	UO_2 - 1st Row only	UC - entire 3-row blanket
$\frac{\xi_o}{T_{c_o}}$	1.2406 - 04	2.4396 - 04	9.3022 - 05
$\frac{\xi_1}{T_{c_1}}$	1.5505 - 04	2.9402 - 04	1.0428 - 04
$\frac{\xi_2}{T_{c_2}}$	2.3864 - 04	4.6555 - 04	1.7462 - 04
$\frac{\xi_3}{T_{c_3}}$	1.6027 - 04	3.1084 - 04	1.1326 - 04

*Radial blankets, all driven by same core.

All linear coefficients, a_{40}, a_{41}, a_{42}, can be determined simultaneously from a single burnup calculation, or even from BOL parameters (but in this case a larger error is to be expected).

Table C.1.2 compares heavy isotope concentrations of Pu-240, Pu-241, Pu-242 calculated using isotopic correlations to "exact" values determined using 2DB calculations. Also shown are the parent Pu-239, U-238 and U-235 concentrations calculated using both 2DB and the simplified versions of the burnup equations developed in this appendix.

Considering the simple nature of the governing relations the agreement shown in Table C.1.2 is quite acceptable.

TABLE C.1.2

COMPARISON OF HEAVY ISOTOPE CONCENTRATIONS CALCULATED USING ISOTOPIC CORRELATIONS AND 2DB†

Time(d) / Isotope	0	300	600	900	1200	2400*	Eq.
Pu-239	0.0 0.0	92.79 97.84	182,18 188.54	267.13 272.48	347.69 350.03	604.40 603.24	C.1.15
Pu-240	0.0 0.0	1.3673 1.3465	5.1845 5.1897	11.0295 11,2503	18.5319 19.2697	56.307 66.4189	C.1.19
Pu-241	0.0 0.0	0.0345 0.0297	0.2447 0.2292	0.7306 0.7452	1.5345 1.7019	7.2234 11.7323	C.1.20
Pu-242	0.0 0.0	0.0002 0.0002	0.0035 0.0034	0.0161 0.0164	0.0453 0.0500	0.4221 0.6894	C.1.21
U-238	17,299 17,299	17,198 17,193	17,090 17,089	16,979 16,984	16,862 16,881	16,411 16,473	C.1.12
U-235	34.230 34.230	31,805 31.636	29.529 29.239	27.417 27.024	25.463 24.976	19.395 18.224	C.1.13

† 3-row Radial Blanket, UO_2-Fueled Core

* ΔT = 150 day time steps, otherwise ΔT = 50 days

** Key:

2DB Eq.

where linear coefficients (a_{40} through a_{42}) were calculated from 2DB results at 900 days.

All quantities are in Kg

APPENDIX C.2

SUMMARY OF GENERAL EQUATIONS FOR FUEL CYCLE COST ANALYSIS IN FBR BLANKETS

A series of studies by Brewer (B4), Wood (W3), and Tagishi (T1) have been carried out at MIT to develop and apply a general expression for the levelized fuel cycle cost of FBR blanket fuel in mills/KwHr. Brewer's topical report (B4) should be referred to for the details of the basic derivations.

Ketabi (K2) and Bruyer (B6) subsequently developed a set of relationships between blanket fuel management parameters such as the optimum irradiation time and generalized economic parameters for some special cases. In the present report we have generalized and extended this previous work.

In this appendix, the equations used as the starting point for the present work are summarized for accounting method A, in which the post-irradiation transactions are treated as non-capitalized, and for accounting method B, in which the Pu revenue and reprocessing cost are capitalized.

C.2.1 Nomenclature

c_1 : Unit Fabrication Cost (\$/Kg HM),

c_2 : Unit Reprocessing Cost (\$/Kg HM),

c_3 : Fissile Material Price (\$/Kg Pu),

$\bar{c}_i$: Modified Unit Cost Component i defined by $\bar{c}_i = c_i \cdot F(-\Delta T_i)$, i.e., the cost present - worthed to either the beginning or the end of the irradiation, as appropriate,

e : Local Levelized Fuel Component of Energy Cost (mills/KwHr),

E : Electrical Energy Produced by the Reactor per year (KwHr/Yr),

f_b, f_s : Debt (Bond) and Equity (Stock) Fractions, respectively,

$F^q(T)$: Carrying Charge Factor for Cost Component q,

M_{HM} : Mass of Heavy Metal Loaded into Blanket Fuel Lot or Zone of Interest,

r_b, r_s : Debt and Equity Rate of Return, respectively,

T : Local Irradiation Time (Yr),

T_q : Time between the Cash Flow Transaction q and the Irradiation Midpoint (Yr) as shown in Fig. C.2.1,

ΔT_1 : The Length of Time from the Fabrication Cash Flow to the Beginning of the Irradiation,

ΔT_2 : The Length of Time from the End of the Irradiation to the Reprocessing Cash Flow,

ΔT_3 : The Length of Time from the End of the Irradiation to the Material Credit Cash Flow,,

X : Discount Rate,

ε_o : Initial Enrichment,

$\varepsilon(T)$: Discharge Enrichment

τ : Income Tax Rate

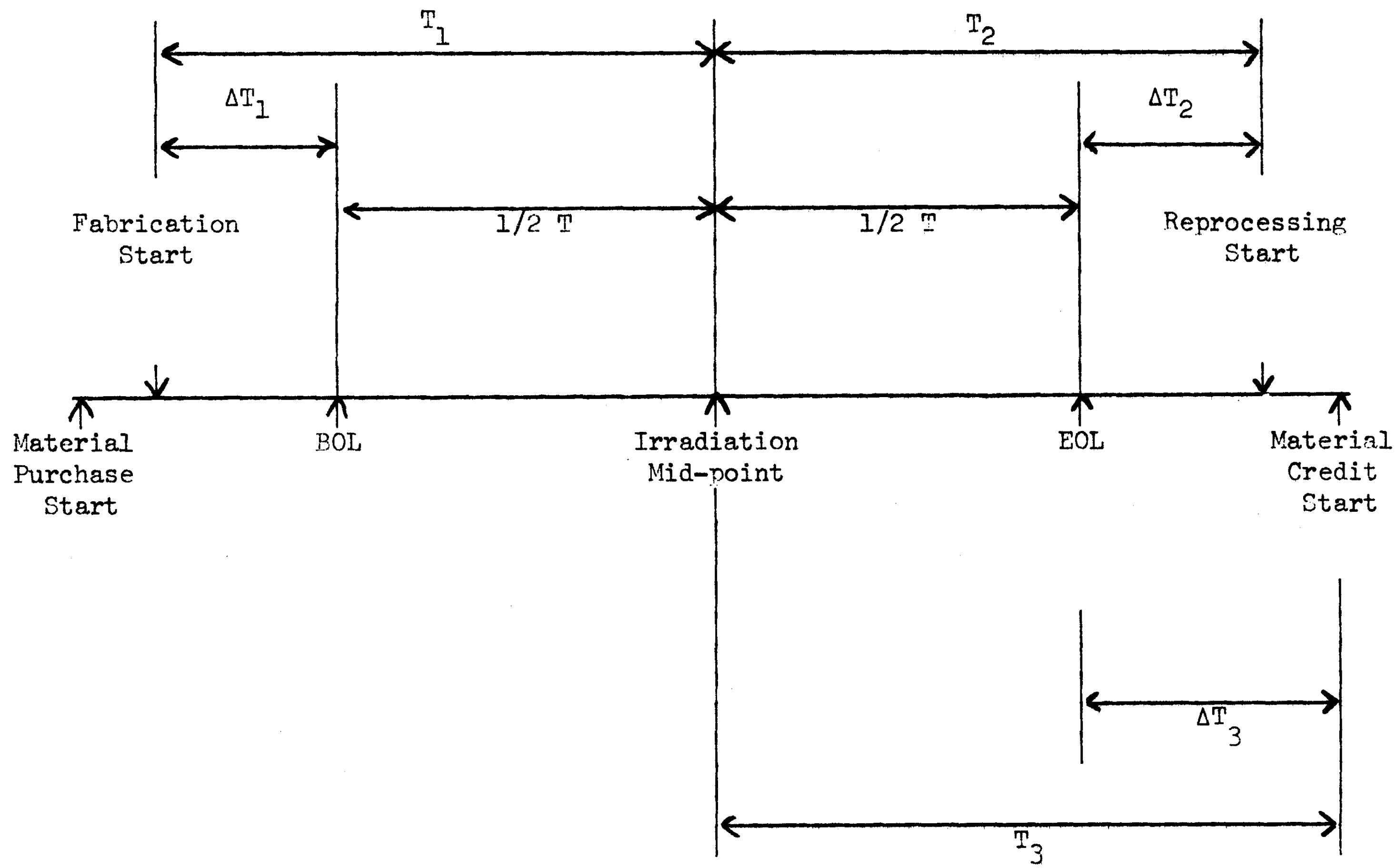

Fig. C.2.1 Timing of Cash Flows for Fuel Cycle Cost Calculations

C.2.2 SUMMARY OF EQUATIONS

	ACCOUNTING METHOD A	ACCOUNTING METHOD B	REMARKS (REF.)
1. Levelized Fuel Cycle Cost Contribution (mills/KWhr)	$e = \frac{1000}{E} M_{HM} \left[\frac{c_3 \varepsilon_o F_o(T)}{T} \right.$		Material Purchase Cost Component
	$+ \frac{c_1 F_1(T)}{T}$		Fabrication Cost Component
	$+ \frac{c_2 F_2(T)}{T}$		Reprocessing Cost Component
	$\left. - \frac{c_3 \varepsilon(T) F_3(T)}{T} \right]$		Material Credit Cost Component
2. Discount Rate (X)	$X = (1 - \tau) r_b f_b + r_s f_s$		(B4)
3. Definition of Transaction Time (Ti)	$T_1 = \Delta T_1 + \frac{T}{2}, \quad \frac{dT_1}{dT} = 1/2$		
	$T_2 = -\Delta T_2 - \frac{T}{2}, \quad \frac{dT_2}{dT} = -1/2$		(K2)
	$T_3 = -\Delta T_3 - \frac{T}{2}, \quad \frac{dT_3}{dT} = -1/2$		

C.2.2 SUMMARY OF EQUATIONS (continued)

	ACCOUNTING METHOD A	ACCOUNTING METHOD B	REMARKS (Ref.)
4. Carrying Charge Factors $[F_i(-Ti)]$	$F_1(-T_1) = \frac{1}{1-\tau}[(1+X)^{T_1} - \tau]$ $\cong e^{\frac{XT_1}{1-\tau}} = e^{\frac{X\Delta T_1}{1-\tau}} e^{\frac{XT}{2(1-\tau)}}$ $= F_1(-\Delta T_1)\, e^{\frac{XT}{2(1-\tau)}}$	$F_1(-T_1) = \frac{1}{1-\tau}[(1+X)^{T_1} - \tau]$ $\cong e^{\frac{XT_1}{1-\tau}} = e^{\frac{X\Delta T_1}{1-\tau}} e^{\frac{XT}{2(1-\tau)}}$ $= F_1(-\Delta T_1)\, e^{\frac{XT}{2(1-\tau)}}$	Method A: Only fabrication cost is capitalized. Method B: All operating costs are capitalized. (B6)
	$F_2(-T_2) = (1+X)^{T_2} \cong e^{XT_2}$ $= e^{-X\Delta T_2} e^{-\frac{XT}{2}}$ $= F_2(-\Delta T_2)\, e^{-\frac{XT}{2}}$	$F_2(-T_2) = \frac{1}{1-\tau}[(1+X)^{T_2} - \tau]$ $= e^{-\frac{X\Delta T_1}{1-\tau}} e^{-\frac{XT}{2(1-\tau)}}$ $= F_2(-\Delta T_2)\, e^{-\frac{XT}{2(1-\tau)}}$	
	$F_3(-T_3) = (1+X)^{T_3} \cong e^{XT_3}$ $= e^{-X\Delta T_3} e^{-\frac{XT}{2}}$ $= F_3(-\Delta T_3)\, e^{-\frac{XT}{2}}$	$F_3(-T_3) = \frac{1}{1-\tau}[(1+X)^{T_3} - \tau]$ $\cong e^{\frac{XT_3}{1-\tau}} = e^{-\frac{X\Delta T_3}{1-\tau}} e^{-\frac{XT}{2(1-\tau)}}$ $= F_3(-\Delta T_3)\, e^{-\frac{XT}{2(1-\tau)}}$	Note exponential function approximation of present worth factors

C.2.2 SUMMARY OF EQUATIONS (continued)

	ACCOUNTING METHOD A	ACCOUNTING METHOD B	REMARKS (REF.)
5. Modified Cost Components $\bar{c}_i = c_i \cdot F_i(-\Delta T_i)$	$\bar{c}_1 = c_1 \cdot F_1(-\Delta T_1) = c_1 e^{\frac{X\Delta T_1}{1-\tau}}$ $\bar{c}_2 = c_2 \cdot F_2(-\Delta T_2) = c_2 e^{-X\Delta T_2}$ $\bar{c}_3 = c_3 \cdot F_3(-\Delta T_3) = c_3 e^{-X\Delta T_2}$	$\bar{c}_1 = c_1 \cdot F_1(-\Delta T_1) = c_1 e^{\frac{X\Delta T_1}{1-\tau}}$ $\bar{c}_2 = c_2 \cdot F_2(-\Delta T_2) = c_2 e^{-\frac{X\Delta T_2}{1-\tau}}$ $\bar{c}_3 = c_3 \cdot F_3(-\Delta T_3) = c_3 e^{-\frac{X\Delta T_3}{1-\tau}}$	
6. (Approximated) Levelized Fuel Cycle Cost Contribution	$\frac{e}{M_{HM}} \propto \frac{\bar{c}_1 e^{r_1 T} + \bar{c}_2 e^{-r_2 T} - \bar{c}_3 \varepsilon(T) e^{-r_3 T}}{T}$		The uranium purchase cost is included in the fabrication charges. (K2)
	$r_1 = \frac{X}{2(1-\tau)}$ $r_2 = \frac{X}{2}$ $r_3 = \frac{X}{2}$	$r_1 = \frac{X}{2(1-\tau)}$ $r_2 = \frac{X}{2(1-\tau)}$ $r_3 = \frac{X}{2(1-\tau)}$	

APPENDIX D

BENCHMARK PROBLEMS FOR THE LARGE CORE CODE EVALUATION WORKING GROUP

D.1 INTRODUCTION

The physics branch of the Reactor Development and Demonstration Division (RDD) of the Energy Research and Development Administration (ERDA), which has the responsibility for the development and evaluation of calculational methods required to establish the technology of full scale liquid metal fast breeder reactors, formed a large Core Code Evaluation Working Group (LCCEWG) in 1975. The tasks of the LCCEWG were identified to be the following:

1. quantify the accuracy and efficiency of current neutronic methods for large cores,
2. identify neutronic design problems unique to large breeder reactors,
3. identify computer code development requirements, and
4. establish priorities for large core benchmark experiments.

The MIT Blanket Research Project has participated as a member of LCCEWG with other members from reactor vendors and government laboratories, with emphasis on the following aspects of the overall effort:

1. verification of the accuracy of cross section data and calculational methods used at MIT to evaluate FBR blanket performance, by comparing in-house results for benchmark problems with results from reactor vendors and national laboratories.

2. Extension of the benchmark problem to analyze the performance of several specific FBR blanket configurations (moderator and fissile seeding in the blanket), and

3. identification of calculational problems in the analysis of FBR blanket performance.

In this appendix, analysis and comparisons are based on the results of a two-dimensional base-case problem supplied by G.E.; a 4-group cross-section set was also supplied by G.E. in CCCC format (K6). Calculational results will be compared with these of other LCCEWG members.

D.2 Reactor Model and Composition

The reactor model for the first LCCEWG code evaluation tests supplied by G.E. is representative of a 1200 MWe (3085 MWth) LMFBR which consists of four regions, i.e., core zone 1, core zone 2, blanket and structure. The X-Y and R-Z geometries are given in Fig. D.1 and D.2 respectively. The assembly pitch is 13.89 cm (vs. 15 cm for other MIT blanket studies) and the blanket thickness is 38.91 cm (vs. 45 cm for other MIT blanket studies). The suggested axial buckling was 4.44×10^{-4} cm^{-2}. Atom densities for each assembly type are given in Table D.1.

D.3 4-group Cross-section Set

A 4-group cross-section set was generated in CCCC format and supplied by G.E. for the benchmark problem. At MIT, it was transformed into 2DB format using the following additional definition of a group absorption cross-section.

$$\sigma_{ab} = \sigma_f + \sigma_c - \sigma_{n2n}$$

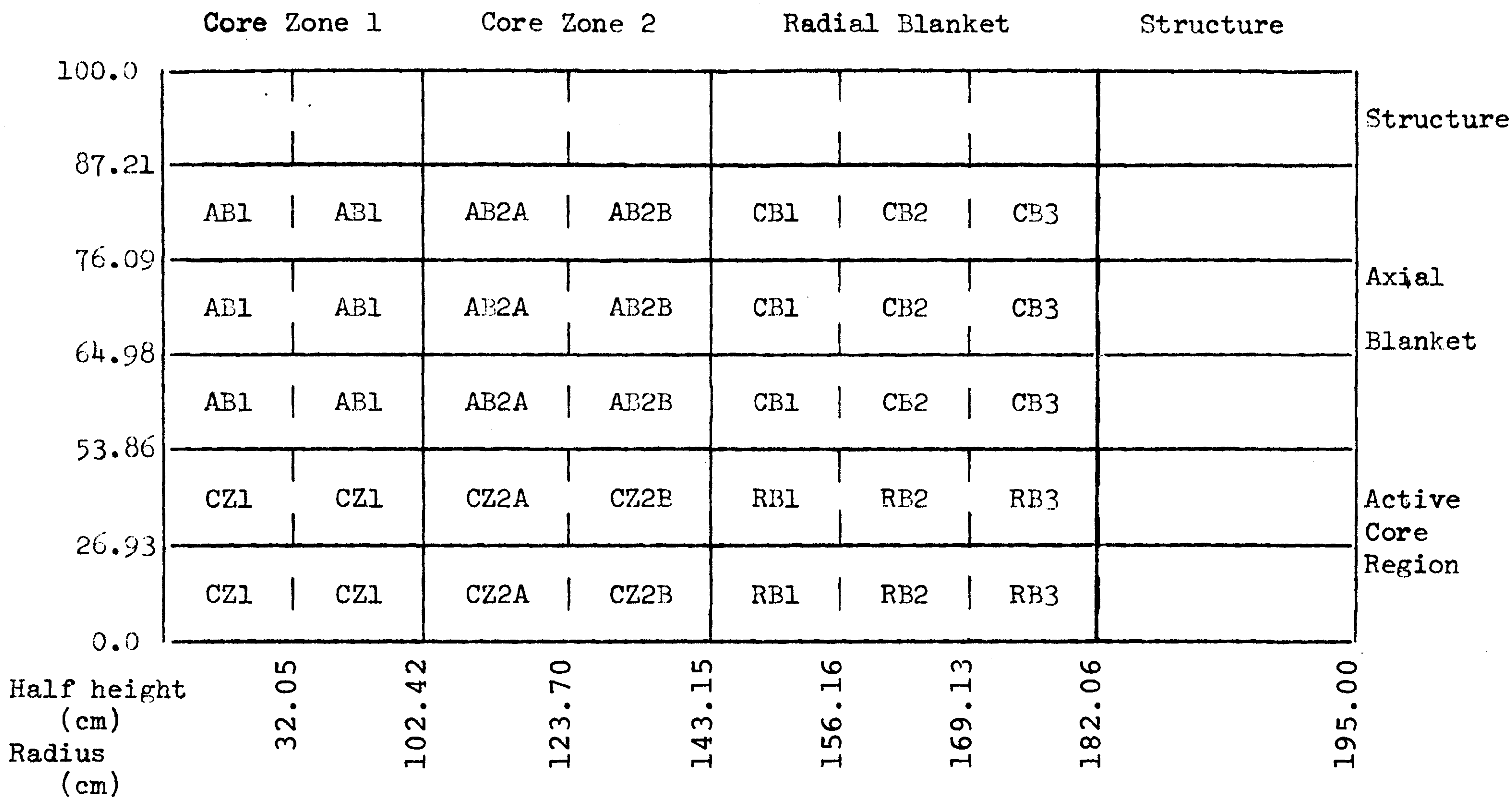

NUMBER OF HEXAGONAL ASSEMBLIES

Radial Region	1	2	3	4	5	6	7	TOTAL
Zone 1 Fuel	18	162						180
Zone 2 Fuel			84	96				180
Radial Blanket					72	78	84	234
Control	1	13	5					19
TOTAL	19	175	89	96	72	78	84	613

Fig. D.1 CORE CONFIGURATION OF 1200MWe BENCHMARK REACTOR

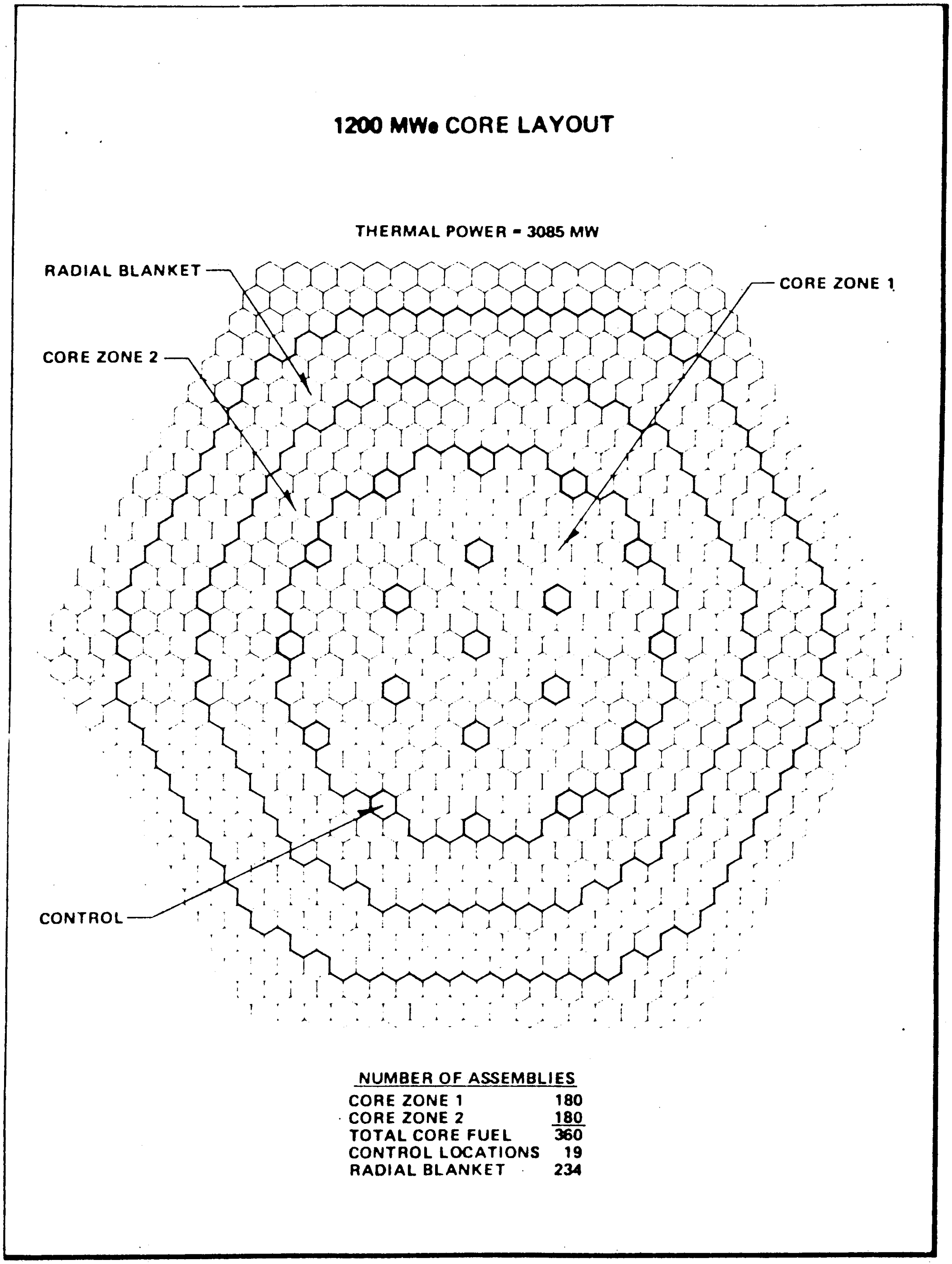

Fig. D.2 1200MWe CORE LAYOUT

TABLE D.1

ASSEMBLY ATOM DENSITIES (atoms/barn-cm)

	CZ1 Fuel	CZ2 Fuel	Blanket	Structure	Control (in)	Control (out)
Pu-239	7.6 - 4	10.1 - 4				
Pu-240	2.9 - 4	4.1 - 4				
Pu-241	1.4 - 4	1.9 - 4				
Pu-242	8.0 -5	1.12 - 4				
U-238	7.69 - 3	7.23 - 3	1.401 - 2			
U-235	1.9 - 5	1.8 - 5	4.2 - 5			
Cr	2.98 - 3	2.98 - 3	1.73 - 3	1.516 - 2	2.98 - 3	2.98 - 3
Fe	6.26 - 3	6.26 - 3	4.04 - 3	3.537 - 2	6.26 - 3	6.26 - 3
Ni	5.26 - 3	5.26 - 3	3.84 - 3	3.368 - 2	5.26 - 3	5.26 - 3
Mo	2.6 - 4	2.6 - 4	1.9 - 4	1.47 - 3	2.6 - 4	2.6 - 4
Na	8.08 - 3	8.08 - 3	6.07 - 3		1.453 - 2	1.832 - 2
B-10					7.64 - 3	
B-11					1.147 - 2	
C					4.78 - 3	
F.P	2.4 - 4	2.4 - 4				
O	1.804 - 2	1.804 - 2	2.802 - 2			

Table D.2 compares cross-sections supplied by G.E. for Pu-239 and U-238 in the core and blanket with the cross-sections used at MIT for most of the other studies in this report.

The energy group structure for both 4-group cross-section sets is approximately the same. The first and second energy groups are very important because of their high neutron group flux, and the G.E. cross-section set generated from (ENDF/B3) is seen to be in accord with the MIT cross-section set within a reasonable error range.

TABLE D.2 COMPARISONS OF 4-GROUP CROSS-SECTIONS USED AT MIT (ABBN) AND G.E.†

Isotope	Group	σ_f	σ_a	$\nu\sigma_f$	σ_{tr}	$\sigma_{g\to g}$	$\sigma_{g-1\to g}$	$\sigma_{g-2\to g}$	$\sigma_{g-3\to g}$
Pu-239 Core Zone 1	1	1.8978	1.9071	6.0519	4.6932	1.9962	0.0	0.0	0.0
		1.8788	1.9207	5.8847	5.0302	2.2757	0.0	0.0	0.0
	2	1.5920	1.7964	4.6421	8.1917	6.3470	0.7842	0.0	0.0
		1.6617	1.8628	4.8294	9.1022	7.1266	0.8250	0.0	0.0
	3	1.9688	3.024	5.6685	13.9951	10.9426	0.04832	0.0057	0.0
		2.2153	3.2398	6.3585	14.7405	11.4857	0.05413	0.0010	0.0
	4	5.7459	10.6652	16.5488	23.0947	12.4239	0.02856	0.00002	0.0
		10.0569	17.0854	28.8628	30.9054	13.8194	0.01513	0.0	0.0
Pu-239 Core Zone 2	1	1.8971	1.9063	6.0523	4.6917	1.9961	0.0	0.0	0.0
		1.8809	1.9926	5.8960	5.0237	2.2686	0.0	0.0	0.0
	2	1.5908	1.7922	4.6401	8.1194	6.2815	0.7835	0.0	0.0
		1.6611	1.8606	4.8288	9.0573	7.0859	0.8240	0.0	0.0
	3	1.9596	3.0023	5.6480	13.957	10.927	0.0457	0.0057	0.0
		2.2032	3.2178	6.3239	14.7070	11.4747	0.05283	0.01	0.0
	4	5.5273	10.267	15.919	22.457	12.190	0.0275	0.0	0.0
		10.0738	17.1278	28.9105	30.9474	13.8193	0.01454	0.0	0.0
U-238 Radial Blanket	1	0.3784	0.4227	1.0468	4.7198	2.5427	0.0	0.0	0.0
		0.2819	0.3675	0.7899	4.7198	3.0311	0.0	0.0	0.0
	2	0.0003	0.1904	0.0008	8.8502	8.5826	1.7449	0.0	0.0
		0.0	0.1833	0.0	9.5596	9.2792	1.1714	0.0	0.0
	3	0.0	0.6150	0.0001	13.0441	12.4115	0.0771	0.0095	0.0
		0.0	0.5719	0.0	13.0632	12.4538	0.0968	0.0159	0.0
	4	0.0004	1.2234	0.0009	11.3609	10.1375	0.0177	0.0001	0.0
		0.0	1.1567	0.0	12.4650	11.381	0.0249	0.0	0.0

†Energy Group structure (Highest Energy in MeV)

	G.E.		MIT
1	16.49000	1	10.5000
2	0.82080	2	0.8000
3	0.04087	3	0.0465
4	0.002035	4	0.00100

Key: G.E. (upper value) / MIT (lower value)

D.4 MIT Results for the LCCEWG Benchmark Problem

D.4.1 Computational Basis

A. Energy Group Structure:

Group	Highest Energy (MeV)	Neutron Velocity (cm/sec)
1	16.49000	1.8760 E + 09
2	0.82080	5.5673 E + 08
3	0.04087	1.5876 E + 08
4	0.002035	4.2981 E + 07

B. Fission Spectrum:

Group	1	2	3	4
	0.75969	0.23715	0.003127	0.00003568

C. Geometry and Code:

1/4 Core - 6 point/Hex.; 2 dimensional diffusion Code (2DB)

D. Cross-section Rearrangement:

4-group cross-section set supplied by G.E. in CCCC format was transfered to 2DB format. Absorption cross-section was defined by

$$\sigma_{ab} = \sigma_f + \sigma_c - \sigma_{n2n}$$

E. Axial buckling: 4.44×10^{-4} cm^{-2}

F. Flat-to-Flat Distance of Fuel Assembly: 13.89 cm

G. Zone Volume (liters): (1/4 core and 1 cm height):

Core Zone 1 (CZ1);	7.5187
Core Zone 2 (CZ2);	7.5187
Blanket (B) ;	9.7743
Structure (S) ;	8.5212
Control Rod (CR) ;	0.79365
Total	34.12655

H. Total Fission Source is normalized to 1.0.

The neutron fission source in a given group g and region Z is given by:

$$S_{gz} = \frac{\chi_g}{k_{eff}} \sum_{g=1}^{G} (\nu\Sigma_f)_{gz}\phi_{gz}$$

where ϕ_{gz} is the total flux for group g in region z. The total fission source is obtained by summing the above expression over all groups and regions.

I. Energy Production: 215 MeV/Fission

J. Boundary Condition: 90° rotation periodic boundary
left boundary: reflective
right boundary: vacuum
Outside core corner: filled with 1% Na
Top boundary: vacuum
Bottom boundary: reflective

D.4.2 Results

A. Case: Base Case - All control rods out except outer-corner control rod in.

B. Convergency Criteria:

$$k_{eff}; \quad \left| k_{eff\ i+1} - k_{eff\ i} \right| \leq 1.0 \times 10^{-6}$$

$$\text{Flux}; \quad \left| (\phi_{i+1} - \phi_i)/\phi_i \right| \leq 1.0 \times 10^{-4}$$

C. Buckling search*: 4.4416 E - 04 cm^{-2}

*suggested value is 4.44×10^{-4} cm^{-2}. Values quoted below are for the fixed buckling case, 4.44 E - 04 cm^{-2}.

D. k_{eff}: 0.99938196

E. Critical Mass* (kg):

Isotope				
Pu-239	2.2670	3.0130	0.0	5.2800
Pu-240	0.8688	1.2280	0.0	2.0968
Pu-241	0.4212	0.5716	0.0	0.9928
Pu-242	0.2417	0.3383	0.0	0.5800
U-238	22.8500	21.4800	54.1100	98.4400
U-235	0.0557	0.0528	0.1602	0.2687

*per cm core height per quarter core

F. Regional Power Distribution (MWth)

Core Zone 1; 391.52

Core Zone 2; 366.85

Blanket; 12.825

Total 771.195 (quarter core)

G. Breeding Ratio*:

$$*BR \equiv \frac{\sum_{C,B} [C^{28} + C^{40}]}{\sum_{C,B} [A^{49} + A^{41} + A^{25}]}$$

Core Zone 1 0.5560

Core Zone 2 0.3677

Blanket 0.2207

Total 1.1444

H. Average Power Density of Core (MWth/liter): 50.4323

I. Average and Regional Peak Fission Rate (#/cm^3-sec):

1. Average Fission Rate in Core; 2.2393 E - 05[@] #/cm^3-sec
2. CZ1 Peak/Average Fission Rate; 1.1456
3. CZ2 Peak/Average Fission Rate; 1.3063

J. Pointwise Neutron Flux Spectrum: (Positions are indicated in Figure D.3)

Group	ϕ ij (#/cm^2-sec)@					
	A	B	C	D	E	F
1	1.3423E-03	1.2415E-03	1.2703E-03	4.5286E-04	2.2020E-06	2.0474E-09
2	6.1067E-03	6.8430E-03	6.1396E-03	2.5580E-03	1.0262E-04	1.2103E-06
3	2.0060E-03	2.5287E-03	2.1142E-03	9.4947E-04	7.9187E-05	6.4281E-07
4	2.8690E-04	5.2172E-04	4.0292E-04	1.4508E-04	3.0639E-05	6.3756E-07
Remarks	The flux in group 1 is a max. here.	Peak Power in CZ1 is here	Peak Power in CZ2 is here			

@ To obtain values compatable with the results of 1/6 core representations, this value should be multiplied by 1.5.

K. Reaction Rate in Each Zone (#/sec-zone):

Isotope Zone	Pu-239	U-238	Fe
CZ1 - F	1.0788E-01	2.6074E-02	0.0
CZ2 - F	1.0307E-01	2.0783E-02	0.0
CZ1 - A	1.3891E-01	2.0401E-01	5.2867E-03
CZ2 - A	1.2988E-01	1.3568E-01	3.6259E-03
B - F	0.0	4.1688E-03	0.0
B - A	0.0	7.8896E-02	8.2367E-04
S - A	0.0	0.0	7.4537E-04

F: Fission A: Absorption

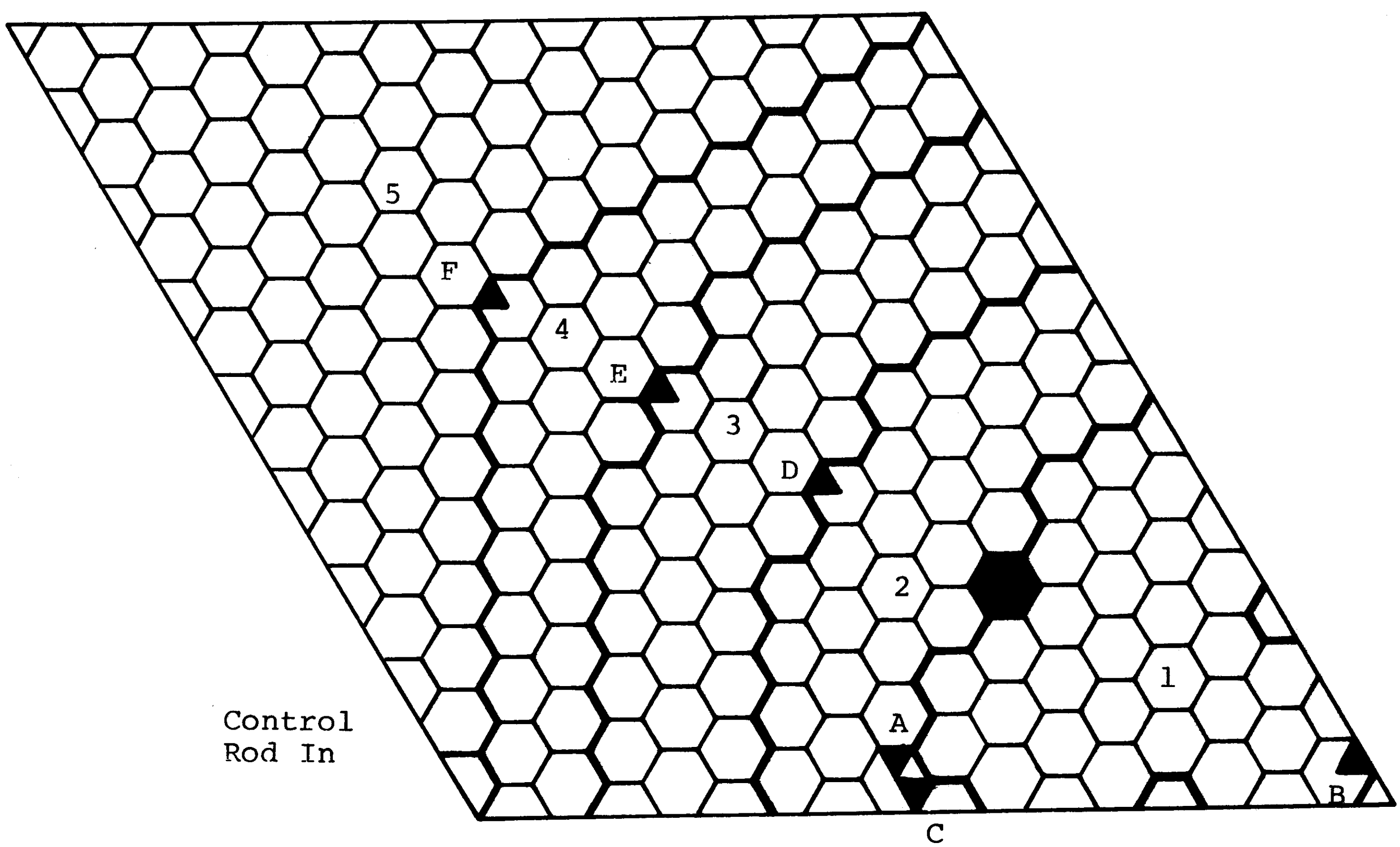

* Regions: 1 Core Zone 1 2 Core Zone 2
3 Radial Blanket 4 Radial Reflector
5 1% Sodium Corner Region

Fig. D.3 CORE LAYOUT WITH 60 ROTATION PERIODIC BOUNDARY

D.5 COMPARISONS OF THE RESULTS OF THE LCCEWG (K6)

Parameters	M.I.T.	G.E.	HEDL	ANL	Range (%)
Codes & Methods	2DB (Diffusion) (6 points/Hex) (1/4 core)	SN2D (Diffusion) (6 points/Hex) (1/6 core)	2DB (Diffusion) (6 points/Hex) (1/6 core)	DIF2D (Diffusion) (6 points/Hex) (1/6 Core)	-
k_{eff}	0.99938	0.99965	0.99958	0.99958	0.03
P_1*	1.1456	1.1579	1.1490	1.1497	0.4
P_2*	1.3063	1.3035	1.3054	1.3053	0.08
BR	1.1444	1.1438	1.1438	1.1438	0.05
Control Worth**	3.76 E-03	3.84 E-03	3.84 E-03	-	2.1
Pu-239					
CZ1-F	1.0788 E-01	1.0828 E-01	1.080 E-01	1.0809 E-01	0.4
CZ2-F	1.0307 E-01	1.0276 E-01	1.030 E-01	1.0301 E-01	0.3
CZ1-A	1.3891 E-01	1.3941 E-01	1.391 E-01	1.3919 E-01	0.4
CZ2-A	1.2988 E-01	1.2949 E-01	1.298 E-01	1.2983 E-01	0.3
U-238					
CZ1-F	2.6074 E-02	2.6163 E-02	2.610 E-02	2.6119 E-02	0.3
CZ2-F	2.0783 E-02	2.0713 E-02	2.076 E-02	2.0766 E-02	0.3
CZ1-A	2.0401 E-01	2.0477 E-01	2.056 E-01	2.0574 E-01	0.8
CZ2-A	1.3568 E-01	1.3528 E-01	1.366 E-01	1.3669 E-01	1.4
B-A	7.8896 E-02	7.8602 E-02	7.902 E-02	7.9045 E-02	0.6
Fe CZ1-A	5.2867 E-03	5.3060 E-03		5.3031 E-03	0.4
CZ2-A	3.6259 E-03	3.6155 E-03	-	3.6291 E-03	0.4
B-A	8.2367 E-04	8.2070 E-04		8.2351 E-04	0.4
S-A	7.4537 E-04	7.3770 E-04		7.4017 E-04	1.0

* P_1: CZ1 Peak to Average Fission Rate

P_2: CZ2 Peak to Average Fission Rate

** (All Control Rods Out - Base Case)/6

L. Na Void Effect for 100% Removal of Na from Each Core Zone and Associated Axial Blanket:

	k_{eff}
Base Case	0.99938196
Without Na in CZ1	1.00442700
Without Na in CZ2	0.99884915
Δk/k in CZ1	0.5048%
Δk/k in CZ2	-0.0533%

M. Control Rod Worth:

	k_{eff}
Base Case	0.99938196
All Control Rods In	0.95374501
All Control Rods Out	1.02192500
Δk/k; All In	-4.5665%
Δk/k; All Out	2.2557%

N. Computation Time 4.92 Min. of Central Precision Time on IBM Model 370 Model 168

D.6 COMMENTS ON THE RESULTS

The LCCEWG benchmark problem was analyzed by the seven organizations and the results were compared in previous section. While MIT used the 90°-symmetry core configurations,rather than 60°-symmetry core configuration which most participants used, all of the computational results of MIT are equally well in agreement with these of other participants.

The points which should be considered more precisely during calculations are

a. Convergence limits for the performance c culations; MIT used 1.0×10^{-6} for the convergence limit of k_{eff}. Loose convergence leads to a different k_{eff} calculation and the variation of breeding ratio is approximately

$$\Delta b \cong -4.6 \; \Delta k_{eff}$$

b. 2DB requires a specific material composition for the area outside of the structural assembly. The neutron reaction rate in the structural assembly is very sensitive to the material used in this region.

APPENDIX E

HETEROGENEOUS FISSILE-SEEDING

E.1 INTRODUCTION

In section 5.3.2, the characteristics of homogeneously and heterogeneously fissile-seeded blankets were discussed. There are very small effects on the core performances caused by the fissile seeding. In this appendix, the effects on the blanket fissile breeding performance for heterogeneously fissile seeded blankets will be discussed. The characteristics for homogeneously fissile-seeded blankets were analyzed in Section 5.3.3.

E.2 BREEDING PERFORMANCE OF HETEROGENEOUSLY FISSILE-SEEDED BLANKETS

Start with the definition of b and assume that U-238 captures and Pu^{49} absorptions are perturbed by events in the blanket only.

$$b_o = \frac{C_T^{28}}{A_T^{49}} \tag{E.1}$$

$$b = \frac{C_T^{28} + \delta C_T^{28}}{A_T^{49} + \delta A_T^{49}} = b_o\left[\frac{1 + \delta C_T^{28}/C_T^{28}}{1 + \delta A_T^{49}/A_T^{49}}\right] \tag{E.2}$$

$$\Delta g = (b - b_o) = b_o\left[\frac{\delta C_T^{28}/C_T^{28} - \delta A_T^{49}/A_T^{49}}{1 + \delta A_T^{49}/A_T^{49}}\right] \tag{E.3}$$

Now assume that small lumps of Pu are dispersed in the blanket such that they absorb neutrons and all fission neutrons produced escape the lump and are absorbed in U-238 in the blanket. Also we assume that fast fissions in U-238 exactly cancel leakage plus parasitic losses - this approximation was shown to be tenable in Section 3.3.4.

Since the core is unaffected, we have in the blanket:

$$\delta C_T^{28} \stackrel{\sim}{=} \delta C_B^{28}, \ \delta A_T^{49} \stackrel{\sim}{=} \delta A_B^{49}, \ A_T^{49} \stackrel{\sim}{=} A_C^{49} \tag{E.4}$$

and

$$\delta C_B^{28} = (\eta_B^{49} - 1)\delta A_B^{49}, \ \eta_B^{49} = \nu F_B^{49}/A_B^{49} \tag{E.5}$$

Thus

$$\Delta g = b_o\left[\frac{(\eta_B^{49} - 1)\dfrac{\delta A_T^{49}}{C_T^{28}} - \dfrac{\delta A_T^{49}}{A_T^{49}}}{1 + \dfrac{\delta A_T^{49}}{A_T^{49}}}\right]$$

$$= b_o\left[\frac{\eta_B^{49} - 1}{C_T^{49}} - \frac{1}{A_T^{49}}\right] \frac{\delta A_T^{49}}{1 + \dfrac{\delta A_T^{49}}{A_T^{49}}}$$

$$= \frac{\delta A_T^{49}}{A_T^{49} + \delta A_T^{49}} \left[\eta_B^{49} - 1 - b_o\right] \tag{E.6}$$

Using the relation $b_o = g_o + 1$, Eq. (E.6) can be rewritten as;

$$\Delta g = \left[\frac{A_B^{49}}{A_B^{49} + A_C^{49}}\right]\left[\eta_B^{49} - (2 + g_o)\right] \tag{E.7}$$

Thus the criterion for positive Δg is

$$\eta_B^{49} \geq 2 + g_o \stackrel{\sim}{\sim} 2.2$$

which is the same as the homogeneous result.

Thus to first order there is no difference between the heterogeneous and homogeneous results.

We can, however, introduce some second order corrections: the fast neutrons emitted by Pu-239 fission can induce U-238 fast fission. Assuming that in the blanket only U-238 removal is very effective, then each fast neutron will produce

$$\left(\frac{\bar{\sigma}_f^{28}}{\bar{\sigma}_r^{28}}\right) \text{ fissions in U-238}$$

where $\bar{\sigma}_f^{28}$ is the fission cross-section for U-238 averaged over the fission spectrum and $\bar{\sigma}_r^{28}$ is the removal cross-section for U-238, also averaged over the fission spectrum.

Thus the net increase in neutron yield is $(\nu-1)\left(\frac{\bar{\sigma}_f^{28}}{\bar{\sigma}_r^{28}}\right)$, and we should replace η_B^{49} by $\eta_B^{49}\left[1 + (\nu-1)\ \frac{\bar{\sigma}_r^{28}}{\bar{\sigma}_r^{28}}\right]$; now the criterion becomes:

$$\eta_B^{49} \geq \frac{2 + g_o}{1 + (\nu-1)\ \frac{\bar{\sigma}_f^{28}}{\bar{\sigma}_r^{28}}} \approx \frac{2.2}{1 + 2 \cdot 1/8} = 1.76$$

Thus we might see some advantage to heterogeneous dispersal of Pu in the blankets - assuming that the preceeding somewhat heuristic derivation is valid. Also note that we neglected leakage into the reflector, which will reduce the advantage, as will parasitic losses, also neglected.

In any event the effect will be small, e.g., let

$$\frac{A_B^{49}}{A_B^{49} + A_C^{49}} = 1/20 \quad \text{and} \quad \eta_B^{49} = 2.2 = 2 + g_o, \quad (\nu-1)\left(\frac{\bar{\sigma}_f^{28}}{\bar{\sigma}_r^{28}}\right) = 0.25, \text{ then}$$

$$\Delta g = 1/20 \cdot (2.2)(0.25) \cong 0.027$$

Thus it will be difficult to achieve an appreciable benefit. Also note that σ_f for Th-232 is a factor of about four less than that of U-238; hence almost no improvement due to fast fission would be expected in Thorium fueled blankets.

However for the U-233/Th-232 cycle in both core and blanket also note that η_B^{23} is probably on the order of 2.3, while $g_o \cong 0.1$, thus since 2.3 > 2.1 there may still be some advantage to heterogeneous seeding.

APPENDIX F

REFERENCES

A1 Aldrich, D.C., "Parfait Blanket Systems Employing Mixed Progeny Fuels", S.M. Thesis, Nuclear Engineering Department, MIT (June, 1976)

A2 Ayer, J. E., et.al., "A Cost Estimate for Remote Refabrication of Metallic Fuels", ANL-6950 (1966).

B1 Barthold, W.I., "Fuel Shuffling in LFMBR Blankets", Argonne National Laboratory, FRA-TM-40 (Aug., 1972)

B2 Barthold, W. P. and J. Beitel, "Potential and Limitations of Heterogeneous LMFBR Reactor Concepts I. Survey Analysis of Radial Parfait Core in the 1200 MWe Class", Argonne National Laboratory, FRA-TM-93 (Feb. 1977)

B3 Bondarenko, I.I., (Ed.), "Group Constants for Nuclear Reactor Calculations", Consultants Bureau, New York (1964).

B4 Brewer, S. T., E. A. Mason and M. J. Driscoll, "The Economics of Fuel Depletion in Fast Breeder Reactor Blankets", COO-3060-4, MITNE-123 (Nov. 1972).

B5 Brown, G. J. and M. J. Driscoll, "Evaluation of High Performance LMFBR Blanket Configurations", COO-2050-4, MITNE-150 (May, 1974).

B6 Bruyer, D., "Breeding-Economics of FBR Blankets having Non-linear Fissile Buildup Histories, S.M. Thesis, Nuclear Engineering Department, MIT (Aug. 1976)

B7 Butler, D. K., et. al., "Use of Beryllium Zones to Enhance Safety of Fast Breeder Reactors" Trans. Am. Nucl. Soc. 8, 239-240 (1965).

C1 Cadwell, W. R., R. F. Byerger and C. J. Pfeifer, "The PDQ-5 and PDQ-6 Programs for the Solution of the Two-dimensional Neutron Diffusion-Depletion Problem", WAPD-TM-477 (June 1965)

C2 Carter, N. E., et. al, "Use of Isotopic Composition Data to Improve Reactor Calculational Techniques", BNWL-5A-4275 (1972).

C3 Caspersson, S. A., R. C. Noyes and J. A. Vitti, "Economic and Nuclear Performance Characteristics of 500 MW(e) Oxide, Carbide and Nitride LMFBR's, Advanced Reactors: Physics, Design and Economics Proc. of the Int. Conf. (Atlanta, Georgia), Pergamon Press (Sept. 1974)

C4 Caspersson, S. A., et. al. A Carbide Radial Blanket for a Demonstration LMFBR", Trans. Am. Nucl. Soc., 18, 277 (1974).

C5 Chang, Y. I., "Review of the French Concept of Heterogeneous Core to Improve the Doubling Time", FRA-TM-77 (Aug. 1975).

C6 Chang, Y. I., W. P. Barthold and C. E. Till, "An Evaluation of the Cylindrical Parfait Core Concept", FRA-TM-88 (April, 1976)

C7 Christensen, D. E., et. al., "Summary of Experience with the Use of Isotopic Correlations Safeguard Techniques", BNWL-SA-4273 (1972).

D1 Driscoll, M. J., et. al. "Safety and Breeding-Related Aspects of Fast Reactor Cores Having Internal Blankets", International Meeting on Fast Reactor Safety and Related Physics, Chicago (Oct. 1976).

D2 Driscoll, M. J., "Notes on Fast Reactor Physics", MIT Subject 22.94 (1968)

D3 Ducat, G. A., M. J. Driscoll and N. E. Todreas, "Evaluation of the Parfait Blanket Concept for Fast Breeder Reactors", COO-2250-5, MITNE-157 (Jan. 1974).

E1 Engle, W. W., Jr., "A Users Manual for ANISN, a One-Dimensional Discrete Ordinates Transport Code with Anisotropic Scattering", K-1693 (March,1967)

F1 Feinberg, S. M., "Fast Gas and Thermal Breeder Reactors" Soviet Atomic Energy, 37(1) (July 1974)

F2 Foggi, C. and D. Frandeli, "Correlations Between Heavy Isotopes in Irradiated Fuel of LWR", EUR-5071 (1973)

F3 Fowler, T. B., et. al., "Nuclear Reactor Core Analysis Code: CITATION", ORNL-TM-2469, Rev. 2 (July 1969)

F4 Furuhashi, Y., "Equation for the Optimum Fuel Irradiation Time in FBR Blankets", Atomic Energy Society of Japan (J), (618), 430-432 (1974) (In Japanese)

G1 Grant, P. J., "Elementary Reactor Physics", Pergamon Press (1966)

H1 Hansen, M. and K. Anderko, "Constitution of Binary Alloys", McGraw-Hill (1958)

H2 Hirons, T. J. and R. D. O'dell, "PHENIX: A Two-Dimensional Diffusion Burnup-Refueling Code", NSE, 39(1), 411 (March 1970)

H3 Hirons, T. J. and R. D. O'dell, "Calculational Modeling Effects on Fast Breeder Fuel Cycle Analysis", LA-4187 (Sept. 1965)

H4 Hoover, J. et. al. "The Fuel Cycle Analysis Stem, REBUS", NSE, 45(1), 52-65 (July 1971)

H5 Howlett, B. W. and A. G. Knapton, "The Uranium-Titanium, Uranium-Zirconium and Uranium-Titanium-Zirconium Alloy Systems", Proc. of the 2nd UN Int. Conf. on the Peaceful Use of Atomic Energy, 6, 104-110 (1958)

K1 Kaufmann, A. R. (Ed.), "Nuclear Reactor Fuel Elements, Metallurgy and Fabrication" (page 651) Interscience Publishers (1962).

K2 Ketabi, M., "The Breeding-Economic Performance of Fast Reactor Blankets", S.M. Thesis, Nuclear Engineering Dept., MIT (May 1975)

K3 Klickman, A. E., et. al., "The Design and Economic Evaluation of Fixed Blankets for Fast Reactors", APDA-156 (Aug. 1963).

K4 Kobayashi, T., S. Kondo and Y. Togo, "Nuclear Characteristics of Sandwich -Blanket Type Core for Power Reactor", NSE, 10(11), 700-702 (Nov. 19 73)

K5 Koch, L., et. al., "Isotope Correlations - A New Tool in Fuel Management", TRANS. Am. Nucl. Soc 20, 339 (April 1975)

K6 Kujawski, E., and H. S. Bailey, "Benchmark Analysis of LMFBR Nuclear Design Methods", the ANS Mathematics and Computation Division National Topical Meeting to be held in Tucson, March 28-30 (1977)

L1 Lake, J. A., et. al., "Breeding Ratio and Doubling Time Characteristics of the Clinch River Breeder Reactor", Advanced Reactors; Physics, Design and Economics, Pergamon Press (Sept. 1974)

L2 Lamarsh, J. L., "Introduction to Nuclear Reactor Theory", Addison-Wesley Publishing Co., Inc. (1966)

L3 Little, W. W., Jr. and R. W. Hardie, "2DB User's Manual, Revision 1", BNWL-831, Rev. 1 (Aug. 1969).

L4 Little, W. W., Jr., R. W. Hardie, L. D. O'dell and R. B. Kidman, "Fuel Management Models and Analysis for the fast Test Reactor", BNWL-SA-2758 (Dec. 1969)

L5 Lynch, J. F. and C. G. Ruderer, (Ed.), "Engineering Properties of Selected Ceramic Materials:, The American Ceramic Society, Inc., Columbus, Ohio (1966)

M1 Masterson, R. E., "The Application of Perturbation Theory and Variational Principles to Fast Reactor Fuel Management", S.M.Thesis, Nuclear Engineering Dept., MIT (Sept. 1974)

M2 Mayer, L., "Studies on the Optimum Design of The Radial Blanket on the Basis of a Steam-Cooled Fast Breeder", EURFNR 377, PSB No. 263/67 (May,1967)

Mayer, L., "Studies on the Optimum Design of the Axial Blanket on the Basis of a Steam-Cooled Fast Breeder", EURFNR-378, PSB No. 271/67 (July 1967)

M3 McIntosh, A. B. and T. J. Heal, (Ed.), "Materials for Nuclear Engineers" Interscience Publishers Inc., New York (1960)

M4 Moorhead, T. P. and A.S.B.Belcher, "Dependence of Breeding upon Some Design Parameters of Large Fast Reactors", Euro Nuclear, 599-603 (Dec. 1965)

M5 Mougniot, J. C. , et. al., "Breeding Gains of Sodium-Cooled Oxide Fueled Fast Reactors", Paper from European Nuclear Conference, April, 1975, Paris ORNL-TR-2994 (1975)

M6 Munno, F. J. and D. Elias, "Reactor Fuel Management Optimization in a Dynamic Environment", Nuclear Technology, 12, 46-55 (1971)

O1 Okrent, D., "Neutron Physics Considerations in Large Fast Reactors", Power Reactor Technology, 7(2), 107-137 (Spring 1964)

O2 Okrent, D., et. al., "Some Nuclear and Safety Considerations in the Design of Large Fast Power Reactors", Proc. of 3rd Int. Conf. on the Peaceful Uses of Atomic Energy, 6(1965)

O3 Okrent, D. and S. D.Hasnain, "On the Design and Management of Fast Reactor Blankets", NSE, 9, 314-322 (1961)

P1 Perks, M. A. and R. M. Lord, "Effects of Axial and Radial Blanket Design on Breeding and Economics", ANL-6791, 367-394 (1963)

P2 Pinnock, R. A., "Parfait Blanket Configurations for Fast Breeder Reactors", S. M. Thesis, Nuclear Engineering Dept., MIT (June 1975)

S1 Samoilov, A. G., et. al., "Dispersion-Fuel Nuclear Elements", Translated from Russian, Israel Program for Scientific Translations, Jerusalem (1968)

S2 Sierra, J. M. and M. Becker, "Sensitivity Analysis for the Fast Reactor Fuel Cycle", Trans. Am. Nucl. Soc., 23, **535** (1976)

S3 Sierra, J. M. and M. Becker, "An Analytical Approach to Fast Reactor Fuel Cycle Analysis", Trans. Am. Nucl. Soc., 22, 713 (1975)

S4 Simcha, G. and R. Salman, "Nuclear Fuel Logistics", Nuclear News, 47-53 (Feb. 1973)

S5 Soltesz, R. G., "Revised WANL ANISN Program User's Manual", WANL-TMI-1967 (April, 1969)

S6 Spitzer, J., "Blanket Shape Optimization in Breeder Reactors", Ph.D. Thesis, the University of New Mexico (1971)

S7 Springsteen, D. F., "Financing for Fuel Cycle", Class Notes for Nuclear Fuel and Power Management Course at MIT (July 1976)

S8 Strasser, A., et. al., "Uranium-Plutonium Carbide Fuels for Fast Breeder Reactors", ANS-100, National Topical Meeting at Detroit, Michigan (1965)

T1 Tagishi, A. and M. J. Driscoll, "The Effect of Reactor Size on the Breeding Economics of LMFBR Blankets", COO-2250-13, MITNE-168 (Feb. 1975)

T2 Tipton, C. R., Jr., (Ed.), "Reactor Handbook" Vol. 1, Materials" Interscience Publishers Inc., New York (1960)

T3 Touloukian, Y. S. , et. al., "Thermal Conductivity (Iron Metallic Solids)", Vol. 2, Thermophysical Properties Research Center (TPRC), Purdue University (1970)

T4 Tzanos, C. P., "Optimization of Material Distributions in Fast Breeder Reactors", MITNE-128, MIT-4105-6 (Aug. 1971)

V1 Vitti, J. A., et. al., "Preliminary Assessment of the Impact of Carbide-Fueled Subassemblies in the CRBRP", Trans. Am. Nucl. Soc., 18, 391 (1974)

W1 Weissert, L. R. and G. Schileo, "Fabrication of Thorium Fuel Elements", AEC Monograph Published by ANS (1968)

W2 Westinghouse Advanced Reactor Development, "Design Analysis of the LMFBR Radial Blanket", WARD 3045T2B-9 (Mar. 1973)

W3 Wood, P. J., "Assessment of Thorium Blankets for Fast Breeder Reactors", COO-2250-2, MITNE-148 (July 1973)

Y1 Yemel'yanov, V. S. and A. I. Sevstyukhin, "The Metallurgy of Nuclear Fuel" Properties and Principles of the Technology of Uranium, Thorium and Plutonium, Pergamon Press (1969)

Z1 DRDT, USAEC, "Reactor Fuel Cycle Cost for Nuclear Power Evaluation", WASH-1099 (Dec. 1971)